Response of *Arabidopsis thaliana* seedlings to lead exposure

Ing Chia Phang

A thesis submitted in partial fulfilment of the requirement for the degree of

Doctor of Philosophy

at the

University of Canterbury

Christchurch, New Zealand

2010

In memory of grandmother.

Abstract

Lead (Pb) is one of the most commonly occurring, highly persistent and widely distributed heavy metal contaminants in the environment. It has a tendency to bioaccumulate in animals and plants, and potentially, it is able to enter the human food chain where it poses a hazard to public health. Generally, conventional remediation technologies applied to decontaminate heavy metals from groundwater and soils are very costly. Hence, phytoremediation has emerged as an ecologically friendly and economically attractive technology that uses green plants to clean up heavy metal contaminated sites. However, a lack of knowledge of the biological processes associated with plant responses to Pb (e.g. Pb uptake, accumulation, translocation, and tolerance) has been a bottleneck for the application of Pb phytoremediation in the field. A model genetic system of higher plants, *Arabidopsis thaliana*, was selected to further examine the physiological, biochemical and molecular events occuring in plants under Pb stress.

The overall aim of this project was to obtain a better understanding of plant responses to Pb contaminants in the early developmental stages of *A. thaliana* seedlings. This research encompassed the physiological responses of *A. thaliana* seedlings to Pb exposure, monitoring their antioxidative defence systems, and investigating the participation of annexin 1 in the response to Pb-mediated oxidative stress. This research also assessed the protective effect of nitric oxide on Pb-induced toxicity of *A. thaliana* seedlings and it isolated a putative Pb tolerant mutant from an EMS-mutagenized M_2 population. A multi-experimental approach was adopted to achieve these objectives.

A. thaliana seedlings were grown on modified Huang & Cunningham (1996) nutrient solution containing 0.8% (w/v) agar, with and without $Pb(NO_3)_2$, under controlled conditions. *A. thaliana* seedlings were insensitive to Pb during seed germination. In treatments with up to 200 μM $Pb(NO_3)_2$, morphological changes and inhibition of root growth were

observed in the 7-d-old seedlings. A tolerance index revealed that $Pb(NO_3)_2$ concentration of 75 μM and higher brought about more than 50% root growth inhibition. Pb was predominantly retained in the roots. Analysis using a graphite furnace atomic absorption spectroscopy indicated that the level of Pb accumulation in *A. thaliana* roots was greatly dependent on the $Pb(NO_3)_2$ concentrations, but only a small fraction of the accumulated Pb was translocated to the shoots (18 - 43%). Transmission electron microscopy analysis showed that Pb was mainly immobilized in the cell walls and intercellular spaces. This was interpreted as a mechanism that minimizes the entry of Pb into cells and interference with cellular functions. Pb that gained entry into the cytoplasm was sequestered into the vacuoles.

The toxicity of Pb in the cytosol of *A. thaliana* seedlings was studied by measuring the H_2O_2 and lipid hydroperoxide levels using a microplate reader. When the $Pb(NO_3)_2$ concentration in the growth medium was 100 μM, the 7-d-old seedlings contained 2.2-fold higher H_2O_2 and 9.6-fold higher lipid hydroperoxide than the control without $Pb(NO_3)_2$. This was followed by an up-regulation of the activity of antioxidative enzymes, including superoxide dismutase (SOD), catalase (CAT), glutathione reductase (GR), glutathione peroxidase (GPX), and general peroxidase (POD) by 2.1-, 3.2-, 2.3-, 1.8- and 4.6-fold, respectively, compared with the control. Pb toxicity is known to trigger oxidative stress, but *A. thaliana* seedlings appeared to be capable of activating cell rescue, defending themselves against harmful oxidative stress and also acclimating to Pb. Data from physiological and biochemical analysis indicate that a combination of avoidance and tolerance mechanisms exists in Pb-treated *A. thaliana* seedlings to maintain the essential cellular metabolism for survival.

Real-time reverse-transcription polymerase chain reaction was used to show the involvement of *AnnAt1* in the response of 7-d-old *A. thaliana* seedlings to a high threshold concentration of Pb. When the seedlings were treated with 100 μM $Pb(NO_3)_2$, *AnnAt1* message levels were up-regulated by 2.12-fold. Pb-mediated oxidative stress may be a component of *AnnAt1* gene expression. *AnnAt1* potentially could be invoked to reduce the toxic effects of Pb stress by acting as ROS and/or Ca^{2+} signals, as a membrane protector, in detoxification of excessive ROS, or in sequestration of Pb.

Pb stress symptoms were less evident in seedlings pre-treated with 1 mM sodium ni-

troprusside (SNP), a nitric oxide (NO) donor. The present study found that exogenous NO did not alter Pb transport into the plants or efflux pumping of Pb at the plasma membrane. However, NO conferred protection to 7-d-old *A. thaliana* seedlings primarily by acting as an antioxidant or a signal for actions to scavenge excessive ROS level. The application of exogenous NO before subjecting to 100 μM $Pb(NO_3)_2$ decreased H_2O_2 back to its original level, and reduced 50% lipid hydroperoxide in the Pb-treated seedlings. As a result, the antioxidative enzyme activities in Pb-exposed seedlings pre-treated with SNP were 23 - 45% lower than those without SNP pre-treatment. Less antioxidative enzyme activities were probably needed to counteract the reduced amount of Pb-induced ROS in *A. thaliana* seedlings.

A post-germination procedure involving prolonged exposure to 150 μM $Pb(NO_3)_2$ was developed to screen an EMS-mutagenized M_2 population of *A. thaliana*. Potential Pb tolerant mutants were selected based on the ability to grow with their roots penetrating into the medium and maintain purple-green leaves without wilting. A minority of the survivors appeared to go into a resting stage and they seemed to have altered transporters that prevented Pb from entering the cells. Only one putative Pb mutant (M_3-1) was recovered from the rescue and set seeds. The M_4 generation of this putative Pb mutant was re-screened for phenotypic confirmation and to determine the regulation of *AnnAt1*. The 7-d-old putative Pb mutant seemed to display enhanced root and shoot growth in the presence of 150 μM $Pb(NO_3)_2$ compared to the wild-type seedlings. The transcript level of *AnnAt1* in this putative Pb tolerant mutant increased by 2.19-fold when exposed to 150 μM $Pb(NO_3)_2$.

Acknowledgements

The journey of my graduate studies was made possible from the generous support, interest and advice from many people. The effort from all individuals has been crucial, either directly or indirectly, making the road travelled less arduous. I would like to take this opportunity to highlight a few of them in no particular order.

First and foremost, I would like to extend my deepest gratitude to my supervisors: Dr. David Leung, Assoc. Prof. Harry Taylor, and Dr. Ashley Garrill. Each gave excellent support, professional guidance, constructive suggestions, and endless advice throughout my studies. Thanks for helping me to develop my thought, contributing towards my understanding, giving constructive comments on draft chapters, being enthusiastic and encouraging, and making my study enjoyable. Most importantly, thanks for having faith and confidence in me.

Special thanks the staffs and students in the School of Biological Sciences for their cooperation, and providing assistance at various occasions. In particular, I thank Manfred Ingerfeld for his expertise in transmission electron microscopy, and Matt Walters for his marvellous photography. Dr. Jason Song for giving advice in molecular biology, David O'Keefe, Thomas Evans and Sandi Suei for sharing tips on molecular techniques, Dr. David Collings for mutant screening advice, and Dr. Jason Tylianakis for statistics advice. I also like to thank Nicole Lauren Manuera for all the management, purchasing and technicality in Plant Biotechnology Laboratory, Jan McKenzie for stereomicroscopy and image analysis, Graeme Young for his prompt support in information technology services, Nicki Judson for administrative works, and Jackie Healy for gel imaging and qPCR set up. I greatly appreciate all my past and present peers from Plant Biotechnology Laboratory: Hossein Alizadeh, Lily Chin, Shugai Zhang, and Seetha Podimanike Wanninayake, for their assistance throughout the progression of this research, invaluable hints, ongoing

discussion, and friendship.

A big thanks to Dr. David Burritt (University of Otago, Dunedin, New Zealand) for providing general methods for ROS and enzyme extractions, and assaying the enzyme activities; as well as Dr. Gregory Clark (University of Texas, Austin, USA) for designing the primer pairs specifically for annexin 1, providing the antibody and sharing knowledge in protein analysis.

I'm grateful to Student Travel Grant from Australasian Society for Ecotoxicology that has encouraged my participation in the 13th Australasian Society for Ecotoxicology Conference in Adelaide, South Australia. I'm also thankful to International Travel Grant from University of Canterbury Students' Association, Student Travel Fund from Biomolecular Interaction Centre, and Phyto Scholar Program from International Phytotechnology Society that have given me the opportunity to participate in the 6th International Phytotechnologies Conference in St. Louis, Missouri, USA. The knowledge and experience gained in both overseas scientific conferences have greatly broaden my horizon. I would also like to acknowledge SLAI Scholarship from Ministry of Higher Education Malaysia and a doctoral fellowship from International Islamic University Malaysia. The financial support has made my study less onerous.

Sincere thanks to all my fellow friends in the Land of Long White Cloud for being the very special person that they are. Their friendship has helped me see through the tough times, and gave a welcome diversion from the rigours of PhD life. Thanks for the great company, proof-reading, moral support, and keeping me sane at all times. Heartfelt gratitude also to all my other friends and relatives in my home country and afar, for their calls, emails, and keeping me in touch with the rest of the world.

Most of all, infinite deep bows of appreciations to my parents, sisters, brother, and loved one. Their unconditional love, dedications, and patience all these years have allowed me to find, realize my potential, and accomplish monstrous tasks. Their nurturing and active support have opened the door for me to explore, and think outside the box. Their faith and encouraging words have been a source of inspiration for me to strive even further. I'm greatly indebted for all they have done, which make a huge difference in my life. I would not have made this far without them.

Contents

List of Figures

List of Tables

Abbreviations

ABA	abscisic acid
ABC	ATP-binding cassette
ADP	adenosine diphosphate
ANOVA	analysis of variance
AnnAt1	annexin 1 gene of *A. thaliana*
AnnAt1	annexin 1 protein of *A. thaliana*
APX	ascorbate peroxidase
AT	adenine-thymine
ATP	adenosine triphosphate
ATPase	adenosine triphosphatase
ATSDR	Agency for Toxic Substances and Disease
BLAST	basic local alignment search tool
BSA	bovine serum albumine
bp	nucleotide base pair
CAT	catalase
Ca^{2+}	calcium
CEC	cation exchange capacity
CHS	chalcone synthase
Col-0	Columbia ecotype
Ct	cycle threshold

cADPR	cyclic ADP ribose
cDNA	complementary DNA
cGMP	cyclic guanosine monophosphate
cm	centimetre
cPTIO	2-(4-carboxyphenyl)-4,4,5,5-tetramethylimidazoline-1-oxyl-3-oxide
Da	dalton
DEPC	diethyl pyrocarbonate
DNA	deoxyribose nucleic acid
DNase	deoxyribonuclease
DTNB	5,5'-dithiobis(2-nitrobenzoic acid)
DTPA	diethylenetriamine pentaacetic acid
DTT	dithiothreitol
d	day
ddH_2O	double-distilled water
dH_2O	distilled water
dL	decilitre
dNTPs	deoxynucleoside triphosphates
EC	enzyme (in standardized nomenclature)
EDDHA	ethylenediaminedi (O-hydroxyphenylacetic) acid
EDTA	ethylenediaminetetra-acetic acid disodium salt
EGTA	ethylene glycol tetraacetic acid
EMS	ethyl methanesulphonate
ERMA	Environmental Risk Management Authority
EtOH	ethanol
e.g.	example given

FW	fresh weight
GC	guanine-cytosine
GF-AAS	graphite furnace atomic absorption spectrophotometry
GMOs	genetically modified organisms
GPX	glutathione peroxidase
GR	glutathione reductase
GSH	glutathione
GSNO	S-nitrosoglutathione
GSSG	glutathione disulfide
GTP	guanosine 5'-triphosphate
g	gram
g/mol	gram per mole
H^+	hydrogen ion
H_2O	water
H_2O_2	hydrogen peroxide
HC	Huang and Cunningham (nutrient solution)
HCl	hydrochloric acid
HEDTA	hydroxyethyl ethylenediamine triacetic acid
HNO_3	nitric acid
h	hour
K^+	potassium ion
kb	thousands (kilo) base pairs
kDa	kilodalton
kg	kilogram
L	litre

LSD	Fisher's least significant difference
log	logarithmic
M	moles pre litre
Mbp	megabases, millions of base pairs
MDA	malondialdehyde
β-ME	beta-mercaptoethanol
MeOH	methanol
m	metre
m^3	cubic metre
mA	milliAmperes
mL	mililitre
mM	milimoles per litre
mg/kg	miligram per kilogram
mg/L	miligram per litre
min	minute
mm	milimetre
MS	Murashige and Skoog (nutrient solution)
MT	metallothionein
NADP	nicotiamide adenine dinucleotide phosphate
NADPH	reduced form of NADP
Na_2EDTA	disodium ethylenediaminetetraacetic acid
NaCl	sodium chloride
NBT	nitro blue tetrazolium
NCBI	National Center for Biotechnology Information
NO	nitric oxide

NO_2^-	nitrate
NO_3^-	nitrite
NOS	nitric oxide synthase
No.	number
NR	nitrate reductase
NTC	no template control
nm	nanometre
$\cdot O_2^-$	superoxide radical
$\cdot OH$	hydroxyl radical
O_2	oxygen
$OONO^-$	peroxynitrite
PAGE	polyacryamide gel electrophoresis
PAL	phenylalanine ammonia lyase
Pb	lead
$Pb(NO_3)_2$	lead nitrate
PC	phytochelatin
PCR	polymerase chain reaction
PEG	polyethylene glycol
PMSF	phenylmethylsulfonyl fluoride
POD	peroxidase
PR	pathogenesis-related
PVP	polyvinylpyrrolidone
ppm	parts per million
qPCR	real-time polymerase chain reaction
RNA	ribonucleic acid

RNase	ribonuclease
ROS	reactive oxygen species
RT	reverse-transcription
rpm	revolutions per minute
SDS	sodium dodecyl sulphate
SE	standard error (of the mean)
-SH	thiol functional group containing sulfur and hydrogen
SNAP	S-nitroso-N-acetylpenicillamine
SNP	sodium nitroprusside
SOD	superoxide dismutase
s	second
sp.	species
T_a	annealing temperature
T_m	melting temperature
TAE	tris-acetate-EDTA
TBS	tris-buffered saline
TBST	tris-buffered saline-Tween-20
TEM	transmission electron microscopy
TEMED	tetra-ethyl-methyl-ethylene-diamide
TI	tolerance index
Tris	tris(hydroxymethyl)methylamine
U	enzyme unit
UV	ultraviolet
V	volt
v/v	volume:volume ratio

w/v	weight:volume ratio
WT	wild-type
YCF1	yeast protein from ATP-binding casette transporter family
%	percent
˚C	degree Celcius
<	less than
>	more than
≤	equal or less than
≥	equal or more than
~	approximately
µE/s/m^2	microEin per second per meter square
µg	microgram
µg/dL	microgram per decilitre
µL	microlitre
µM	micromoles per litre
µm	micron

Chapter 1

Introduction and literature review

1.1 Heavy metals

The term *heavy metals* is widely used as a subset for metals and semi-metals (metalloids), and are responsible for contamination leading to toxicity or ecotoxicity. However an IUPAC technical report considered the term to be arbitrary and imprecise (Duffus, 2002). Heavy metals are often categorized by atomic density, which is rarely a biologically significant property (Phipps, 1981; Duffus, 2002). Hence, it is more useful to refer to it as *trace metals*, which are found in low concentrations, typically < 1 ppm (i.e. 1 mg/L), in a specific source, including soil, plant, or ground water (Phipps, 1981). In plants, trace metals are grouped either as essential micronutrients, or non-essential toxic elements according to their effects on plant growth (Hagemeyer, 1999). Chromium (Cr), copper (Cu), iron (Fe), manganese (Mn), molybdenum (Mo) and zinc (Zn) are examples of essential micronutrients. Non-essential elements include cadmium (Cd), cobalt (Co), fluorine (F), mercury (Hg), lead (Pb), selenium (Se), vanadium (V) and tungsten (W) (Pilon-Smits, 2005). The essential micronutrients are toxic to plants when it is at high concentrations in the soils. They are able to inhibit many physiological and biochemical process of most life forms (Saxena *et al.*, 1999). In this thesis, the term *heavy metals* will be used instead of non-essential trace metals, as the former has been a widely recognised usage in toxicological research.

Heavy metals are natural elements that are present in bedrocks. At low background levels, they are not pollutants but their elemental nature means they are persistent and

cannot be removed from the environment by simple microbial degradation. Heavy metal pollution arises when their levels are abnormally high relative to normal background levels (Greger, 1999), and can range from less than 1 mg/kg to 100,000 mg/kg in soil (Yang *et al.*, 2005). Natural contamination originates from excessive weathering (both chemically and physically) of mineral and metal ions from rocks, and by displacing certain contaminants from groundwater or subsurface layers of the soil (Saxena *et al.*, 1999; McIntyre, 2003). Human activity, however, is the key contributor to heavy metal pollution. For example, heavy metals may originate from the following sources: metalliferous mining and smelting; agricultural and horticultural practices, including the application of fertilizers, herbicides and pesticides, and sewage sludges; fossil fuel combustion; metallurgical industries; electronics, chemical and other industrial sources; waste disposal; sports shooting; warefare and military training (Alloway, 1995). Excessive levels of heavy metals in soils lower soil quality, reduce crop yield and the quality of agricultural products (Yang *et al.*, 2005). They are also major hazards to human health and pose a serious threat to the ecosystem.

1.2 Lead (Pb)

1.2.1 Chemical and physical properties

Lead (Pb) is a dense, soft, highly malleable, and non-corrosive metal (Davies, 1995). It is one of the various types of heavy metals, and has an atomic number of 82, molecular weight of 207.2 g/mol and a specific gravity of 11.34. The melting point of Pb is 327.4°C, and the boiling point is 740°C (Agency For Toxic Substances & Disease Registry, 2007b; American Elements, 2009). There are three oxidation states of Pb: Pb(0), the metal; Pb(II); and Pb(IV) (Agency For Toxic Substances & Disease Registry, 2007b). Pb(II) is the form in which it primarily exists in the environment. Pb is bluish-grey in colour and present in the earth's crust at a very low concentration, averaging 16 µg/g soil (Koeppe, 1981). However, it is rarely found naturally as a metal [Pb(0)], but in combination with two or more other elements to form Pb compounds. In natural sources, Pb is released from volcanoes, windblown dust and erosion (Agency For Toxic Substances & Disease Registry, 2007b).

1.2.2 Pb pollution

Anthropogenic sources are the major contributors to Pb pollution. Because of a low melting point and an excellent resistance to corrosion, there has been an extensive use of Pb. Pb can be found in building construction, metal production (solder and pipes), paints, batteries, cable covering, plumbing, ammunition, and devices to shield X-rays (Davies, 1995; Agency For Toxic Substances & Disease Registry, 2007b; American Elements, 2009). Hence, the world's environmental levels of Pb have increased more than 1000-times over the past three centuries (Agency For Toxic Substances & Disease Registry, 2007b).

At uncontaminated sites, Pb is present at less than 20 mg/kg in the soil (Davies, 1995). Since Pb and its compounds are abundant in nature, there is a growing concern on Pb contamination. In Britain, Pb concentration in surface soils exceed 1000 mg/kg at severely contaminated areas (Thornton, 1981). Furthermore, Pb compounds tends to accumulate in soils and sediments due to their low solubility (Davies, 1995). Pb tends to bind to the surfaces of clay minerals and organic colloids, and forms insoluble Pb chelates with organic matter (Thornton, 1981). Pb has been detected in more than 1272 of the 1684 National Priority List sites identified by the Environmental Protection Agency (EPA) (Agency For Toxic Substances & Disease Registry, 2007b). In the USA, Pb levels range from 1 to 6900 mg/kg although the regulatory limit in this country is 600 mg/kg (Salt *et al.*, 1998). In fact, Pb is ranked after Arsenic as the second most hazardous subtance, by the Agency For Toxic Substances & Disease Registry (2007a). The toxicity of Pb on living organisms, its widespread occurence in the environment, its persistence, and its bioaccumulative nature highlight the importance of this study.

1.2.3 Pb in the environment

Elemental Pb does not degrade or breakdown in the environment. Instead, Pb compounds are changed into other forms of Pb by sunlight, air and water (Agency For Toxic Substances & Disease Registry, 2007b). Accumulation over time leads to higher concentrations of Pb in the environment. Historically, leaded gasoline was the primary source of Pb emission to the environment. This Pb is then moved continuously between air, water, and

soil by natural chemical and physical processes. Pb in the form of suspended particles in air are removed from the atmosphere by weather, runoff, precipitation, dry deposition of dust, and river flow before settling to the ground (Agency For Toxic Substances & Disease Registry, 2007b). Once Pb falls onto soil, it will adhere to soil particles, forming relatively stable organic complexes. The movement of these immobile forms of Pb from soil into groundwater depends on the type of Pb compound and soil characteristics, such as temperature, pH, soil texture, particle size, and organic matter content (Hettiarachchi & Pierzynski, 2004; Agency For Toxic Substances & Disease Registry, 2007b).

Pb exists in both water and soil for a very long period of time and has been reported to remain in the environment for 150 to 5000 years (Kumar *et al.*, 1995; Saxena *et al.*, 1999). Huang *et al.* (1997) reported that Pb in soil solution is usually less than 0.1% of total soil Pb, thereby Pb availability is limited. Hence, a low percentage of soil Pb is available to plant roots, and a small amount of that is translocated to shoots (Thornton, 1981). Soil inactivation with chemical amendments has been used to temporarily treat Pb-contaminated sites. These sites are long-term pollution sources to human and animals through accidental ingestion or inhalation (Lasat, 2002). Severe Pb contamination in soils may result in loss of vegetation and groundwater contamination. Subsequently, Pb levels may build up in plants, animals, and human body from areas where air, water or soil are contaminated with Pb, causing Pb toxicity.

1.2.4 Pb and human health

Pb has no known essential or beneficial effects for humans. Instead, Pb poisoning is a serious health concern throughout the world (Davies, 1995). For example, Pb poisoning is found to cause health problems to 800,000 children between age of one to five in USA (Lasat, 2002). Since Pb is not metabolized in the body, it accumulates in the soft tissues. Pb can enter the human body through inhalation (i.e. Pb-contaminated dust or Pb-based paint), where 30 - 50% of these inhaled particles are retained in the respiratory tract before being absorbed into the body. Consumption of contaminated food and water are the main entry routes of Pb into the human body. Drinking water can be contaminated by Pb that is leached from Pb-soldered joints or leaded pipes in water distribution systems or individual houses, whereas food may be contaminated by improperly glazed pottery

or ceramic dishes. Crops grown at heavily industralized areas tend to be exposed to Pb. Plants take up Pb from soils, which eventually enters into the human's food chain (World Health Organisation, 2001).

When ingested or inhaled, Pb is absorbed by the gastrointestinal tract and accumulates in blood, soft tissues, and the mineralizing tissues (bones and teeth). Pb binds to the SH-group of enzymes and displaces other essential metal ions. Hence, metabolism for heme biosynthesis, nervous and kidney function, reproduction and cardiovascular, hepatic, endocrine, and gastrointestinal processes are inhibited. Pb toxicity is more pronounced among children, where 10 μg/dL of blood Pb level can impair their mental development, causing behavioral difficulty and learning problems. In addition, Pb level in blood as low as 10 μg/dL decreases the activities of several heme biosynthesis enzymes and elevates blood pressure level. High Pb levels can affect the central nervous system and cause anaemia in both adults and children. Acute Pb poisoning may lead to convulsions, coma and death (World Health Organisation, 2001).

1.3 Heavy metal remediation technologies

As mentioned earlier, heavy metals are persistent and cannot be degraded from the environment. Therefore, remediation of such pollutants requires physical removal or conversion to a non-toxic form. Selection of appropriate remediation technology to clean-up these inorganic pollutants is dependent on the characteristics of the contaminated land, form and concentration of the contaminants, availability and effectiveness of the remediation technologies, cost and performance of the technologies, and probable end use of the remediated land (Saxena *et al.*, 1999).

1.3.1 Conventional remediation technologies

Conventional remediation technologies are colloquially termed as "pump-and-treat" and "dig-and-dump" techniques (Saxena *et al.*, 1999). They can be divided into *in situ* and *ex situ* remediation. *In situ* technologies treat the contaminants at the site where pollution occurs, whereas *ex situ* technologies relocate contaminants to a separate treatment facility (Iwamoto & Nasu, 2001). The most commonly used technologies for remediation are

summarized by Saxena *et al.* (1999) in Table 1.1.

However, the application of conventional chemical and physical treatment technologies is limited to small contaminated areas and accessibility to the contaminated sites could be an issue. Furthermore, soils may become infertile and unsuitable for agricultural purposes after washing (Saxena *et al.*, 1999).

The most important drawback is the high cost often associated with these technologies. For example, soil removal and burial costs close to $1 million per acre (Salt *et al.*, 1998). *In situ* remediation for volatile or water-soluble pollutants averagely costs US$ 10 - 100 per m^3, landfill or low-temperature thermal treatment costs US$ 60 - 300 per m^3, special landfill arrangement or high temperature thermal treatment costs US$ 200 - 270 per m^3, and extensive management techniques for radionuclides costs US$ 1000 - 3000 per m^3 (Cunningham *et al.*, 1995). In year 1999, cleaning up heavy metal contaminated sites in US alone was estimated to cost US$ 7.1 billion (Saxena *et al.*, 1999). Although the use of *in situ* conventional remediation technologies are generally less expensive than *ex situ* technique, the use of these technologies are still not economically viable.

1.3.2 Bioremediation contaminants, polluted substances

Bioremediation exploits microorganisms to detoxify, degrade, or reduce the concentration of contaminants in polluted soil or water back to its original condition. Bioremediation has been applied to clean up contaminated groundwater, soils, lagoons, sludges, and process-waste streams. A successful case of bioremediation is the treatment of Exxon Valdez oil spill happened at the Alaskan shoreline of Prince Williams Sound in 1989 (Boopathy, 2000). Like conventional remediation technologies, bioremediation can be broadly classified into *in situ* and *ex situ* approaches. Some examples of *in situ* and *ex situ* bioremediation specified by Boopathy (2000) are found in Table 1.2.

In situ bioremediation offers several advantages over the conventional remediation technologies. It allows detoxification of polluted sites without excavating the contaminants. This eliminates transportation cost, is applicable to diluted and widely diffuse contaminants, and minimises site disruption (Iwamoto & Nasu, 2001). A few examples of bioremediation technologies are bioattenuation, biostimulation, and bioaugmentation.

Microorganisms are capable of degrading synthetic, or recalcitrant chemical com-

Remediation technologies	**Process involved**
Soil flushing	Physical separation by vertical or horizontal leaching using a fluid, followed by collection and treatment of the leachates in basins or trench infiltration systems.
Pneumatic fracturing	Injecting pressurized air into the soil to develop cracks in low permeability areas, thereby enhancing the extraction efficiencies of other *in situ* technologies.
Solidification/ stabilization	Physically enclose the contaminant in a stabilized mass or through chemical interactions induced between the stabilizing agent and the contaminant.
Vitrification	Use thermal energy to melt the soil to enable physical or chemical stabilization.
Electrokinetics	Mobilize the contaminants as charged species towards polarized electrodes placed in the soil. The migrated contaminants can be removed or treated *in situ*.
Chemical reduction/ oxidation	Chemically convert the contaminants into less hazardous, more stable, less mobile and/or inert forms.
Soil washing	Separation of contaminants absorbed to fine soil particles using an aqueous solution, through size separation, gravity separation, or attrition scrubbing.
Excavation, retrieval and off-site disposal	Removal and transportation of the contaminated soil to an off-site treatment and disposal facility.

Table 1.1: Conventional remediation technologies (Saxena *et al.*, 1999).

Bioremediation	**Process involve**
Land farming	Contaminated soils are treated in a solid-phase treatment system.
Composting	Contaminated materials are mixed with a bulking agent in an aerobic and thermophilic treatment process, using static or aerated piles.
Bioreactors	Liquids or slurries are biodegraded in a container or reactor.
Bioventing	Contaminated soils are treated by inducing oxygen flow into the soil to enhance microbial activity.
Biofilters	Air emissions are treated using microbial stripping columns.
Bioaugmentations	Contaminated media are treated by the addition of bacterial cultures.
Biostimulation	Soils and groundwater are treated by adding various nutrients to stimulate the population of indigenous microbes.
Intrinsic bioremediation	Contaminants are metabolized by innate microbes where only regular monitoring is done.

Table 1.2: Examples of bioremediation (Boopathy, 2000).

pounds, such as trichloroethylene (e.g. methanotrophs, phenol oxidizers, toluene oxidizers, ammonia oxidizers and propene utilizers), polychlorinated biphenyl, 2,4,6-trinitrotoluene, dioxin-like compounds (e.g. polychlorinated dibenzo-*p*-dioxins and polychlorinated dibenzofurans) and toxic metals (Iwamoto & Nasu, 2001). Introduced microbes, or those already on site, may utilize organic pollutants as a carbon or energy source. Hence, toxic organic substrates are transformed into innocuous end products, such as carbon dioxide and water (Suthersan, 1997). However, application of bioremediation to organic pollutants is more effective than inorganic compounds. Heavy metals such as Cd and Pb are not readily absorbed or captured by microorganisms (Suthersan, 1997). Furthermore, the transformation of moderately toxic elemental Hg(II) and Hg(0) into more hazardous methylmercury (MeHg) by anaerobic bacteria caused human mercury poisoning in Minamata Bay, Japan (Meagher, 2000).

1.3.3 Phytoremediation

1.3.3.1 Definition and classes

With the growing concern of heavy metal pollution and inadequacies of conventional remediaton technologies, an emerging low-cost and ecologically friendly alternative has gained interest from the public. This technology that uses plants to clean-up nature (soil and water) has been termed phytoremediation (from the Greek prefix *phyto* which means plant, and the Latin suffix *remedium* which is to cure or restore) (Cunningham *et al.*, 1997; Saxena *et al.*, 1999). Decontamination of heavy metals is technically difficult, as inorganic contaminants tend to bind to the soil matrix (Section 1.5.1). Since inorganic contaminants cannot be mineralized, they must be physically removed or converted into a biologically inert form (Cunningham & Ow, 1996). Phytoremediation is useful in these circumstances, because plants are able to bioaccumulate these heavy metals in parts which are above ground. Then, plants are harvested for removal of heavy metals, and further concentrated by incineration or recycling for industrial use (Salt *et al.*, 1998).

Phytoremediation is defined by Salt *et al.* (1998) as "the use of green plants to remove pollutants from the environment or to render them harmless". It can be applied to organic and inorganic pollutants present in soil, water and air. Meagher (2000) identifies

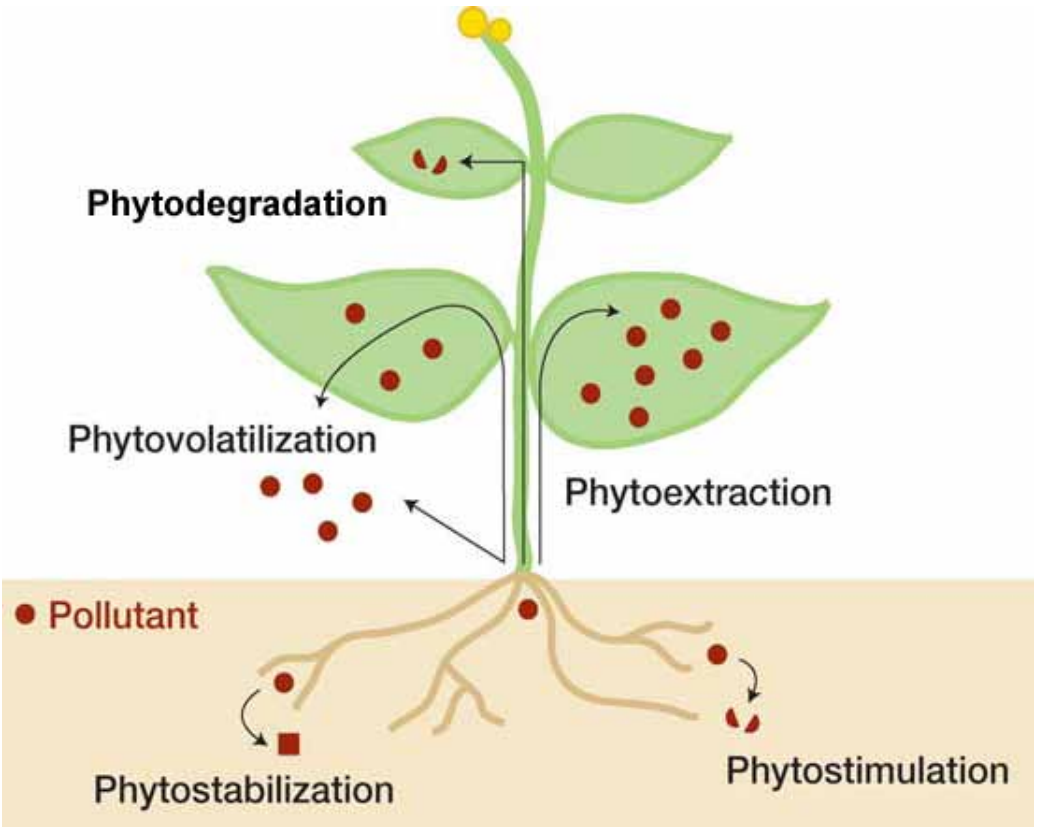

Figure 1.1: Phytoremediation technology (Pilon-Smits, 2005).

five ways to phytoremediate these elemental pollutants: absorption, transport, transport and translocation, hyperaccumulation, and transformation of toxic elements. Salt *et al.* (1998) and Pilon-Smits (2005) classify phytoremediation into five subgroups as shown in Figure 1.1, and they are further explained in Table 1.3. Among these, phytoextraction, rhizofiltration and phytostabilization have the most commercial potential (Saxena *et al.*, 1999).

1.3.3.2 Advantages

Phytoremediation has gained popularity as a publicly acceptable way to remediate heavy metal contaminants in the past 15 years due to its many advantages (Pilon-Smits, 2005). Saxena *et al.* (1999) has outlined its many advantages as follows:

1. *Cost*: Phytoremediation is in general ten-fold cheaper than engineering-based re-

Phytoremediation techniques	**Definition**
Phytoextraction	Plants are used to extract metals and organics from the polluted soil, and accumulate them in their tissues, before harvest the above ground shoots for removal.
Phytodegradation	Plants and associated microorganisms are used to degrade complex organic-metal pollutants via enzymatic activities.
Rhizofiltration/ phytostimulation	Plant roots are used to absorb, precipitate and concentrate metal pollutants from waste water streams.
Phytostabilization	Plant roots are used to stabilize, demobilize and bind to pollutants in the soil matrix, thereby reducing their bioavailability (via precipitation in root rhizosphere). Soil erosion, leaching, and runoff are also prevented by plant roots.
Phytovolatilization	Plants are used to absorb, then volatilize pollutants from soil into the atmosphere.

Table 1.3: Phytoremediation strategies and its definitions compiled from Salt *et al.* (1998) and Pilon-Smits (2005).

mediation approaches, such as pump-and-treat system (Pilon-Smits, 2005). The cost of phytoremediation is US$ 10000 - 30000 per acre (Suresh & Ravishankar, 2004). Growing plants is relatively inexpensive. Furthermore, there are potential economic returns for some plant species used for phytoremediation which offset the technical costs.

2. *Application scale*: Plants can be sown or translocated in large areas.

3. *Environmentally friendly and ecologically safe*: *In situ* application methods reduce the exposure of polluted substrates (Pilon-Smits, 2005). Transportation of contaminants is not necessary, thereby minimizing environmental disruption that might arise from excavation and burial. Plants concentrate and reduce the amount of hazardous waste. Hence, smaller reclamation facilities are required to extract heavy metals.

4. *Broad applications*: Phytoremediation can be easily implemented to a range of pollutants, including toxic metals, organics and radionuclides. Furthermore, plants increase the aeration of the soil so that microorganisms can degrade organic contaminants and assist uptake of heavy metals. Phytostabilization reduces top soil erosion, whereas rhizofiltration maintain a healthy ecosystem by enhancement of rhizospheric micro-fauna and flora.

5. *Aesthetic value*: Plants beautify the landscape of contaminated sites.

1.3.3.3 Limitations

Although phytoremediation has many advantages, it also has a number of limitations, as explained below:

1. *Remediation depth*: Plant roots must be in the contamination zone, so that the plants can reach and absorb the pollutants (Cunningham & Ow, 1996; Suresh & Ravishankar, 2004; Pilon-Smits, 2005). The roots of most heavy metal-accumulating plants distinguished thus far are short, only penetrate into shallow depths, and have a small biomass (Yang *et al.*, 2005).

2. *Plant growth requirement*: Plants require oxygen, water and nutrient to grow. Therefore, soil properties (e.g. texture, pH and salinity) and pollutant concentrations must be within the limits of plant tolerance (Cunningham *et al.*, 1995). The ability of plants to tolerate multiple contaminants might also pose a challenge (Saxena *et al.*, 1999). In addition, naturally occuring hyperaccumulators generally have slow growth rates and low biomass (Salt *et al.*, 1998).

3. *Bioavailability*: Pollutants must be bioavailable for uptake into plant tissues. Hence, phytoremediation might not be applicable to meet safety regulations if only a small amount of the pollutant is readily bioavailable (Pilon-Smits, 2005).

4. *Translocation from roots to shoots*: Certain heavy metals, such as Pb, are poorly translocated from roots to shoots. Less than 30% was translocated in the best Pb translocating plants (Huang *et al.*, 1997). Therefore, harvesting the aerial parts for heavy metal removal is not an efficient approach to remediate soil contamination.

5. *The possibility of leaching*: Highly water soluble contaminants may leach from the plant roots and require containment (Cunningham *et al.*, 1995). Use of chelating agents, such as water soluble Na_2EDTA, to increase bioavailability of Pb in soils could contaminate groundwater (Wu *et al.*, 1999).

6. *Time*: Phytoremediation is a slow process and may take several years to decrease metal contents to an acceptable level compared to conventional remediation methods (Pilon-Smits, 2005). The slow growth and low biomass of plants may require long-term commitment.

7. *Entry into food chain*: Contaminants accumulated in senescing tissues such as leaves may release back into the environment when they drop to the ground. There is also a possibility where animals feed on these leaves, thereby pass the contaminant into the food chain. The volume of polluted biomass must be reduced and disposed in an ecologically sound manner.

1.3.3.4 Phytoremediation in New Zealand

In Australasia, phytoremediation was pioneered by the late Professor R. R. Brooks on heavy metal hyperaccumulating plants (Robinson & Anderson, 2007). The current phytoremediation works focus on biopumps, where plants are employed to reduce the mobility of contaminants and magnify the *in situ* degradation of pesticides. In New Zealand, companies such as HortResearch (www.hortresearch.co.nz) and Soil and Earth Science Group of the Institute of Natural Resources at Massey University (soils-earth.massey.ac.nz) have phytoremediation projects. Phytoremediation is mainly applied to restore lands deteriorated by agricultural and silvicultural production in the country. It has been successfully tested on serpentinite waste-rock piles in Waikato, New Zealand (Robinson & Anderson, 2007). Hence, phytoremediation is a promising technology for research and commercial development in this country.

1.4 Plants for phytoremediation

1.4.1 Characteristics of a plant ideal for phytoremediation

Proper selection of plant species for phytoremediation is the prerequisite for successful application of remediation methods. Ideally, a suitable plant for phytoremediation possesses the following properties: (a) fast-growing, (b) high biomass, (c) hardy, (d) tolerant to pollution, (e) are able to hyperaccumulate metals in the aerial parts, (f) widely distributed and highly branched root system, (g) easy to harvest, (h) easy to grow and have a wide geographic distribution, and (i) repulsive to herbivores to prevent the extracted metals from escaping into the food chain (Karenlampi *et al.*, 2000; Pilon-Smits, 2005; Yang *et al.*, 2005; Kotrba *et al.*, 2009).

Generally, plant selection will be affected by the candidate plant's ability to accumulate metals, its growth rate and planting density (Saxena *et al.*, 1999). For phytoextraction of inorganic contaminants, plants ideal for phytoremediation should have a high capability of metal uptake, translocation, and accumulation within harvestable tissues. For phytodegradation, candidate plants must have a large and dense root systems, as well as contain an abundant amount of degradative enzymes. Meanwhile, plant species that have

a large root surface area for promoting microbial growth and are able to produce specific exudate compounds for microbial activity favor phytostimulation (Pilon-Smits, 2005).

1.4.2 Strategies of plants in responding to heavy metals

Baker & Walker (1990) reported that plants may be divided into three basic types of response to metal-contaminated soils (Figure 1.2).

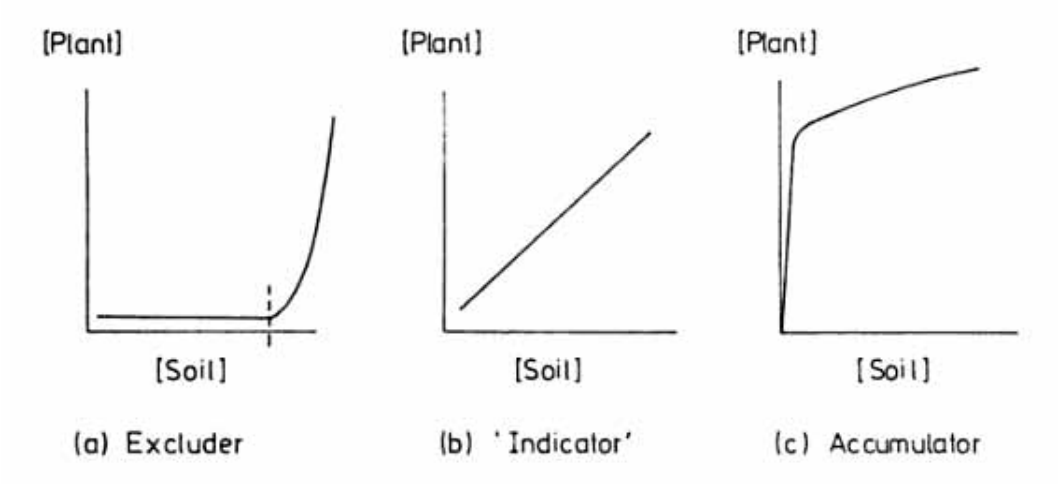

Figure 1.2: Basic strategies of metal uptake by the above-ground parts of plants. [Plant], metal concentration in plant (vertical axis) in relation to [Soil], substrate concentrations in soil (horizontal axis) (Baker & Walker, 1990).

1. *Excluders*: Plants with the ability to avoid or restrict metals from entering their aerial parts. Relatively low metal concentrations are maintained in the shoots, but they can still contain high levels of metals in their roots. Translocation of metals from root to shoot, where leaf:root metal concentration ratio is < 1, is a characteristic of excluders (Baker *et al.*, 2000).

2. *Accumulators*: Plants capable of accumulating high levels of metals in the shoots without causing toxicity to the cells, irrespective of metal concentrations in the soils. The ratio of leaf:root metal concentration of accumulators is > 1. A particular category of these plants are hyperaccumulators, which are able to grow on

metalliferous soils without any symptom of phytotoxicity (Baker *et al.*, 2000; Fischerova *et al.*, 2006). These plant species have the ability to accumulate as much as 100-fold more inorganic elements than other species grown in the same condition (Pilon-Smits, 2005). Hyperaccumulating plants contain more than 0.01% (w/w) of Cd, 0.1% (w/w) of Co, Cu, Pb and Ni, or 1% (w/w) of Mn and Zn on a dry weight basis. About 400 plant species known worldwide are identified as hyperaccumulators, a majority of them accumulating Ni (Baker *et al.*, 2000; Fischerova *et al.*, 2006). These plants have attracted considerable interests because of their potential use in phytoremediation. However, Pb hyperaccumulators are comparatively rare. To date, only 14 taxa have been identified (Baker *et al.*, 2000). *Thlaspi rotundifolium*, for example, can accumulate up to 8200 mg/kg Pb in the shoot, whereas *T. caerulescens* can accumulate up to 2740 mg/kg Pb. However, like other Pb-hyperaccumulating species reported in the literature, these plant species are only useful for studying metal tolerance and accumulation mechanisms, because their slow growth and small biomass may limit their application in phytoremediation (Huang *et al.*, 1997).

3. *Indicators*: Plants in which the metal concentrations in shoot reflect metal concentrations in the soil.

1.4.3 Challenges in selecting plants for Pb phytoremediation

To date, there is no ideal plant species with all the desired phytoremediation properties (see Section 1.4.1). All plants take up heavy metals on a varying degrees depending on genetic factors of the plant species and environmental factors associated with the metals (Baker *et al.*, 2000). Hence, phytotechnologies are based on the appropriate plant properties in selecting suitable plant species for remediation (Pilon-Smits, 2005).

To phytoremediate Pb in the field, a high biomass Pb hyperaccumulator that can tolerate high levels of Pb is most desirable. Because the solubility of Pb in soil solution and plant tissues is low, synthetic chelating agents including EDTA have been used to induce Pb hyperaccumulation. *Zea mays* and *Pisum sativum* accumulated Pb in excess of 1% (w/w) dry weight (Huang & Cunningham, 1996; Huang *et al.*, 1997). This was because

EDTA could maintain Pb in a soluble form. Pb translocation from roots to shoots was significantly increased. Accumulation of Pb in the shoots of *Brassica juncea* up to 1.5% (w/w dry weight) was also observed when the plants were grown in Pb-contaminated soil amended with EDTA (Blaylock *et al.*, 1997). However, high solubility of Pb-EDTA complex caused 37.9% of initial total Pb in soil to leach down the soil profile. Consequently, a phytotoxic effect was observed in *Trifolium pratense* (Greman *et al.*, 2001). This poses potential risks and increased environmental stress.

In order to overcome the challenges in plant selection, Memon & Schroder (2009) suggested four research areas for advancing phytoremediation technologies: (1) metal-accumulating ability of various plant species in relation to heavy metal concentrations in the soil, physico-chemical properties of the soil, and plant growth conditions; (2) identification of metal uptake, transport, and accumulation by looking into the involvement of metal transporters, chelators (e.g. metallothioneins and phytochelatins) and detoxification; (3) physiological, biochemical, and molecular mechanisms of plant-metal interaction; and (4) the importance of natural variation and evolution on metal accumulation in plants.

1.4.4 *Arabidopsis thaliana*: a phytoremediation study

1.4.4.1 The thale cress

Arabidopsis thaliana is a small flowering plant widely used as a model system in plant biological research (Meinke *et al.*, 1998; The Arabidopsis Information Resource, 2009). It is commonly known as thale cress, and belongs to the mustard or crucifer family (Brassicaceae or Cruciferae). *A. thaliana* is a weed that is naturally distributed in Europe, Asia and North America. It is a self-pollinated diploid plant with five pairs of chromosomes (2n = 10). Genetic, biochemical and physiological investigations of *A. thaliana* have been carried out intensely in the laboratory for more than 40 years (The National Science Foundation, 2009). The main advantage of *A. thaliana* is that it has the smallest genome among the higher plants (100 Mbp). Thus, extensive genetic characterization, genomic sequencing, and molecular genetic manipulation (Peer *et al.*, 2003) are desirable features of *A. thaliana*. Examples of research performed using *A. thaliana* as given by

Meinke *et al.* (1998) are: chemical and insertional mutagenesis, crosses and introduction of DNA by plant transformation, extensive collections of mutants with differing phenotypes, and diversification of chromosome maps of mutant genes and molecular markers. The small size of *A. thaliana* plants enables researchers to grow them in a confined laboratory environment. Its fast life cycle, ability to produce a large seed set, and small seed size (Delhaize *et al.*, 1993; Lightner & Caspar, 1998) enable researchers to test hypotheses quickly and efficiently. Therefore, improvements in plants of economic and cultural importance can be rapidly perfected, based on the knowledge gained from the established literature relating to *A. thaliana* (Meinke *et al.*, 1998; The National Science Foundation, 2009).

1.4.4.2 *Arabidopsis thaliana* as a model system for studying Pb tolerance

The scarcity of Pb-hyperaccumulating plants, coupled with a lack of basic physiological and genetic information associated with this trait, suggests a model plant system should be studied. Hence, *A. thaliana* was selected for this project as the experimental plant. Although *A. thaliana* is not a plant of choice for Pb phytoextraction in the field due to its small size, it has characteristics that make it an attractive experimental system for studying Pb tolerance in plants (Chen *et al.*, 1997). Firstly, *Arabidopsis* is a member of the Brassicaceae family, from which 25% of documented metal hyperaccumulators (Peer *et al.*, 2003), such as *T. caerulescens* (Baker *et al.*, 2000) and *Brassica juncea* (Kumar *et al.*, 1995), have been identified. Secondly, its Pb-accumulation patterns are similar to other hyperaccumulators. Hence *A. thaliana* can be used to investigate the mechanisms of uptake, translocation, accumulation, tolerance and detoxification in other species (Chen *et al.*, 1997). Thirdly, *Arabidopsis* has a rich history relating to the physiology and biochemistry of responses to metal toxicity and accumulation in plants. Genes that play a role in metal metabolism have been identified (Cobbett, 2003). Fourthly, *A. thaliana* mutants can be created with the aid of mutagenic agents, such as ethyl methanesulphonate (EMS), which are commercially available for research purposes. These mutant lines can be screened for progeny with desirable traits, and certain mutants in metal tolerance and/or sensitivity have now been isolated and characterized (Section 1.7.2). Altered metal homeostasis in several *Arabidopsis* ecotypes have been identified, and natural variations in this

species may also be a source of genetic information (Chen *et al.*, 1997). Therefore, genetic mechanisms controlling Pb accumulation and tolerance should be elucidated for engineering transgenic plants in the future. In this regard, the role of annexin 1 gene (*AnnAt1*) for Pb phytoremediation (Chapter 5), and putative Pb mutants isolated (Chapter 7) were studied in this thesis.

1.4.4.3 *Arabidopsis thaliana* in other heavy metal-related studies

Since the 1960s, *A. thaliana* has been extensively utilized as a model system to study basic plant processes and responses to various stress conditions, including nutrient deficiency and metal toxicity. Comparison has been made between *A. thaliana* and other species. For example, Bert *et al.* (2000) compared population of *A. halleri* from contaminated and uncontaminated sites to *A. thaliana*, and found that *A. halleri* and not *A. thaliana* is a Zn hyperaccumulator that can grow on Zn, Pb, and Cd contaminated conditions. A leaf slice test demonstrated that the metal tolerance level of *A. thaliana* is low, with a half effective concentration values (EC_{50}) of 2.5 mM for Zn, and 1.9 mM for Cd (Cho *et al.*, 2003). Polec-Pawlak *et al.* (2007) developed a method using size-exclusion chromatography coupled to an isotope specific mass spectrometer (SEC-ESI-MS) to characterize the involvement of cell wall components (e.g. galacturonic acid) in Pb deactivation in *A. thaliana*. These studies allow researchers to understand the degree of phytotoxicity of various heavy metals in plants, as well as to isolate hyperaccumulator plants with potential for phytoremediation. Characterization of the components involved in metal uptake, distribution, and long-distance transport could contribute to the knowledge of plant-metal homeostatic networks (Puig *et al.*, 2007).

To understand the defence mechanism of plants exposed to heavy metals, multiple authors have studied their biochemical-physiological responses, and heavy metal-induced signal transduction pathways in plants. For example, exposure of *A. thaliana* to Cd (Cho & Seo, 2005; Maksymiec & Krupa, 2006; Saffar *et al.*, 2009), Cu (Drazkiewicz *et al.*, 2004; Maksymiec & Krupa, 2006) and Al (Richards *et al.*, 1998) have resulted in H_2O_2 accumulation, leading to oxidative stress, the basic reaction of plants to toxic levels of heavy metal concentration. A general increase of antioxidative enzymes was also observed (Drazkiewicz *et al.*, 2006; Semane *et al.*, 2007). These results provide a framework

of plants' response to toxic levels of heavy metals and detoxification strategy.

A. thaliana has also been screened to isolate mutant plants conferring certain altered elemental characteristics. Man1, a Mn accumulator, has been isolated from F_2 population (Delhaize, 1996). Cad1, a Cd-sensitive mutant, has also been isolated (Howden *et al.*, 1995b). These Cad1 mutants were deficient in inaugurating Cd-peptide complexes, demonstrating the importance of phytochelatins for Cd tolerance in plants. These and similar screens are used to identify novel genes that affect metal accumulation or tolerance. Therefore, *A. thaliana* is particularly useful for elucidating the molecular and genetic basis of heavy metal tolerance in plants.

1.5 Heavy metal uptake by plants

Heavy metal uptake varies considerably, depending on plant species and the types of heavy metals. Chin (2007) summarized three key issues in relation to heavy metal uptake, which will be discussed in this section: 1) bioavailability of heavy metals, 2) root uptake and xylem transport, 3) toxicity and detoxification.

1.5.1 Bioavailability of heavy metals and affecting factors

Heavy metal bioavailability is one of the key factors leading to the success of phytoremediation (Huang *et al.*, 1997; Lasat, 2002). Bioavailability is the metal concentrations that are available for uptake into plants. Different metals have different mobilities in the soils. Hence, total metal concentration in contaminated sites do not necessarily correspond to bioavailability (John & Leventhal, 1995). For example, Zn and Cd occur primarily as a soluble form in the soil and thus are readily bioavailable for plant uptake. On the other hand, Pb tends to remain bound and immobile within the soil matrix. Thus Pb occurs in the form of insoluble precipitates, including phosphates, carbonates and hydroxides, which are mostly unavailable for plant uptake (Lasat, 2002). The release of metals from mineral deposits is strongly influenced by soil physical, chemical, and biological properties (John & Leventhal, 1995; Saxena *et al.*, 1999). These physico-chemical processes subsequently affect heavy metal toxicity in plants (Table 1.4). Therefore, a better understanding of metal bioavailability enables assessment of the potential toxicity of metal

elements and their compounds. This has important implications for phytoremediation.

1.5.1.1 Physical factors

Physical factors are mainly related to the texture, clay and organic matter of the soils as outlined in the following.

1. *Size and texture*: Higher level of heavy metals can be retained in fine-textured (e.g. clay) than coarse-textured soils (e.g. sand).

2. *Organic matter content*: High organic matter content reduces metal bioavailability because heavy metals tend to bind with organic matter (Saxena *et al.*, 1999).

1.5.1.2 Chemical factors

Soil chemistry, including factors described in the following, affect metal bioavailability.

1. *pH*: Low pH (acidic) increases metal bioavailability by releasing metals into the environment through H^+ ion activity (Figure 1.3). Metals have to compete with H^+ ions for negative affinity binding sites on soil particles (John & Leventhal, 1995; Huang & Cunningham, 1996; Greger, 1999; Saxena *et al.*, 1999). Bioavailability of heavy metals in soil can be easily manipulated using soil acidifiers and ammonium-containing fertilizers (Saxena *et al.*, 1999).

2. *Redox potential (Eh)*: Low Eh enhances bioavailability of heavy metals by donating electrons to soil solutions, thus converting insoluble heavy metals to soluble forms (Saxena *et al.*, 1999).

3. *Cation exchange capacity (CEC)*: Metal bioavailability is lower in soil with higher CEC because metal ions have a tendency to remain in the soils (Saxena *et al.*, 1999).

4. *Chelating agents*: Chelating agents increase metal bioavailability by forming soluble metal-chelate complexes that are readily taken up by plants. Metal chelating molecules, known as phytosiderophores, are secreted by the plant roots to chelate and solubilize soil-bound metals. Natural chelators are compounds of low molecular weight, such as sugars, organic acids, amino acids and phenolics. EDTA is a

Parameter	Effect on metal toxicity
Temperature	Increases at higher temperature
Light	Toxicity is light dependent in some cases
pH	Low pH increases toxicity
Redox potential	Negative redox potential decreases toxicity
Monovalent cations (Na and K)	Decrease in toxicity with increasing concentrations
Divalent cations (Ca, Mg, Mn and Fe)	Decrease in toxicity with increasing concentrations
Heavy metals	Synergistic/antagonistic depending on metal combination, concentration and sequence of addition
Anions (Acetate, phosphate, nitrate and sulphate)	Reduce toxicity
Extracellular products (organic acids, polyphenols, polysaccharides, polypeptides)	Reduce toxicity
Sulphur containing amino acids	Reduce toxicity
Sediment fractions (suspended solids and colloids)	Reduce toxicity

Table 1.4: Effect of physico-chemical factors on metal toxicity, adapted from Mallick & Rai (2002).

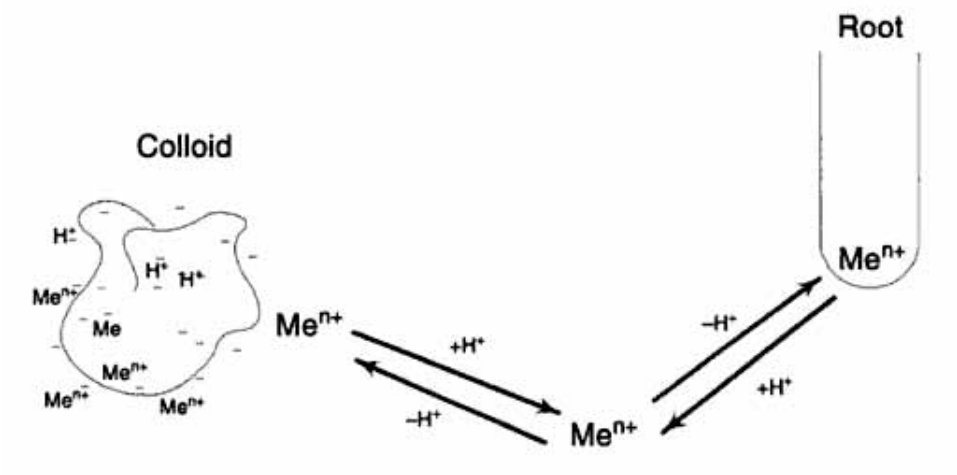

Figure 1.3: Effect of pH on metal uptake in soil (Greger, 1999).

type of synthetic chelating agent that has been added to contaminated soils to increase metal solubility (Saxena *et al.*, 1999). The effectiveness of synthetic chelators decreases from EDTA to HEDTA, DTPA, EGTA, and EDDHA (Huang *et al.*, 1997). By decreasing the size of Pb particles and altering its charge characteristics, synthetic chelates managed to overcome two major limiting factors in Pb phytoremediation: the low bioavailability of Pb in the soils by reducing the sorption of Pb to soil particles, and the low Pb translocation from roots to shoots. Blaylock *et al.* (1997) and Huang *et al.* (1997) have shown that Pb accumulation increased by 1.5% (w/w) of shoot dry weight in maize, and more than 1% (w/w) Pb shoot dry weight in *Zea mays* and *Pisum sativum*, respectively. Chelator-assisted phytoextraction also enhanced the bioavailability of Cd, Cu, Ni and Zn in soil (Blaylock *et al.*, 1997). However, the possibility of metal-leaching is a risk associated with the chelate-assisted phytoextraction approach (Geebelen *et al.*, 2002).

5. Cations: Ca^{2+} for example, competes with Pb for exchange sites on root and soil surface. Hence, the bioavailability in soil can be decreased by liming (Thornton, 1981).

1.5.1.3 Biological factors

Biological factors are mainly related to plant genotype and rhizospheric microbes (Saxena *et al.*, 1999).

1. *Plant genotype*: Different plant species have different metal uptake potential. There is also variation among genotypes of the same species (Greger, 1999). Metals are taken up biologically through membrane transporter proteins (Pilon-Smits, 2005). Dicots were reported to accumulate higher heavy metal concentrations than monocots because they have more negatively charged-metal binding sites (CEC) in their cell wall (Greger, 1999; Saxena *et al.*, 1999). However, Huang *et al.* (1997) reported that Pb accumulation in shoots of *Zea mays* (a monocot) is higher than in *Brassica juncea* (a dicot).

2. *Rhizospheric microbes*: The presence of microbes associated with plant roots can affect plant uptake of inorganics by modifying the pH around roots (Saxena *et al.*, 1999). Microbes also enhanced metal uptake by stimulating plant root growth, producing metabolites that affect gene expression coding for transporter protein in plants, as well as increasing bioavailability of metals in soils (Pilon-Smits, 2005). In addition, root-microbes interaction improves heavy metal bioavailability by secreting proton, organic acids, phytochelatins, amino acids, and enzymes (Yang *et al.*, 2005), as shown in Figure 1.4.

1.5.2 Metal uptake and transport

Roots are the primary site of ion exchange with the external environments, and regulate the influx and efflux of ions to plants. In this case, the plasma membrane controls the entry of heavy metals into the cytoplasm. Hence, the membrane integrity under heavy metal stresses needs to be maintained as it is an important determinant of the plant tolerance to heavy metals. Key steps involved in heavy metal uptake by plants are summarized by Clemens *et al.* (2002) in Figure 1.5.

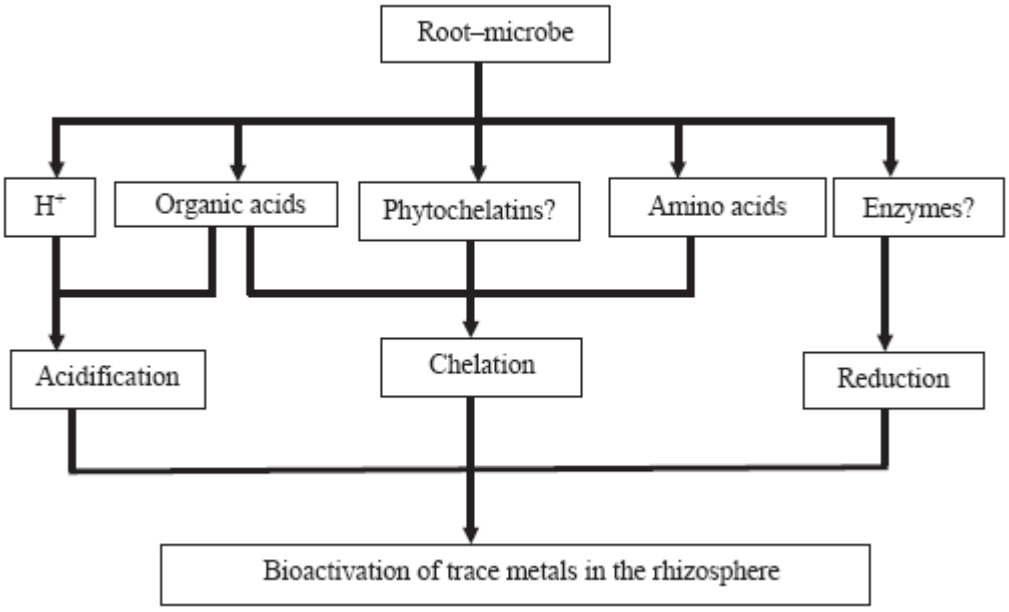

Figure 1.4: Heavy metal bioavailability in the rhizosphere by root-microbe interaction (Yang *et al.*, 2005).

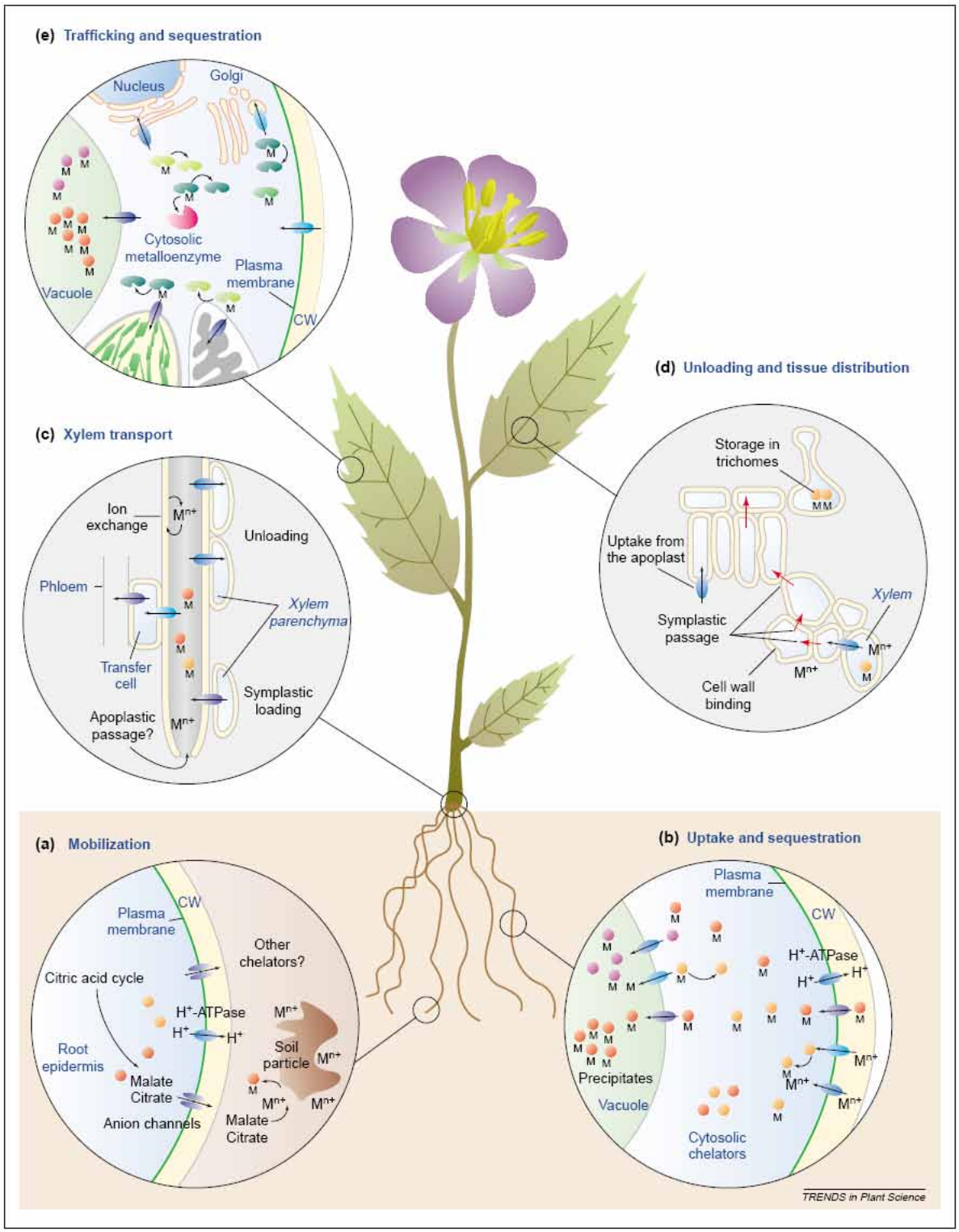

Figure 1.5: Heavy metal uptake in plants (Clemens *et al.*, 2002).

1.5.2.1 Mobilization and uptake from soil

Acidification and release of phytosiderophores from the rhizosphere increased bioavailability of metals (Clemens *et al.*, 2002). Heavy metals that are taken into the plant roots are trapped by the negative charges of the cell wall structure (metal ions are positively charged), or transport apoplastically through the plasma membrane into the cytoplasm (Greger, 1999).

1. *Passive transport*: When the cell wall's metal ion concentration is high, metals diffuse or flow into the cytoplasm in a non-metabolic, passive process (Greger, 1999).

2. *Active transport*: Inorganics exist as ions and cannot pass through membranes, but are taken up into the root cytoplasm with the aid of membrane transporter proteins (Pilon-Smits, 2005), such as channel proteins (e.g. Ca^{2+}-channels) and H^{+}-coupled carrier proteins (e.g. H^{+}-ATPases) (Clemens *et al.*, 2002). More than 150 different cation transporters have been identified in *A. thaliana* (Pilon-Smits & Pilon, 2002). Constitutive expression of a Zn transporter in *T. caerulesens* is one of the mechanisms underlying Zn hyperaccumulation (Pilon-Smits, 2005).

1.5.2.2 Compartmentation and sequestration within the roots

During metal transportation through the plant, about 75 - 90% metals are found in the roots, of which a majority is bound on the cell walls (Greger, 1999). Metal ions in the cytoplasm bind to various negative charged macromolecules, either as soluble forms, or as part of the cellular structure (e.g. cell wall). Soluble metal ion complexes in the cytoplasm are those conjugated with organic acids (e.g. citrate, malate, histidine), thiol-rich polypeptides (e.g. phytochelatins, glutathione), or cysteine-rich metallothioneines. These chelated metals are transported across the tonoplast membrane into the vacuole (Figure 1.6) as part of the detoxification mechanisms so that the pollutants can do least harm to the cell, or exported to the shoot through the xylem (Salt *et al.*, 1998; Greger, 1999; Pilon-Smits, 2005).

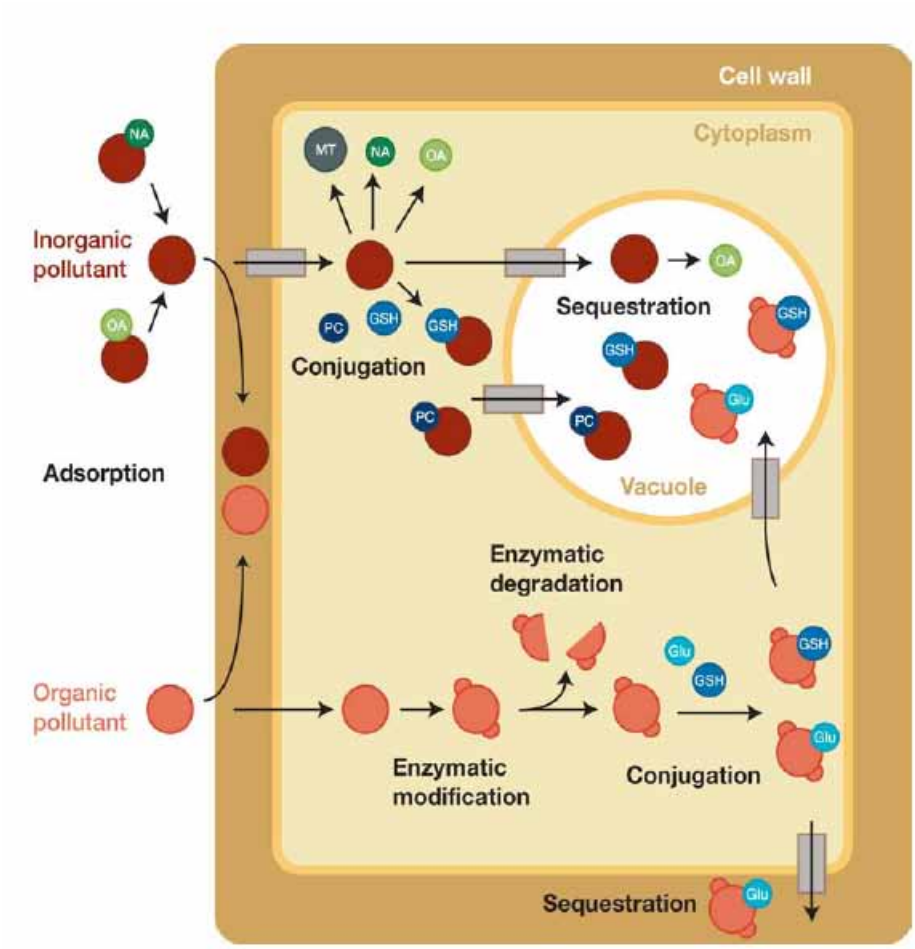

Figure 1.6: Sequestration of inorganic pollutants into vacuole and apoplast (Pilon-Smits, 2005). Metals are chelated by glutathione (GSH), glucose (Glu), metallothioneins (MT), nicotianamine (NA), organic acids (OA), and phytochelatins (PC), and transported via active transporters (boxes with arrows).

1.5.2.3 Xylem loading and transport

Translocation of metal ions from roots to shoots require membrane transport proteins, which are yet to be discovered (Clemens *et al.*, 2002; Pilon-Smits, 2005). This is because metal ions from soil solutions or root apoplast must cross the endodermis and suberised Casparian strips before entering the xylem, which is a difficult process. It is thought that the younger part of the roots facilitate most of the metal uptake process as their Casparian strips are not fully developed (Greger, 1999). Metal movement from the root into the xylem is controlled by three processes: metal sequestration inside the root cells, symplastic transport into the stele, and release into the xylem (Clemens *et al.*, 2002). Some metal ions are chelated during xylem transport to avoid adhesion to the xylem cell wall. For example, Zn is chelated with organic acids, Cu is complexed with amino acids, Cd is transported as a divalent ions, while Ni as a Ni-peptide (Greger, 1999). Transpiration builds a negative pressure in the xylem, allowing water and solutes to transport the metal ions from roots to shoots (Pilon-Smits, 2005). Heavy metal translocation to the shoot is influenced by transpiration rate, root uptake, radial transport and xylem loading (Saxena *et al.*, 1999).

1.5.2.4 Distribution, sequestration and storage in leaf cells

Metal accumulation and distribution patterns vary between species and within genotypes of a species. In general, the distribution of metals decreased from fibrous roots to storage roots, stems and leaves (Greger, 1999). When metal ions in the xylem sap reach the apoplast of the leaves, specific membrane transporter proteins such as ABC-type transporter, metallochaperones, and P-type ATPase pumps are required to import these metals into leaf cells (Clemens *et al.*, 2002; Pilon-Smits, 2005). Inorganics are sequestered in places such as vacuole, cell wall, epidermis and trichomes where they are least harmful to cellular processes. Plants with higher levels of cytosol-vacuole transporter activities have shown to be more efficient in storing toxic inorganics (Pilon-Smits, 2005).

1.5.3 Heavy metal toxicity and detoxification

Excess heavy metal concentrations are toxic to plants. Heavy metals cause three types of unfavorable processes in biological systems by: (1) inactivation of several enzymes by binding with their thioyl-, histidyl- and carboxyl-groups, (2) intensification of reactive oxygen species production processes that lead to oxidative stress, and (3) displacement of essential cations from specific binding sites causing inactivation of antioxidant enzymes and nutrient deficiency (Dietz *et al.*, 1999; Hall, 2002; Sharma & Dietz, 2009). These processes destroy cell structure and metabolism. Heavy metal-tolerant plants are capable of regulating the metal uptake, accumulation and elimination from the cells. These mechanisms are important to protect the cells against the toxic effect of heavy metals and to maintain an optimal level of essential metal elements for proper cellular functioning (Malecka *et al.*, 2008). These mechanisms are described in more details in the following section.

1.6 Mechanisms of heavy metal tolerance in plants

Heavy metal tolerance is the key prerequisite for phytoremediation. Generally, plants adopt two strategies to prevent the accretion of excess metal concentrations in the cytoplasm that leads to toxicity symptoms: avoidance and tolerance mechanisms. Verkleij & Schat (1990) defined avoidance as the ability to hinder excessive metal uptake into plants. On the other hand, tolerance is defined as the ability to cope with excess metals that accumulate within the plants. These complex mechanisms vary, depending on the type of metal, metal concentration, plant species, organs, and developmental stage (Navari-Izzo & Quartacci, 2001).

1.6.1 Avoidance mechanisms

At low metal concentration, plants undergo avoidance mechanisms including metal exclusion, translocation and complexation in the cytoplasm (Navari-Izzo & Quartacci, 2001). Plants maintain a low toxic metal concentration in the cytoplasm by stopping the metals from being transported across the plasma membrane (Tong *et al.*, 2004; Yang *et al.*, 2005).

These plants alter their membrane permeability, change the metal-cell wall binding capability, increase exudation of metal-chelating substances, and stimulate efflux pumping of metal out of the cells (Verkleij & Schat, 1990; Hall, 2002; Yang *et al.*, 2005). The middle lamella acts as the main barrier to prevent Pb penetration into cytoplasm (Malecka *et al.*, 2008).

1.6.1.1 Plant cell wall

One of the most distinct mechanisms of metal tolerance and accumulation is by embedding the potentially toxic metals in the plant cell walls (Memon & Schroder, 2009). Metal ions have an affinity to negative charged polygalacturonic acids in the cell walls, in a decreasing order from Pb to Cr, Cu, Ca and Zn (Ernst *et al.*, 1992). By binding metals to specific sites in the cell walls of epidermis and mesophyl, the amount of free metal ions that entering the cells is reduced. Using a cation exchange technique, Zn was found to alter carbohydrate composition of the cell wall in *Agrostis capillaris* (Ernst *et al.*, 1992). Using electron microscopical techniques, Pb was reported to increase polysaccharides in the cell wall and its thickness in *Allium cepa* (Wierzbicka, 1998). However, such metal-specific tolerance mechanism is still difficult to interpret in detail (Ernst *et al.*, 1992).

1.6.1.2 Plasma membrane

The plasma membrane is the primary site of heavy metal toxicity (e.g. membrane damage) resulting in altered membrane permeability (Verkleij & Schat, 1990; Hall, 2002). The failure of plasma membrane in controlling the entry of heavy metals into the cytoplasm may lead to the disruption of normal cellular and whole plant function (Dietz *et al.*, 1999). Ernst *et al.* (1992) and Hall (2002) pointed out that Cu caused K^+ efflux leakage in *Agrostis capillaris*, *Silene vulgaris*, and *Mimulus guttatus* by oxidation and cross-linking of protein thiols, inhibition of membrane proteins (e.g. H^+-ATPase), or alteration of membrane lipid's composition and fluidity. However, both low and high concentration of Zn protects membrane lipids and proteins against oxidation (Ernst *et al.*, 1992). It is also thought that active efflux mechanisms of plasma membrane prevents metal ions from entering the cytosol. One of the few examples of this exclusion mechanism is Cu (di Toppi & Gabbrielli, 1999; Hall, 2002). Metal-tolerant plants are usually efficient in preventing

the presence of toxic concentrations of free heavy metal cations in the cytoplasm, and thereby avoiding the development of oxidative stress (Dietz *et al.*, 1999). To date, it is unclear whether efflux transporters are generally involved in mediating metal uptake and homeostasis in the plasma membrane (Ernst *et al.*, 1992; Hall, 2002).

1.6.1.3 Exudation of metal-chelating substances

Most metal ions require continuous chelation once they have gained entry into the cell (Clemens, 2001). In the cytoplasm, plants release organic and inorganic substances that are capable of chelating or precipitating metals. The main inorganic compounds in ligand detoxification are phosphates and silicates, while organic compounds are phytochelatins, metallothioneins, organic acids, amino acids, cell wall proteins, cell wall pectins and polyphenols (Chin, 2007). These metal-chelating compounds reduce free metal ion concentration in the cell, thereby reducing their phytotoxicity (Salt *et al.*, 1998). For example, in the wheat roots, oxalic acid chelated Al to form non-toxic Al-oxalate which accumulated in the leaves (Hall, 2002). Plants may precipitate Zn as Zn-phytate for detoxification. Plants may also detoxify Pb by intra- and extracellular precipitation of Pb as Pb-carbonate, -sulphate and -phosphate (Salt *et al.*, 1998). In *Rauwolfia serpentina*, phytochelatin synthesis was induced when 1 mM Pb was added into the medium, in order to sequester Pb ions in plants (Grill *et al.*, 1987).

1.6.1.4 Compartmentalization

Pb may be detoxified from the cells when Pb-containing vesicles fuse with plasma membrane in *Allium cepa* (Wierzbicka, 1998). Metals in the shoot cells are sequestered in the apoplast or in specialized cell types (e.g. epidermal cells, mesophyll cells or trichomes) (Eapen & D'Souza, 2005). For example, Cd, Mn and Pb were found in leaf trichomes (Salt *et al.*, 1998).

At the whole plant level, metal ions tend to be retained in the roots of tolerant plants rather than in shoots (Baker, 1981). There is a hypothesis that plants are able to translocate metals into leaves, which are then removed as a result of natural leaf shedding. Zn, for example, accumulates in leaves especially during the last week prior to leaf shedding, thereby using leaf fall as a means of reducing the level of toxic metals inside the plant

body (Ernst *et al.*, 1992).

1.6.2 Tolerance mechanisms

Various mechanisms have been suggested to account for abiotic stress and tolerance in plants. At high metal concentrations, primary barriers (e.g. plasma membrane) are broken down and lose their function. Inadequate avoidance mechanisms causes the concentration of metal ions increases in the plant body, closely followed by production of free radicals that impose oxidative stress. Plants need to undergo biochemical changes to defend against metal-induced oxidative stress (Navari-Izzo & Quartacci, 2001). Sharma & Dietz (2009) illustrated heavy metal-induced changes in the schematic diagram shown in Figure 1.7. The tolerance mechanisms must be able to limit the activity of potentially harmful metal species in the cytosol (Ernst *et al.*, 1992). Therefore, heavy metal ions that enter the cytoplasm are inactivated by chelation, by convertion into a less toxic form, or by compartmentalization (Hall, 2002; Yang *et al.*, 2005). The degree of heavy metal-generated cell damage relies on: (1) the rate of free radical and reactive oxygen species formation, and (2) the efficiency of detoxification and repair mechanisms (Dietz *et al.*, 1999). With information on the relationship between the effects of heavy metals and oxidative stress, it may be possible to alter the cellular metabolism involved in antioxidative defense.

1.6.2.1 Vacuolar compartmentalization

Excess metal ions must be removed from the cytoplasm. This can be achieved by efflux of ions or compartmentalization into the vacuole (Hall, 2002). Earlier studies on Zn and Cd have shown that the vacuole is the main storage site of these toxic metals. It has often been postulated that this tolerance mechanism may be due to an increased ability to transport metals into the vacuole. For example, overexpression of a Zn transporter (*ZAT*) has been shown to increase Zn tolerance by sequestration of Zn in the vacuole (Hall, 2002). Yeast mutants incapable of accumulating Cd-PC complex (*hmt1*) in the vacuole are Cd-sensitive (Salt *et al.*, 1998).

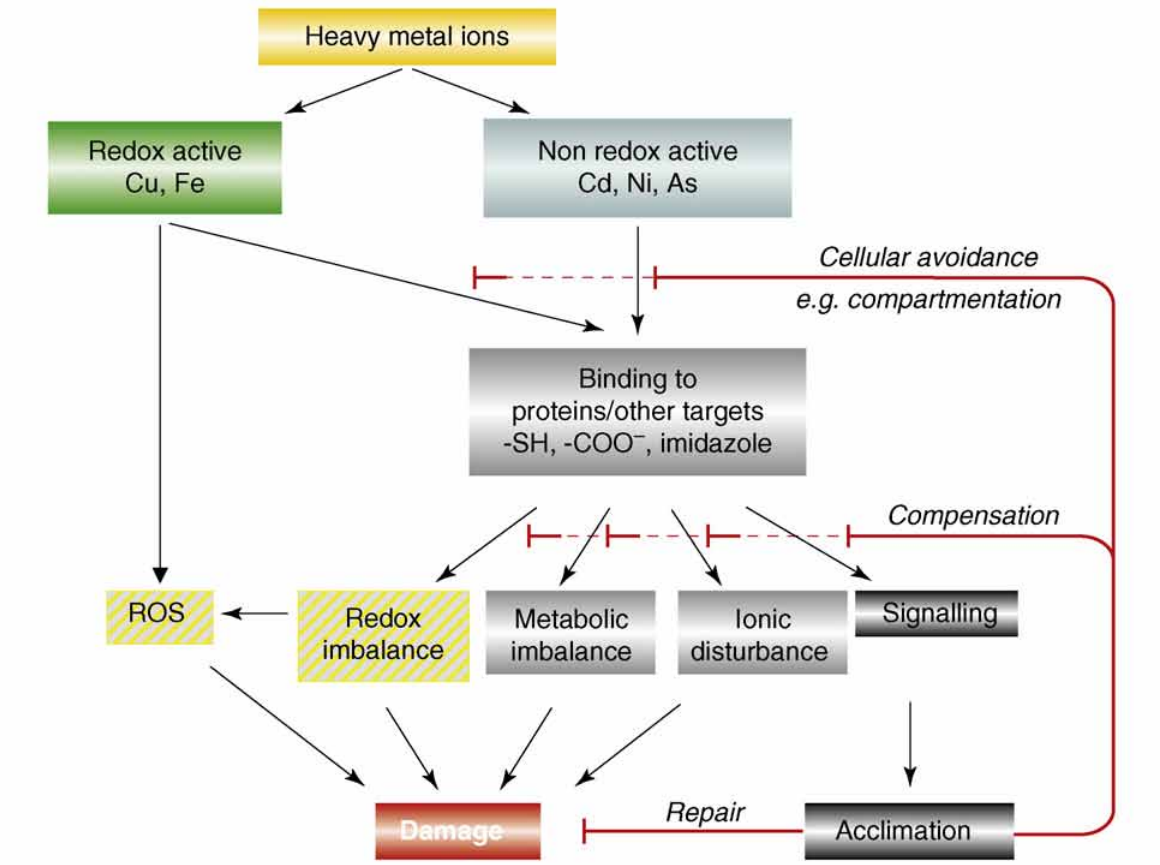

Figure 1.7: Biochemical changes induced by heavy metals (Sharma & Dietz, 2009).

1.6.2.2 Generation of reactive oxygen species in plants

Reactive oxygen species (ROS) is a term used to describe a group of products generated from an electron reduction of molecular oxygen (O_2) (Wojtaszek, 1997; Apel & Hirt, 2004), as shown in Figure 1.8. These molecules are highly reactive due to the presence of an unpaired electron (Dietz *et al.*, 1999). The most common ROS molecules are superoxide radical ($\cdot O_2^-$), hydrogen peroxide (H_2O_2) and hydroxyl radical ($\cdot OH$). In plants, the main sites of ROS formation are chloroplasts, peroxisomes and mitochondria.

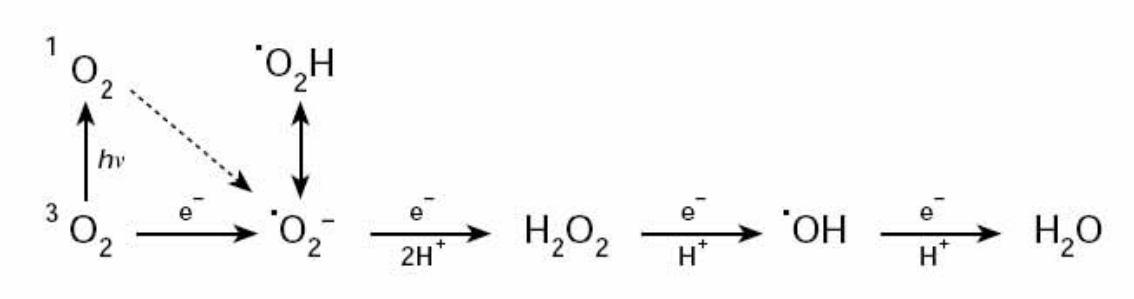

Figure 1.8: ROS production (Wojtaszek, 1997).

Under normal conditions (Figure 1.9a), ROS are by-products of various plant metabolic pathways localized in different cellular compartments. ROS act as protectants, signal molecules and/or enzyme substrates in the biological system (Apel & Hirt, 2004). For example, in the Fenton reaction of photosynthesis and respiratory electron transport chain (in the chloroplast and mitochondria), ROS is involved in the metal ion transition (Fe^{2+}, Cu^{+}). ROS also plays a role as cellular indicators of stress and secondary messengers. This is followed by alteration of gene expression and translation to enzyme chemistry. The lowest levels of ROS inside a cell are maintained by the relevant protective mechanisms and scavenged by different antioxidative defence components. However, the equilibrium between production and scavenging of ROS are perturbed by adverse environmental factors (e.g. heavy metals). The rapid, transient production of huge amounts of ROS overrides these protective mechanisms. Thus, ROS levels rise rapidly and exceed the capacity of cell defense mechanisms, termed as oxidative stress (Bolwell & Wojtaszek, 1997; Wojtaszek, 1997; Blokhina *et al.*, 2003; Apel & Hirt, 2004; Gratao *et al.*, 2005).

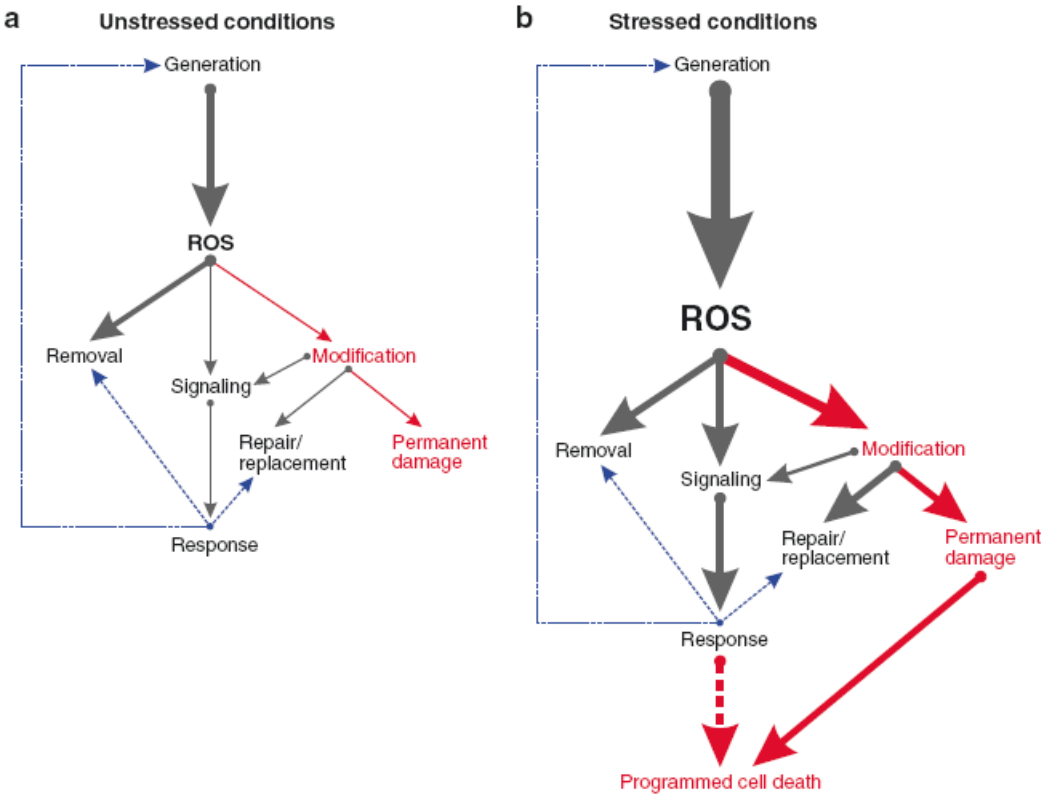

Figure 1.9: The relationship between ROS generation, removal, signalling, repair, and damage in plant cells under (a) unstressed, and (b) stressed conditions (Moller *et al.*, 2007).

1.6.2.3 Oxidative burst in plants and consequences

The level of oxidative stress in a cell is determined by the amount of $\cdot O_2^-$, H_2O_2 and $\cdot OH$ radicals (Gratao *et al.*, 2005). As a result of heavy metal stress, an increased concentration of ROS in plant cells could exert a variety of damaging effects on lipids, proteins, carbohydrates and nucleic acids (Figure 1.10). By binding to thiol groups, Pb decreases the efficiency of oxidation-reduction enzymes in electron transport system (Malecka *et al.*, 2001). By binding to nucleic acids, Pb aggregates and condenses chromatin, stabilizes the DNA double helix, and inhibits DNA replication and transcription. Severe lipid peroxidation, protein denaturation and DNA mutations will eventually cause cell death (Figure 1.9b).

Lipids are very susceptible to the catalysis of peroxidative reactions by Pb (Stohs & Bagchi, 1995), causing electron leakage from the plasma membrane. Excess metal ions alter the amounts, ratio and saturation of membrane lipids. As a result, lipid membranes change its fatty acid composition, which eventually leads to membrane damage by peroxidation of membrane lipid. Increased lipid peroxidation is considered to be an indication of oxidative stress (Devi & Prasad, 1999). Free radicals ($R\cdot$), including hydroxyl ($OH\cdot$) and peroxyl ($ROO\cdot$), initiate lipid peroxidation by abstracting a hydrogen atom from the polyunsaturated fatty acid side chain (-CH) in a membrane. The carbon-centered radical (-C$\cdot$) reacts instantly with oxygen to produce fatty acid side chain peroxyl radical (-$CO_2\cdot$), which attacks adjacent fatty acid side chains. This reaction chain continues (Figure 1.11) and lipid peroxide (-CO_2H) accumulates in the membrane (Ahmad, 1995; Devi & Prasad, 1999; Hogg & Kalyanaraman, 1999).

1.6.2.4 Antioxidative defence in plants

Due to of the speed and extent of ROS-induced cellular damage, plants must be able to mount a rapid and effective scheme of detoxification. A suite of enzymatic and non-enzymatic antioxidative defense mechanisms is available and inducible upon initiation of a ROS burst (Figure 1.12). As explained in the previous section, antioxidative defense systems of the plants provide adequate cellular protection against ROS under normal conditions. However, plants suffer from the toxic effects of increased oxidative stress when the generation of ROS exceeds the cellular defense system. Consequently, plants exhibit

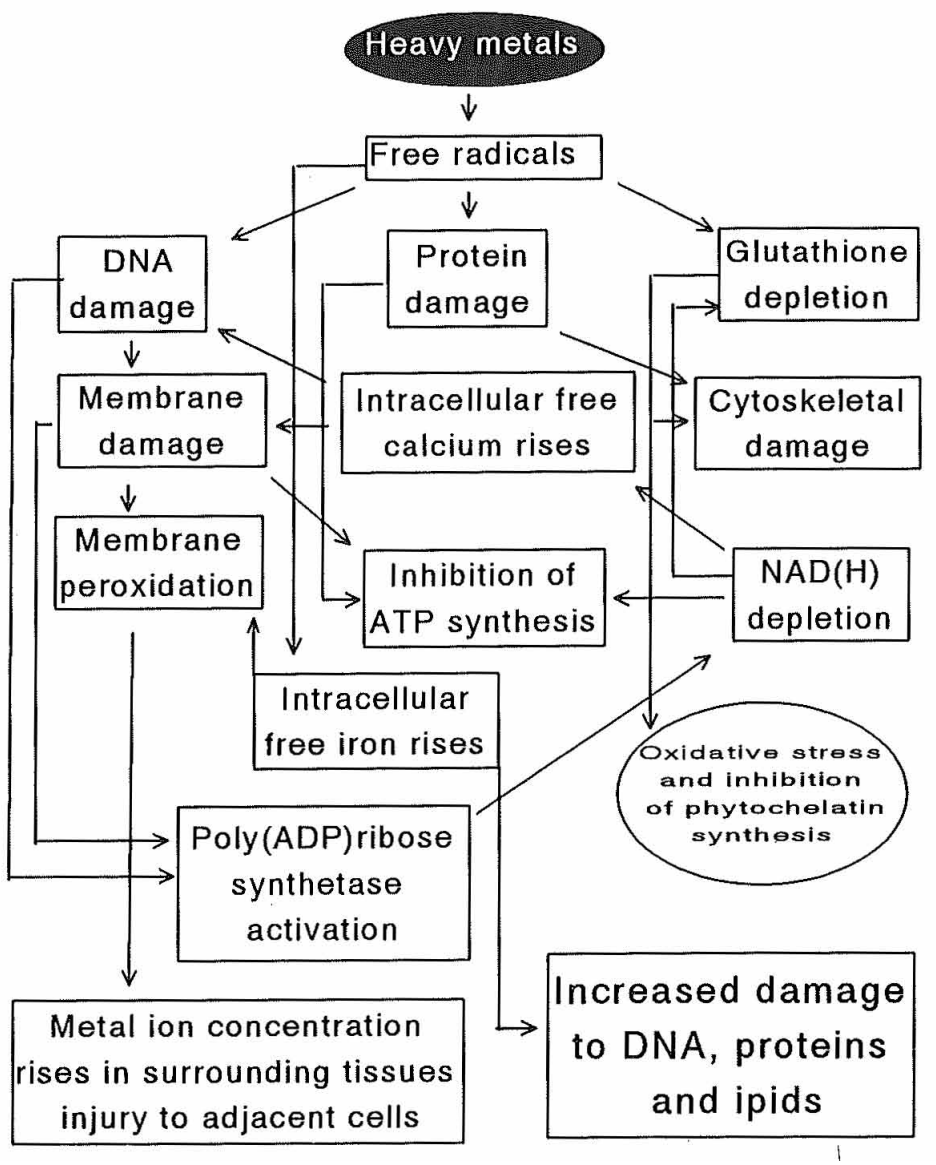

Figure 1.10: Cell components damaged by heavy-metal generated free radicals (Devi & Prasad, 1999).

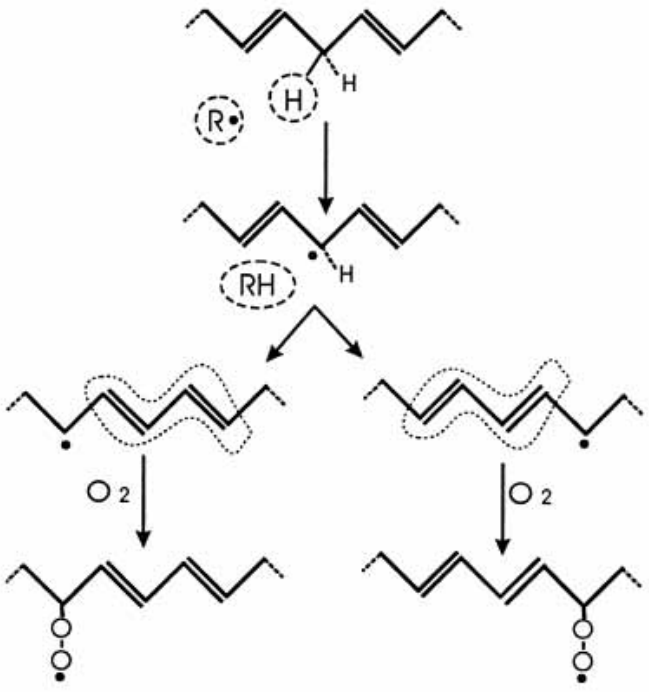

Figure 1.11: Lipid peroxidation (Hogg & Kalyanaraman, 1999).

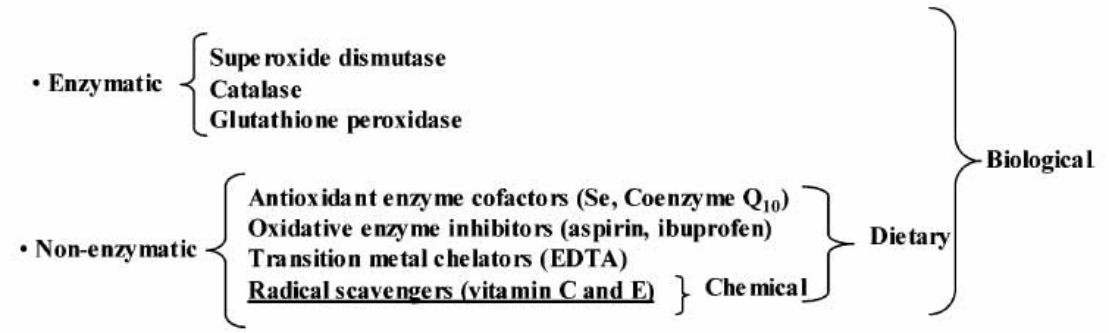

Figure 1.12: Enzymatic and non-enzymatic antioxidantive defence system (Huang *et al.*, 2005).

an increased antioxidative defense to counteract the increament of oxidative stress, by removing excess ROS in order to avoid a build-up of ROS (Table 1.5). An antioxidant is any molecule that has the ability to scavenge ROS without becoming a destructive radical itself (Gratao *et al.*, 2005). Examples of non-enzymatic antioxidants are glutathione (GSH), ascorbate, phenolic compounds, polyamines, carotenoids, α-tocopherols (vitamin E), ascorbic acids (vitamin C), flavonoids, and alkaloids (Dalton, 1995; Dietz *et al.*, 1999; Apel & Hirt, 2004). Examples of enzymes capable to remove, neutralize or scavenge free radicals and oxy-intermediates in the enzymatic antioxidant defence systems that are of interest in this study are:

1. *Superoxide dismutase*: Within a cell, SOD (EC 1.15.11) is the first line of antioxidative defence system which catalyzes the destruction of the superoxide anion ($^{\cdot}O_2^-$) into hydrogen peroxide (H_2O_2) and molecular oxygen (O_2) (Equation 1 in Figure 1.13). SOD is located throughout the cell, and is differentiated by their metal cofactor: a Cu/Zn-isoform in the cytosol and chloroplast, Mn-isoform in the mitochondria and peroxisomes, and Fe-isoform in the chloroplast (Ahmad, 1995; Dalton, 1995; Grene, 2008).

2. *Catalase*: CAT (EC 1.11.1.6) acts sequentially to SOD, converting hydrogen peroxide (H_2O_2) to water (H_2O) and oxygen (O_2). CAT has the simplest reaction (Equation 2 in Figure 1.13), requiring neither a cofactor nor a high affinity for its sub-

Mechanisms	**Substrate**	**Product**	**Cellular localization**
Superoxide dismutase	$^{\cdot}O_2^-$	H_2O_2	Chloroplast, cytoplasm, mitochondria, peroxisomes
Catalase	H_2O_2	H_2O	Mitochondria, peroxisomes
Peroxidases	H_2O_2	H_2O	Many locations
Ascorbate/glutathione cycle	H_2O_2	H_2O	Chloroplast, cytoplasm, mitochondria, peroxisomes
Glutathione peroxidases	H_2O_2	H_2O	Chloroplast, cytoplasm, endoplasmic rediculum, mitochondria
	Lipid hydroperoxides		
	Other hydroperoxides		
Peroxiredoxin system	H_2O_2	H_2O	Chloroplast, cytoplasm, mitochondria, nucleus
	Alkyl hydroperoxides		
	Peroxinitrites		
Thioredoxin system	H_2O_2	H_2O	Chloroplast, cytoplasm, mitochondria
Glutaredoxin system	H_2O_2	H_2O	Chloroplast, cytoplasm, mitochondria, secretary pathway
	Hydroperoxides		
Carotenes and tocopherol	$^1O_2$	O_2	Chloroplast

Table 1.5: Removal of ROS in plants (Moller *et al.*, 2007).

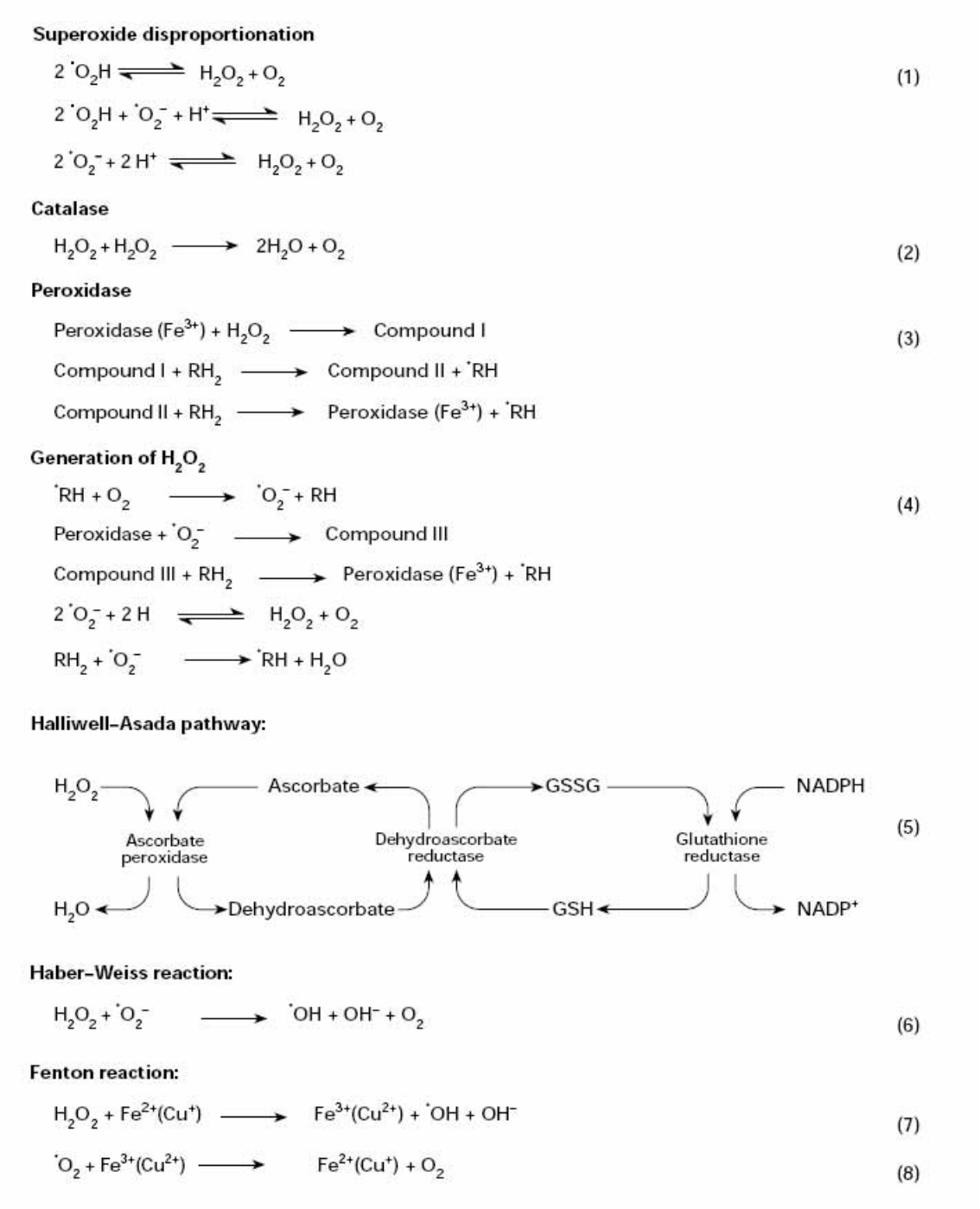

Figure 1.13: Chemical equations depicting major reactions determining the fate and possible interconversions of ROS in plants (Wojtaszek, 1997).

strate. Thus, in a physiological setting, CAT is responsible for removal of excess ROS during stress. CAT is found predominantly in peroxisomes (Ahmad, 1995; Dalton, 1995). The equilibrium of SOD and CAT is essential in determining the steady-state level of $^{\cdot}O_2^-$ and H_2O_2 (Gratao *et al.*, 2005).

3. *Peroxidase*: POD (EC 1.11.1.7) is a heme-containing protein that utilizes H_2O_2 to oxidize organic and inorganic substrates. Recently, a POD known as guaiacol peroxidase utilizes guaiacol as an electron donor and is localized throughout the cells. The other groups of peroxidases scavenge H_2O_2 using cytochrome-c, glutathione, pyridine nucleotide and ascorbate as electron donors (Ahmad, 1995; Verma & Dubey, 2003).

4. *Glutathione reductase*: GR (EC 1.6.4.2) is a flavoprotein that is distributed widely in the cytosol, mitochondria and membrane-bound organelles (e.g. endoplasmic reticulum). It is one of the enzymes in the ascorbate-glutathione cycle (Equation 5 in Figure 1.13), and catalyzes the NADPH-dependent reduction of glutathione disulphide (GSSG) to glutathione (GSH). A high GSH/GSSG ratio is important for maintaining the proper redox conditions in all aerobic organisms (Ahmad, 1995; Dalton, 1995; Verma & Dubey, 2003).

5. *Glutathione peroxidase*: GPX (EC 1.11.1.9) detoxifies H_2O_2 to H_2O, directly using GSH as a reducing agent. The GPX cycle involves the regeneration of GSH from GSSG by GR (Figure 1.14). Cytosolic GPX also catalyzes the oxidation of lipid hydroperoxides and other hydroperoxides (Ahmad, 1995).

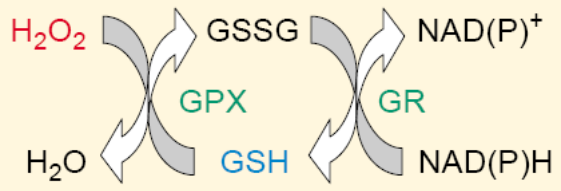

Figure 1.14: The GPX cycle (Mittler, 2002).

In most reported studies, heavy metals can induce oxidative stress, but the regulation of antioxidants is varying (Gratao *et al.*, 2005). The reason for this is partially due to the differences in experimental factors, such as plant species, tissue type, metal type, metal concentration, and the duration of metal exposure.

1.7 Improving phytoremediation with biotechnology

The remediating features of plants are commonly incomplete (see Section 1.4.3). Song *et al.* (2003) suggested two main criteria that must be satisfied for a plant to be considered well-suited for phytoremediation of heavy metals: (1) the plant must be able to translocate heavy metals from root to shoot, and (2) it must compartmentalize heavy metals that have been taken up to prevent them from interferring with cellular metabolism or harming plant cells. A number of strategies has been elaborated to achieve these criteria. Conventional breeding programs have been carried out to combine the desired traits of hyperaccumulator plants, which are often slow-growing, low-biomass, and tightly associated with a specific habitat, with fast-growing, high-biomass varieties (Cunningham & Ow, 1996). However, the anatomical differences between plants, which lead to sexual incompatibility, may hinder the success of this approach (Yang *et al.*, 2005). Biotechnology could overcome this limitation by manipulating desired biochemical and genetic mechanisms that are important to phytoremediation via direct gene transfer. The same objectives can also be achieved by obtaining mutants for heavy metal tolerance via chemical mutagenesis.

1.7.1 Genetic modification approach

Genetic engineering has been employed for the development of transgenic plants that exhibit a desired trait by introducing foreign DNA into the genome of plant cells. With the aim to improve the biochemical and genetic basis of phytoremediation properties in plants, the genetic modification approach has gained significant momentum in the recent years. Scientists have exploited the natural characteristics of hyperaccumulating plants (e.g. root uptake, metal sequestration and translocation) and inserted metal-tolerance genes into non-hyperaccumulators. Plants have also been genetically engineered with

novel traits from microorganisms and mammals (Karenlampi *et al.*, 2000; Kramer & Chardonnens, 2001; Arthur *et al.*, 2005; Eapen & D'Souza, 2005).

For a plant to stand as a probable candidate for phytoremediation and genetic manipulation, it should posses the properties referred to earlier (Section 1.4.1) and be susceptible for genetic transformation (Karenlampi *et al.*, 2000; Kotrba *et al.*, 2009). Some examples of candidate plants are *Brassicae juncea*, *Helianthus annuus*, *Liliodendron tulipifera*, and *Nicotiana glaucum* (Kotrba *et al.*, 2009). Some of the possible targets for genetic manipulation are shown in Figure 1.15.

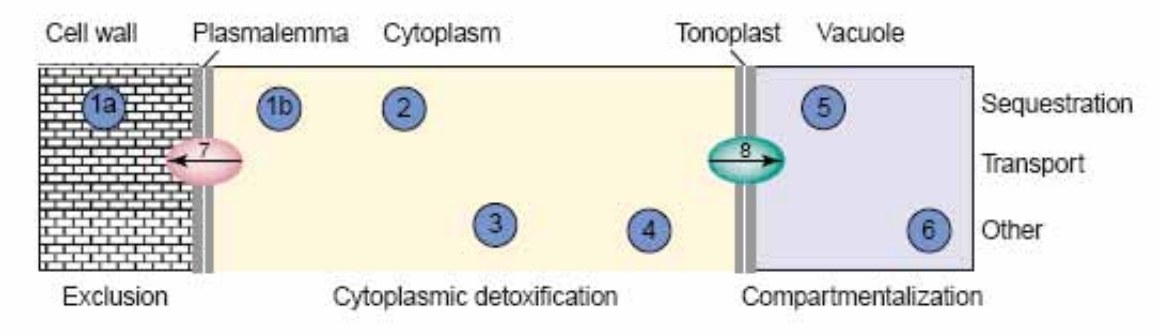

Figure 1.15: Potential targets for genetic modification (Tong *et al.*, 2004). Some of the possible targets are: biosynthesis of (1a) extra-, (1b) intracellular enzymes, and (2) chelating proteins; modification of (3) metal ions oxidation state, (4) metabolic pathways in reducing heavy metal stress, (5) metal complexing process, (6) metal ions solubility enzymes, (7) transporters that pump metal ions from cytoplasm to the apoplastic space, and (8) transporters that pump metal-complexes or free ions into the vacuole (Tong *et al.*, 2004; Eapen & D'Souza, 2005).

1.7.1.1 Transgenic plants

In order to improve a plant's capability to decontaminate environmental pollutions, genes with unique metabolic capabilities (as mentioned previously) were transferred from microorganisms to plants. Most genes used in engineering metal tolerance of plants for phytoremediation originate from microorganisms. One of the most groundbreaking works is the engineering of plants to detoxify highly toxic organomercurial compounds and reduce toxic ionic mercury (Hg^{2+}) into volatile elemental mercury (Hg^{0}) (Arthur *et al.*, 2005;

Eapen & D'Souza, 2005; Kramer, 2005). Two bacterial genes, *merA* and *merB*, which code for organomercurial lyase and mercuric ion reductase respectively, have been transferred to *Arabidopsis*, tobacco and poplar. These transgenic plants can tolerate high level of mercury-contaminants.

Another two examples of successfully engineered phytoremediators are: (1) transgenic Indian mustard that overexpressed the ATP-sulfurylase gene (*APS*) had 4-fold and 3-fold higher APS activity and selenium (Se) accumulation, respectively, than wild-type plants (Eapen & D'Souza, 2005; Yang *et al.*, 2005); and (2) transgenic *Arabidopsis* plants that overexpressed both arsenate reductase (*AsrC*) and γ-glutamyl cysteine synthetase gene (γ-*ECS*) accumulated up to 17-fold greater fresh shoot weight and as much as 3-fold more arsenic (As) accumulation than wild-type plants (Yang *et al.*, 2005). Phytoremediation using transgenic plants is reviewed further by Kramer & Chardonnens (2001), Pilon-Smits & Pilon (2002) and Kotrba *et al.* (2009).

However, genetic engineering for the improvement of Pb-extracting plants is rare, mainly due to the lack of genes conferring Pb tolerance and accumulation. A few exceptions to this are the yeast protein YCF1 from *Saccharomyces cerevisiae* (ATP-binding cassette [ABC] transporter that pumps Cd and Pb into the vacuole), *AtPDR12* (ABC transporter), *AtHMA3* (P_{1B-2} subgroup of the P-type ATPase family that sequesters Pb in vacuole), *ACBP1* (acyl-CoA-binding proteins that accumulates Pb in shoots), and the wheat gene *TaPCS1* (encodes phytochelatin synthase). An increase in tolerance and accumulation of Cd and Pb was found in transgenic *A. thaliana* plants that overexpressed *YCF1* (Song *et al.*, 2003). Deletion of *YCF1* in yeast cells resulted in hypersensitivity to Pb. *AtPDR12*-overexpressing *A. thaliana* plants were more resistant to Pb and accumulated less Pb in the shoots, compared to wild-type plants (Lee *et al.*, 2005). In contrast, *AtPDR12*-knockout plants (*atpdr12*) did not grow well and accumulated more Pb in the shoots, compared to wild-type plants. Overexpression of *AtHMA3* improved *Arabidopsis* tolerance to Pb by 2- to 3-fold (Morel *et al.*, 2009). Transgenic *ACBP1*-overexpressing plants accumulated significantly more Pb in the shoots, where *acbp1*-sensitive line was unable to do so (Xiao *et al.*, 2008). Genetically modified shrub tobacco (*Nicotiana glauca*) overexpressing *TaPCS1* accumulated 36-fold more shoot Pb contents under hydroponic conditions, and as much as 6-fold Pb in mining soils, compared to wild-type plants (Martinez

et al., 2006).

1.7.1.2 Potential risks associated with transgenic plants

Biosafety is an issue of major concern in genetic engineering. Davison (2005) has reviewed potential risks that come with transgenic phytoremediation plants. These include: (1) transgene flow, (2) antibiotic resistance markers in transgenic plants, (3) cross contamination of human and animal foods, and (4) effect of transgenic plants on the rhizosphere ecology. The main risk involves gene flowing from transgenics to wild relatives, which could cause a loss of genetic diversity and plant extinction (Davison, 2005; Kotrba *et al.*, 2009). The genes in plant genome could also be acquired and expressed by microbes via horizontal gene transfer. Hence, a risk-mitigation method is needed to ensure that transgenes (foreign genes inserted into a host organism) will not escape into the environment (Davison, 2005). Introduction of a heterologous gene in plastids could curb transgene flow (Kotrba *et al.*, 2009). This is because maternal inheritance of chloroplast DNA and pollen transmission of plastid DNA are rare. The possibility of gene flow could also be reduced by fusing the desirable gene alongside a second one that demonstrates benefit under agricultural conditions but not functioning in the wild (Davison, 2005; Kotrba *et al.*, 2009). Over the last ten years, researchers who have worked on genetic modification of plants for remediation of heavy metal pollutants have come together to evaluate the suitability of a specific gene to develop useful transgenic phytoremediators (Kotrba *et al.*, 2009). Although genetically modified phytoremediators have many benefits, their economic perspective and environmental safety are still uncertain. Currently, transgenic plants are being field tested to assess the associated risks and benefits (Pilon-Smits, 2005).

In New Zealand, the Environment Risk Management Authority (ERMA) strictly regulates the use, field trials, and release of genetically modified organisms (GMOs). The possible risks and benefits of genetically modified plants for phytoremediation should be contemplated thoroughly. Since the risks associated with transgenic phytoremediation plants are still controversial, the genetic modification approach is not the focus of this study.

1.7.2 Chemical mutagenesis approach

Unlike transgenic plants, a non-GMO approach allows plants to be tested directly under real field conditions for improved metal extraction potential (Nehnevajova *et al.*, 2009). A powerful approach in obtaining plants with enhanced heavy metal tolerance and accumulation is through mutagenesis. Mutagenesis produces mutants with heritable alterations in the genomes, phenotypes and physiological responses, which are critical for determining the biological functions of genes in plants. Various approaches for mutagenesis involving chemical, physical (e.g. x-ray, UV and gamma-ray irradiation), and biological (e.g. introduction of T-DNA and heterologous transposons) methods have been developed (Lightner & Caspar, 1998). Each has advantages and disadvantages for the study of gene function. In this thesis, the focus is on chemical mutagenesis.

1.7.2.1 Ethyl methane sulfonate as a mutagen

Chemical mutagenesis such as using methyl methanesulfonic acid (MMS), nitrosomethylurea (NMU), and diepoxybutane (DEB) as mutagens, has the advantage of producing organisms with high mutation rates. Ethyl methane sulfonate (EMS) mutagenesis in *Arabidopsis* is the most extensively applied technique. This is mainly because EMS is highly mutagenic, causes low mortality, and can be conducted in any laboratory with a fume hood (Lightner & Caspar, 1998; Maple & Moller, 2007).

EMS is an alkylating agent that donates an ethyl group to nucleic acid, leading to base mispairing. An alkylated guanine pairs with a thymine base, and thus produces essentially GC $\rightarrow$ AT transitions, which causes an amino acid change or deletion (Lightner & Caspar, 1998; Maple & Moller, 2007). The advantages of EMS mutagenesis as described by Maple & Moller (2007) are: (1) EMS generates irreversible genome mutations in bulk, allowing mutagenesis process without the need to screen large amounts of individual mutants, and (2) EMS mutagenesis generates mutants that have lost their function, as well as novel phenotypes including dominant or functional proteins due to alterations of specific amino acids.

1.7.2.2 EMS mutagenized *Arabidopsis thaliana*

As described earlier (Section 1.4.4.1), *A. thaliana* is ideal for conducting mutation experiments mainly because of its small size, short life cycle, large seed sets, small seed size, and its natural tendency to self-fertilize. M_1 generation refers to individuals that are treated directly with mutagen, whereas M_2 generation refers to progeny that are derived from self-fertilization of M_1 popoulations thereby producing homozygous recessive mutations. Hence, M_2 generation is mainly used in mutant screening (Lightner & Caspar, 1998).

Over the past 20 years, there have been several thousands of identified *Arabidopsis* mutants defective in various plant growth and development which have been saved as genetic stocks (Meinke *et al.*, 1998). These mutations interfere with basic metabolism (e.g. amino acid, lipid, mineral uptake), cellular and physiological processes (e.g. photosynthesis, light perception and chloroplast differentiation), developmental processes (e.g. root growth, gametogenesis, seed formation, flowering, senescence), metabolic and signal transduction pathways (e.g. response to hormone, pathogens, environmental signals), structural genes, and mechanisms controlling genetic regulation (e.g. transcription factors, DNA binding sites) (Redei, 1992; Meinke *et al.*, 1998). The elucidation of physiological, biochemical, genetic and molecular attributes of *Arabidopsis* mutants has yielded valuable insights into all areas of biological research.

Lehle Seeds (USA) is a commercial supplier of EMS mutagenized *Arabidopsis* seeds. Although purchasing EMS mutated M_2 seeds from a commercial source allows limited control of the initial genotype used and the way seeds are pooled, it is safer for researchers because EMS is highly carcinogenic and volatile.

1.7.2.3 Mutants and phytoremediation studies

Mutagenesis treatment has been used successfully to induce tolerance to various abiotic stresses. Novel genes with a key role to improve metal concentration characteristics have been identified. Based on the phenotypic display in comparison to the wild-type, new mutant variants of *A. thaliana* (Howden & Cobbett, 1992; Howden *et al.*, 1995b,a; Vliet *et al.*, 1995; Delhaize, 1996; Larsen *et al.*, 1996; Chen *et al.*, 1997; Navarro *et al.*, 1999), *B. juncea* (Schulman *et al.*, 1999), barley (Nawrot *et al.*, 2001; Zhu *et al.*, 2003), legumes

(Ellis *et al.*, 2003), peas (Tsyganov *et al.*, 2007), and sunflowers (Nehnevajova *et al.*, 2007), have been isolated (Table 1.6). The subsequent characterization and genetic analysis of these mutants provide a better understanding of the mechanisms that govern heavy metal toxicity, tolerance, accumulation, stress signalling, and antioxidative defence in plants.

In Pb-related studies, Chen *et al.* (1997) initiated a research program to screen EMS-mutagenized *Arabidopsis* M_2 populations to identify mutants with increasing Pb accumulation and tolerance. More than 500,000 seedlings were screened, using root length as an indicator. Three mutants, APb2, APb7 and APb8 were isolated. These mutants were able to accumulate levels of Pb in the shoots more than twice of that in wild-type plants. They also accumulated elevated levels of Mn, Cu, Mg, Zn and S. A possible mutation in the *man1* gene controlling the regulation of metal-ion and uptake or homeostasis has been suggested. Schulman *et al.* (1999) has developed a new screening method by incubating *B. juncea* seedlings in a solution containing radioisotopes of the investigated metals. Subsequent visualization of metal accumulation in the tissue was detected with a phosphorimager. Twenty one Pb-accumulating mutants were isolated from the screening of 50,000 M_2 seedlings. Subsequent characterization of mutant 7/15-1 suggested Pb accumulation was due to the enhanced cell wall binding and precipitation in the roots. The eventual characterization of such genes may provide tools for genetic engineering to enhance Pb phytoremediation.

1.8 Potential genes for phytoremediation: annexins

Significant progresses have been made in the past fifty years in resolving the physiological and biochemical mechanisms of heavy metal toxicity. However, current understanding of the fundamental of these molecular mechanisms is still scanty. It is vital to find the genes that participate in the metal homeostasis network, particularly in heavy metal tolerance and uptake. Identification of the genes or proteins involved in heavy metal stress responses is necessary to understand their molecular mechanisms. This knowledge should help the development of novel plants for phytoremediation usage (Aarts & Fiers, 2003; Yang *et al.*, 2005; Ahsan *et al.*, 2009). As a starting point, hyperaccumulators are potentially good

ID	Feature	Plant	Mutant phenotype in comparison to wild-type plants	Reference
man1	Manganese accumulator	*Arabidopsis thaliana*	Accumulated 7.5 times Mn, 4.6 times Cu, 2.8 times Zn, 1.8 times Mg, 2.7-fold S higher in leaves, and 10-fold more Fe in roots, when grown in soil.	(Delhaize, 1996)
als	Aluminium sensitive	*A. thaliana*	Root growth was inhibited in the presence subtoxic level of $AlCl_3$ (0.75 mM). Root growth was inhibited by 36% in Col-0 and Ws-0, while 64% in La-0 when grown in gel with 1.0 mM $AlCl_3$.	(Larsen *et al.*, 1996)
cdht1, *cdht4*	Cadmium hypertolerant	*A. thaliana*	Root growth was longer than 2 mm upon exposure to 200 µM $CdCl_2$, and accumulated 56% less total Cd.	(Navarro *et al.*, 1999)
cad1	Cadmium sensitive, phytochelatin synthase deficient	*A. thaliana*	Leaves growth was inhibited by 2- to 3-fold over a period of 3 d in 6 µM $CdSO_4$, Cd accumulation remain the same over that periods. Further experiment with *cad1-1* on 0.8% nutrient agar containing 3 µM $CdSO_4$ showed the gradual chlorotic leaves and discrete brown pigment in roots. Also sensitive to Hg.	(Howden & Cobbett, 1992; Howden *et al.*, 1995a,b)
cup1	Copper sensitive	*A. thaliana*	Growth was inhibited on medium containing 5 µM $CuSO_4$, most sensitive to Cu, slightly sensitive to Cd, and less sensitive to Hg. The leaves accumulated 2- to 3-fold more Cu in the presence of 5 or 20 µM $CuSO_4$, and 2- to 4- fold more Cd in the presence of 3 µM $CdSO_4$.	(Vliet *et al.*, 1995)
cup2	Copper sensitive	*A. thaliana*	Poorly grown on medium containing 50 µM $CuSO_4$; look stunted with short roots and fewer initiated roots when grown on higher $CuSO_4$ concentrations.	(Larkin *et al.*, 1999)
APb2, APb7, APb8	Pb accumulator	*A. thaliana*	Longer root growth, lower shoot dry weight, and 3-fold higher Pb concentrations in shoots when grown in hydroponic culture with 4.1 mg/L Pb. Also accumulated higher Mn, Cu, Mg, Zn and S levels in the same medium.	(Chen *et al.*, 1997)

Table 1.6: Isolation of mutants for phytoremediation.

ID	Feature	Plant	Mutant phenotype in comparison to wild-type plants	Reference
7/15	Pb accumulator	*Brassica juncea*	Roots accumulated 3.6 times higher Pb, stunted root growth (shorter and thicker), decreased root cell size (cells failed to elongate), stunted and thickend hypocotyl, 37% more cell-wall material on in roots.	(Schulman *et al.*, 1999)
RL819/2, RL820/6	Aluminium tolerance	*Hordeum vulgare*	Longer roots, and higher root tolerance index. Roots exhibited no hematoxylin stainability at the 0.03 mM Al^{3+}, no or partial stainability at 0.06 mM Al^{3+}, and partial stainability at 0.09 mM Al^{3+}.	(Nawrot *et al.*, 2001)
M_3, M_{10}, M_{25}	Aluminium tolerance	*H. vulgare*	Relative cell growth was > 26% higher in modified MS treated with 30 µM Al, Al accumulation was significantly lower.	(Zhu *et al.*, 2003)
raz	Require additional Zn	*Medicago truncatula*	Leaf necrosis was evident. Higher concentrations of Zn, Mn and Cu were found in most tissues, while higher Fe was observed in roots. Reduction of general growth, and leaf loss was 48% higher in medium containing low nutrients: 3 µM Zn and 0.2 µM Mn. Leaf necrosis was reduced when plants contained high level of Zn.	(Ellis *et al.*, 2003)
$SGECd^t$	Cd tolerance and accumulation	*Pisum sativum*	Grew normally without exhibiting any stress symptoms in the presence of 3 µM $CdCl_2$, accumulated 3- and 3.5-fold more Cd in roots and shoots, respectively. Higher Mg and Ca contents in roots, and Mg, Ca, Zn, Mn and B in shoots.	(Tsyganov *et al.*, 2007)
M_2 14/185/04	Giant mutant	*Helianthus annuus* L.	Increased metal concentrations of Cd, Zn, and Pb by 1.8-, 2.7-, and 3.0-fold, respectively. Significantly enhanced metal extraction ability in the above ground parts: 7.5-fold for Cd, 9.2-fold for Zn, and 8.2-fold for Pb.	(Nehnevajova *et al.*, 2007)

Table 1.6: Isolation of mutants for phytoremediation (continued from the previous page).

source of genes suitable for phytoremediation (Clemens *et al.*, 2002; Eapen & D'Souza, 2005).

Numerous studies have shown that plant stress responses vary from species to species and from stressor to stressor. There are common stress-related genes reacting to different abiotic stresses, including ROS detoxification and stress-specific response genes (Aarts & Fiers, 2003). To date, heat shock protein (*hsp*) genes are the most extensively characterized stress response genes, particularly in *Drosophila*, *Saccharomyces cerevisiae* and *Escherichia coli* (Grover *et al.*, 2001). Induction of *hsp* genes was reported in response to cold, drought, salinity and anaerobic stress. Heat shock protein (HSP) chaperone function that is essential to protect cells from stress, as well as maintain normal cellular functions (Rhee *et al.*, 2000; Grover *et al.*, 2001; Hall, 2002). They are ubiquitous, encoded by nuclear genes, and localized in cytoplasm, mitochondria, chloroplast and endoplasmic reticulum (Grover *et al.*, 2001). On the other hand, several studies have suggested the involvement of Ca^{2+} in various intracellular signaling processes, and modulating many metabolic and developmental activities in plants (Sanders *et al.*, 1999). Upon stimulation by abiotic stress, Ca^{2+} is released from intracellular storage (e.g. endoplasmic reticulum, mitochondrion, chloroplast and vacuole), enters the cells via Ca^{2+} channels, and thus increasing its concentration in the cytosol (Figure 1.16).

Annexin, a Ca^{2+}-dependent phospholipid binding protein, is structurally related to HSP. It can function as a chaperone, and has several other functions and biochemical properties similar to HSP (Rhee *et al.*, 2000; White *et al.*, 2002). It has become known as an important target for manipulating Ca^{2+} level in plant cells (Clark *et al.*, 2005). Coupled with the studies by Gidrol *et al.* (1996), Kovacs *et al.* (1998), Rhee *et al.* (2000), Kush & Sabapathy (2001), Lee *et al.* (2004), Gorecka *et al.* (2005), Cantero *et al.* (2006), Gorecka *et al.* (2007) and Chandran *et al.* (2008), it would seem that annexins may participate in the response of plants to heavy metal stress. Therefore, the possible participation and role that annexins play in protecting plant cells from Pb-mediated stress has become a focus in this study.

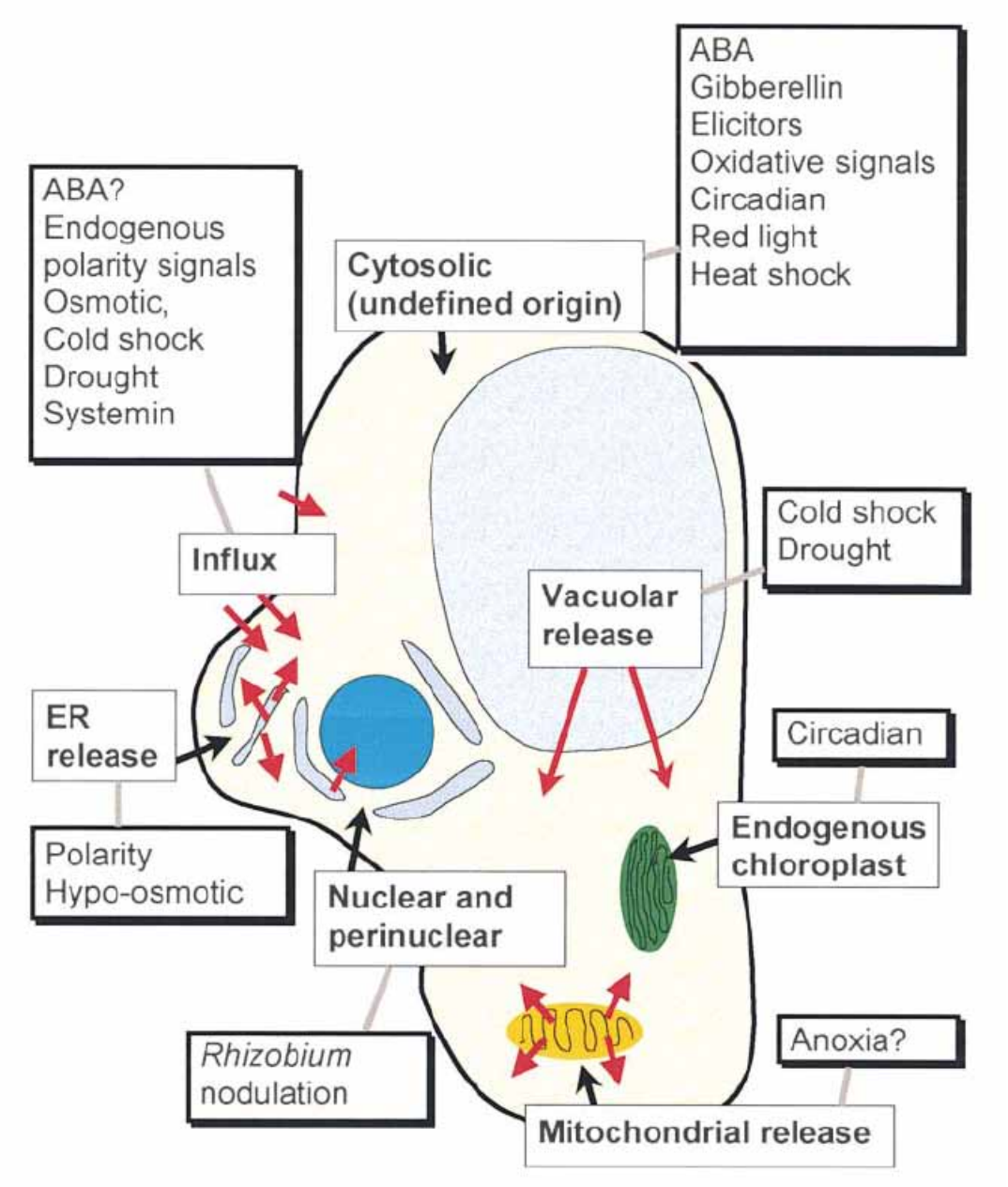

Figure 1.16: Schematic diagram depicting the origins and locations of calcium signals from the external medium, ER, mitochondrion, chloroplast, vacuole, cytosolic, nuclear and perinuclear in response to specific stimuli (Sanders *et al.*, 1999). Red arrows indicate the principal Ca^{2+} fluxes.

1.8.1 Discovery of annexins in plants

Ca^{2+} is known to modulate many metabolic and developmental activities in higher plants. This has led researchers to examine the existence of annexins, which are a diverse, multigene family of Ca^{2+}-regulated phospholipid-binding and membrane-binding proteins in higher plants (Smallwood *et al.*, 1990, 1992; Clark & Roux, 1995; Delmer & Potikha, 1997; Gerke & Moss, 2002). An annexin-like protein in higher plants was first discovered by Boustead *et al.* (1989). This research was conducted by a plant science team and an animal annexin research group at University of Leeds (Delmer & Potikha, 1997). The authors found two Ca^{2+}-dependent phospholipid-binding proteins of molecular weight 34 and 35 kDa in tomato that can cross react with antibodies against 2 different human annexins. Purification and partial sequence analysis showed substantial sequence homology between tomato annexins and animal annexins (Smallwood *et al.*, 1990). Since then, research on plant annexins has yielded information about the importance of annexins in plant growth and development. Annexin-like proteins have been isolated, for example, from pea, cotton, celery, pepper and ferns (Delmer & Potikha, 1997). These soluble or membrane-bound, hydrophilic proteins contribute up to 0.1% of the total extractable protein in plant cells (Clark & Roux, 1995; Delmer & Potikha, 1997). A majority of annexin genes are expressed in the whole plant and it is a typical membrane channel protein (White *et al.*, 2002).

The origin of the name annexin comes from Greek *annex*, which mean "bring/ hold together", reflecting the principal property of most annexins (Gerke & Moss, 2002). Annexins bind and hold certain biological structures such as membrane constituents together. In the late 1970s and early 1980s, annexins were named according to their biochemical properties, including synexin, chromobindins, calcimedins, lipocortins and calpactins (Gerke & Moss, 2002).

1.8.2 Annexins in *Arabidopsis thaliana*

A. thaliana, which has eight annexin genes (*AnnAt1* - *AnnAt8*), is used in this research. These eight annexin genes share from 30% to 81% deduced amino acid sequence identity (Clark *et al.*, 2005). They encode proteins of molecular mass 36.0 - 36.6 kDa (Clark *et al.*,

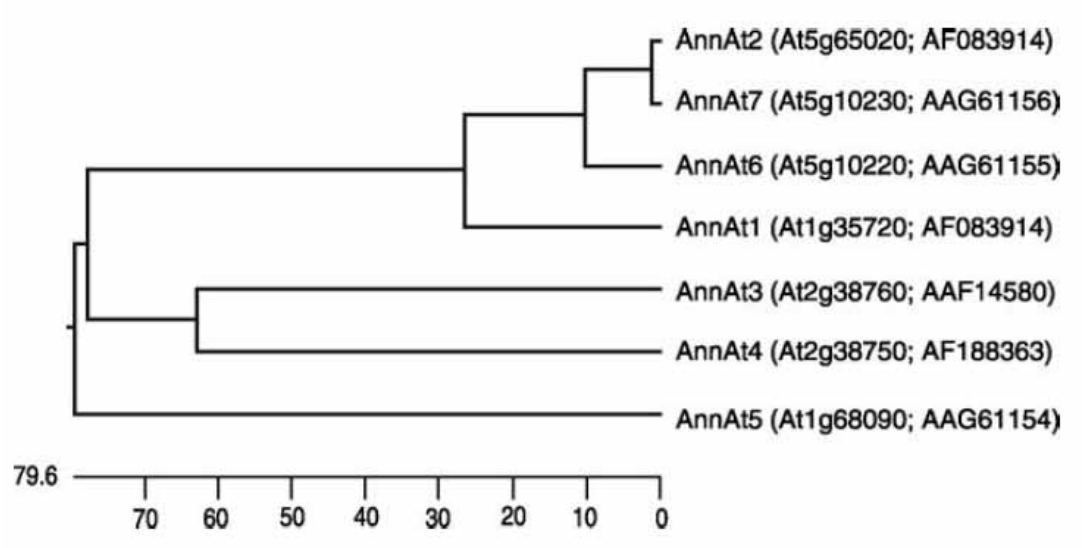

Figure 1.17: Dendogram showing sequence relationships among the seven annexin proteins identified in *Arabidopsis thaliana* (White *et al.*, 2002).

2001). *AnnAt1* is the main annexin in *Arabidopsis*. Although all *Arabidopsis* annexins are found to be expressed in roots, only *AnnAt1* and *AnnAt2* have been studied in detail. *AnnAt1* was first found to be involved in stress signalling by Gidrol *et al.* (1996) (see Section 1.8.4.2). White *et al.* (2002) shows the sequence relationships among the seven *Arabidopsis* annexin proteins (Figure 1.17).

1.8.3 Structure and functions

Annexins possess the characteristic four repeats of 70 - 75 amino acids and the sequence GXGTD motif within the endonexin fold for Ca^{2+} binding (White *et al.*, 2002; Mortimer *et al.*, 2008), as shown in Figure 1.18. This conserved C-terminal domain, also known as the "annexin core", is α-helical and forms a compact disk with a slightly curved planar structure (Figure 1.19) and a central pore lined with conserved hydrophilic residues (Gerke & Moss, 2002; White *et al.*, 2002; Rescher & Gerke, 2004; Mortimer *et al.*, 2008). It is likely for these conserved regions within the encoded proteins to play a role in Ca^{2+} binding and ion channel formation (White *et al.*, 2002). The first and fouth repeated domains in plants are known to have the endonexin sequence (Mortimer *et al.*, 2008).

The N-terminal region precedes the core domain and is variable in length, amino acid sequence and diversity, and in the sites of secondary modifications like phosphorylation, glycosylation, or acetylation (Liemann & Lewit-Bentley, 1995). In plants, it is only about 10 amino acids long (Mortimer *et al.*, 2008). This variation accounts for the functional differences in annexins (Clark & Roux, 1995). The N-terminal region mediates regulatory interactions with protein ligands and regulates the annexin-membrane association, as it contains binding motifs for protein partners, sites for post-translational modifications and alternative splicing (Gerke & Moss, 2002; Rescher & Gerke, 2004).

Annexins function in many essential cellular processes, such as membrane trafficking, transmembrane channel activity, mitogenic signal transduction, cell-matrix interactions in animal tissues, phospholipids metabolism and DNA replication (Clark & Roux, 1995; Proust *et al.*, 1996). In plants, annexins appear to be involved in secretion, callose synthase activities, as substrate for protein phosphorylation, Ca^{2+} channels activities, interaction with actin, nucleotide phosphodiesterase acitivity and peroxidase activity (Proust *et al.*, 1996; Gerke & Moss, 2002; Mortimer *et al.*, 2008). Ca^{2+} regulatory mechanisms, in plants share many similarities with animals (Delmer & Potikha, 1997).

Gidrol *et al.* (1996) discovered the shared sequence homology between N-terminal region of *Arabidopsis* and a heme-binding region of many plant peroxidases (Figure 1.20). Peroxidases are enzymes that bind H_2O_2 via the heme group and catalyze its break-down and detoxification (see Section 1.6.2.4).

1.8.4 Major experimental approaches

Identification of plant annexins has been performed through amino acid sequence, antibody cross-reactivity and functional similarities (Kovacs *et al.*, 1998). In earlier studies, annexin was identified by probing with the appropriate DNA sequences. However, this was not gene-specific. Therefore, monoclonal or polyclonal antibodies and gene-specific probes capable of recognizing specific annexin proteins and genes (Delmer & Potikha, 1997) has been used in the recent years. Many of the previous studies used a polyclonal antibody that had been produced against the annexins for screening of an expression library prepared from mRNA of a respective plant. The polyclonal antibody was used to recognize the protein and hence, indicate annexin expression in all major tissues of plant

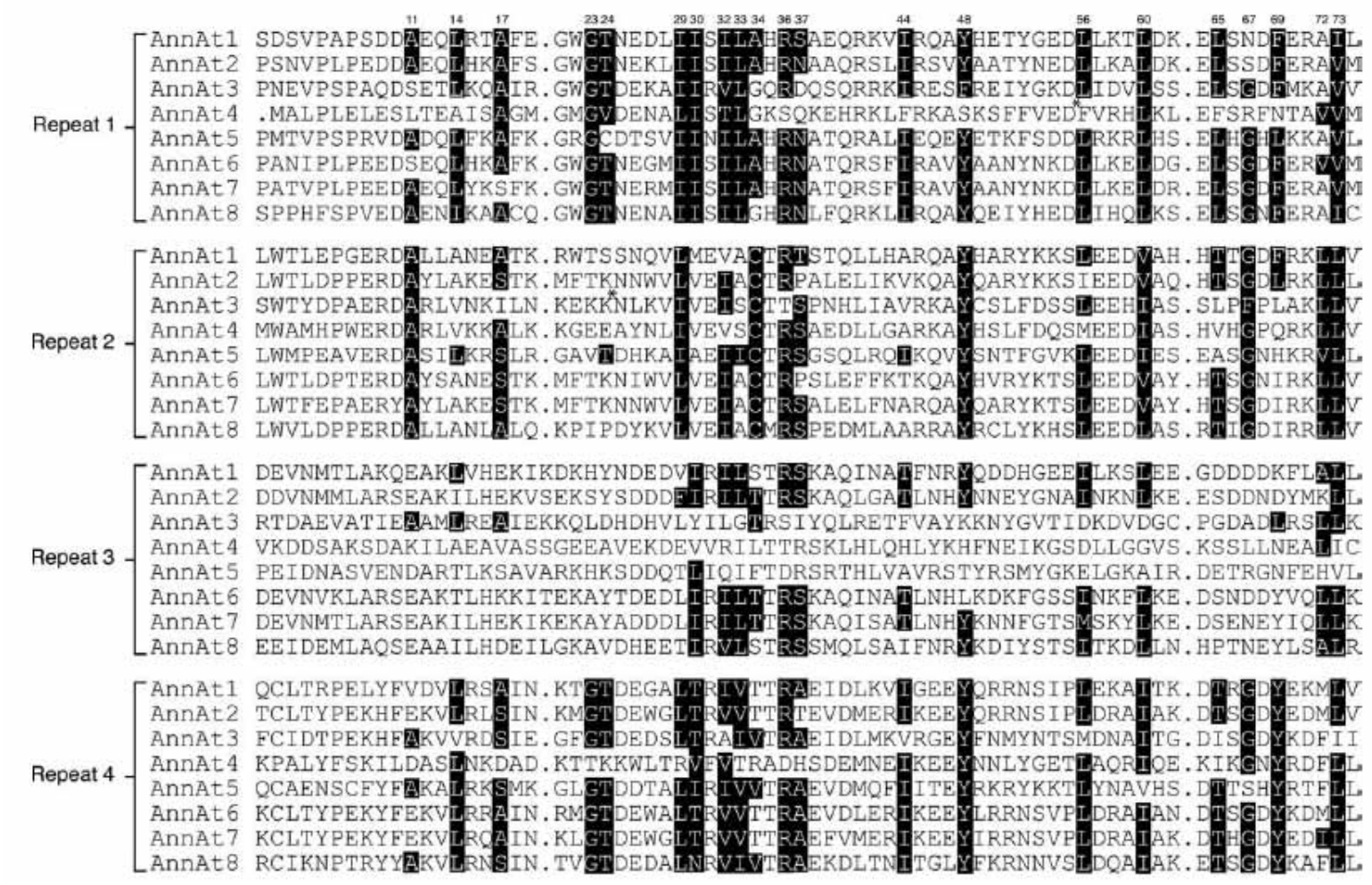

Figure 1.18: Sequence alignment of *Arabidopsis* annexin repeats (Cantero *et al.*, 2006).

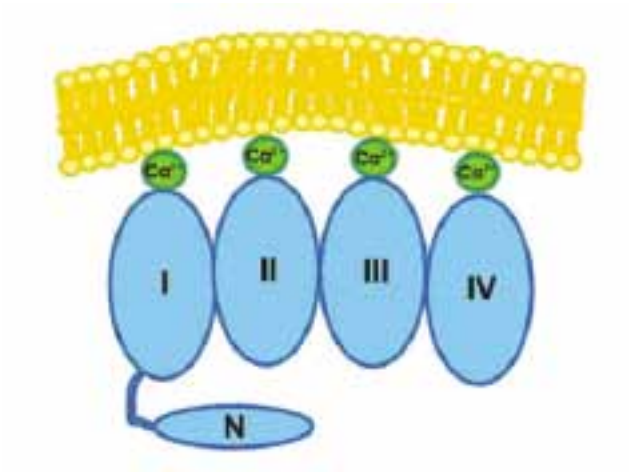

Figure 1.19: The slightly concave disc of animal annexins structure (Mortimer *et al.*, 2008). Each of the four conserved domains (I-IV) of animal annexin (blue) binds to a single Ca^{2+} ions (green), and associates with phospholipid membrane (yellow).

Figure 1.20: Homology between N terminus of *Arabidopsis* annexin and heme-binding domain of various plant peroxidases (Gidrol *et al.*, 1996). Shaded boxes indicate identical amino acid residues between *Arabidopsis* annexin (ANXarb) and peroxidases from *Arabidopsis* (ARATH), horseradish (ARMRU), turnip (BRARA), and peanut (ARAHY). Dashes indicate gaps that maximize the alignment, while a dot (•) indicate the heme-binding proximal histidine in the peroxidase sequences. Numbers show on the left are amino acid positions.

(Delmer & Potikha, 1997). For example, antiserum raised against p33/p35 from maize only cross-react with a 32 kDa polypeptide in crude and partially purified extracts from bell peppers (Proust *et al.*, 1996).

Meanwhile, Clark *et al.* (2005) developed anti-AnnAt1 and anti-AnnAt2 polyclonal antibodies that were raised in guinea pigs against two peptides synthesized based on a 31 amino acid sequence (amino acids 200 - 231) of the two *Arabidopsis* annexins (AnnAt1 and AnnAt2). The antibodies were used in Western blots for protein analysis and immunolocalization studies. In addition, quantitative real time RT-PCR was performed to measure the transcription levels of the *Arabidopsis* annexins, as it detects relative expression of genes more accurately (Cantero *et al.*, 2006).

1.8.4.1 Localization of annexins

Annexins are relatively abundant in cells. A majority of them are found in the cytoplasm or intracellular membrane, while a minority of them is detected in the nucleus. In alfalfa, AnnMs2 is found to be localized in the nucleolus by indirect immunofluorescence microscopy using affinity purified annexin antibody (Kovacs *et al.*, 1998). The authors suggested that AnnMs2 aids in the synthesis, assembly and transportation of ribosomes, and also maintains the nucleolar structure.

Immunolocalization studies have shown that secretory cell types contain high concentrations of plant annexins. They are found in the outer root cap cells, epidermal cells (including root hairs), developing vascular tissue, and tip of polar cell growth (Clark & Roux, 1995). Hence, annexins take part in the Golgi-mediated secretion of newly synthesized cell wall and plasma membrane. AnnAt1 is expressed pre-dominantly in all root cells, except those at the root tip, where it is only found in the outer rootcap cells (Clark *et al.*, 2001; Lee *et al.*, 2004). On the other hand, AnnAt2 is localized in endodermal cells close to the root-hypocotyl junction and epidermal root tip cells (Clark *et al.*, 2001).

The greatest difference between the staining patterns of anti-AnnAt1 and anti-AnnAt2 in the root is that anti-AnnAt2 stain was absent from the elongation zones (Clark *et al.*, 2005). Nevertheless, localization of anti-AnnAt2 is more obvious than anti-AnnAt1 in hypocotyls and cotyledons of 1 to 2-d-old seedlings. It is suggested that during early development of seedlings, translational control of gene expression might be very low or

not operational. Annexin in cytoplasm may also move to nucleus and perinuclear region to protect important genetic information from stress or facilitate the folding of stress-generated unfolded molecules (Rhee *et al.*, 2000). Factors that influence the localization of annexins are plant species, tissue type, and cytosolic Ca^{2+} concentration (Mortimer *et al.*, 2008).

1.8.4.2 Annexin gene expression

AnnAt1 was first found to be involved in stress response by Gidrol *et al.* (1996), on the basis of its ability to rescue an $\triangle$*oxyR* mutant in *E. coli* by exhibiting peroxidase acitivity to compensate for catalase deficiency. This study was further supported by Kush & Sabapathy (2001) who showed that *AnnAt1* can protect against oxidative cellular damage. Gorecka *et al.* (2005) confirmed the property of inherent peroxidase activity for AnnAt1 protein. This protein limits the excessive levels of ROS during oxidative burst in plants and its expression is upregulated in the presence of H_2O_2. A higher expression level of antioxidant enzymes is caused by an adaptive defense mechanism that protects cells from oxygen toxicity. Thus, this feature should enable *AnnAt1* to play a role in stress signaling.

Mimosa annexin also participated in nyctinastic and seismonastic movement (Hoshino *et al.*, 2004). Thus, the involvement of annexins in Ca^{2+} signaling pathways is associated with many plant responses. The authors suggested that *AnnAt1* may be a part of the plant cells response to osmotic stress.

Annexin gene expression is linked with the proliferation, differentiation, or transformation of cells (Gerke & Moss, 2002). It is influenced by environmental and developmental signals. Proust *et al.* (1996) showed the active secretion of annexin from pepper during fruit ripening, where its mRNA levels rose markedly by approximately 3.5-fold.

Annexin mRNA of *Medicago sativa* (*AnnMs2*) was induced in response to abscicic acid (Kovacs *et al.*, 1998). The level of *AnnMs2* mRNAs increased as alfalfa cell was treated with NaCl (50 mM or above), mannitol (0.3 - 0.6 M) and 1 h with PEG (5%). However, *AnnMs2* mRNA level did not increase with 10 and 15% PEG concentration, or a longer treatment period, although the transcript level was always higher than control.

From the experiment conducted by Cantero *et al.* (2006), the message level for *AnnAt1* of 7-d-old *Arabidopsis thaliana* seedlings increased 39-fold after 2 h with drought

treatment, or 42-fold with salt treatment. However, that for *AnnAt2* decreased by about 11-fold in the two treatments. It was suggested that annexin might help Ca^{2+}-signalling transduction in mediating plant adaptation to high salt concentrations and regulate Na^{+} transportation.

1.8.4.3 Inconsistencies in gene expression results

A few controversial results have been reported. Rhee *et al.* (2000) showed an increase of annexin I to heat, hydrogen peroxide and sodium arsenite. Kovacs *et al.* (1998) showed changes in alfalfa annexins expression when fruits ripen, cell cycle progresses, and in response to abiotic stresses and abscisic acid. During germination and early seedling growth, *annAt1* and *annAt4* T-DNA insertion mutants were sensitive to salt, abscisic acid and osmotic stress (Lee *et al.*, 2004). In this study, treatment with salt decreased AnnAt1 protein level in cytosol but increased in the membrane fraction. In another study, *AnnAt1* mRNA level in the roots of 2-week-old seedlings was not affected despite treatment with 250 mM NaCl for 2 h or longer. However, *AnnAt1* transcript levels in 7-d-old *A. thaliana* seedlings exposed to 250 mM NaCl increased more than 40-fold after 2 h treatment (Cantero *et al.*, 2006). Therefore, the authors suggest that the different findings might be related to different developmental stages, tissue sources or techniques used for annexin gene expression studies.

1.9 Nitric oxide in plants

Since the first groundbreaking discovery of nitric oxide (NO) in plant defense signalling by Delledonne *et al.* (1998) and Durner *et al.* (1998), research on NO in plants has increased significantly. NO is involved in many physiological and developmental processes, respiration, senescence and maturation, abiotic and biotic stresses (Arasimowicz & Floryszak-Wieczorek, 2007). However, the various NO functions in plants makes it relatively difficult to study.

1.9.1 Chemical and physical properties of nitric oxide

NO in its basic form is a free radical gas. It is highly reactive and highly diffusive, and rapidly permeates cell membranes (Lamattina *et al.*, 2003; Neill *et al.*, 2003; Arasimowicz & Floryszak-Wieczorek, 2007; Palavan-Unsal & Arisan, 2009). Under physiological conditions, the NO radical ($NO^{\cdot}$) tends to convert into other redox forms (Figure 1.21A): one-electron oxidation of NO produces nitrosonium cation (NO^{+}), while one-electron reduction forms nitroxyl anion (NO^{-}) (Arasimowicz & Floryszak-Wieczorek, 2007). In the presence of transition metals (Me^{+x}), NO produces metal-nitrosyl complexes that affects regulatory of transcription factors and certain enzymes. In the presence of superoxide ($^{\cdot}O_2^{-}$) and hydrogen peroxide (H_2O_2), NO readily reacts with the compounds to produce peroxynitrite ($OONO^{-}$). Peroxynitrite causes serious damage to cell structures by reacting with -SH groups of proteins and polyunsaturated radicals of membrane lipids. In the presence of oxygen, NO is oxidized to NO_2, which subsequently produces nitrate (NO_2^{-}) and nitrite (NO_3^{-}). The chemical reactions of NO are shown in Figure 1.21.

1.9.2 Source of nitric oxide

There are several potential NO sources in plants, relying on the species, cells and tissues, growth conditions and activation of the appropriate signalling pathways (Neill *et al.*, 2003; Arasimowicz & Floryszak-Wieczorek, 2007; Palavan-Unsal & Arisan, 2009). In plants, NO is synthesized enzymatically and non-enzymatically, as shown in Table 1.7. However, there are still many uncertainties concerning NO biosynthesis (Neill *et al.*, 2008).

1.9.3 Nitric oxide as a signal molecule

The properties of NO make it a good signalling molecule. Its simple structure, together with its small size, high diffusivity, and ability to directly influence second messengers are factors that make it so (Arasimowicz & Floryszak-Wieczorek, 2007). Biosynthesis of cyclic GMP (cGMP) and cyclic ADP ribose (cADPR), increament of cytosolic-free Ca^{2+} levels, activation and suppression of protein kinases, phosphatases, transcription factors and ion channels play a role in NO signalling responses in plant cells (Palavan-Unsal & Arisan, 2009). This is achieved via redox or an additive chemistry. NO has

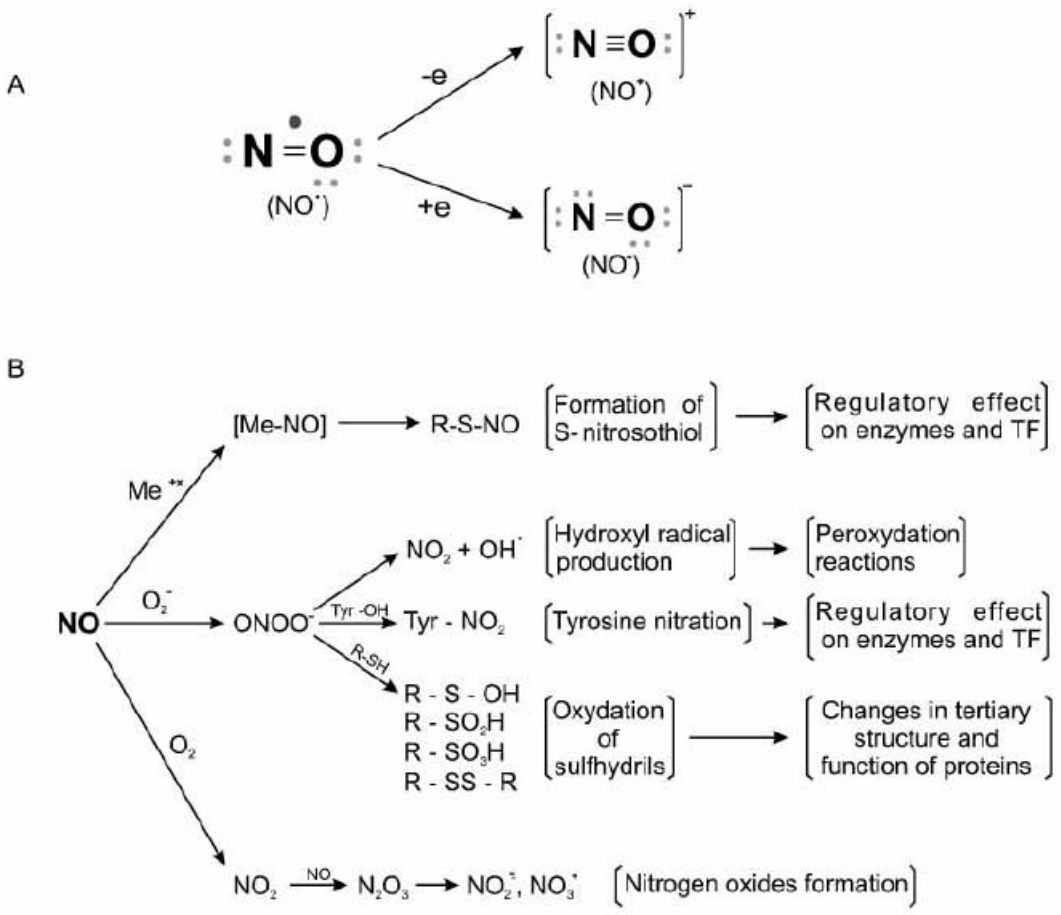

Figure 1.21: Chemistry of nitric oxide (Lamattina *et al.*, 2003). (A) Interconversion of NO radical ($NO^{\bullet}$) into nitrosonium cation (NO^{+}) and nitroxyl anion (NO^{-}). (B) Chemical reactions of NO and their potential biological activity.

Source of NO	Substrate	Localization
Enzymatic		
Nitric oxide synthase (NOS)	L-arginine	Mitochondria, peroxisomes, cytoplasm, chloroplasts
Nitrate reductase (NR)	NO_2^-	Cytoplasm
Xanthine oxidoreductase (XOR)	NO_2^-	Peroxisomes
Nitrite: NO reductase (Ni-NOR)	NO_2^-	Plasma membrane (root)
Peroxidase	*N*-hydroxy-arginine	
Cytochromes P450	*N*-hydroxy-arginine	
Non-enzymatic		
Ascorbate	NO_2^-	
Carotenoid	Nitrogen dioxide (NO_2)	

Table 1.7: Source of nitric oxide in plants (Neill *et al.*, 2003; Arasimowicz & Floryszak-Wieczorek, 2007; Neill *et al.*, 2008; Palavan-Unsal & Arisan, 2009).

been found to have a major impact in plant responses to several abiotic stresses, such as heat, chilling, drought, salt, UV irradiation, and ozone exposure (Wink *et al.*, 1993; Beligni & Lamattina, 1999b, 2000; Beligni *et al.*, 2002; Delledonne *et al.*, 2002; Sudha & Ravishankar, 2002; Wendehenne *et al.*, 2004; Dubovskaya *et al.*, 2007; Lei *et al.*, 2007; Shi *et al.*, 2007; Zhao *et al.*, 2007; Hong *et al.*, 2008; Li *et al.*, 2008; Qiao *et al.*, 2009; Wang *et al.*, 2009; Zhang *et al.*, 2009). Stress-induced signal transduction pathways by NO are shown in Figure 1.22.

1.9.4 The effect of nitric oxide on gene expression

Induction of gene expression by NO was firstly shown in plant-pathogen interactions. Tobacco plants infected with tobacco mosaic virus (TMV) have been reported to have an increased NOS activity, while NO donors (S-nitrosoglutathione, GSNO or S-nitroso-N-acetylpenicillamine, SNAP) instigated phenylalanine ammonia lyase (*PAL*) and pathogenesis-related (*PR-1*) gene expression (Durner *et al.*, 1998). A NO donor (sodium nitroprusside, SNP) also induced *PAL* and chalcone synthase (*CHS*) gene expressions in soybean (Delledonne *et al.*, 1998). However, there is no definite way to identify the NO-dependent intracellular signalling pathways leading to the activation or suppression of these genes (Grun *et al.*, 2006). Metal- and thiol-containing proteins are main targets for NO (Beligni & Lamattina, 2001). For example, in the presence of an electron acceptor, cysteine thiol reacts with NO and S-nitrosylated proteins were created (Neill *et al.*, 2003). Post-translational modification of these proteins could affect the function of stress-related, signalling, metabolic, and nuclear regulatory proteins (Grun *et al.*, 2006). NO might directly interact with S-nitrosylation, ADP-ribosylation, heme groups and other transition metals that are present in transcription factors (TFs), thereby changing their activity and gene expression levels. NO might also modulate the activity of TFs by altering the activity of signalling pathways through cGMP, cADPR and Ca^{2+}/ calmodulin pathway (Beligni & Lamattina, 2001; Neill *et al.*, 2003). Further aspects of the modulation of gene expression through NO are reviewed by Grun *et al.* (2006).

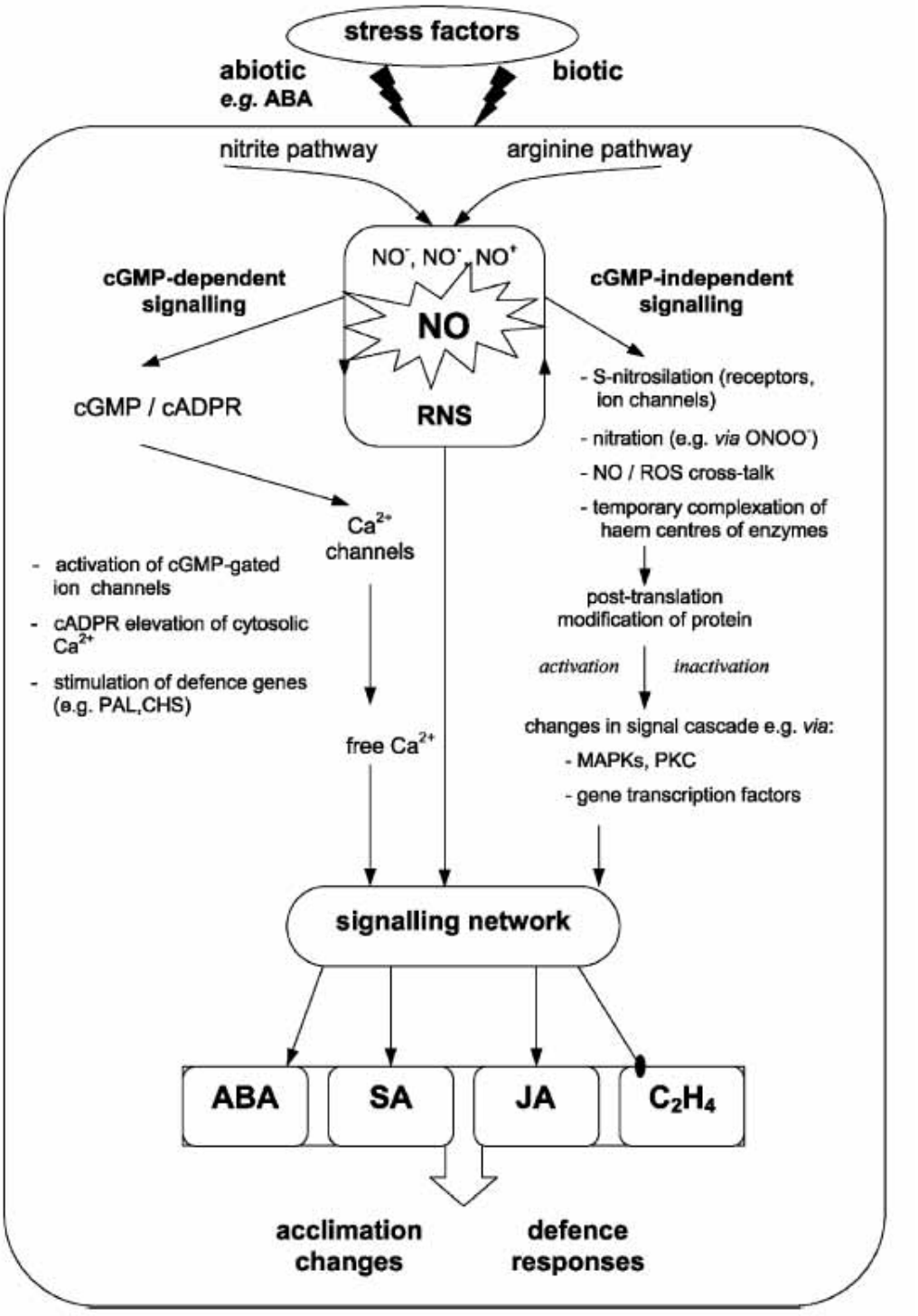

Figure 1.22: Signal transduction pathways involving NO in response to abiotic and biotic stresses (Arasimowicz & Floryszak-Wieczorek, 2007). ABA: abscisic acid, cADPR: cyclic ADP ribose, CHS: chalcone synthase, cGMP: cyclic GMP, C_2H_4: ethylene, JA: jasmonic acid, MAPK: mitogen activated protein kinase, PAL: phenylalanine ammonia lyase, ROS: reactive oxygen species, RNS: reactive nitrogen species, SA: salicylic acid.

1.9.5 Nitric oxide and heavy metals

As explained earlier, plants exposed to heavy metals are subjected to oxidative stress, which results in overproduction of ROS. ROS could act as signal transducers in plant defense responses, and also could cause cellular damage. NO-generating systems are also activated upon being triggered by different stressing environmental conditions (Figure 1.23). Depending on its concentration, NO reactivity with ROS accounts for both toxicity and protection (Beligni & Lamattina, 1999a, 2001). At a high concentrations of NO, the formation of $OONO^-$ from NO and $^{\cdot}O_2^-$ is deleterious to lipids, proteins and DNA. However, at a low concentrations of NO, peroxides have proven to be much more toxic than NO and $OONO^-$. Therefore, NO protects cells from ROS damage. Several researchers have reported that NO is able to scavenge metal-induced ROS, and it participates in the antioxidant cellular system (Kopyra & Gwozdz, 2003; Hsu & Kao, 2004; Laspina *et al.*, 2005; Wang & Yang, 2005; Yu *et al.*, 2005; Kopyra *et al.*, 2006; Hu *et al.*, 2007; Qiang *et al.*, 2007; Singh *et al.*, 2008; Zhang *et al.*, 2008; Singh *et al.*, 2009). Studies on the protective effects of exogenously supplied NO on heavy metal toxicity are summarized in Table 1.8. Furthermore, heavy metals suppressed internal NO production in plants, thereby inducing cellular damage (Rodriguez-Serrano *et al.*, 2006, 2009). The relationship between SNP pre-treatment and Pb-induced oxidative damage was investigated in this study.

1.10 Technical approaches used in this project

1.10.1 Graphite-furnace atomic absorption spectrophotometer

Atomic absorption spectrophotometry (AAS) is routinely used to determine many trace elements in a variety of sample matrices. The limited sensitivity of flame AAS for detecting most elements is significantly improved by a graphite furnace (GF) AAS. The sensitivity and detection limit of GF-AAS is 20 - 1000 times better than conventional AAS. GF-AAS is based on the following principle: Pb in the samples is atomized at a relatively high temperature and absorbs light at a wavelength characteristic of the element of interest. The amount of light absorbed is linearly correlated with the concentration of

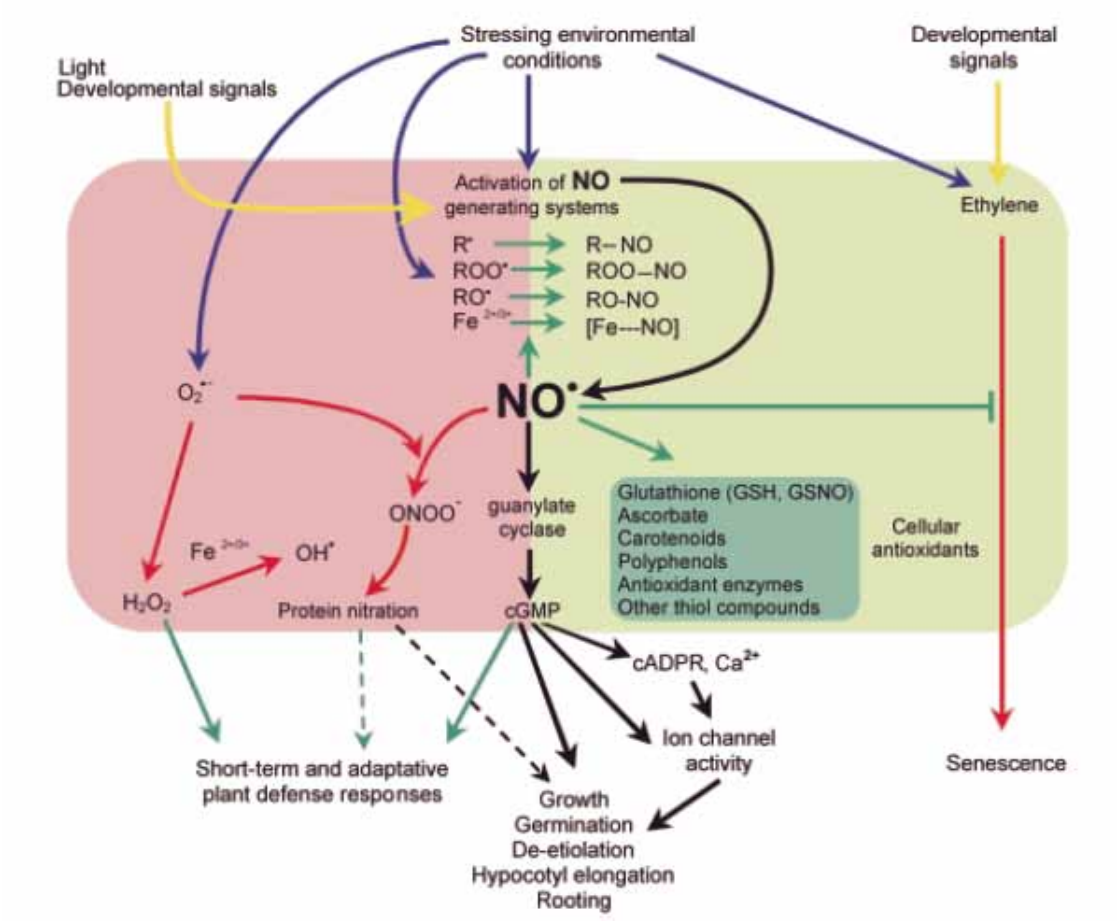

Figure 1.23: Schematic diagram showing the effect of nitric oxide in plants (Beligni & Lamattina, 2001). NO reaction with ROS accounts for cytotoxic (pink area) and cyto-protective (green area). R•: non-oxygen free radicals, RO•: alcoxyl radicals, ROO•: peroxyl radicals, OH•: hydroxyl radicals, $OONO^-$: peroxynitrite, GS-NO: nitrosoglutathione, cGMP: cyclic GMP, cADPR: cyclic ADP-ribose.

Heavy metals	Plants	Key findings	Reference
Cd	*Oriza sativa* L.	NO donors (PBN, SIN-1, SNP, and ASC + $NaNO_2$) decreased Cd-induced toxicity and MDA content. SNP prevented Cd-induction of H_2O_2 and MDA contents, decreased GSH and ASC contents, and increased the specific activities of antioxidant enzymes. SNP also prevented Cd accumulation by NH_4^+, decreased the activity of GS, and increased the specific activity of PAL. ∴ NO was able to scavenge H_2O_2.	(Hsu & Kao, 2004)
Cd	*Triticum aestivum* L.	SNP significantly decreased Cd-mediated lipid peroxidation, H_2O_2 level and electrolyte leakage in wheat roots. SNP also restored antioxidant enzymes by reducing SOD, GPX, CAT and GR activities. The protective role of NO was observed in the histochemical localization of lipid peroxidation, plasma membrane integrity and $^{\bullet}O_2^-$. ∴ NO quenched ROS, reduced oxidative damage and cellular injury.	(Singh *et al.*, 2008)
Cd	*Helianthus annuus* L.	NO reversed dry weight loss and chlorophyll degradation caused by Cd, reduced lipid peroxidation, recovered CAT activity and GSH levels, enhanced ASC content, and restored SOD activity. ∴ NO attenuated Cd-induced oxidative damage and conferred higher tolerance.	(Laspina *et al.*, 2005)
Cd	*Glycine max* L.	SNP restored Cd-inhibited cell growth, stimulated SOD activity, reduced $^{\bullet}O_2^-$, H_2O_2 and oxidized protein levels. ∴ NO scavenged ROS directly, mobilized SOD and reduced the level of oxidized proteins.	(Kopyra *et al.*, 2006)
Pb, Cd	*Lupinus luteus* L.	SNP improved seed germination, reduced the metal-damaging effect on root growth and morphology, increased SOD activity, changed POX and CAT activities, and decreased $^{\bullet}O_2^-$ level. ∴ NO stimulated SOD acitivity and/or direct scavenging of $^{\bullet}O_2^-$.	(Kopyra & Gwozdz, 2003)

Table 1.8: Effects of exogenously supplied nitric oxide on heavy metals-induced stress in plants. Key findings are those in comparison to control (without pre-treatment with NO donor, but with heavy metal treaments). ∴ indicates conclusion made by the authors. PBN: N-tert-butyl-phenylnitrone, SIN-1: 3-morpholinosydonimine, SNP: sodium nitroprusside, ASC: ascorbic acid, $NaNO_2$: sodium nitrite, MDA: malondialdehyde, GS: glutamine synthetase, NH_4^+: ammonium.

Heavy metals	Plants	Key findings	Reference
Al	*Cassia tora* L.	SNP treatment significantly increased root elongation by decreasing Al accumulation in root apices. NO also decreased lipid peroxidation, ROS, lipoxygenase and antioxidant enzymes. Such effects were confirmed by histochemical staining of lipid peroxidation and loss of membrane integrity in roots. ∴ NO promoted plant tolerance to Al toxicity.	(Wang & Yang, 2005)
Al	*Hibiscus moscheutos*	SNP alleviated the inhibitory effect of Al, NOS and NR on root elongation. ∴ NO changed the regulation of genes involved in cell elongation.	(Tian *et al.*, 2007)
As	*O. sativa* L.	SNP ameliorated the negative effect of As-mediated root and coleoptile growth, decreased MDA, $^{\bullet}O_2^-$, root oxidizability and H_2O_2 contents, and partially reversed As-induction of SOD, APX, GPX and CAT activities. ∴ ROS scavenging activity of NO protected rice against As-induced toxicity oxidative stress.	(Singh *et al.*, 2009)
Cu	*T. aestivum* L.	SNP greatly improved wheat seed germination subjected to Cu, retained higher amylase activities, stimulated SOD and CAT activities, decreased lipoxygenases activities, sustained a lower MDA, and H_2O_2 contents. No significant difference in seed Cu contents was found. ∴ NO enhanced the antioxidative capacity.	(Hu *et al.*, 2007)
Cu	*O. sativa* L.	SNP reduced Cu toxicity and NH_4^+ accumulation in leaves, inhibited protein reduction and MDA content, prevented early increase and late decrease in H_2O_2, and restored Cu-mediated SOD, POX and GR specific activities. ∴ NO was capable of scavenging the active oxygen species.	(Yu *et al.*, 2005)
La	*O. sativa*	SNP inhibited La uptake and translocation from roots to shoots, restored GSH content, SOD and GPX acitivities, and decreased H_2O_2 level. ∴ NO increased the activities of antioxidant enzymes, thus preventing La-induced oxidative stress.	(Qiang *et al.*, 2007)

Table 1.8: Effects of exogenously supplied nitric oxide on heavy metals-induced stress in plants (continued from the previous page). Key findings are those in comparison to control (without pre-treatment with NO donor, but with heavy metal treaments). ∴ indicates conclusion made by the authors.

the analyte present. Hence, a calibration curve from standards of known concentrations can be used to determine the concentration of the samples. The main advantages of GF-AAS are: (1) high sensitivity and low detection limit, (2) the automated process provides fast, reliable and accurate measurement, (3) minimal sample preparation and analytes can often be measured directly (Schlemmer *et al.*, 1999; Csuros & Csuros, 2002).

1.10.2 Transmission electron microscopy

Transmission electron microscopy (TEM) is one of the most practical approaches to study the patterns of Pb deposition within plant cells and cellular organelles. Antosiewicz & Wierzbicka (1999) confirmed the suitability of using conventional electron microscopy to study the distribution of Pb deposits in onion (*Allium cepa* L.) root cells. Since only 3.8% Pb were lost during fixation and other TEM processes, this method is suitable for ultrastructural observation of Pb. Various aspects of Pb uptake and accumulation have been examined in *A. cepa* L. using TEM. This includes Pb migration through the root tissues (Wierzbicka, 1987), translocation of Pb through the middle lamella of root cap cells (Wierzbicka, 1987), resumption of mitotic activity in root tips by Pb (Wierzbicka, 1994), Pb accumulation in the apoplast of root tips (Wierzbicka, 1998), constitutional tolerance to Pb (Wierzbicka, 1999a), Pb prolonged the cell cycle (Wierzbicka, 1999b), and encapsulation of Pb in small vesicles in the cytoplasm of epidermal cells (Wierzbicka *et al.*, 2007).

TEM has also been used to study localization of Pb in *Chamaecytisus palmensis* (Jarvis & Leung, 2001), *Pinus radiata* (Jarvis & Leung, 2002), *Zea mays* (Malone *et al.*, 1974), and *Pisum sativum* (Malone *et al.*, 1974; Malecka *et al.*, 2001, 2008).

1.10.3 Real-time RT-PCR

Reverse transcription following quantitative real-time polymerase chain reaction (qRT-PCR) analysis is widely used to quantify the steady-state of mRNA levels. This quantitative nucleic acid sequence analysis has an important role in basic research, molecular diagnostics, clinical microbiology, clinical oncology, and biotechnology (Bustin, 2002; Klein, 2002). Other methods that have been used for quantification of transcription

are northern blotting, *in situ* hybridisation, RNase protection assays, and cDNA arrays (Bustin, 2000). However, low sensitivity is the main limitation of these techniques. In contrast to classical PCR, real-time PCR (Figure 1.24) measures the amplified PCR product at each cycle throughout the exponential phase, allowing precise and accurate quantification (Gachon *et al.*, 2004).

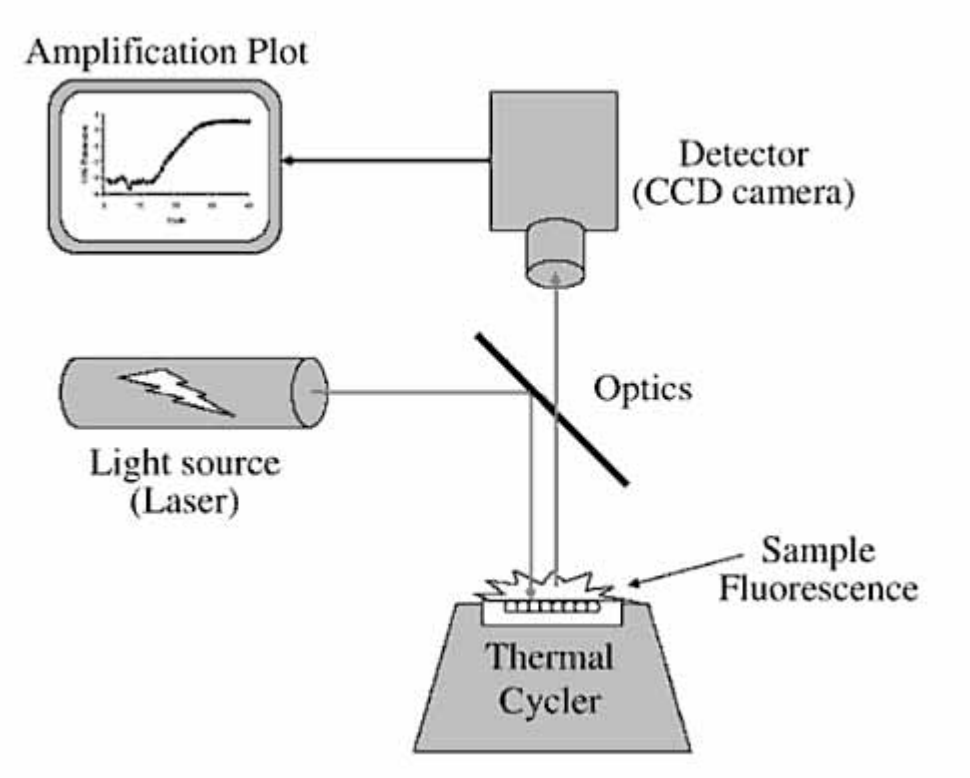

Figure 1.24: Schematic diagram of real-time PCR setup (Peirson & Butler, 2007)

1.10.3.1 PCR amplification

PCR is performed on a single or double-stranded (ds) DNA template. The reaction is carried out by temperature cycling (Figure 1.25), and consists of two oligonucleotide primers flanking DNA sequence of interest, dNTPs (the four nucleotide triphosphates), a heat-stable polymerase, and Mg^{2+} in the buffer (Kubista *et al.*, 2006). Firstly, a melting temperature (T_m) of 95˚C separates the double-stranded DNA. Then a low annealing temperature (T_a) allows primers to bind to DNA template. Lastly, an optimum temperature

of 72˚C is set, enables polymerase to synthesize a new DNA strand by incorporating the dNTPs (Kubista *et al.*, 2006).

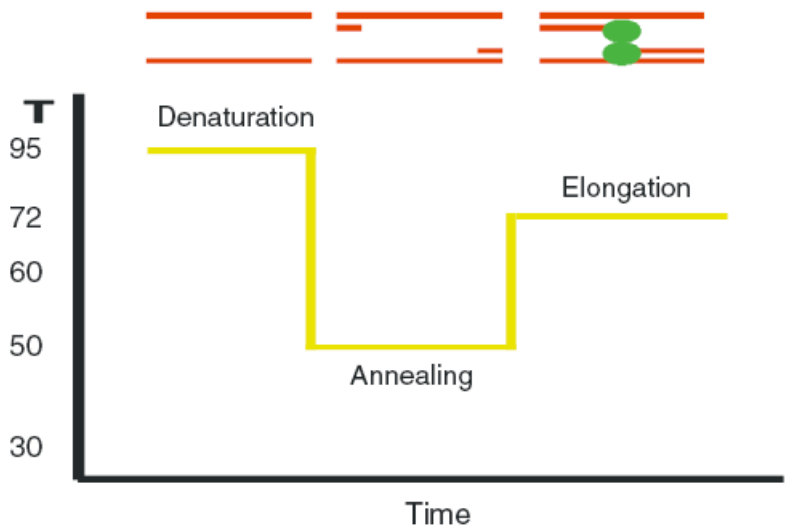

Figure 1.25: The PCR temperature cycle (Kubista *et al.*, 2006).

1.10.3.2 The qRT-PCR process

The two-step qRT-PCR approach is more sensitive than the one-step qRT-PCR reaction (Kubista *et al.*, 2006). A stable cDNA pool is generated in the two-step approach, allowing indefinite storage (Bustin, 2000). Additionally, two-step qRT-PCR eliminates the formation of primer-dimer artifacts and genomic co-amplification, thus enables higher reproducibility (Vandesompele *et al.*, 2002a). Steps required prior to gene expression analysis are illustrated in Figure 1.26.

Firstly, total RNA is isolated from the sample, and DNase treatment is performed to eliminate any contaminating genomic DNA template that may produce false positive amplification signals (see Section 1.10.3.5). Alternatively, this is prevented by designing two primers that hybridize at different exons but contains ≥ 1 intron, or designing a primer strand that spans across an exon/exon boundary (Kubista *et al.*, 2006). After that, mRNA is copied to cDNA by reverse transcription (RT). Since it is important to maximize the

quantity of mRNA from a small sample of RNA, a mix of random hexamers and oligo (dT) primers is used in the experiments, allowing total reverse transcription (Bustin, 2000; Kubista *et al.*, 2006). Random hexamers bind unspecifically along each RNA template (includes tRNA, rRNA and mRNA), copy and produce many cDNA of interest. Oligo(dT) primers bind to the poly(A) tail and synthesize from the 3'-end of the mRNA. Lastly, quantification of gene expression is measured by a real-time PCR using SYBR Green (Figure 1.27), a fluorescent dye. SYBR Green is specific for any double-stranded but not single-stranded DNA during the amplification of the PCR product.

1.10.3.3 Principle of qRT-PCR

Gachon *et al.* (2004) summarized the principles of qRT-PCR (Figure 1.28) as follows: (1) cDNA containing a specific target is reverse-transcribed from isolated RNA, and used in qRT-PCR to accurately measure the concentrations of a gene of interest present in independent samples. Each sample is mixed with a fluorochrome (e.g. SYBR Green, hybridization probes, TaqMan, molecular beacon, and scorpion), specific primers, and reaction mix (Taq, dNTP and buffer). (2) During the PCR amplification, fluorescence is generated when a specific product is detected. The cycle number at the exponential phase of fluorescence gives the best PCR amplification efficiency. The point where the fluorescence intersects the threshold is known as the *Ct*. The amplification plot, where Ct = $f(\log_{10}$ initial concentration of the specific target), is the end result of real-time PCR. It is also known as growth curve of fluoresence (Peirson & Butler, 2007). (3) The amount of a target product of interest can be calculated from the calibration curve of known starting materials or standards. This is because the copy number is proportional to the DNA concentration within the reaction.

1.10.3.4 Advantages of qRT-PCR

Real-time PCR has several features that makes it an attractive method for gene expression studies (Gachon *et al.*, 2004). It is characterized by a wide dynamic range of quantification (Klein, 2002). It detects gene of interest rapidly, specifically and sensitively. The benefits are explained in the following:

1. *Rapidity*: Compared to classical PCR, real-time PCR produces reliable data rapidly.

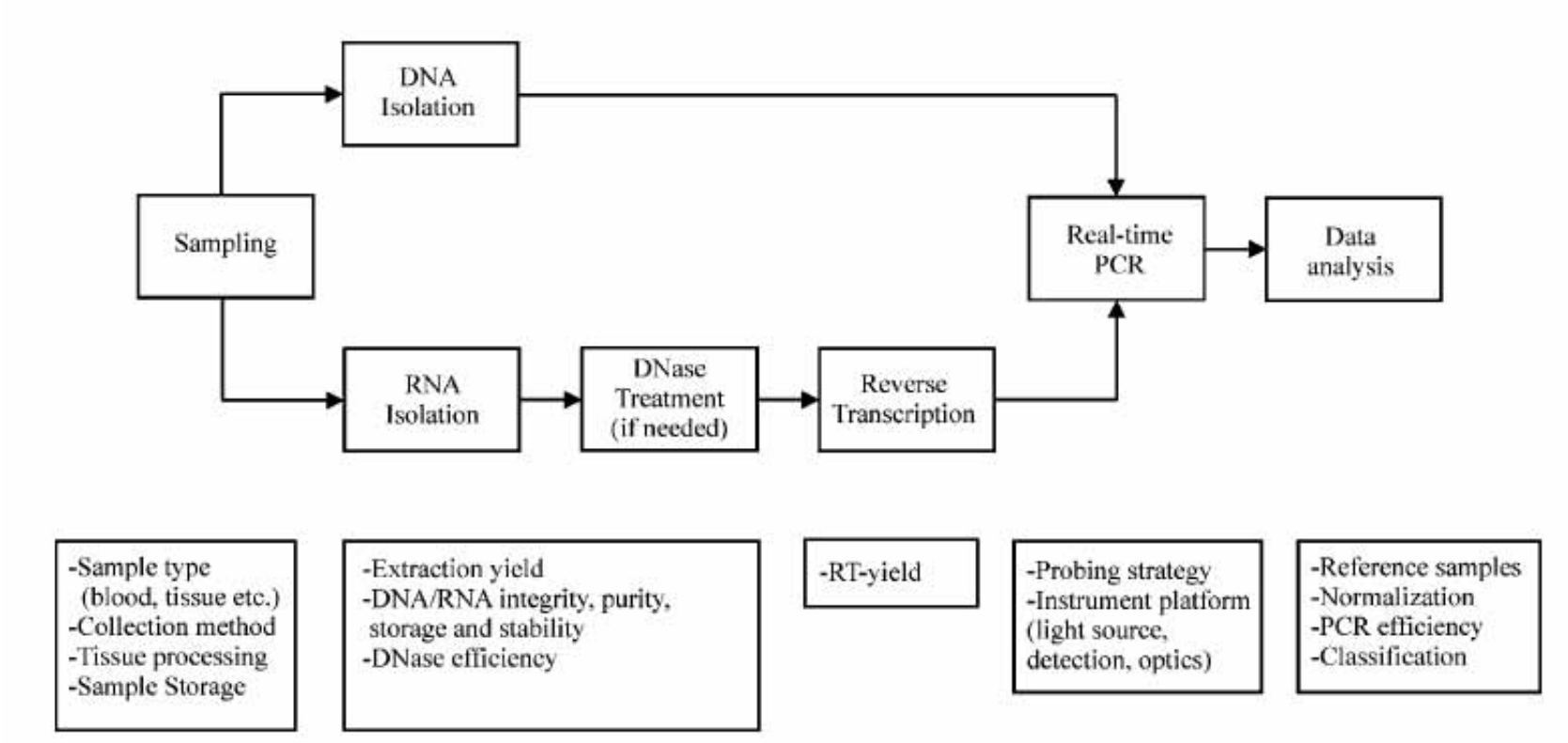

Figure 1.26: RNA and DNA analysis from biological samples (Kubista *et al.*, 2006). Boxes at the bottom indicate sources of variation at each step.

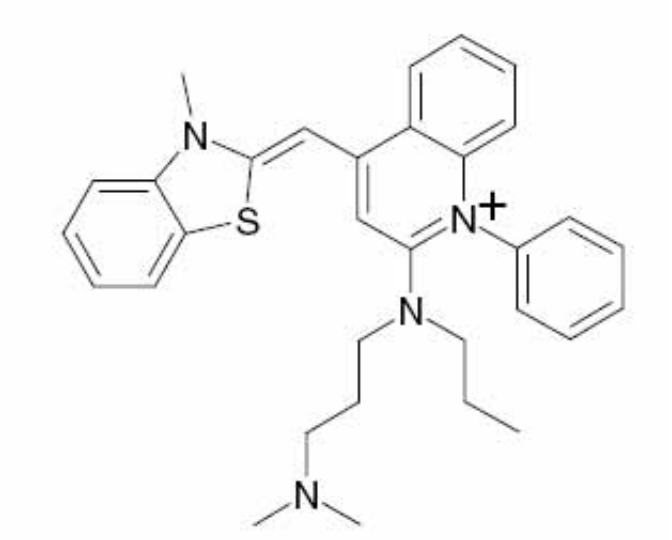

Figure 1.27: Structure of SYBR Green (Kubista *et al.*, 2006).

A modern real-time PCR machine uses capillaries and heats by light, rather than tubes and heating block, respectively. This reduces the duration required to heat the PCR mixture, from 15 s to 1 - 2 s (Gachon *et al.*, 2004). A large number of samples (e.g. 384 well plates) can be analyzed together using this automated technology, thus the cost of operation can be decreased (Klein, 2002). Moreover, qRT-PCR records amplification of DNA in real-time, thereby reducing resources in term of effort and time (Gachon *et al.*, 2004).

2. *Sensitivity*: Real-time PCR is highly sensitive and capable of detecting samples of < 5 copies, enabling the quantification of gene expression from a very limited amount of starting materials (Klein, 2002; Gachon *et al.*, 2004). Intercalating agents, such as SYBR Green, detects PCR amplification in real-time.

3. *Specificity*: Real-time PCR gives highly precise results, with less than 2% standard deviation of Ct values (Klein, 2002). The melting curve program checks the specificity of PCR process directly after the completion of a PCR run (Gachon *et al.*, 2004). Alternatively, the specificity of an amplicon can be checked with gel electrophoresis and DNA sequencing.

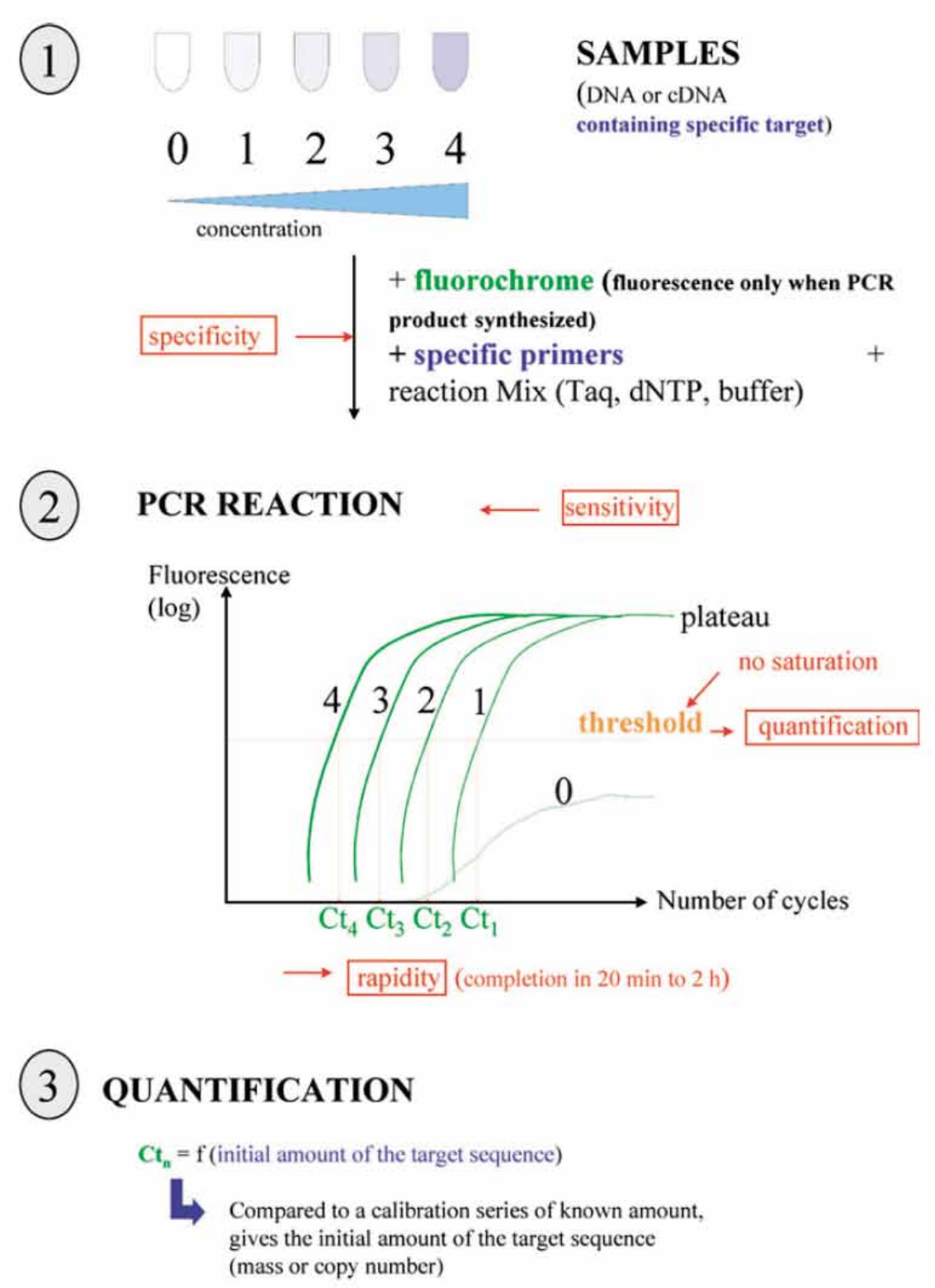

Figure 1.28: Principles of quantitative real-time PCR (Gachon *et al.*, 2004).

4. *Flexibility of quantification methods*: Real-time PCR enables analysis of multiple samples from extremely low to high concentrations, and allows customization of the cycle number necessary to reach the Ct value (Gachon *et al.*, 2004). Hence, this method compares mRNA levels in different sample populations, discriminates between closely related mRNAs, and characterizes mRNA expression patterns and structures (Heid *et al.*, 1996). Absolute and relative quantification methods are used in gene expression studies.

5. *Minimum cross contamination risk*: Post-PCR steps are not required, thereby preventing the possibility of cross-contamination by PCR products (Klein, 2002).

1.10.3.5 Important considerations in qRT-PCR

Reliability of qRT-PCR data is essential, where linearity, precision, specificity, limitation of detection and quantification must be taken into account (Vaerman *et al.*, 2004). To achieve biologically meaningful results, it is important to implement several procedures and precautions to minimize experimental error. These procedures can be incorporated into a protocol at many stages (Figure 1.29), including sampling, total RNA isolation, and design of the internal reference. The following strategies must be considered carefully when optimising the specificity, sensitivity, and reproducibility of the reactions.

1. *Sample size and collection*: Ensuring replicate samples are of a similar size, by sampling similar tissue volumes or weights, is the first stage of reducing experimental error. However, this can be difficult due to the nature of biological samples (Huggett *et al.*, 2005). Materials should be harvested from ≥ 3 biological replicates for statistical analysis, frozen immediately in liquid nitrogen, and stored at -80˚C to minimize RNA degradation (Udvardi *et al.*, 2008).

2. *RNA quality*: It is well known that RNA is sensitive to degradation during sample handling and storage. Contamination with RNases need to be prevented at all times (van Pelt-Verkuil *et al.*, 2008a). It is important to perform RNA quality control to accurately quantify small gene expression difference in PCR. In addition, degraded RNA samples greatly affect gene expression results (Perez-Novo *et al.*, 2005). The integrity of RNA can be assessed based on the 18S and 28S ribosomal bands after

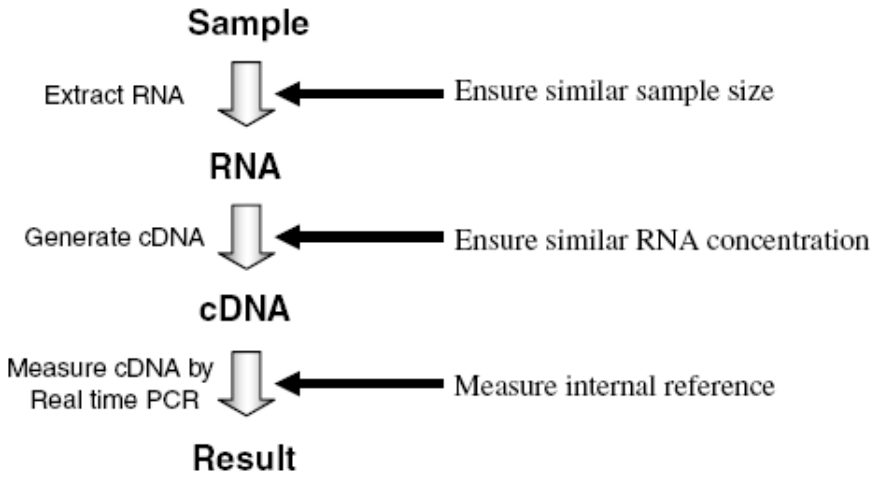

Figure 1.29: Real-time RT-PCR processes (Huggett *et al.*, 2005). A good normalisation strategy is recommended on the right.

agarose gel electrophoresis (Fleige & Pfaffl, 2006). Using spectrophotometric techniques, a ratio of $A_{260}/A_{280} > 1.8$ and $A_{260}/A_{230} > 2.0$ indicates the isolated RNA is of high quality (Perez-Novo *et al.*, 2005; Udvardi *et al.*, 2008). RNA should be processed immediately or otherwise, stored at -80˚C (van Pelt-Verkuil *et al.*, 2008a).

3. *DNase treatment*: Any genomic DNA template could generate a false positive result and affect gene expression data. Therefore, a DNase treatment is highly recommended after RNA isolation. A negative control (isolated RNA + RT mix without reverse transcriptase) can be added to detect any genomic DNA contamination (van Pelt-Verkuil *et al.*, 2008a). However, it is important to remove the DNase prior to any RT step, because the presence of DNase interferes with cDNA synthesis process (Bustin, 2002).

4. *cDNA synthesis*: Reverse transcription often causes variation and data discrepancy in RT-PCR experiments. This is because RNA samples have inherent variation and are rather unstable. RNA transcripts may also display significant secondary structure, affecting the ability of reverse transcriptase to generate cDNA (Freeman *et al.*, 1999; Bustin, 2000, 2002; Bustin *et al.*, 2005). As a result, the synthesized

cDNA may not represent the actual quantity of RNA starting materials. Hence, similar priming strategy, reaction conditions and RNA input must be used in all experiments. A robust reverse transcriptase without RNaseH activity should be used to maximize the cDNA yield (Udvardi *et al.*, 2008). The choice of primers (e.g. specific primers, random hexamers or oligo-dT primers) may also determine the sensitivity and accuracy of gene quantification. Alternatively, this is prevented by designing two primers that hybridize at different exons but contains ≥ 1 intron, or designing a primer strand that spans across an exon/exon boundary (Kubista *et al.*, 2006).

5. *Primer design*: Generally, a good primer pairs should have similar melting temperatures (T_m = 60 $\pm$ 3˚C), 40 - 60% GC content, 18 - 25 nucleotides in length, yield relatively short PCR amplification products (100 - 200 nucleotides), absence of primer dimers formation, and ~100% amplification efficiency (Udvardi *et al.*, 2008). Lowe *et al.* (1990) encourage researchers to choose primer pairs that flank an intron-exon border and synthesize a small amplified product (0.2 - 0.5 kb) near the 3'-end of the target sequence. The 3'-untranslated region is generally more unique than the coding sequence because it permits better identification of the amplified products (Lowe *et al.*, 1990; van Pelt-Verkuil *et al.*, 2008d; Udvardi *et al.*, 2008). Prior to selection, the specificity of each primer should be tested using BLAST to minimize the influence of non-target binding sites, thus maximizing amplification efficiency (Bustin *et al.*, 2005). The authors also recommended using automated melting curve program based on SYBR Green-I chemistry to evaluate the primers at the end of PCR run.

6. *Internal controls*: Accurate quantification by qRT-PCR relies on the normalisation of gene expression data with a stably expressed reference gene (Bustin, 2002; Vandesompele *et al.*, 2002b; Andersen *et al.*, 2004; Brunner *et al.*, 2004; Pfaffl *et al.*, 2004; Radonic *et al.*, 2004; Huggett *et al.*, 2005; Nicot *et al.*, 2005; Remans *et al.*, 2008; Guenin *et al.*, 2009). Reference genes, also known as housekeeping genes, are used to standardize the differences in quantity and quality of starting materials, RNA preparation and cDNA synthesis. This is possible because both reference

and target genes undergo the same preparation steps (Radonic *et al.*, 2004; Huggett *et al.*, 2005). The most commonly used reference genes are β-actin, tubulin, microglobulins, glyceraldehyde-3-phosphate dehydrogenase (GAPDH), ribosomal units (18S or 28S rRNA), albumins, cyclophilin, hypoxanthine-guanine phosphoribosyl transferase (HPRT), and ubiquitin (Thellin *et al.*, 1999; Bustin, 2000; Pfaffl, 2001; Czechowski *et al.*, 2005; Huggett *et al.*, 2005). Ideally, a reference gene should not be regulated or influenced by the experimental condition (Radonic *et al.*, 2004). However, this is not always the case with traditional housekeeping genes and could compromise gene expression studies (Czechowski *et al.*, 2005; Nicot *et al.*, 2005; Remans *et al.*, 2008). Therefore, it is necessary to ascertain which reference gene is best to normalize the target gene expression under designated experimental condition, and validate with BestKeeper (Pfaffl *et al.*, 2004), geNorm (Vandesompele *et al.*, 2002b), or NormFinder (Andersen *et al.*, 2004) softwares. Reference gene validation softwares for improved normalization are further reviewed by Vandesompele *et al.* (2009). Remans *et al.* (2008) had identified the best three reference genes (*AT5G15710* F-box protein, *AT2G28390* SAND family protein, and *AT5G08290* mitosis protein YLS8) from *A. thaliana* exposed to Cd and Cu, and suggested the suitability of these genes for studying gene expression in plants exposed to other heavy metals.

7. *PCR conditions and optimization*: Typically, PCR amplification protocols comprises 30 - 50 cycles of denaturation of initial nucleic acid template/activation of thermostable DNA polymerase, amplification, extension, and cooling phase (van Pelt-Verkuil *et al.*, 2008c). The primer anealing temperature and time must be optimized to maximize amplification efficiency and minimize incompletely amplified, non-specific, or extraneous 'primer-dimer' products arising from primer-primer self- or cross- homologies (Lowe *et al.*, 1990). To ensure the quality of PCR, PCR efficiency should be determined from calibration curve or amplification plots because it reflects the sensitivity and specificity of a PCR reaction (van Pelt-Verkuil *et al.*, 2008b). In order to produce reliable data and allow detection of both up- and down-regulation of gene expression, it is vital to select conditions that enable measurements of broad analytical range of RNA expression (van Pelt-Verkuil

et al., 2008c). A small difference in amplification efficiencies between the PCR capilaries may severely affect the final concentration of amplified product, causing under- or over-estimation of gene expression level (Peirson & Butler, 2007). The mean Ct values of all tested samples should be within ± 1 (Udvardi *et al.*, 2008).

8. *Technical control*: In order to limit technical errors in PCR reaction setup, it is necessary to standardize and minimize pipetting steps. Master mix consisted of cDNA and qPCR reagents can be prepared before aliquoting a standard volume into each reaction well (Udvardi *et al.*, 2008). No template control (NTC) should be incorporated in all PCR reaction to check for contaminations. The total cDNA concentration must be the same in all samples to ensure reliability of result yield (Guenin *et al.*, 2009). In addition, Udvardi *et al.* (2008) recommended running real-time PCR on target and reference genes in parallel.

1.10.3.6 Quantification of gene expression and statistics

There are two types of quantification for qRT-PCR (Freeman *et al.*, 1999; Pfaffl, 2001; Peirson & Butler, 2007). Relative quantification is based on the relative expression of a target gene that is standardized by a stably expressed reference gene. It is adequate for most biological research. On the other hand, absolute quantification states the copy number of a specific RNA per cell or unit mass of tissue, based on a calibration curve. Thus, it requires a number of extra conditions, which are more technically demanding (Freeman *et al.*, 1999; Peirson & Butler, 2007; Pfaffl, 2001). Two mathematical models have been developed for relative quantification: the efficiency calibrated model (Pfaffl, 2001), and the $2^{-\triangle\triangle C_t}$ model (Livak & Schmittgen, 2001). Four statistical approaches for analysis of qRT-PCR data have been reported by Yuan *et al.* (2006). Several computer programs have also been established for analysis of transcript levels, such as REST (Pfaffl *et al.*, 2002), LinRegPCR (Ramakers *et al.*, 2003), and qBase (Hellemans *et al.*, 2007).

1.10.4 Western blotting

Proteins are synthesized from mRNA, but they do not reflect the mRNA expression levels in the samples. These proteins may undergo post-translational modification to function

in response to a given treatment. Western blotting is a commonly applied analytical technique to detect a specific protein from a protein mixture, by binding of antibodies to a specific antigen (Lee, 2007). It uses sodium dodecyl sulphate-polyacrylamide gel electrophoresis (SDS-PAGE) to separate protein extracts, based on their molecular mass. The separated proteins are then transferred from the gel to a membrane, where they are detected using antibodies specific to the target protein and visualized with a chemiluminescent reagent or a colorimetric method. Clark *et al.* (2005) used western blot and found two *Arabidopsis* annexins that function in Golgi-mediated secretion during early growth and development of seedlings (see Section 1.8.4.1). Using this technique, Lee *et al.* (2004) suggested that AnnAt1 and AnnAt4 play a vital role in osmotic stress and ABA signalling in a Ca^{2+}-dependent manner.

1.11 Objectives and structure of the thesis

The extensive use of Pb attributing to its low melting temperature and anti-corrosive properties has raised public health and environmental concern. This heavy metal contaminant is likely to enter human's food chain, eventually affecting the nervous system, kidney function and reproduction system of the human body. Its widespread occurence, persistence, immobility and bioaccumulative nature highlight the importance of remediation research, including phytoremediation. This emerging low-cost and ecologically friendly technology is particularly useful to remove Pb pollutant from the environment, because like other heavy metal contaminants it cannot be mineralized.

The overall aim of the research is to obtain a better understanding of Pb phytoremediation, using *Arabidopsis thaliana* as a model system. *A. thaliana* is an appealing experimental system for studying Pb tolerance in plants, mainly due to the scarcity of Pb-hyperaccumulating plants and a lack of basic physiological and genetic information associated with the ideal traits for Pb phytoremediation. The project was designed to grow the plants in a controlled environment of a Petri dish. The reasonings, specific objectives (in bold) and format of the thesis towards accomplishing this research are:

Chapter 1

In order to provide the background knowledge related to the scope of the present investigation, this chapter present a general introduction and literature review that embrace all aspects of the study.

Chapter 2

This chapter outlines the general details of plant materials and growth conditions used in various experiments, the culture media, experimental procedures, analytical instruments and techniques, as well as statistical analysis of data obtained.

Chapter 3

Plants are regularly exposed to unfavorable conditions that impose stress. Plants exposed to Pb stress make specific changes in their cell physiology to avoid or tolerate the stress. However, the mechanisms to reduce the effects of Pb vary from plant species, developmental stage, culture medium, Pb concentration and bioavailability. Basic growth responses to increasing Pb concentrations result in characteristic uptake response curve, the phases of which correspond to ranges of tolerance and toxicity. These basic physiological responses underpin biochemical and molecular studies of stress response to Pb in *A. thaliana* seedlings. Hence, *A. thaliana* were grown on modified Huang & Cunningham (1996) medium, containing up to 200 µM $Pb(NO_3)_2$, for 7 d. The experimentations were conducted as follows:

1. To **study the physiological effect of Pb on the growth of *A. thaliana* seedlings and symptoms of toxicity**, which are particularly evident from morphological observation. The root length of seedlings grown in different concentrations of Pb were measured.

2. To **evaluate the pattern of Pb uptake and translocation in *A. thaliana* seedlings** using a graphite furnace atomic absorption spectroscopy.

3. To **identify the possible sites of Pb localization/ sequestration and subcellular damage that might occur within the plant cell** using transmission electron microscopy.

Chapter 4

Pb has been shown to induce oxidative stress in various plant species by generation of lipid peroxidation and ROS. Similar to physiological level, the extent of biochemical change in plants brought about by Pb exposure is greatly dependent on Pb concentration and plant species. As Pb stress is intensified, the level of antioxidative enzyme activities might be increased as a defense mechanism against Pb-induced ROS, or decreased as a result of enzyme inactivation. Hence, this chapter seeks to better understand the mechanisms of Pb-induced oxidative stress that correlate with the physiological studies, and the way seedlings respond by tolerating, or acclimating to the presence of Pb. Experiments were performed to **assess the oxidative stress of *A. thaliana* seedlings by measuring lipid hydroperoxide, ROS and antioxidative defence capacity**. The antioxidative enzyme activities examined were superoxide dismutase, catalase, glutathione peroxidase, glutathione reductase and general peroxidases.

Chapter 5

Pb phytoremediation has been delayed due to the lack of Pb-related genes or proteins. Therefore, finding functional genes or proteins associated with Pb tolerance and uptake can advance the fundamental understanding of molecular mechanisms of stress responses. Annexins have been shown to be involved in many abiotic stresses and limit excessive level of ROS. It would seem that annexins could also play in protecting plant cells from Pb-mediated stress. This chapter seeks to **determine whether annexin 1 (*AnnAt1*) participates in Pb stress** by comparing its gene expression between Pb stressed and non-stressed *A. thaliana* seedlings using real-time PCR, and to **establish the possible relationship between Pb stress and *AnnAt1* in *A. thaliana* seedlings**.

Chapter 6

NO is an important signalling molecule in plant development and defense responses. It is suggested to scavenge heavy metal-induced ROS and change the antioxidant cellular system. Depending on its concentration, NO provokes both beneficial and harmful effects in plants. This chapter **investigates the protective effect of an exogenous supply of ni-**

tric oxide on Pb-induced toxicity, uptake, accumulation and tolerance in *A. thaliana* seedlings. The physiological and biochemical responses of 7-d-old seedlings were studied, and assessed if these responses are similar to the literatures. Experiments were also performed to **examine if the protective effect of nitric oxide alters the transcript level of *AnnAt1***.

Chapter 7

Chemical mutagenesis may contribute to identification of novel genes by producing Pb mutants with heritable alterations in the genomes, phenotypes and physiological responses. This chapter seeks to **screen EMS-mutagenized *A. thaliana* M_2 populations to identify Pb mutants with increasing Pb accumulation and tolerance**. The putative Pb mutants were isolated and grown for seed collection. Subsequent experiments **characterized the putative Pb mutant plants** by investigating the changes in morphology, Pb accumulation, sequestration, and regulation of *AnnAt1*.

Chapter 8

The final chapter presents an overall summary of studies undertaken in this project to advance our understanding in Pb phytoremediation using *A. thaliana* as a model system. Future research from the outcome of current works is also recommended.

Chapter 2

General materials and methods

2.1 Plant material and growth conditions

Wild-type *Arabidopsis thaliana* ecotype 'Columbia' (Col-0) seeds purchased from Lehle Seeds (Round Rock, TX, USA) were weighed into a 1.5 mL Eppendorf tube according to the number of seeds required (~5000 seeds/0.1 g). Seeds in the tube were surface-sterilized with 20% (v/v) bleach for 10 min, and rinsed thoroughly five times with distilled water in the laminar flow cabinet. The seeds were suspended in ~1 mL sterile dH_2O and cold-treated at 4˚C in the dark for 2 - 4 d to break dormancy and synchronize germination. Using a sterile Pasteur pipette, $\pm$150 seeds were placed evenly (Figure 2.1) across a 9 cm diameter Petri plate containing an agar medium (described in Section 2.2).

All agar plates were placed on the bench inside a growth room with continuous lighting (24 h photoperiod at 26.5 µE/s/m^2, 22˚C) in a completely randomized design.

2.2 Culture medium and its composition

Huang & Cunningham (1996) nutrient solution modified by Chin (2007) was used throughout this thesis, and is referred to as modified HC medium. This nutrient solution containing 0.8% (w/v) agar and salts (in Appendix A.1.1) at pH 4.5 - 5.0 was specially formulated for use in the Pb accumulation study. Acidic pH and low P concentration (0.5 µM KH_2PO_4) were chosen to prevent precipitation of Pb. This should ensure maximum Pb solubility in the medium.

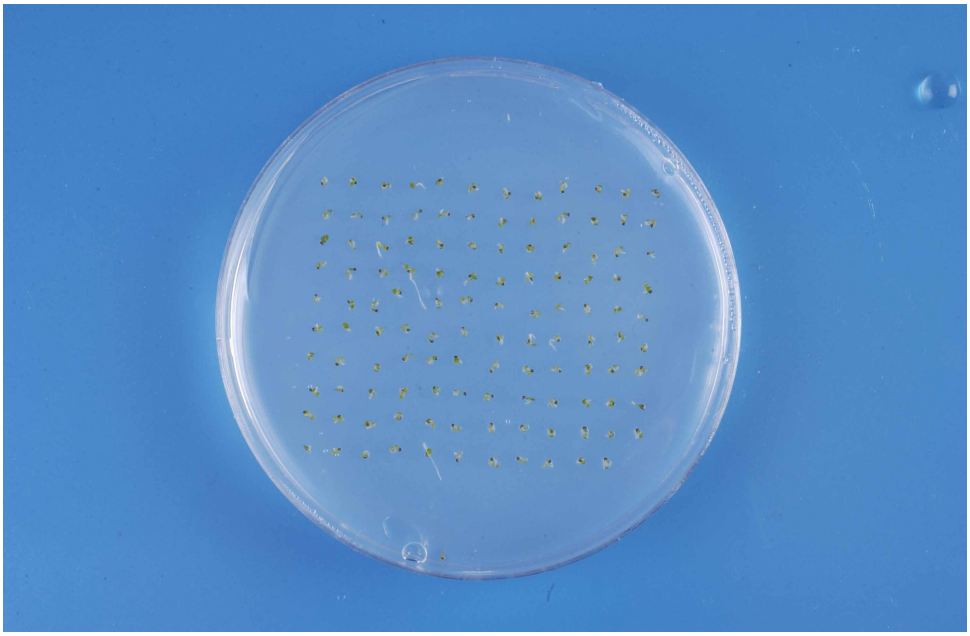

Figure 2.1: View of a culture plate from above showing the arrangement of seeds. There are approximately 150 seeds per plate.

The major salt stock (50 mL 10x concentrate) and minor salt stock (5 mL 100x concentrate) were mixed with 395 mL nanopure H_2O in a 500 mL glass bottle. The pH of the solution was adjusted to 4.7 with 0.1 M HCl using a pH meter (E350B, Metrohm, Herisau, Switzerland). Then, 4 g bacteriological grade agar (Danisco, Copenhagen, Denmark) was added and the solution was heated to dissolve the agar. The total volume of the solution was brought to 500 mL with nanopure H_2O before autoclaving at 121˚C for 20 min. After the autoclaved medium was cooled to ~50˚C, it was poured into sterile Petri dishes, each containing about 25 mL in the laminar flow cabinet. Upon solidification, the agar plates were sealed in a clean bag and kept at room temperature.

2.3 Pb treatments

Pb treatments were applied as lead nitrate, $Pb(NO_3)_2$ (BDH, Poole Dorset, UK). Stock solution of 0.1 M $Pb(NO_3)_2$ were prepared in a 100 mL polypropylene bottle and kept at 4˚C, for up to 6 months. The required Pb concentrations ranging from 25 µM to 200 µM,

or as specified, were added to the modified HC medium before pH adjustment. Non-Pb treatments served as controls.

2.4 Acid washing procedure

Since cations bound to the glassware and plasticware could compete with Pb at the uptake sites of a plant root, acid washing was indispensable. All glassware and plasticware, before and after use, were submerged overnight in an acid bath containing 10% (v/v) HNO_3 (BDH, Poole Dorset, UK) to remove potentially contaminating metal ions on the surface. Following acid wash, the laboratory items were triple-rinsed with dH_2O to ensure complete removal of all contaminants and remaining acid. Glassware and plasticware were inverted, drained and dried in a 50˚C oven before use. Unused items were capped for storage.

2.5 Appearance and morphology of seedlings

One week after sowing cold-stratified seeds, *A. thaliana* seedlings grown on modified HC medium were randomly selected and photographed using a stereomicroscope (Leica MZ 12.5) supplied by Vashaw Scientific Inc. (Norcross, GA, USA) that was connected to a digital camera (AxioCam HRc, Carl Zeiss Inc., Jena, Germany). A fibre optic cool light (KL1500 LCD, Schott AG, Mainz, Germany) was used to control lighting onto the specimens. Digital images were collected for a morphological study of *A. thaliana* seedlings in response to Pb toxicity. In this thesis, the term *seedlings* refers to 7-d-old *A. thaliana* with *root* and *shoot* as shown schematically in Figure 2.2.

2.6 Root length measurement

Ten seedlings were randomly collected from each horizontal plate and immediately laid across an agar plate to keep them moist. Petri dishes were placed on a black background for contrast and photographed using Nikon D1x camera fitted with a Nikon 60 mm Macro lens. A ruler was photographed under the same magnification for calibration.

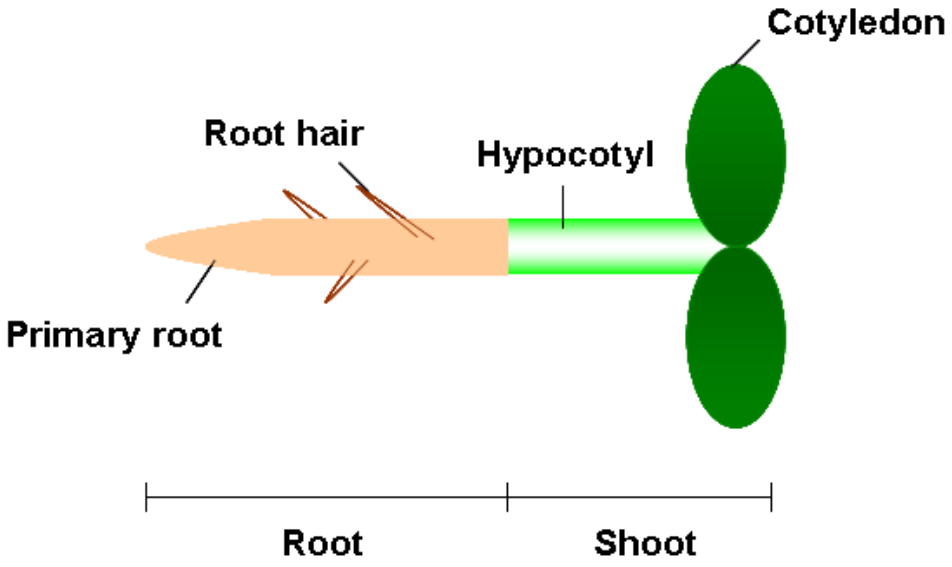

Figure 2.2: Schematic diagram of an *A. thaliana* seedling.

The root length was measured using Image-Pro Plus version 4.5 (Media Cybernetics Inc., Bethesda, MD, USA). The arithmetic mean of ten measurements was considered as one replicate to compensate for the variation in root length. For each of the investigations of the effects of Pb and other factors reported in subsequent chapters, at least two independent experimental series were carried out. Each of these experiments comprised of three replicates in each of the different experimental treatments.

2.7 Tolerance index

The mean of root length obtained for each Pb treatment in independent experiments was used for calculation of the tolerance index (TI). TI was defined by Wilkins (1957) as:

$$\text{Tolerance index (TI)} = \frac{\text{Mean of root length on agar medium containing Pb}}{\text{Mean of root length on control medium (without Pb)}} \text{x } 100\%$$

2.8 Graphite furnace atomic absorption spectroscopy

2.8.1 Metal extraction protocol

The total concentration of Pb in plant materials subjected to different treatments was determined following acid digestion. After 7 d of growth, ten seedlings were randomly selected from each agar plate. Samples were desorbed in 1 mM Na_2EDTA for 1 min to remove surface adherent Pb, washed thoroughly five times with nanopure H_2O, and blotted dry on a paper towel. Seedlings were excised into roots and shoots, and collected at the bottom of a 14 mL polypropylene tube. Concentrated HNO_3 (1 mL) was added and digestion of the plant materials was performed in a fume hood overnight in a water bath at $60 \pm 0.5^{\circ}C$. Nanopure H_2O of 9 mL was added into each tube to dilute the concentrate acid for suitability to work at the bench. Samples were diluted to 1% (v/v) HNO_3 with ddH_2O and mixed thoroughly in a 1 mL sample cup before GF-AAS analysis. At least two independent experiments with three replicates in each treatment were carried out. Reagent blanks (in the absence of plant material) were included to check for contamination.

2.8.2 Preparation of standard solutions

The graphite furnace atomic absorption spectrophotometer (GF-AAS) was calibrated each time it was used. A bulk standard solution containing 100 µmol/L $Pb(NO_3)_2$ was freshly prepared (analytical grade BDH) in 1% (v/v) HNO_3. The stock solution was serially diluted to 20, 50, 100, and 200 nmol/L $Pb(NO_3)_2$ working standard solutions. HNO_3 (1%, v/v) was prepared to zero the machine.

2.8.3 GF-AAS measurement

All quantitative Pb analysis was performed through a graphite furnace atomic absorption spectrophotometer (GBC Avanta with autosampler, GBC Scientific Equipment Pty. Ltd., Dandenong, Australia). The furnace method is ideal for sensitive measurements of samples with discrete volumes (1 - 100 µL). Basic checks including nitrogen gas and water supplies, graphite tube, lamp ignition, injection capillary, alignment of the workhead in the optical beam, slit height, and position of the autosampler trays were performed auto-

Step (#)	Temperature (˚C)	Ramp time (s)	Hold time (s)	Gas type	Read signal	Graphics
1			Inject sample			
2	40	5.0	1.0	Inert	Off	Off
3	95	10.0	10.0	Inert	Off	Off
4	150	10.0	1.0	Inert	Off	Off
5	400	10.0	10.0	Inert	Off	Off
6	400	1.0	0.0	None	Off	On
7	2000	1.0	1.0	None	On	On
8	2200	1.0	1.0	Inert	Off	On
9	40	11.3	1.0	Inert	Off	Off

Table 2.1: GF-AAS time/temperature program for the determination of Pb element in a 20 µL of injected sample volume in 1% (v/v) HNO_3.

matically upon starting up the machine.

The absorption due to Pb was measured at a wavelength of 217 nm using a Pb hollow cathod Super Lamp (GBC Scientific) operated at 8 mA lamp current and 1.0 nm slit width and using a deuterium continuum lamp for background correction. The furnace temperature program is summarized in Table 2.1. The machine was zeroed with 1% (v/v) HNO_3 at initial start-up, and rescaled with 1% (v/v) HNO_3 and 200 nmol/L $Pb(NO_3)_2$ after every ten samples.

2.8.3.1 Estimation of Pb content

For each sample, duplicate absorbance readings were taken and interpolated against calibration curves (an example is given in Appendix A.9), calculated automatically by the GBC Avanta software (version 1.33). Overrange samples were diluted with 1% (v/v) HNO_3 to obtain readings within the calibration curve. The Pb contents of plant materials were expressed as nmol/plant.

2.9 Transmission electron microscopy

The TEM methods outlined below are based on those of Jarvis (2001).

2.9.1 Samples preparation for TEM

Seedling samples, exposed and non-exposed to Pb, were randomly selected, desorbed in 1 mM Na_2EDTA for 1 min to remove surface adherent Pb, and washed thoroughly five times with dH_2O. Before fixation, the seedlings were dissected into roots and shoots.

2.9.2 Preparation of ultra-thin sections for TEM

Fixation, dehydration and infiltration steps were performed in a fume hood.

2.9.2.1 Fixation

Root and cotyledon tissue samples obtained from approximately similar locations were cut into thin slices (< 1 mm) using a scapel, and immediately placed in a small glass vial containing freshly made 3% (v/v) glutaraldehyde in 0.075 M sodium phosphate buffer, pH 7.2 (Appendix A.2.1). The tissues were fixed under partial vacuum for 3 h at room temperature before storing overnight at 4˚C. Following removal of fixative, the samples were rinsed in 0.075 M sodium phosphate buffer (twice for 10 min and then for 30 min). The samples were post-fixed in 1% (v/v) osmium tetroxide (OsO_4) in 0.075 M sodium phosphate buffer for 2 h at room temperature.

2.9.2.2 Dehydration

Post-fixed samples were dehydrated with a series of 20, 40, 60, and 80% (v/v) acetone for 10 min at each concentration. The dehydrated samples were transferred to 100% acetone three times, each for 15 min.

2.9.2.3 Infiltration

The samples were infiltrated with Spurr's resin (Electron Microscopy Sciences, Fort Washington, PA, USA). The first infiltration step was with one part of Spurr's resin and two

parts of 100% acetone, placed overnight on a slow rotating wheel at room temperature. The second infiltration step was with three parts of Spurr's resin and one part of 100% acetone, placed on a slow rotating platform for more than 3 h at room temperature.

2.9.2.4 Embedding

Samples were transferred to shallow plastic caps containing 100% Spurr's resin, placed on a glass Petri dish, and polymerized in a 60˚C oven overnight.

2.9.2.5 Ultramicrotomy

Specimens cut from resin blocks were glued to *stubs* (empty gelatin capsules filled with hardened epoxy resin), before setting overnight at room temperature. The excess resin of the stubs were trimmed to produce desired sections of the tissues. Ultra-thin sections of approximately 90 - 100 nm were cut with a ultramicrotome (LKB2128 Ultratome, Uppsala, Sweden) using a diamond knife and mounted on a copper grids (Electron Microscopy Sciences, Fort Washington, USA). Ultra-thin sections were unstained for viewing.

2.9.3 Microscopy, scanning of TEM negatives and image collection

The coppper grids were viewed using Hitachi H600 transmission electron microscope at 75 kV. Micrographs of regions of interest were taken on Kodak Electron Image Film SO-163 (8.3 x 10.2 cm). Developed negatives were scanned using Epson Perfection 1200U scanner and stored on a compact disc as TIF files.

2.10 Sample collection for biochemical and genetic studies

After 7 d of growth, seedlings were collected with straight fine point forceps into a sterilized pre-weighed 1.5 mL Eppendorf tubes placed on ice. The forceps were submerged in 100% ethanol for sterilization before use. Each tube was weighed immediately to minimize drying of specimens that might produce inaccurate data. Then, samples were flash

frozen in liquid nitrogen and stored at -80˚C until use. Similar steps were repeated for collection of replicates in each of the treatments. Fresh weight was calculated by substrating the weight of the empty tube.

2.11 Sample extractions for ROS and antioxidative enzyme assays

General methods for extraction of H_2O_2, lipid hydroperoxide and antioxidative enzymes (SOD, CAT, GR, GPX, POD) were provided by Dr. David J. Burritt (Department of Botany, University of Otago, Dunedin, New Zealand). Potassium phosphate buffer preparation is outlined in Appendix A.2.2. When required, frozen plant tissues were ground to a fine powder in liquid nitrogen using a mini plastic pestle in a 1.5 mL Eppendorf tube. All ground tissues were kept on ice and then processed further as described in Sections 2.11.1, 2.11.2 and 2.11.3. Supernatants obtained after centrifugation of the tissue homogenates were stored at -80˚C until analysis.

2.11.1 Hydrogen peroxide

Ice-chilled 100 mM potassium phosphate buffer (pH 6.4) containing 5 mM KCN and the catalase inhibitor hydroxylamine (0.5 mM) were added to the ground tissues (3 mL/g FW). The homogenates were centrifuged at 15,000 rpm for 15 min at 4˚C. The supernatant was used as the crude extract for the assay of hydrogen peroxide. Extracts for H_2O_2 assay were sealed with nitrogen gas before storage at -80˚C.

2.11.2 Lipid hydroperoxide

Methanol:chloroform (2:1 v/v) was added to the ground tissues (3 mL/g FW) and incubated for 1 min. Deionised water was added (2 mL/g FW) and mixed for 30 s. The chloroform phase at the bottom was transferred to a new Eppendorf tube after phase separation and used as the crude extract for the assay for lipid hydroperoxide. Crude extracts were stored at -80˚C.

2.11.3 Antioxidative enzymes (SOD, CAT, GR, GPX, POD)

Ice-chilled 100 mM potassium phosphate buffer (pH 7.0) containing 0.1 mM Na_2EDTA, 1% (w/v) PVP-40, 1 mM PMSF and 0.5% (v/v) TritonX-100 was added to the ground tissues (4 mL/g FW). The homogenates were centrifuged at 15,000 rpm for 15 min at 4˚C. The supernatants were used as the crude extracts for the assay of enzyme activities. Crude extracts were stored at -80˚C.

2.12 Assays for hydrogen peroxide, lipid hydroperoxide and antioxidative enzymes

All assays and enzymes activities were measured at 25˚C on a PC-controlled Perkin Elmer (Wallac) 1420 multilabel counter (Perkin Elmer, San Jose, California, USA), fitted with a temperature-controlled cell and an auto-dispenser. Data were processed by the WorkOut 2.0 software package (Perkin Elmer, San Jose, California, USA).

2.12.1 Hydrogen peroxide

Hydrogen peroxide (H_2O_2) concentrations were determined colorimetrically according to Cheeseman (2006). The differences in absorbance between 550 and 800 nm were calculated. Serial dilution of 30% (v/v) H_2O_2 (Merck Ltd, Palmerston North, New Zealand) was used to prepare a standard curve. The concentration of H_2O_2 in all standards was calibrated by measuring the absorbance at 240 nm and using an extinction coefficient of 43.6 M^{-1} cm^{-1}. H_2O_2 concentrations in the extracts were obtained by referring to the standard curve and expressed as nmol H_2O_2 per g FW.

2.12.2 Lipid hydroperoxide

Determination of lipid hydroperoxides followed the work of Mihaljevic *et al.* (1996) adapted for a microplate reader. Absorbance was read at 480 nm. Serial dilution of t-butyl hydroperoxide was used to prepare a standard curve. Lipid hydroperoxide contents in the extracts were obtained by referring to the standard curve and expressed as nmol lipid hydroperoxide per g FW.

2.12.3 Antioxidative enzymes

2.12.3.1 Superoxide dismutase

Superoxide dismutase (SOD, EC 1.15.1.1) activity was determined by its ability to inhibit cytochrome c reduction according to Banowetz *et al.* (2004). One unit of SOD is the quantity of enzyme that inhibits cytochrome c reduction by 50% in a coupled system with xanthine oxidase at pH 7.8 and 25˚C. The reaction mix contained 125 µL of piperazine-1,4-bis(2-ethanesulfonic acid) (Pipes) buffer (pH 7.8), 0.4 mM o-dianisidine, 0.5 mM DTPA, 26 µM riboflavin, and 50 µL enzyme extract (dH_2O as control). Samples were measured immediately (t = 0 min) and after illumination under 18 W fluorescent lamps placed 12 cm above the plate for 30 min. Absorbance was read at 450 nm. A regression analysis was used to generate a standard curve for SOD activity based on the change in A_{450} using bovine liver SOD (Sigma-Aldrich, St. Louis, MO, USA). Specific SOD activities in the extracts were interpolated against the standard curve and expressed as units SOD per mg total protein.

2.12.3.2 Catalase

Catalase (CAT, EC 1.11.1.6) activity was determined according to Maral *et al.* (1977), as adapted by Janssens *et al.* (2000). The reaction mix contained 100 µL of 100 mM phosphate buffer (pH 7.8), 100 mM Na_2EDTA, 1 µM H_2O_2, and 50 µL enzyme extract (dH_2O as control). After incubation at 25˚C for 30 min, 50 µL of a solution containing 20 mM luminol and 11.6 units/mL horseradish peroxidase (Sigma-Aldrich, St. Louis, MO, USA) were injected into each well. The light emission intensity was measured and it is proportional to the H_2O_2 remaining in the mixture. Absorbance was recorded at 240 nm. A regression analysis was use to generate a standard curve for CAT activity based on the intensity of light emission using purified bovine liver CAT (Sigma-Aldrich, St. Louis, MO, USA). Specific CAT activities in the extracts were interpolated against the standard curve and expressed as µL of H_2O_2 consumed per min per mg total protein.

2.12.3.3 Glutathione reductase

Glutathione reductase (GR, EC 1.6.4.2) activity was determined according to Cribb *et al.* (1989) with minor modification. The reaction mix contained 150 µL of 100 mM sodium phosphate buffer (pH 7.6), 0.1 mM DTNB, 10 µL NADPH (10 mg/mL; 12 mM) and 50 µL enzyme extract (dH_2O as control). The reaction was initiated by the addition of 10 µL GSSG (1 mg/mL; 3.25 mM). Absorbance was read at 415 nm for 3 min at 30 second intervals. Plates were shaken automatically before each reading. The rate of increase in A_{415} per min was calculated. A regression analysis was used to generate a standard curve for GR activity based on the change in A_{415} using standard wheat germ GR (Sigma-Aldrich, St. Louis, MO, USA). Specific GR activities in the extracts were interpolated against the standard curve and expressed as µmol oxidized glutathione reduced per min per mg total protein.

2.12.3.4 Glutathione peroxidase

Glutathione peroxidase (GPX, EC 1.11.1.9) activity was determined according to Paglia & Valentine (1967) with modification for microplate reader usage. The reaction mix contained 170 µL of 50 mM Tris-HCl buffer (pH 7.6), 5 mM EDTA, 0.14 mM NADPH, 1 mM GSH, 3 units/mL GR (from wheat germ, Sigma-Aldrich; EC 1.6.4.2) and 20 µL enzyme extract (dH_2O as control). The reaction was initiated by the addition of 20 µL 2.1 mM t-butyl hydroperoxide. Absorbance was read at 340 nm for 3 min at every 30 second interval, by monitoring the consumption of NADPH. Plates were shaken automatically before each reading. A regression analysis was used to generate a standard curve for GPX activity based on the change in A_{340} using bovine erythrocyte GPX (Sigma-Aldrich, St. Louis, MO, USA). Specific GPX activities in the extracts were interpolated against the standard curve and expressed as µmol per min per mg total protein.

2.12.3.5 Peroxidase

Peroxidase (POD, EC 1.11.1.7) activity was determined according to Gorecka *et al.* (2005) and adapted for microplate reader assays. The reaction mix for the fluorometric method contained 50 mM potassium phosphate buffer (pH 7.4), 2 mM H_2O_2, Amplex Red reagent

(Sigma-Aldrich, St. Louis, MO, USA) at a final concentration of 100 μM, and enzyme extract (horseradish peroxidase as positive control, and BSA as negative control). Absorbance was read at 590 nm, by monitoring the florescence emission of resorufin, a product oxidized from the Amplex Red reagent. Specific POD activities were expressed in relative fluorescence unit per mg total protein.

2.13 Agarose gel electrophoresis

2.13.1 Agarose gel preparation

Agarose gel (1%, w/v) electrophoresis was performed using a Bio-Rad Mini Sub™ DNA Cell (Bio-Rab Laboratories Inc., Hercules, CA, USA) apparatus. Agarose (0.3 g, Bio-Rad) was heat dissolved in 30 mL 1x TAE buffer (see Appendix A.2.3). Before gel setting, 3 μL SYBR® Safe DNA Gel Stain (Invitrogen, San Diego, CA, USA) was added and mixed well by swirling gently. After this, the gel solution was poured slowly into the gel rack to avoid bubble formation.

2.13.2 Gel electrophoresis

Each sample (5 μL) was mixed with 1 μL loading buffer (30% (v/v) glycerol and 0.25% (v/v) bromophenol blue). DNA 100 bp molecular weight marker XIV (2 μL, Roche Diagnostics GambH, Mannheim, Germany) was loaded alongside with DNA samples. Electrophoresis was carried out at a constant voltage setting of 80 V for 1 h at room temperature.

2.13.3 Gel visualization and photography

Agarose gel was examined under UV illumination and photographed using the SynGene Chemi Genius Bioimaging System (Synoptics Ltd., Cambridge, UK). Images were stored in the computer in TIF or JPG files.

2.14 Elimination of RNase for molecular biology work

Since RNase contamination present in the environment threatened the integrity of RNA at all stages, care was taken to eliminate the possibility of RNase contamination. Before commencing each molecular task, the surface of the lab bench, the laminar flow cabinet, glassware, plasticware, pipettors, and other equipment were wiped with RNaseZap® (Sigma-Aldrich, St. Louis, MO, USA). Gloves were to be wore at all times and wiped with RNaseZap frequently. LabServ® RNase-free microcentrifuge tubes (Fisher Scientific, Waltham, MA, USA) and filtered pipette tips (Axygen Inc., Union City, CA, USA) were used. Glassware was autoclaved prior to use. Then, the glassware was washed with RNaseZap® in the laminar flow cabinet. After swirling gently to ensure that the internal surface of the glasswares were in contact with the solution, it was rinsed three times with DEPC-H_2O (Appendix A.2.4).

2.15 Preparation of nucleic acid

2.15.1 Isolation of total RNA

Frozen tissues ($\leq$ 100 mg) were ground in liquid nitrogen to a fine powder using a mini plastic pestle that had been soaked in 3% (v/v) H_2O_2 overnight. Total RNA was extracted from disrupted tissues using RNeasy Plant Mini Kit (Qiagen GmbH, Hilden, Germany) following the manufacturer's procedure with slight modification as described below.

Tissue disruption, RNA extraction and precipitation: Firstly, 450 µL Buffer RLT working solution (10 µL β-mercaptoethanol per 1 mL Buffer RLT) was added to each sample tube, which was then vortexed and incubated at 56˚C for 2 min to assist tissue disruption. Then, the lysate was transferred to a lilac QIAshredder spin column placed in a 2 mL collection tube, and centrifuged at 15,000 rpm for 2 min to remove cell debris and homogenize the lysate. The supernatant was then transferred to a new RNase-free microcentrifuge tube without disturbing the cell debris pellet in the collection tube. Ethanol (100%, v/v) was added (1 volume of supernatant: 0.5 volume of ethanol) to clear the lysate and mixed immediately by pipetting. The sample, including any precipitate, was transferred to a pink RNeasy spin column placed in a 2 mL collection tube. The lid was

closed and centrifuged at 10,000 rpm for 15 s. The flow-through was discarded. All centrifugations were carried out at room temperature.

Elimination of genomic DNA contamination: On-column DNase digestion was carried out with an RNase-Free DNase kit (Qiagen GmbH, Hilden, Germany) according to the manufacturer's procedure (see Appendix A.2.5) to eliminate genomic DNA contamination that can serve as a template during PCR and lead to dubious results. A 350 µL volume of Buffer RW1 was added to the spin column and incubated for 5 min at room temperature. After centrifugation at 10,000 rpm for 15 s, the flow-through was discarded, and 10 µL DNase I stock solution was added to 70 µL Buffer RDD. Mixing was carried out by gently inverting the tube as DNase I is sensitive to physical denaturation. The mixture was centrifuged briefly to collect residual liquid from the wall to the bottom of the tube. DNase I incubation mix (80 µL) was added directly to the RNeasy spin column membrane and incubated at room temperature for 15 min. After this, 350 µL Buffer RW1 was added to the spin column, centrifuged at 10,000 rpm for 15 s, and the flow-through was discarded completely without contacting the spin column.

RNA wash: To wash the spin column membrane, 500 µL Buffer RPE working solution (1 volume of Buffer RPE concentrate: 4 volumes of 100 % v/v ethanol) was added, and centrifuged at 10,000 rpm for 15 s. The flow-through was discarded. This step was repeated by adding 500 µL Buffer RPE working solution and centrifuged at 10,000 rpm for 2 min to ensure that no ethanol was carried over during RNA elution. The RNeasy spin column was removed from the old collection tube with the flow-through, and placed in a new 2 mL collection tube. After this, it was centrifuged at 15,000 rpm for 1 min to eliminate any possible carry-over of Buffer RPE or residual flow-through.

Elution of RNA from RNeasy spin column: RNase-free H_2O (40 µL) was added to the spin column membrane that was placed on top of a new 1.5 mL collection tube, and incubated at room temperature for 10 min. After centrifugation at 10,000 rpm for 1 min, the RNA eluate was pipetted back onto the spin column membrane and re-centrifuged to obtain a higher final RNA yield. Lastly, RNAsecure Reagent (Ambion, Austin, TX, USA) was diluted to a final concentration of 1x in the RNA extract and mixed well. The mixture was incubated at 60˚C for 10 min, and cooled to room temperature. Isolated RNA was divided into smaller aliquots in RNAse-free microcentrifuge tube, and stored at -80˚C

until use.

2.15.2 Quantification of isolated RNA

The concentration of each RNA sample was measured by pipetting 2 µL RNA extract onto the pedestal of NanoDrop® ND-100 Spectrophotometer (BioLab Nanodrop Technologies, Wilmington, DE, USA). The purity of RNA can be estimated from the ratio of the readings at 260 nm and 280 nm (A_{260}/ A_{280}), as stated by Udvardi *et al.* (2008). A ratio of $\geq$ 1.8 indicates that RNA preparation is of high quality. Alternatively, RNA purity can be estimated from the ratio of the readings at 260 nm and 230 nm (A_{260}/ A_{230}). A ratio of $\geq$ 2.0 indicates that RNA preparation is pure.

2.15.3 Integrity of isolated RNA

Gel electrophoresis is the most common technique that allows visualization of discrete intact ribosomal bands and may be used to estimate the degree of RNA degradation. The integrity and size distribution of total RNA was assessed by 1% (w/v) agarose gel electrophoresis using a Bio-Rad Mini Sub™ DNA Cell apparatus (Bio-Rab Laboratories Inc., Hercules, CA, USA). SYBR® Safe DNA Gel Stain (3 µL, Invitrogen, San Diego, CA, USA) was added to agarose gel and mixed well before solidification. DNA 100 bp molecular weight marker XIV (2 µL, Roche Diagnostics GambH, Mannheim, Germany) was loaded into the first lane. Isolated RNA extract (5 µL) was mixed with 1 µL loading buffer before it was placed into a well. Agarose gel electrophoresis was performed at 80 V for 1 h. The gel was examined under a UV illuminator and photographed using the SynGene Chemi Genius Bioimaging System (Synoptics Ltd., Cambridge, UK).

The sharpness of the bands and the ratio of 28S rRNA to 18S rRNA was assessed for RNA integrity. Sharp bands without smearing indicated no RNA degradation was observed. The ratio of 28S rRNA to 18S rRNA of approximately 2:1 indicated that the RNA purified was of high integrity. The absence of extra high molecular weight band confirmed the absence of genomic DNA.

2.15.4 Reverse-transcriptase for synthesis of cDNA

First-strand complementary DNA (cDNA) synthesis was carried out using two-step RT-PCR according to the instructions from Transcriptor Reverse Transcriptase (Roche Diagnostics GambH, Mannheim, Germany). Reagents were thawed and placed on ice before starting. Firstly, denaturation of RNA secondary structure was performed by incubating 1 µg RNA, 1 µL Oligo-p$(dT)_{15}$ primer (50 pmol), 1 µL random hexamer primer p$(dN)_6$ (100 pmol), and DEPC-H_2O in a total volume of 13 µL at 65˚C for 10 min.

The mixture was put immediately on ice for 5 min. Then, 7 µL master mix comprising 4 µL transcriptor RT reaction buffer (5x), 0.5 µL RNAse inhibitor (40 U/µL), 2 µL dNTP-mix (10 mM) and 0.5 µL transcriptor reverse transcriptase (20 U/µL) was added into each mixture. The mixture in a microcentrifuge tube was briefly spun to send it to the bottom of the tube.

The total 20 µL reaction mixture was incubated at 25˚C for 10 min, followed by 55˚C for 30 min in a MJ Research PTC-200 Peltier Thermal Cycler (MJ Research Inc., Waltham, MA, USA) or a Bio-Rad DNA Engine Peltier Thermal Cycler (Bio-Rad Laboratories Inc., Hercules, CA, USA). The reaction was inactivated by heating to 85˚C for 5 min. Following the preliminary tests to select cDNA concentration, a 10-fold dilution of the synthesized cDNA was made using DEPC-H_2O and stored at -20˚C for subsequent PCR analysis.

All chemicals were purchased from Roche Diagnostics GambH (Mannheim, Germany). Each reaction mixture containing a total volume of 20 µL was set up in a RNase-free microcentrifuge tube. An outline of the reverse transcription (RT) procedure used is given in Table 2.2.

2.16 Real-time PCR

2.16.1 Primers

PCR primers were designed using web Primer3 (Rozen & Skaletsky, 2000) based on the cDNA sequences obtained from the open access database, NCBI (http://www.ncbi.nlm.nih-.gov/Entrez/) in Appendix A.4. A standard set of criteria governing the primer sequence

1) Denaturation of RNA secondary structure

Reagent	**Volume (µL)**	**Final concentration**
Template RNA	X	1 µg
Oligo-p$(dT)_{15}$ primer	1.0	50 pmol
Random hexamer primer p$(dN)_6$	1.0	100 pmol
DEPC-H_2O	13-1-1-X	variable
Final volume for denaturation	*13.0*	

Incubate at 65˚C for 10 min, then immediately place on ice for 5 min

2) Master mix preparation

Reagent	**Volume (µL)**	**Final concentration**
Transcriptor RT reaction buffer (5x)	4.0	1x
RNAse inhibitor (40 U/µL)	0.5	20 U
dNTP-mix (10 mM)	2.0	1 mM
Transcriptor reverse transcriptase (20 U/µL)	0.5	10 U
Total volume of reaction mixture	*20.0*	

Vortex to mix well, spin briefly to collect at the bottom

3) Incubation 25˚C for 10 min, then 55˚C for 30 min

4) Inactivation of RT enzyme Heat at 85˚C for 5 min, then place on ice

Table 2.2: Procedure for reverse transcription.

selection were used: similar melting temperature (T_m = 60 ± 3˚C), 18 - 25 nucleotides in length, 40 - 60% GC content, yielded a short PCR product (100 - 200 bases), and 90 - 110% PCR amplification efficiency (van Pelt-Verkuil *et al.*, 2008e; Udvardi *et al.*, 2008). Then, a NCBI-BLAST database search (http://www.ncbi.nlm.nih.gov/BLAST) against the *Arabidopsis* (*Arabidopsis thaliana*) transcript database was performed on the resulting primer pair sequences. This ensures the uniqueness of the target sequence and avoids amplification of primers pairs on other templates. Primer-BLAST (http://www.ncbi.nlm.nih-.gov/tools/primer-blast/) developed by NCBI was also used in the selection of primer pairs. Summary of selected primer pairs generated by the programs are shown in Appendix A.5.

Candidate primers were tested in real-time PCR. A dissociation curve (Section 2.17.1) was generated to check for specificity of the amplification product and further confirmed by agarose gel electrophoresis (Section 2.17.2). Upon validation, the selected primer pairs were used for real-time PCR (Table 2.3). The other housekeeping genes are shown in Chapter 5.

All primers were purchased from Invitrogen (Santa Diego, CA, USA). Ice-chilled DEPC-H_2O was added to dissolve the lyophilized primer to a stock concentration of 100 µM. This primer stock solution was calculated using the number of nmoles stated in the certificate of analysis provided by Invitrogen. The primer working solution of 6 µM was prepared by diluting with DEPC-H_2O. Both primer stock solution and working solution were stored at -20˚C for subsequent PCR analysis.

Gene	**Forward primer**	**Reverse primer**
Mitosis protein YLS8	TCCCGTGAACTGGTTTCATT	CAACGGCTTCCAAATTTCAT
Annexin 1	GGAACAGCATTCCTTTGGAG	GCAGCTTATGTTTCTCTGTGGA

Table 2.3: Primer sequences for real-time PCR.

Components	Volume (µL)	Final concentration in reaction mixture
Diluted cDNA template	1.0	
FastStart SYBR Green Master	10.0	1x
DEPC-H_2O	7.0	
Total volume	*18.0*	

Table 2.4: PCR mix for one reaction before mixing with specific primers.

2.16.2 Preparation of the real-time PCR reaction mix

The PCR mix was prepared according to the procedure for FastStart SYBR Green Master (Roche Diagnostics GambH, Mannheim, Germany). Before starting, all reagents were thawed, briefly spun to the bottom of a microcentrifuge tube, pipetted up and down to mix, and placed on ice. In a 1.5 mL RNAse-free microcentrifuge tube, each 20 µL reaction contained 1 µL diluted cDNA template, 1 µL each of the forward and reverse primers from the respective working solutions (6 µM), 10 µL FastStart SYBR Green Master, and 7 µL DEPC-H_2O. "No template control" (NTC) contained 1 µL DEPC-H_2O instead of diluted cDNA.

Technical errors in real-time PCR were lessened by standardizing and minimizing the number of pipetting steps. When there was more than one reaction, the PCR mix was prepared by multiplying the quantity in the 'Volume' column in Table 2.4 by z, where z = the number of reactions to be run + one additional reaction. Diluted cDNA was mixed with the other PCR components (in Table 2.4) before the required aliquote was placed into a thin-wall PCR tube (Axygen Inc., Union City, CA, USA) containing the specific primer pairs. This was followed by a brief centrifugation to obtain the samples at the bottom of the PCR tubes.

2.16.3 Real-time PCR condition

To minimize variation between PCR runs, aliquots of the PCR reaction mix (as prepared in Section 2.16.2) containing primers of target and reference genes were performed in the

Program setting	Cycles	Target temperature (˚C)	Hold time
Prevention of carry-over contamination	1	50	2 min
Activation of FastStart Taq DNA Polymerase	1	95	10 min
PCR	40		
Denaturation		95	15 s
Annealing of primers		54	60 s
Extension		72	30 s

Table 2.5: Program settings for amplification of *AnnAt1* by real-time PCR.

same PCR run. Real-time PCR was performed in a 96-well reaction plate with a thermal cycler (Stratagene Mx3005P™, Agilent Technologies Inc., Santa Clara, CA, USA). Thermal cycling conditions in Table 2.5 were used in real-time PCR. Fluorescent data were acquired at the end of extension phase, using MxPro3005P software (Stratagene, Agilent Technologies Inc., Santa Clara, CA, USA).

2.17 Specificity of the PCR amplification product

2.17.1 Melting curve

An automated melting curve program in the MxPro3005P (Stratagene, Agilent Technologies Inc., Santa Clara, CA, USA) was conducted after 40 cycles to check for specificity of amplification (Table 2.6). All PCR amplification products were melted at 95˚C, annealed at 55˚C, and followed by a gradual increase in temperature at a heating rate of 0.1˚C per second. Continuous fluorescent data were collected until the reaction reached 95˚C, where the major PCR product melted to form single strand.

The melting peak was obtained by plotting the negative first derivative of raw fluorescence, R'(T) to pinpoint the temperature. The presence of a single homogenous melting peak for all sample reactions showing that PCR amplification was specific. The NTC sample was evaluated for the presence of primer-dimer formation. It was acceptable if only a small wide peak was observed at a lower temperature indicating a small amount of

Program setting	Cycles	Target temperature (˚C)	Hold time (s)
Melting	1		
Segment 1		95	60
Segment 2		55	30
Segment 3		95	30

Table 2.6: Program setting for melting curve analysis by real-time PCR.

primer-dimer formation.

2.17.2 Agarose gel electrophoresis

An optimized assay yielded only a single specific product. Specificity of real-time PCR amplification was double-checked with gel electrophoresis to confirm the presence of a single product with the expected size. This acted as an additional control to determine real-time PCR product specificity besides the dissociation curve data. Procedure for agarose gel electrophoresis was carried out as explained in Section 2.13.

2.18 Quantification of gene expression

2.18.1 Relative quantification method

The relative quantification method was used to quantify the relative copy number of *AnnAt1* in unknown samples, compared to the control sample. Ct is defined as the instant where the fluorescence signal is first detected as it rises significantly above the background fluorescence (van Pelt-Verkuil *et al.*, 2008e). The Ct value was calculated by MxPro3005P software (Stratagene, Agilent Technologies Inc., Santa Clara, CA, USA). Differences in Ct values between unknown samples and the control sample were expressed as fold-changes (up- or down-regulated) relative to the control sample. The PCR efficiency of gene-specific and internal control primers were determined beforehand. The relative expression of *AnnAt1* was then normalised to the expression of the mitosis protein YLS8,

the stably expressed reference gene transcript. Then, the relative expression ratio was determined based on the PCR efficiency and Ct of the investigated transcript according to the formula:

$$\text{Ratio}=\frac{(E_{\text{AnnAt1}})^{\triangle Ct_{\text{AnnAt1}}(\text{Mean control-Mean sample})}}{(E_{\text{ref}})^{\triangle Ct_{\text{ref}}(\text{Mean control-Mean sample})}}$$

(E = average real-time PCR reaction efficiency; Ct = differences of Ct values between control and treatement) (Pfaffl, 2001; van Pelt-Verkuil *et al.*, 2008e)

2.18.2 Statistical analysis for gene expression

To confirm the accuracy and reproducibility of real-time PCR, each PCR reaction was performed in triplicate with no-template controls. The entire experiment, including RNA isolation, reverse transcription and real-time PCR analysis was repeated. This yielded at least two independent experimental replications. Results (Ct values) obtained from MxPro3005P (Stratagene, Agilent Technologies Inc., USA) were analyzed in REST 2008 (Pfaffl *et al.*, 2002), using pair-wise randomization test. *P*-values which were less than or equal to 0.05 were considered significant.

2.19 Preparation of total protein extract

The total protein extraction protocol was modified from Weigel & Glazebrook (2002). Frozen tissues (~100 mg) were ground in liquid nitrogen to a fine powder using a mini plastic pestle. Fresh PMSF (2 mM) was prepared each time a homogenization buffer was used. Ice-cold protein extraction buffer (Appendix A.2.6) consisted of 50 mM Tris-acetate (pH 7.9), 100 mM potassium acetate, 1 mM Na_2EDTA, 1 mM DTT, 20% (v/v) glycerol, 2 mM PMSF, and Complete mini-protease inhibitor cocktail tablets (1 tablet per 5 mL total volume; Roche Diagnostics GambH, Mannheim, Germany) were added to the powdered tissue (1 mL/g FW). Following the preliminary tests, a high concentration of protease inhibitor was required to avoid proteolysis of the protein of interest. Immediately after gentle suspension of tissue in the homogenization buffer on ice, samples were clarified by

centrifugation at 15,000 rpm for 5 min at 4˚C. The supernatant was transferred to a new sterilized Eppendorf tube without disturbing the cell debris pellet. This was re-centrifuged at 15,000 rpm for 5 min at 4˚C to further eliminate the cell debris. Isolated total protein was divided into smaller aliquots and stored at -80˚C until use.

2.20 Estimation of protein concentration

The protein contents of the crude extracts were quantified following the work of Bradford (1976). BSA (Gibco, Invitrogen, San Diego, CA, USA) was used to generate a standard curve over 4 dilution points (0, 25, 50 and 100 µg/mL) that were measured in triplicate. A standard curve was plotted from the mean absorbance value at 595 nm, by linear regression in Microsoft Office Excel 2003 (Microsoft Corporation, Redmond, WA, USA). Crude extracts were diluted by adding homogenization buffer at appropriate ratios. Then, 1 mL Bradford reagent was added to 100 µL diluted crude extract (buffer as control), vortexed and incubated for 5 min at room temperature. Absorbance was read at 595 nm, using SmartSpec™ Plus spectrophotometer (Bio-Rab Laboratories Inc., Hercules, CA, USA) or NovaSpec II spectrophotometer (Pharmacia, Cambridge, England). Distilled water was used to zero the spectrophotometer. Protein concentrations of the extracts were obtained by referring to the standard.

2.21 SDS-Polyacryamide gel electrophoresis

Reagents and buffer for SDS-PAGE are described in Appendix A.2.7.

2.21.1 Gel preparation

Proteins in the crude extracts were separated by size using one-dimensional discontinuous SDS-PAGE as per Laemmli (1970) with slight modification, using a Mini-PROTEAN III gel apparatus (Bio-Rab Laboratories Inc., Hercules, CA, USA). Briefly, a 12% separating gel was prepared by adding 2 mL acrylamide/bis (30%, w/v) to 1.25 mL Tris-HCl (1.5M, pH 8.8) containing 50 µL SDS stock (10%, w/v) and 1.675 mL dH_2O. Polymerization was initiated by adding 25 µL of freshly prepared ammonium persulphate (10%, w/v) and

10 µL TEMED. This solution was poured into the space of a glass sandwich formed by two glass plates in the Mini-PROTEAN III gel apparatus.

A 4% stacking gel was prepared by adding 650 µL acrylamide/bis (30%, w/v) to 1.25 mL Tris-HCl (0.5 M, pH 6.8) containing 50 µL SDS stock (10%, w/v) and 3.05 mL dH_2O. Polymerization was also initiated by the addition of 25 µL of freshly prepared ammonium persulphate (10%, w/v) and 10 µL TEMED.

2.21.2 Sample preparation

Three volumes of crude extracts were mixed with one volume of 4x Laemmli SDS sample buffer containing 8% (w/v) SDS, 40% (v/v) glycerol, 20% (v/v) β-ME, and 0.5% (w/v) bromophenol blue in 0.25 M Tris-HCl (pH 6.8). After a brief centrifugation to collect the mixture at the bottom of the tube, samples were boiled for 3 min. Then, 10 µg of the remaining protein samples were used to pipette into each of the designated lanes on the gel.

2.21.3 Running condition

A prestained Bio-Rad low range SDS-PAGE standards (5 µL; Bio-Rab Laboratories Inc., Hercules, CA, USA) was loaded into the first well of a vertical gel. This allowed monitoring of the protein migration during an electrophoretic run and estimation of protein size. An approximately equal volume of 1x Laemmli SDS sample buffer was added into empty wells to ensure even migration of the dye front as the gel was running. Tris-HCl (25 mM, pH 8.3) containing 192 mM glycine and 0.1% (w/v) SDS was used as the running buffer. Electrophoresis was carried out at 30 mA at a constant voltage setting of 200 V for 39 min.

2.21.4 Polyacryamide gel staining

After the SDS-PAGE, proteins were visualized by staining with 0.1% (w/v) Coomassie Blue R-250 (Gibco BRL, Gaithersburg, MD, USA) in a fixative containing 10% (v/v) acetic acid and 40% (v/v) methanol for 30 min with gentle shaking. The gel was destained with several changes of 10% (v/v) acetic acid and 40% (v/v) methanol for approximately 1

h to remove background. After that, the gel was photographed using the SynGene Chemi Genius Bioimaging System (Synoptics Ltd., Cambridge, UK).

2.22 Western blotting

Western blot was used to detect the expression level of AnnAt1 protein in response to Pb treatments. The reagents and buffer for western blotting were described in Appendix A.2.8.

2.22.1 Transfer and blocking

Protein in the crude extracts (35 µg) were first resolved by SDS-PAGE (Section 2.21) and transferred to a nitrocellulose membrane. The membrane was placed on top of the gel and sandwiched between 5 layers of Whatman filter papers (2-3 mm thick) which was cut to an appropriate size. The membrane and filter papers were wet beforehand with 1x blotting bufffer consisted of 20 mM Tris-HCl (pH 8.3), 150 mM glycine and 20% (v/v) methanol. A stack of absorbance papers was placed on top of the sandwich and assembled in place so that the buffer solution moved up to the paper by capilary action, bringing the proteins with it.

After an overnight transfer process, the stack was disassembled. The transfer of the prestained markers in a lane on the membrane indicated that most of the proteins of interest were also transferred. This marker lane was excised from the membrane for future reference. The remainder of the membrane was incubated in a blocking solution containing 1% (w/v) BSA in TBST (0.9%, w/v, NaCl; 20 mM Tris-HCl, pH 7.5; and 0.05%, v/v, Tween-20) for 30 min on a gentle shaker. The membrane was then rinsed twice, each for 30 min in TBST.

2.22.2 Immunodetection

A primary antibody for AnnAt1, which had been raised against peptides that were synthesized on the basis of a 31 amino acid sequence (amino acids 200-231) in guinea pig (Clark *et al.*, 2005), was obtained from Dr. Gregory B. Clark and Dr. Stanley J. Roux

(Department of Molecular Cell and Developmental Biology, University of Texas, Austin, Texas, USA). Diluted primary antibody in the blocking solution was added to the surface of the membrane and incubated overnight at room temperature. After washing the membrane thrice with TBST for 10 min each, diluted secondary antibody in blocking solution was placed onto the surface of the membrane and incubated at room temperature for 1 h with gentle shaking. The secondary antibody applied was phosphatase-labeled goat anti-guinea pig IgG (H+L) (Sigma-Aldrich, St. Louis, MO, USA), as per Clark *et al.* (2005). The membrane was again washed thrice with TBST for 10 min each. Alkaline phosphatase activity was recognized by NBT-BCIP (Nitro blue tetrazolium:5-bromo-4-chloro-3-indolyl phosphate).

2.23 Statistical analysis

All values are presented as means with its standard error (SE), with a minimum of three replicates. Independent experiments were repeated at least twice. STATISTICA 8 (StatSoft Inc., Tulsa, OK, USA) was used to perform statistical analysis in this thesis. In earlier studies, Minitab 14 Student (Minitab Inc., Stage College, PA, USA) and SPSS 13.0 Windows for Integrated Student Version (SPSS Inc., Chicago, IL, USA) were used.

Firstly, all data were tested for homogeneity of variance (Hartley's F-max) to determine if the data required transformation prior to Analysis of Variance (ANOVA). When the resulting F-max ratio was greater than the critical value of the corresponding tabular value, data were square-root or $\log_{10}$ transformed to improve its distribution around the mean and fit the assumption of ANOVA. Hartley's F-max was re-tested prior to ANOVA. All data presented in this thesis passed Hartley's F-max test.

The difference between the means of treatments were tested with One-way ANOVA (or Factorial ANOVA to test the interaction effect between two or more treatment variables). *P*-values which were less than or equal to 0.05 were considered significant. Statistically significant treatments were then compared using the Fisher's Least Significant Difference (LSD) test. Different letters in graphs or tables indicate significant differences at $p < 0.05$.

Chapter 3

Physiological responses of *Arabidopsis thaliana* seedlings to Pb exposure

3.1 Introduction

Plants exposed to Pb stress make specific changes in their cell physiology to avoid or tolerate the stress. In this chapter, the physiological responses of *Arabidopsis thaliana* seedlings to Pb exposure grown in a controlled environment of Petri plates are reported. Seven-d-old seedlings were used in the present study because the early developmental stages in the life of a plant must trigger future physiological and biochemical processes (Singh *et al.*, 1997). Consistent with these authors review, prolonged exposure to the toxic effects of Pb at the physiological level was found to be lethal to *A. thaliana* in the preliminary study. Plants that were unable to survive were unsuitable for the type of experiments reported in this study.

Basic growth responses to increasing Pb concentrations exhibit a characteristic uptake response curve, the phases of which correspond to ranges of tolerance and toxicity. A tolerance index (TI) was determined according to Wilkins (1957). The patterns of Pb uptake and translocation in plants were assessed using graphite furnace atomic absorption spectroscopy (GF-AAS) and transmission electron microscopy (TEM). The Pb localization studies provided an insight into the possible sites of metal sequestration and changes in subcellular structure that might occur in plants exposed to Pb. The Pb accumulation capacity of roots and shoots in *A. thaliana* seedlings extends our knowledge of how plant

cells are able to tolerate the presence of Pb and contributes to the success of Pb phytoremediation techniques. The physiological responses of *A. thaliana* seedlings to Pb exposure underpin the biochemical and molecular studies in the following chapters.

3.2 Materials and methods

3.2.1 Plant material and culture conditions

Approximately 150 *A. thaliana* ecotype 'Columbia' seeds were sown on an agar plate containing modified Huang & Cunningham (1996) nutrient solution (see Sections 2.1 and 2.2). There were three replicate plates in each Pb treatment group.

3.2.2 Assessment of Pb toxicity and plant growth

3.2.2.1 Germination rate

After 7 d of growth, the number of seedlings producing roots and shoots were recorded and the germination percentage was scored as follows:

$$\text{Germination percentage (\%)} = \frac{\text{Number of seedlings producing roots and shoots after 7 d}}{\text{Total number of seeds sown on agar plate (~150)}} \text{ x } 100\%$$

This experiment which comprised of three replicates was repeated twice.

3.2.2.2 Appearance and morphology

One week after sowing cold-stratified seeds, 15 *A. thaliana* seedlings were randomly selected and photographed (see Section 2.5). Digital images were collected for a morphological study of *A. thaliana* seedlings in response to Pb toxicity (0, 50, 100, 150 and 200 µM $Pb(NO_3)_2$), including changes in the shape, appearance and colour of roots and cotyledons.

3.2.2.3 Effect of Pb on growth rate (Fresh weight)

Twenty seedlings were randomly transferred with straight fine point forceps into each of the three pre-weighed 1.5 mL Eppendorf tubes that was placed on ice. Each tube was weighed immediately to minimize drying of specimens. A similar procedure was used for collection and weighing of seedlings after each of the Pb treatments. Fresh weight was calculated by subtracting the weight of the empty tube. This experiment which comprised of three replicates for each treatment (0, 50, 100, 150 and 200 µM $Pb(NO_3)_2$) was repeated twice.

3.2.2.4 Root length measurement

Ten seedlings were randomly collected and photographed using Nikon D1x camera fitted with a Nikon 60 mm Macro lens (see Section 2.6). The mean of ten measurements was considered as one replicate to compensate for the variation in root length. Three independent experimental series were carried out; each of these experiments comprised of three replicates each of the different Pb treatments (0, 25, 50, 75, 100, 150 and 200 µM $Pb(NO_3)_2$).

3.2.2.5 Tolerance index

The mean of the root lengths obtained for each Pb treatment in three independent experiments (from Section 3.2.2.4) was used for calculation of the tolerance index (TI). The formula is shown in Section 2.7.

3.2.3 Rhodizonate test

The sodium rhodizonate test allowed visual observation of Pb residues *in situ* (on the seedlings). A colorimetric procedure was conducted according to Jurkiewicz *et al.* (2001). In this experiment 2-week-old *A. thaliana* seedlings were used. Ten plants were randomly selected for investigation and washed thoroughly in dH_2O three times. Samples were soaked in the staining solution consisting of 0.2 g potassium rhodizonate (Sigma-Aldrich) in 100 mL tartaric acid-sodium bitartrate buffer (pH 2.8) for 1 h at room temperature. The buffer was prepared by adding 3 g tartaric acid (Sigma-Aldrich) and 3.8 g sodium

bitartrate in 200 mL nanopure H_2O. Ten mL staining solution were used in each 5 cm diameter Petri dish placed on a piece of white paper for contrast. After removing the staining solution, samples were washed with tartaric acid-sodium bitartrate buffer for 10 min, and photographed using a Nikon D1x camera fitted with Nikon 60 mm Macro lens. Then, the same specimen was observed under a dissecting microscope. The formation of pink colour as a result of Pb rhodizonate precipitation on Pb-containing samples indicates the presence of Pb.

3.2.4 Graphite furnace atomic absorption spectroscopy

The total concentration of Pb in plant materials from different treatments (0, 50, 100, 150 and 200 μM $Pb(NO_3)_2$) was determined following acid digestion. After 7 d of growth, 10 seedlings were randomly selected and desorbed in 1 mM Na_2EDTA for 1 min, washed thoroughly five times with nanopure H_2O, and excised into roots and shoots. Concentrated nitric acid (HNO_3) was added and digestion of plant materials was performed overnight in a water bath at 60 $\pm$ 0.5˚C (see Section 2.8). Two independent experiments were carried out; each contained three replicates in which duplicate absorbance readings were taken and interpolated against calibration curves. The Pb contents of plant materials were expressed as nmol/plant.

3.2.5 Transmission electron microscopy

Replicates of 10 seedlings each that were exposed and non-exposed to Pb (0, 50, 100, 150 and 200 μM $Pb(NO_3)_2$) were randomly selected, desorbed in 1 mM Na_2EDTA for 1 min, and washed thoroughly five times with dH_2O. Primary root and cotyledon tissue samples from a (approximate) similar locations were cut into thin slices (< 1 mm) and fixed in 3% (v/v) glutaraldehyde in 0.075 M sodium phosphate buffer (pH 7.2) for 3 h. After post-fixation of the samples in 1% (w/v) OsO_4 dissolved in the same buffer for 2 h, dehydration was accomplished with a series of acetone (20, 40, 60, 80 and 100%, v/v). This is followed by infiltration and embedding in Spurr's resin, and ultra-thin slices (90 - 100 mm) were cut with an ultramicrotome using a diamond knife mounted on a copper grid. In this study, unstained sections were adequate for viewing using a Hitachi H600

transmission electron microscope at 75 kV. Micrographs of regions of interest were taken on Kodak Electron Image Film SO-163 (see Section 2.9).

3.2.6 Statistical analysis

The mean values and standard error of the mean (SE) were calculated from a minimum of three replicates. Independent experiments were repeated at least twice. Statistical analysis was performed as described in Section 2.23. $P < 0.05$ was indicated by different letters in the graphs or tables.

3.3 Results

3.3.1 Seed germination and early seedling growth

In the preliminary trials, it was found that $Pb(NO_3)_2$ concentrations that were greater than 200 μM were lethal to 7-d-old *A. thaliana* seedlings. Therefore, these concentrations were not used in the present study. Radicles were seen to protrude from seeds on d 2 - 3 after sowing seeds. The emergence of radicles was slightly slower in seeds exposed to high $Pb(NO_3)_2$ concentrations (150 and 200 μM) in comparison to the control without $Pb(NO_3)_2$, by 1 - 2 d. Although Pb-treated seedlings displayed symptoms of toxicity, and growth lagged behind that of the controls, there was no statistically significant inhibition of germination with variation in $Pb(NO_3)_2$ concentrations. By 7 d, approximately 90 - 95% seeds germinated from media containing 0 to 200 μM $Pb(NO_3)_2$ (Figure 3.1).

As $Pb(NO_3)_2$ concentrations increased, the growth of 7-d-old *A. thaliana* seedlings was visibly affected. The Pb toxicity symptoms appeared to be concentration-dependent (Figure 3.2). In the control treatment without $Pb(NO_3)_2$, the roots looked healthy and normal. The seedlings that were grown in the presence of 25 μM $Pb(NO_3)_2$ looked similar to the control. In response to exposure to 150 and 200 μM $Pb(NO_3)_2$, seedlings appeared to be severely affected. Their roots appeared to be short and thickened, with the number of root hairs decreased. The colour of the roots in Pb-treated seedlings changed from creamy white to brown.

As $Pb(NO_3)_2$ dosage increased, wilting and browning at the edge of cotyledon became

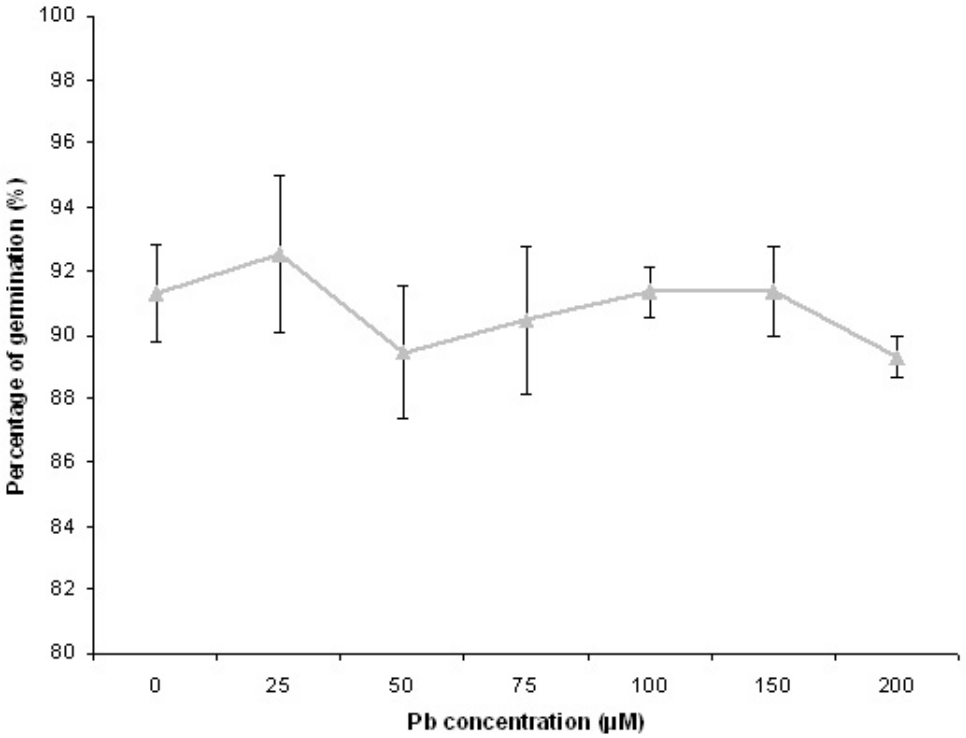

Figure 3.1: Effect of Pb treatment on the germination of *A. thaliana* seeds. Representative results from one of the two independent experiments are presented (n = 3). No statistically significant difference was detected. The scale bars indicate standard error of the means.

Pb concentration (μM)	Tolerance index (%)	Standard error of the mean
0	100.00	-
25	81.57	±3.43
50	57.68	±1.89
75	36.16	±2.25
100	30.30	±3.06
150	22.64	±1.95
200	17.10	±1.37

Table 3.1: Tolerance index of 7-d-old *A. thaliana* seedlings grown in varying concentrations of $Pb(NO_3)_2$. Values were calculated from the means of root length measurements of three independent experiments (n = 3).

more evident. In contrast, Pb stress was less evident when seedlings were exposed to lower $Pb(NO_3)_2$ concentrations.

3.3.2 Fresh weight of seedlings

After 7 d of growth, the greatest reduction (almost 50% of the controls, 0.607 ± 0.019 mg) of fresh weight of *A. thaliana* seedlings occured in response to 200 μM $Pb(NO_3)_2$, 0.333 ± 0.012 mg (Figure 3.3). There was a slight reduction in seedling fresh weight in response to 50 μM $Pb(NO_3)_2$, 0.530 ± 0.012 mg. The inhibitory effect of 100 and 150 μM $Pb(NO_3)_2$ on seedling fresh weight was 0.443 ± 0.003 mg and 0.390 ± 0.015 mg, respectively.

3.3.3 Effects of Pb on root growth

The extent of root inhibition in *A. thaliana* seedlings was found to be proportional to the $Pb(NO_3)_2$ concentration in the medium (Figure 3.4). Based on the tolerance index (Table 3.1), 75 μM $Pb(NO_3)_2$ and above brought about more than 50% root growth inhibition.

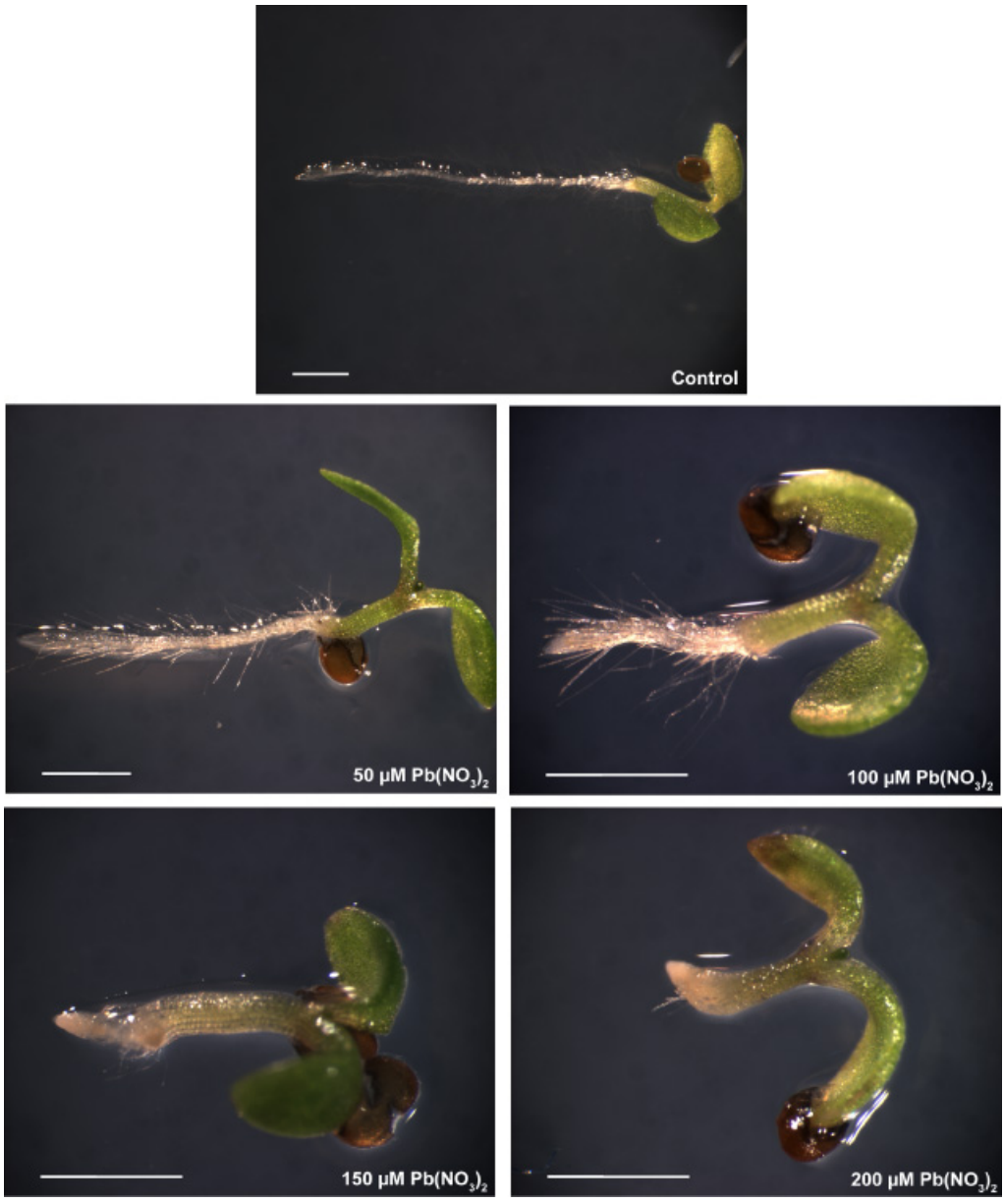

Figure 3.2: Response of 7-d-old *A. thaliana* seedlings to varying concentrations of $Pb(NO_3)_2$. The changes in the shape, appearance and colour of roots and cotyledons were observed. The scale bars indicate 1 mm.

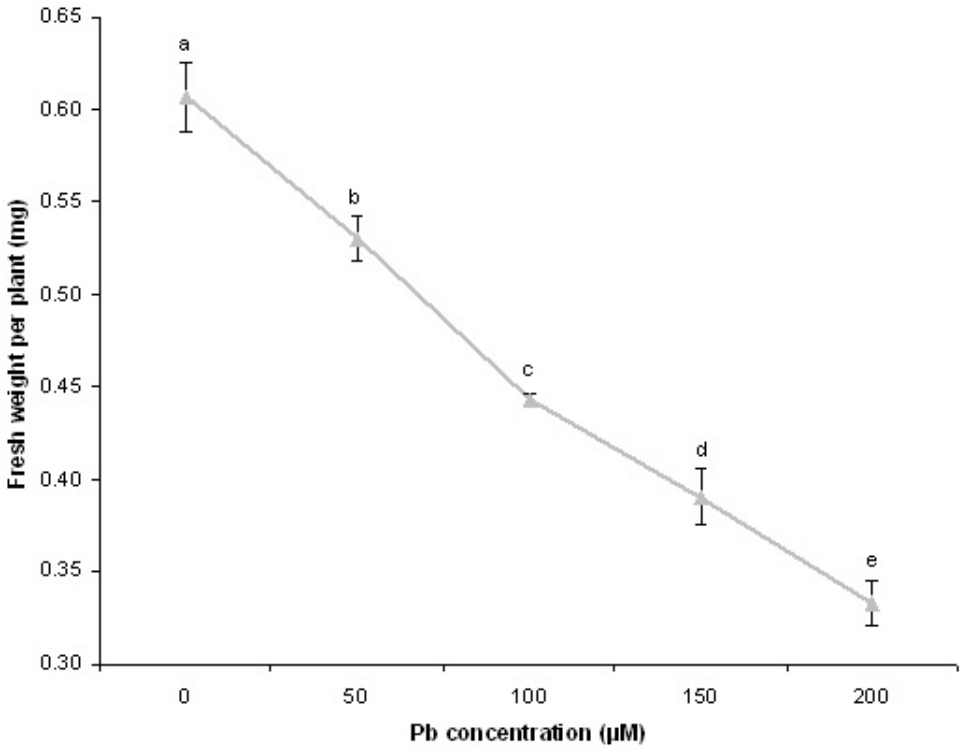

Figure 3.3: Effect of Pb treatment on fresh weight of *A. thaliana* seedlings. Data are representative of two independent experiments, showing standard error of the mean (n = 3). Different letters in the graph represent significant differences at $p < 0.05$, according to one-way ANOVA and multiple comparison using Fisher's LSD test.

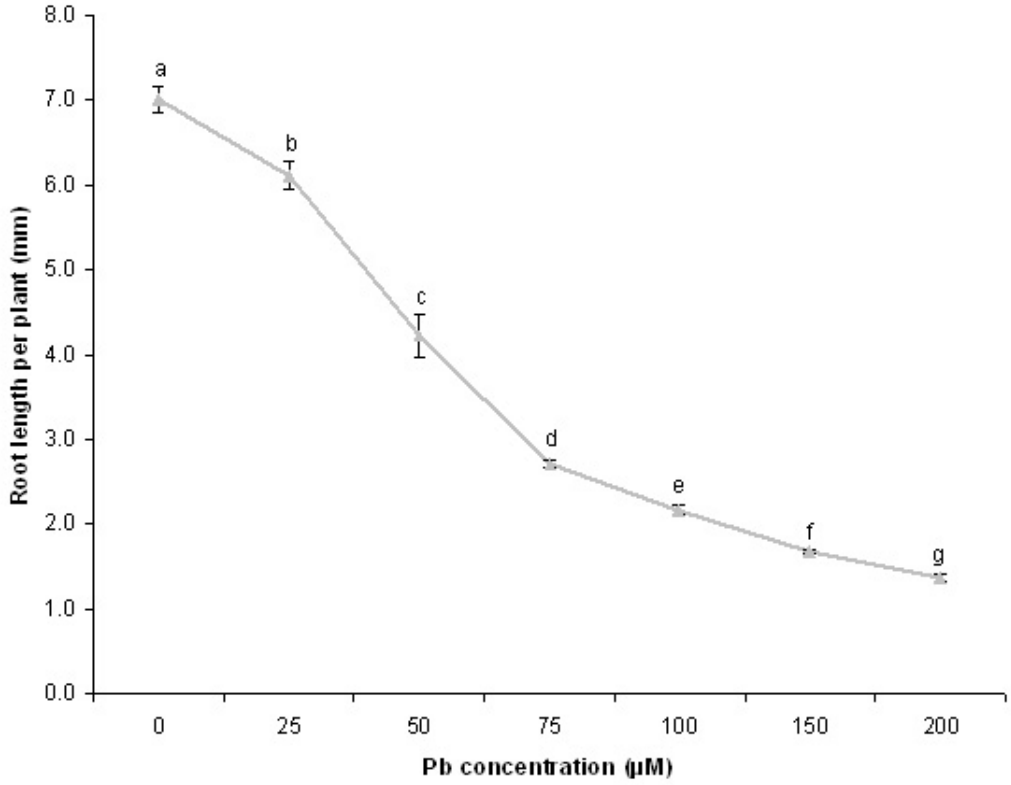

Figure 3.4: Effect of Pb treatment on root length of 7-d-old *A. thaliana* seedlings. Representative results from one of the three independent experiments are presented. Each independent experiment comprised three replicates of each Pb treatments combination (n = 3). Each replicate (n) is derived from the average of root length measurements calculated from ten seedlings. For each treatment, the mean root length $\pm$ standard error has been given a different letter indicates significant differences at $p < 0.05$, according to one-way ANOVA and multiple comparison using Fisher's LSD test.

3.3.4 Histochemical localization of Pb residues

The histochemical rhodizonate method allowed direct visualization of Pb in the seedlings. The formation of pink colour as a result of Pb rhodizonate precipitation indicates the presence of Pb. In seedlings treated with 50 μM $Pb(NO_3)_2$, pink colouration was only observed in the roots (Figure 3.5). Pb deposits were observed in the roots and at the edge of a few cotyledons following exposure to 100 μM $Pb(NO_3)_2$. In the 150 and 200 μM $Pb(NO_3)_2$ treatments, the whole roots and more than 50% of the cotyledons were stained pink.

3.3.5 Graphite furnace atomic absorption spectroscopy

3.3.5.1 Pb content in roots

Generally, the level of Pb accumulation in the roots of 7-d-old *A. thaliana* seedlings increased with increasing $Pb(NO_3)_2$ concentration in the medium. A dramatic increase of 4.5-fold Pb uptake occured when $Pb(NO_3)_2$ concentration was increased from 50 to 100 μM in the medium (Figure 3.6).

3.3.5.2 Pb content in shoots

The shoot Pb content depends on the Pb taken up by the roots and then its translocation from root to shoot. In general, the uptake of Pb by the shoot increased with increasing Pb concentrations in the medium (Figure 3.7). The percentages of Pb translocated from roots to the shoots [Pb content in shoots / (Pb content in shoots + Pb content in roots) x 100%] were 26.2, 18.1, 30.5 and 42.8% after 7 d on agar medium containing 50, 100, 150 and 200 μM $Pb(NO_3)_2$, respectively.

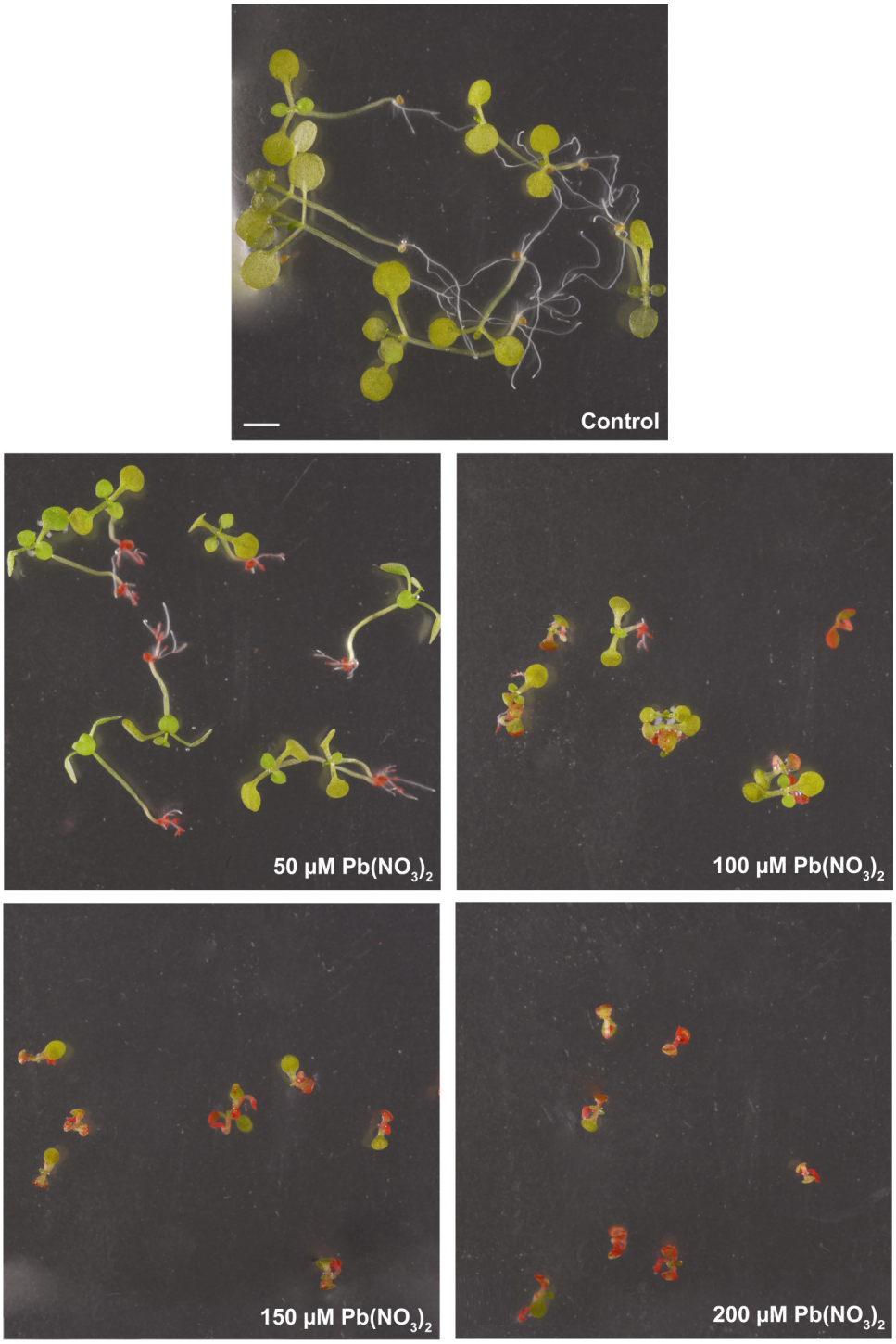

Figure 3.5: Detection of Pb on 2-week-old *A. thaliana* seedlings to varying concentrations of $Pb(NO_3)_2$. Pb was visualized by the rhodizonate method. The pink stains indicate Pb-rhodizonate precipitates. The scale bar indicates 2 mm.

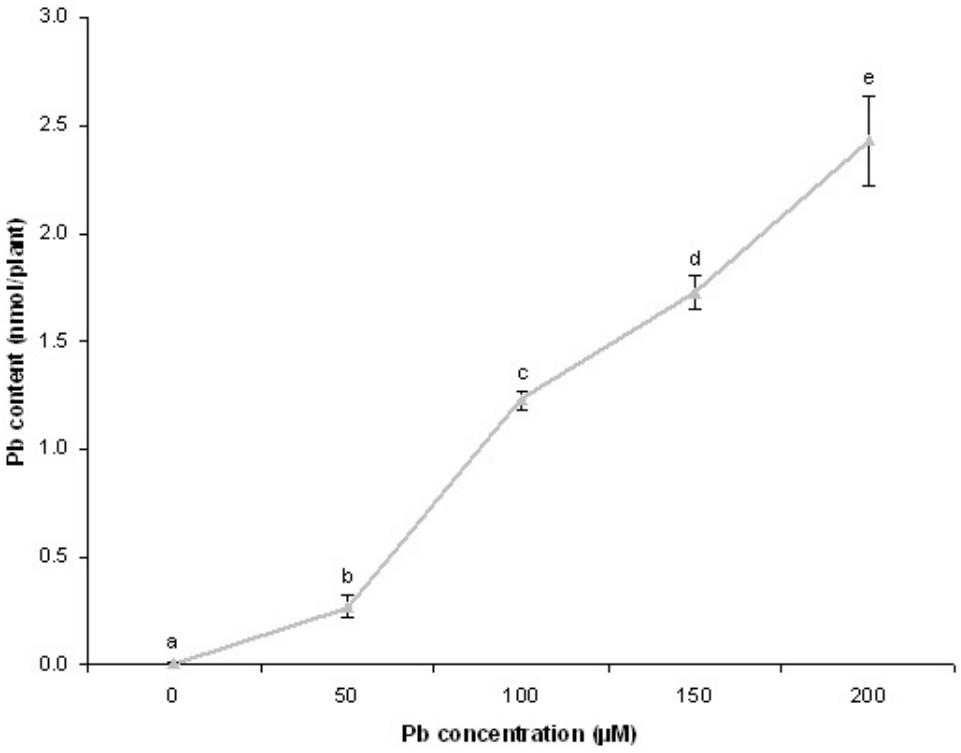

Figure 3.6: Pb content in root of 7-d-old *A. thaliana* seedlings grown in different Pb concentrations. Values are means from two independent experiments with three replicates (n = 6). The bars indicate standard error of the means. Different letters in the graph represent significant differences at $p < 0.05$, according to one-way ANOVA and multiple comparison using Fisher's LSD test.

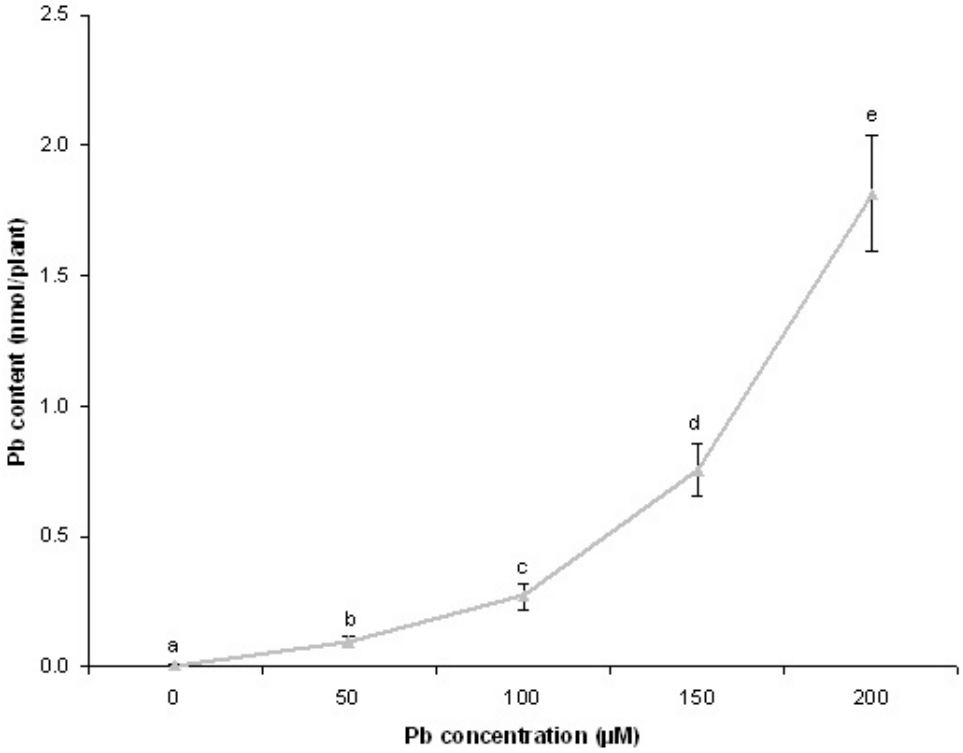

Figure 3.7: Pb content in shoot of 7-d-old *A. thaliana* seedlings grown in different Pb concentrations. Values are means from two independent experiments with three replicates (n = 6). The bars indicate standard error of the means. Different letters in the graph represent significant differences at $p < 0.05$, according to one-way ANOVA and multiple comparison using Fisher's LSD test.

3.3.6 Transmission electron microscopy

3.3.6.1 Distribution of Pb in roots

The control micrographs were used as a basis for comparison (Figure 3.8). In roots of *A. thaliana* seedlings exposed to a low $Pb(NO_3)_2$ concentration (50 µM), a few fine Pb grains were only observed in the cell wall regions (Figures 3.9 and 3.10). When $Pb(NO_3)_2$ concentration was increased to 100 µM, heavy Pb deposits were embedded in the cell wall regions and in the vacuole with high density (Figure 3.11). TEM revealed that most of the large Pb deposits were found in the thick segments of the cell wall, whereas small-grained deposits were located in the cell wall near the plasmalemma. As shown in Figure 3.12, discrete clumps of large Pb particles can be seen in the middle lamella. This situation was even more evident in the treatment with 200 µM $Pb(NO_3)_2$, as heavy Pb deposits filled up the intercellular spaces (Figure 3.13). Pb particles were also evident along the tonoplast, in the vacuole (Figure 3.14), cell wall and cytoplasm (Figure 3.15). Pb was present in two forms: as distinct congregates of relatively large electron-dense particles and evenly disseminated fine grains. A small number of Pb grains were also observed in a few vesicles. These large Pb particles have sharp angular edges with a very grainy, crystalline appearance.

No destructive changes appeared in the ultrastructure of cellular organelles after growth of seedlings in the (selected) doses of Pb, up to 200 µM $Pb(N_3)_2$. These cellular organelles include the mitochondria and endoplasmic reticulum.

3.3.6.2 Distribution of Pb in cotyledons

Micrographs of the control are shown to provide a basis for comparison of Pb accumulation in the cotyledons (Figures 3.16 and 3.17). In the treatment with 50 µM $Pb(NO_3)_2$, Pb deposits were not observed in the chloroplasts (Figure 3.18) and only very fine Pb grains were detected in intercellular spaces (Figure 3.19). When seedlings were grown on a medium containing 100 µM $Pb(NO_3)_2$, extremely fine Pb particles were present in the cell wall region near the plasmalemma, within the chloroplast, and central vacuole (Figures 3.20 and 3.21). There appeared to be more Pb deposits in the 100 µM $Pb(NO_3)_2$ (Figure 3.22) than in the 50 µM $Pb(NO_3)_2$ treatment. In the 200 µM $Pb(NO_3)_2$ treatment,

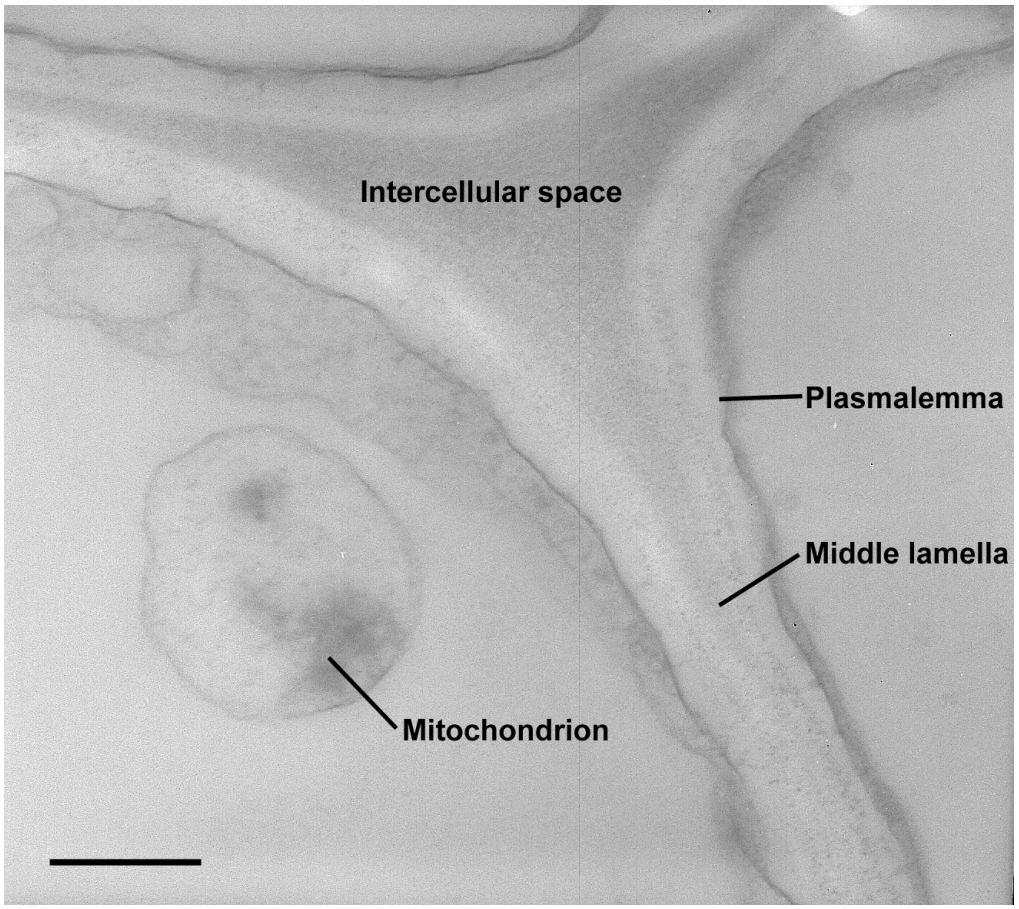

Figure 3.8: Transmission electron micrograph of an unstained ultra-thin section of the root from a 7-d-old *A. thaliana* seedling grown in the absence of Pb. Magnification of the micrograph was at 25,000 X. Bar = 500 nm.

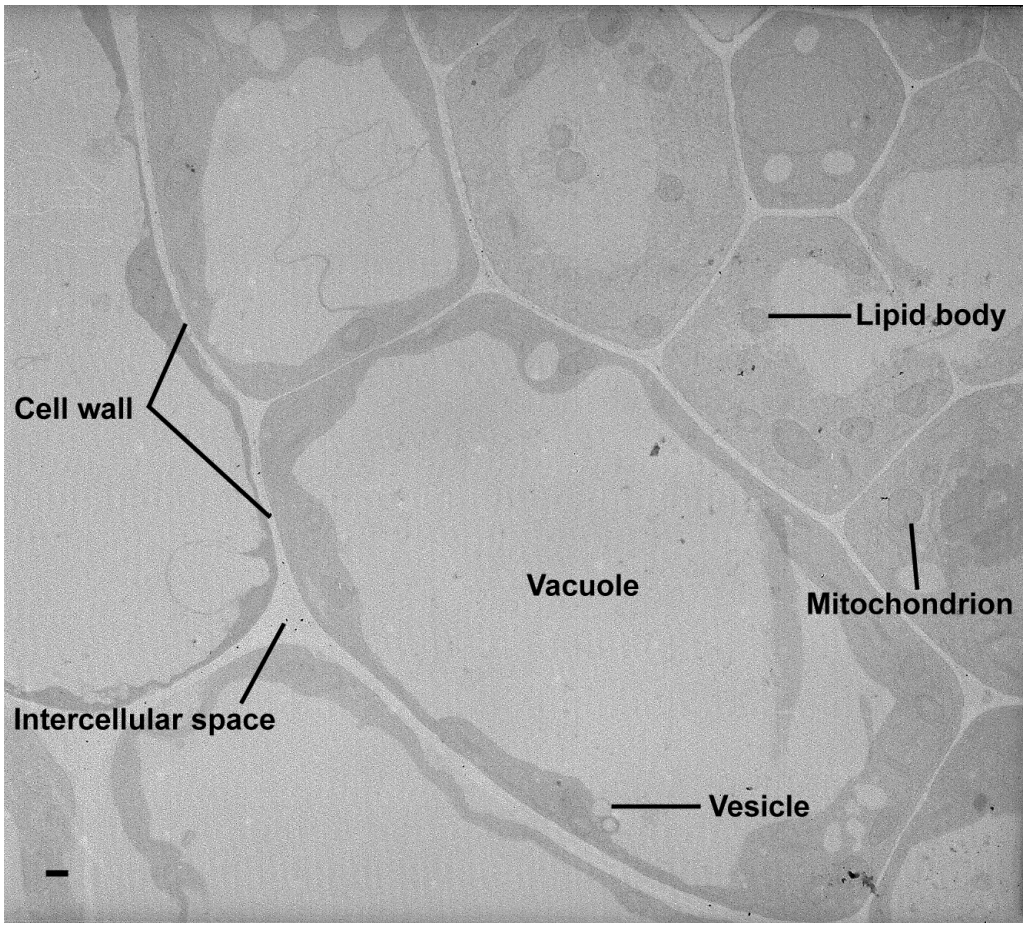

Figure 3.9: Transmission electron micrograph of an unstained ultra-thin section of the root from a 7-d-old *A. thaliana* seedling grown in medium containing 50 μM $Pb(NO_3)_2$. Magnification of the micrograph was at 3,500 X. Bar = 500 nm.

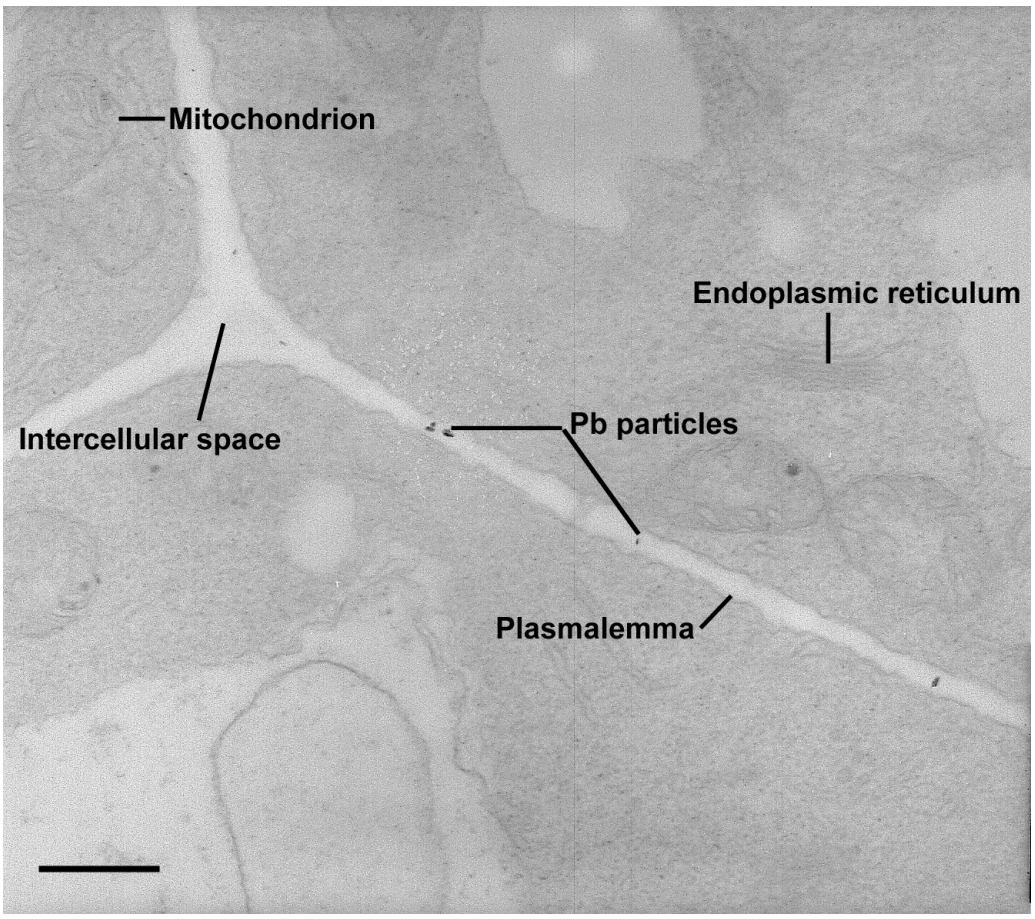

Figure 3.10: Transmission electron micrograph of an unstained ultra-thin section of the root from a 7-d-old *A. thaliana* seedling grown in medium containing 50 µM $Pb(NO_3)_2$. Magnification of the micrograph was at 20,000 X. Bar = 500 nm.

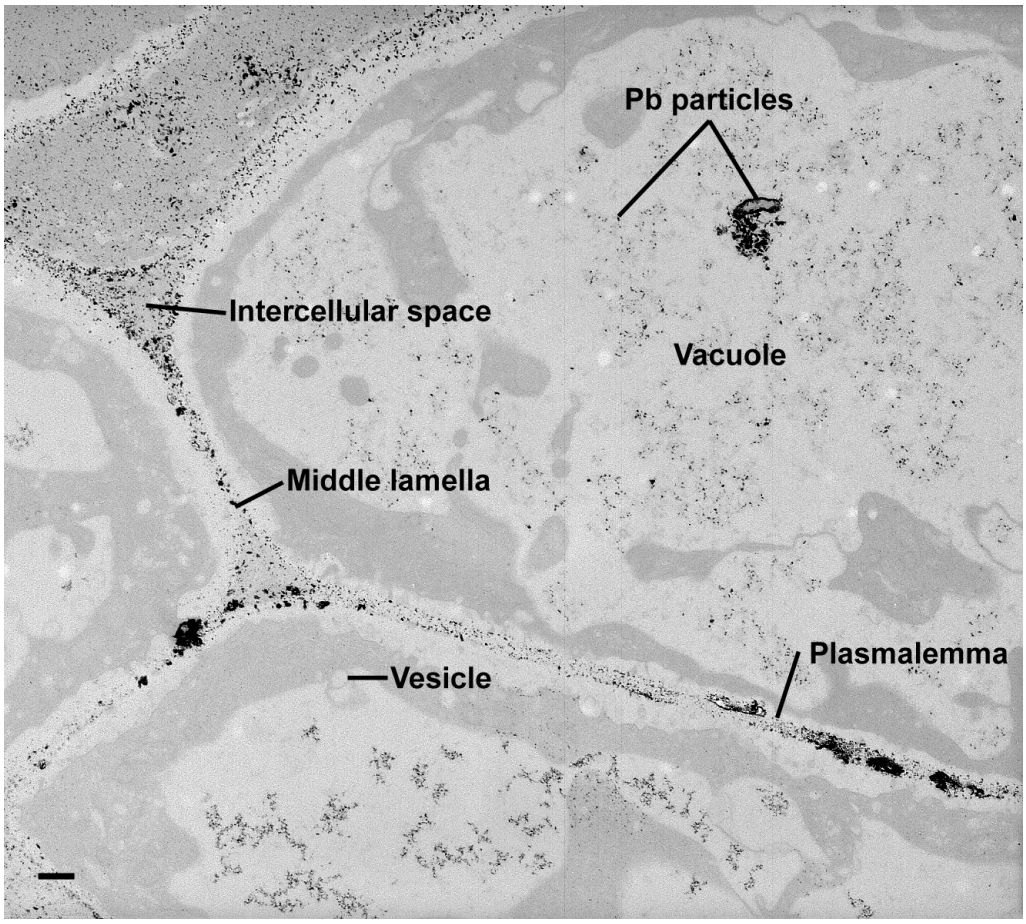

Figure 3.11: Transmission electron micrograph of an unstained ultra-thin section of the root from a 7-d-old *A. thaliana* seedling grown in medium containing 100 μM $Pb(NO_3)_2$. Magnification of the micrograph was at 6,000 X. Bar = 500 nm.

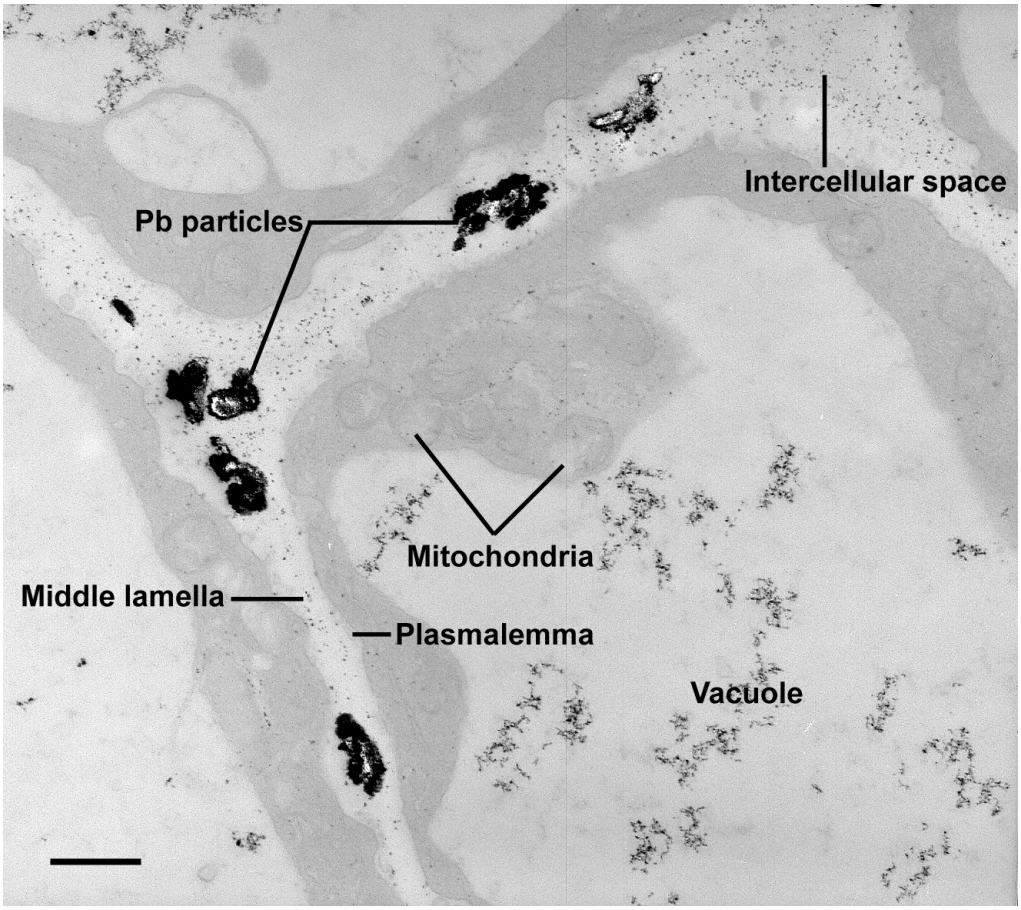

Figure 3.12: Transmission electron micrograph of an unstained ultra-thin section of the root from a 7-d-old *A. thaliana* seedling grown in medium containing 100 μM $Pb(NO_3)_2$. Magnification of the micrograph was at 15,000 X. Bar = 500 nm.

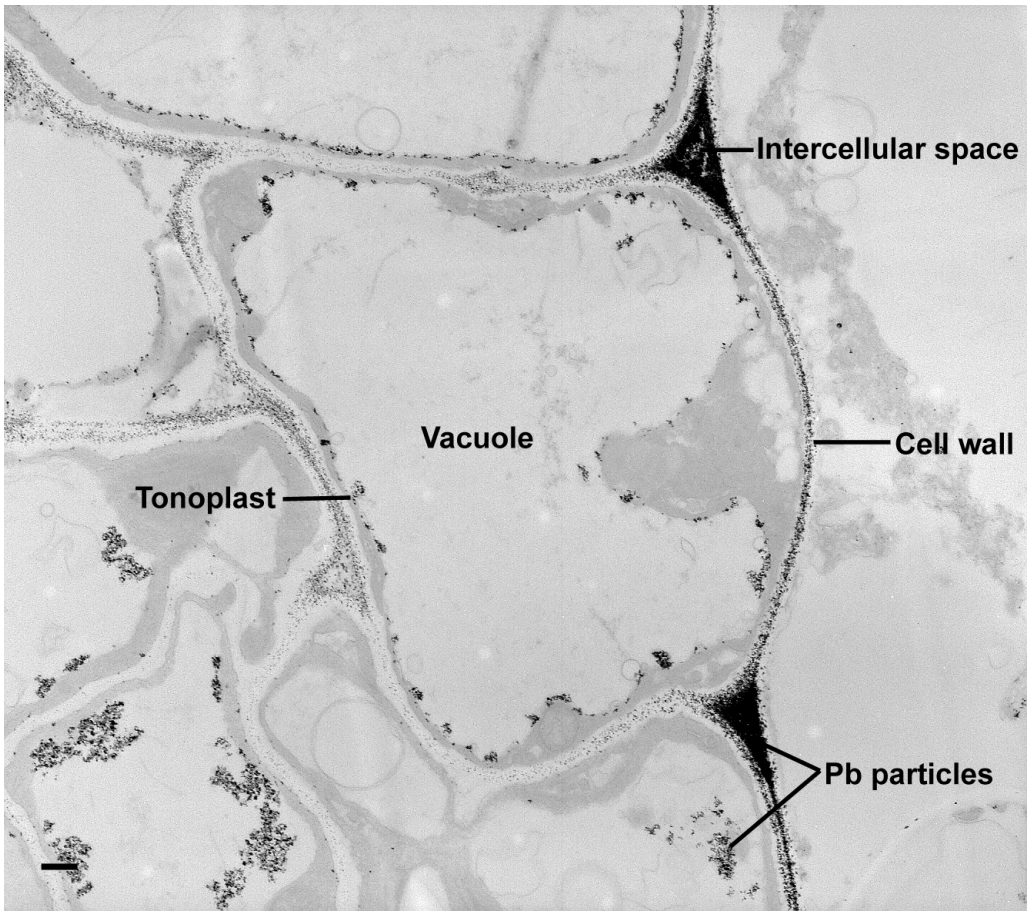

Figure 3.13: Transmission electron micrograph of an unstained ultra-thin section of the root from a 7-d-old *A. thaliana* seedling grown in medium containing 200 μM $Pb(NO_3)_2$. Magnification of the micrograph was at 6,000 X. Bar = 500 nm.

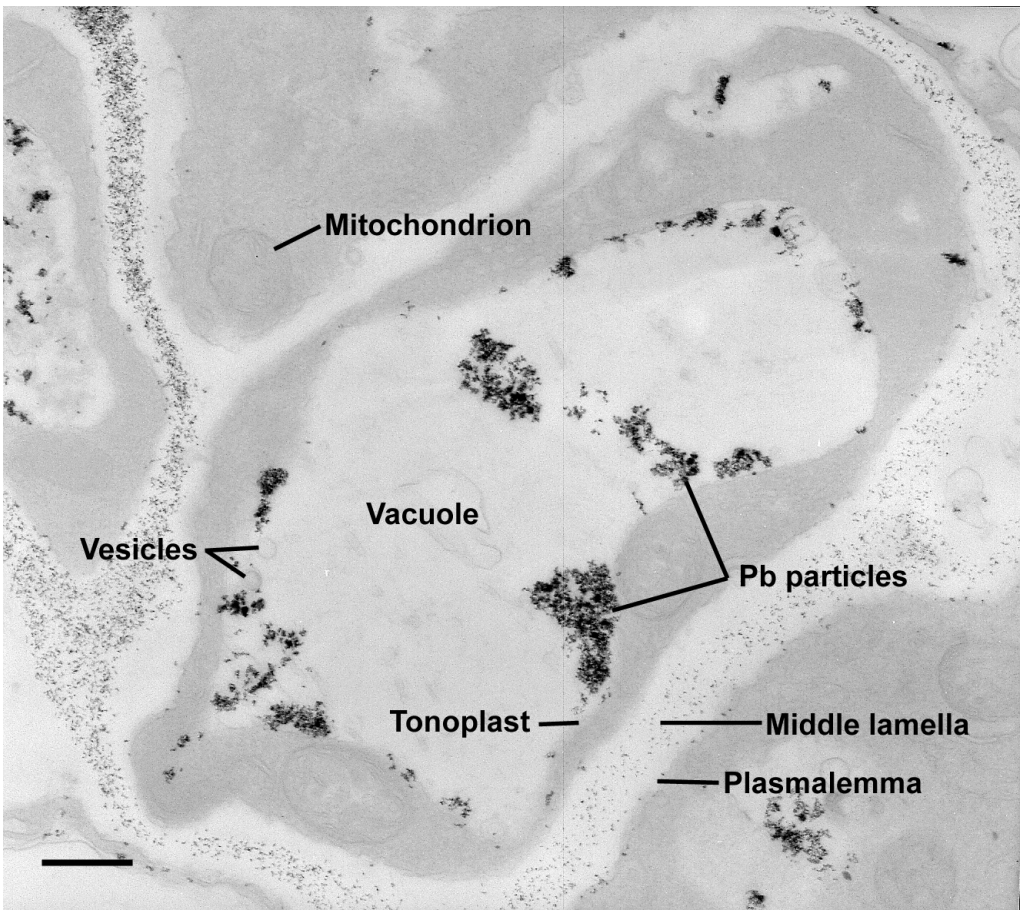

Figure 3.14: Transmission electron micrograph of an unstained ultra-thin section of the root from a 7-d-old *A. thaliana* seedling grown in medium containing 200 μM $Pb(NO_3)_2$. Magnification of the micrograph was at 15,000 X. Bar = 500 nm.

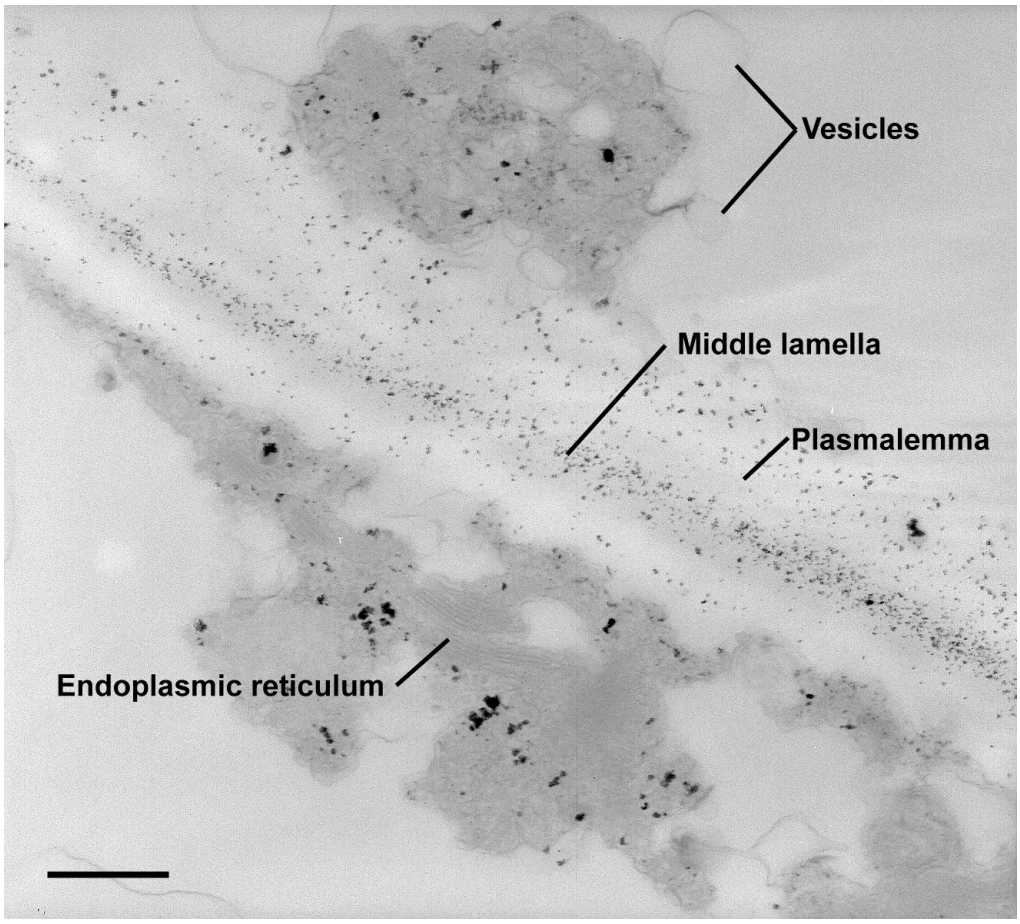

Figure 3.15: Transmission electron micrograph of an unstained ultra-thin section of the root from a 7-d-old *A. thaliana* seedling grown in medium containing 200 μM $Pb(NO_3)_2$. Magnification of the micrograph was at 20,000 X. Bar = 500 nm.

medium-size crystal-like Pb particles were evident in the cell wall region (Figure 3.23), but finer grains were evenly dispersed within the chloroplasts. There was also a high level of Pb accumulation and heavy deposition in the central vacuole (Figure 3.24).

3.4 Discussion

3.4.1 Preliminary experiments

Modified Huang and Cunningham (HC) medium was chosen as the basal culture medium for studying Pb accumulation and tolerance as it is relatively similar to characteristics of Pb-contaminated soil. Pb tends to interact with other nutrient elements (e.g. Ca, P and Zn) during nutrient absorptions, translocation and consumption (Chen *et al.*, 1997). Thus, a minimal medium allowed seedling growth and lessened the competition between Pb-nutrient uptake. This culture medium has a low pH (4.5 - 5.0) and a reduced P concentration to ensure maximum Pb bioavailability. Lead phosphate precipitates were observed in the medium if the P concentration in the unmodified HC was used.

Initially, seeds sown on Petri plates were placed vertically in the growth room. However, the side of the cotyledon in contact with the modified HC medium containing 200 μM $Pb(NO_3)_2$ appeared to be more severely affected (brown) than the side not in direct contact with agar medium. In addition, stunted seedling growth increased the likelihood and surface area of cotyledon-agar contact. This raised the concern that Pb may enter the plants via direct contact of cytoledon with agar if the plates were stood in a vertical orientation. This may complicate interpretation of Pb accumulation levels in the seedlings. Therefore, Petri plates were placed horizontally in the growth room for the present experiments.

Due to the relative small size of 7-d-old *A. thaliana* seedlings, fresh weight difference was not used as an indication of Pb toxicity. This is because the water content in plants might have evaporated into the surrounding during harvesting, leading to experimental inaccuracy. The use of root length as an indication of Pb toxicity was considered more appropriate in this study.

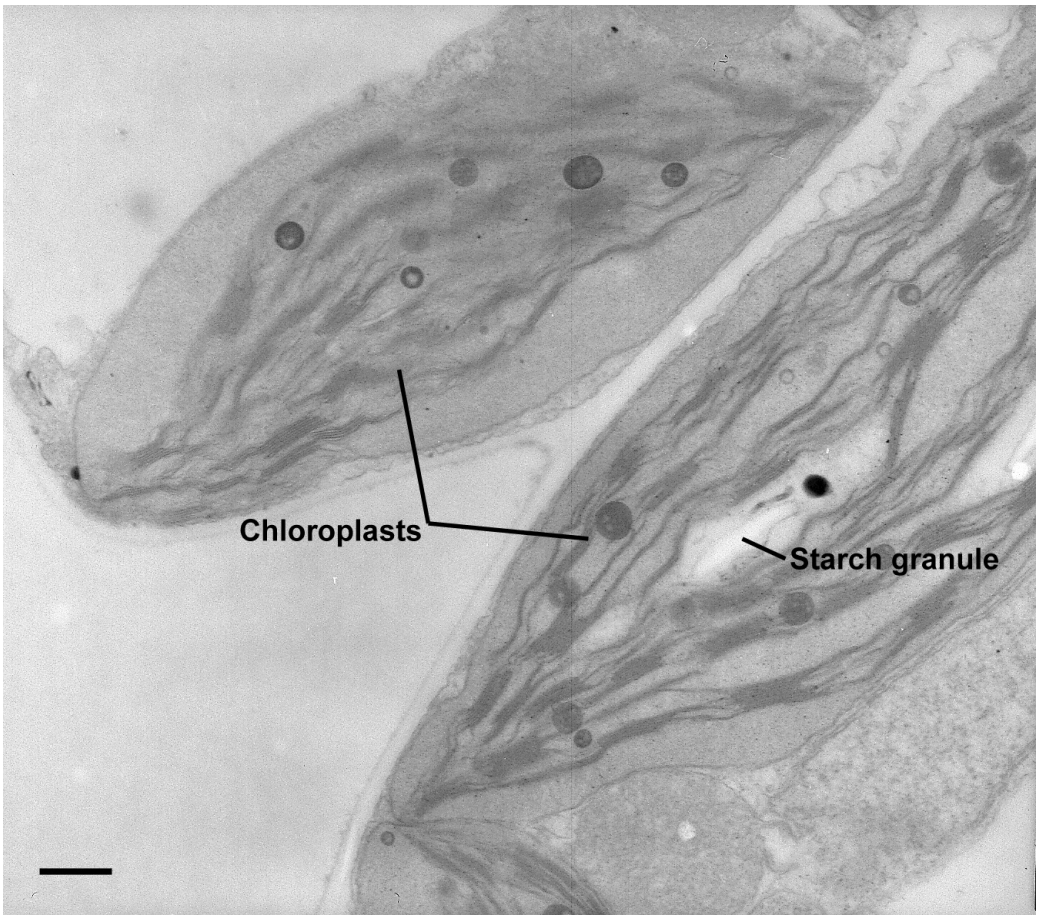

Figure 3.16: Transmission electron micrograph of an unstained ultra-thin section of the cotyledon from a 7-d-old *A. thaliana* seedling grown in the absence of Pb. Magnification of the micrograph was at 12,000 X. Bar = 500 nm.

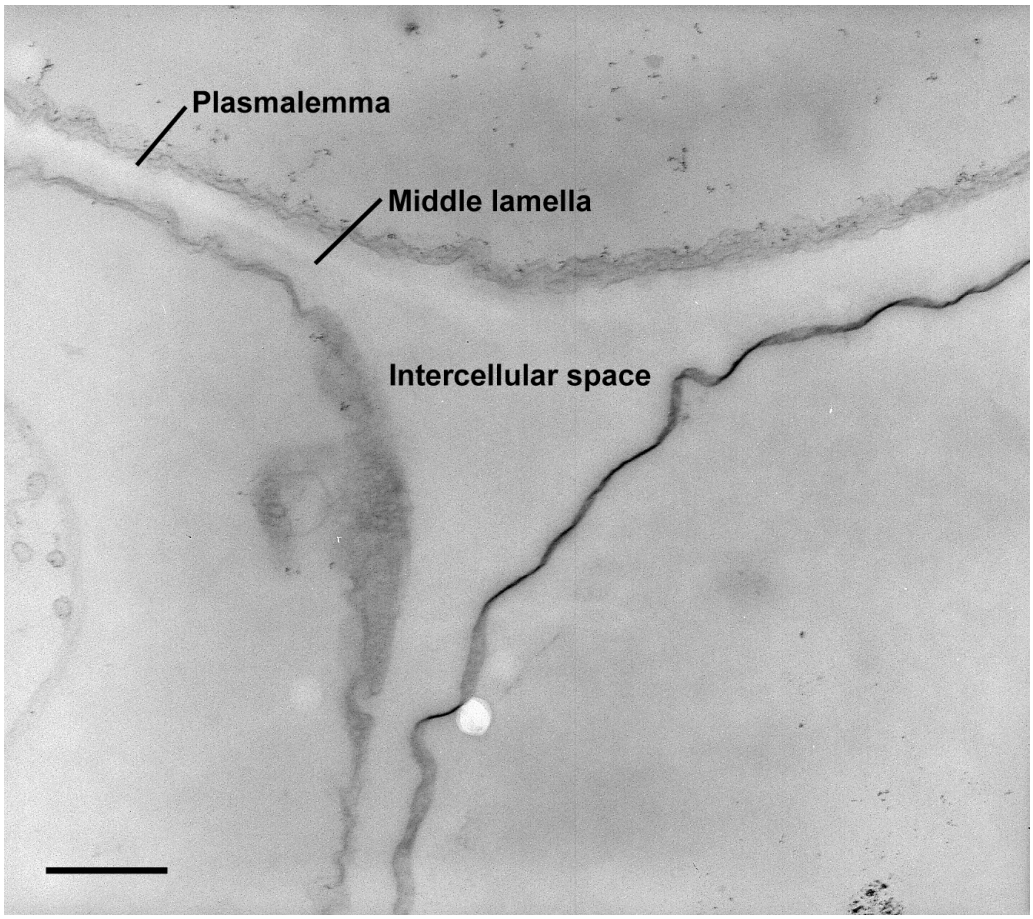

Figure 3.17: Transmission electron micrograph of an unstained ultra-thin section of the cotyledon from a 7-d-old *A. thaliana* seedling grown in the absence of Pb. Magnification of the micrograph was at 20,000 X. Bar = 500 nm.

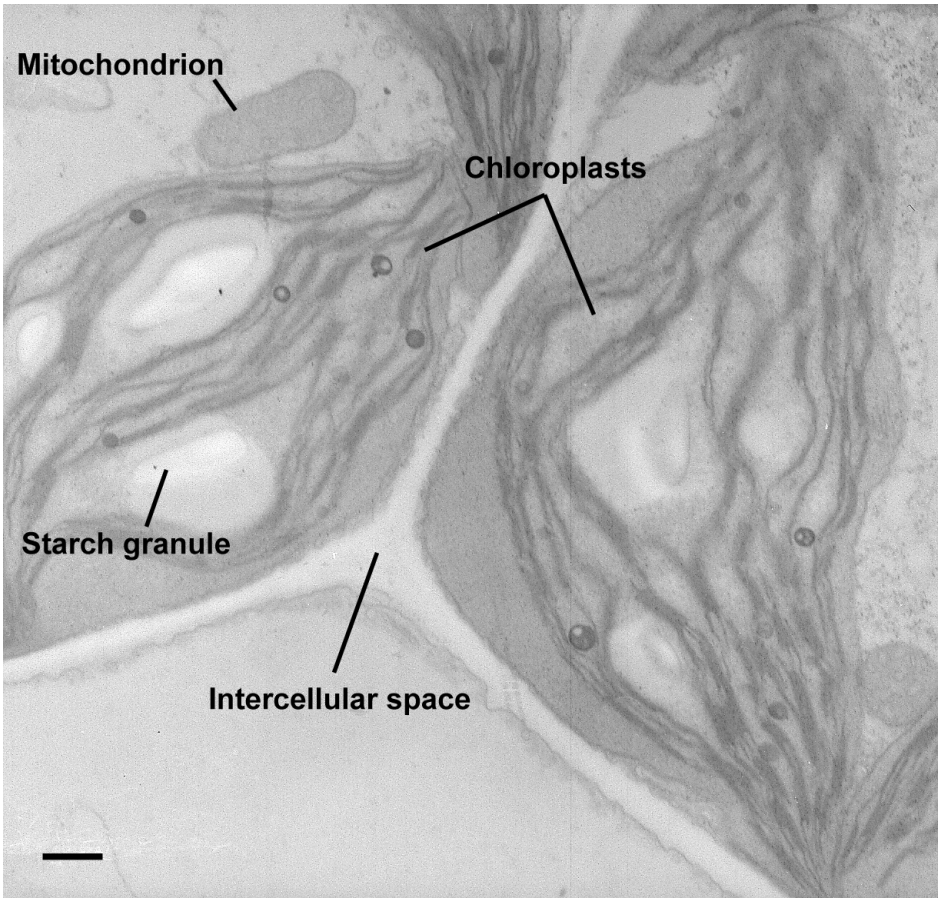

Figure 3.18: Transmission electron micrograph of an unstained ultra-thin section of the cotyledon from a 7-d-old *A. thaliana* seedling grown in medium containing 50 µM $Pb(NO_3)_2$. Magnification of the micrograph was at 10,000 X. Bar = 500 nm.

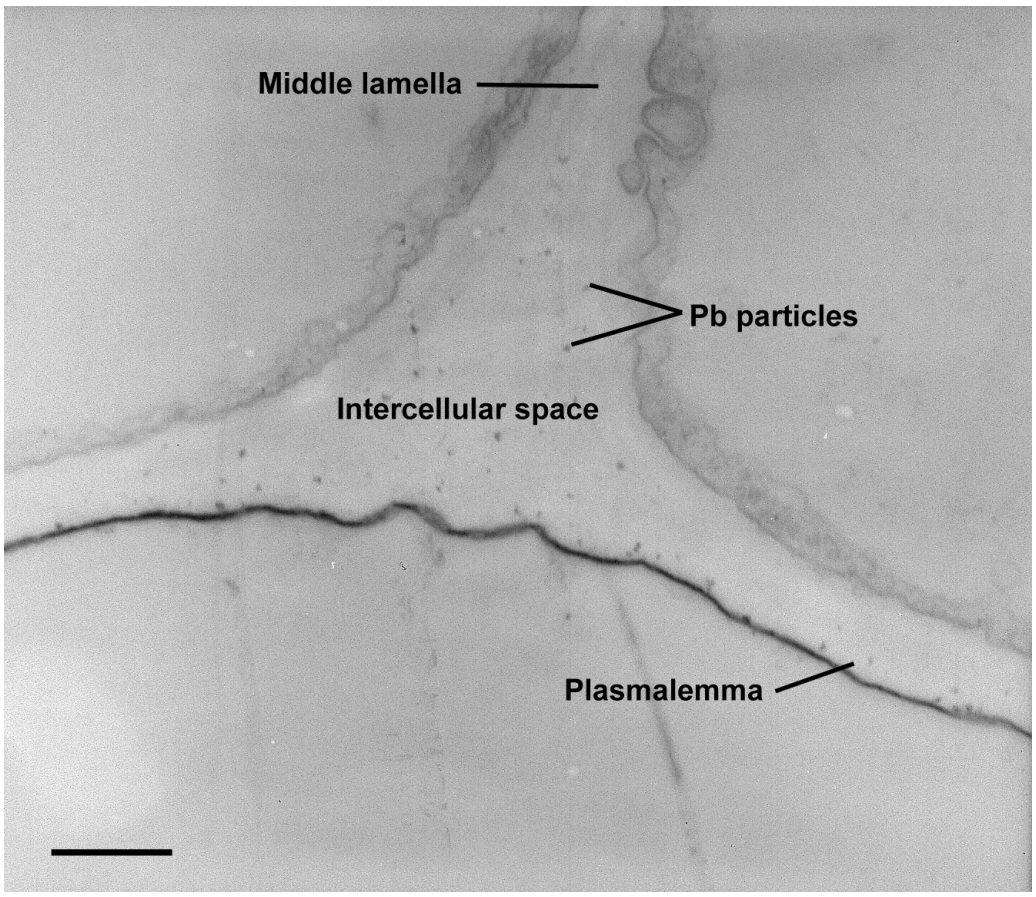

Figure 3.19: Transmission electron micrograph of an unstained ultra-thin section of the cotyledon from a 7-d-old *A. thaliana* seedling grown in medium containing 50 μM $Pb(NO_3)_2$. Magnification of the micrograph was at 20,000 X. Bar = 500 nm.

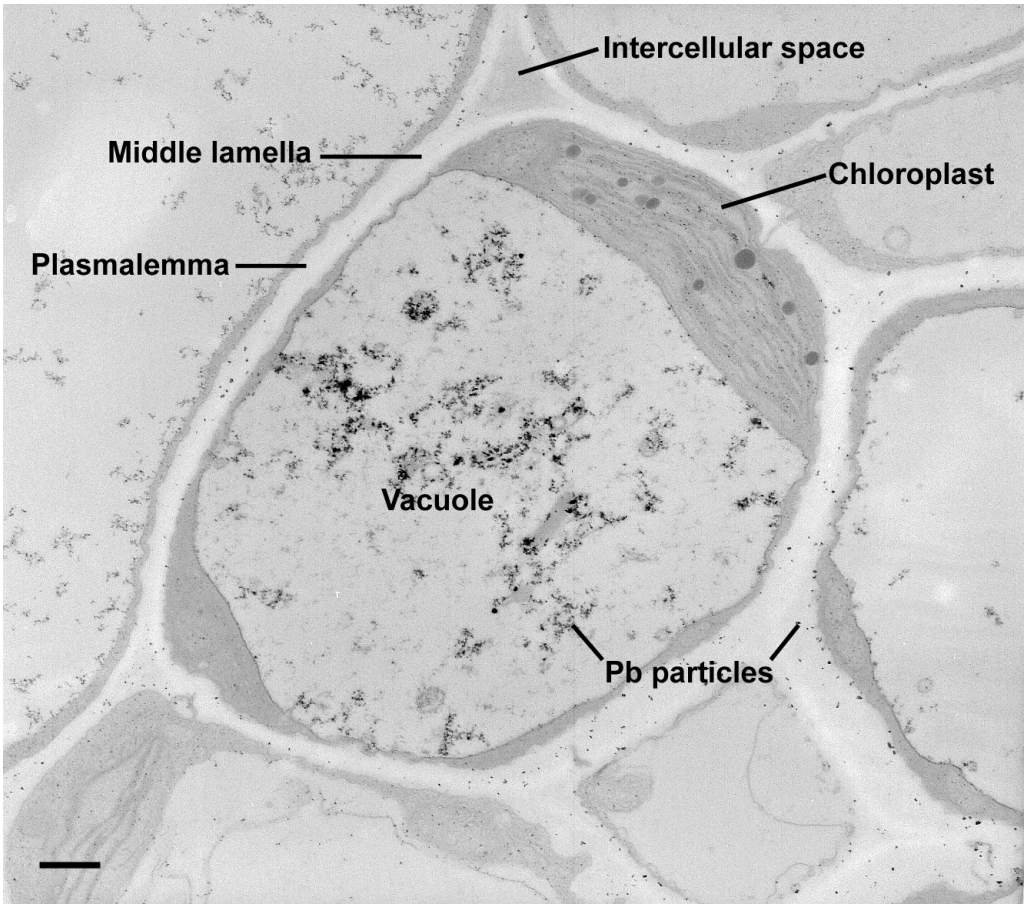

Figure 3.20: Transmission electron micrograph of an unstained ultra-thin section of the cotyledon from a 7-d-old *A. thaliana* seedling grown in medium containing 100 µM $Pb(NO_3)_2$. Magnification of the micrograph was at 10,000 X. Bar = 500 nm.

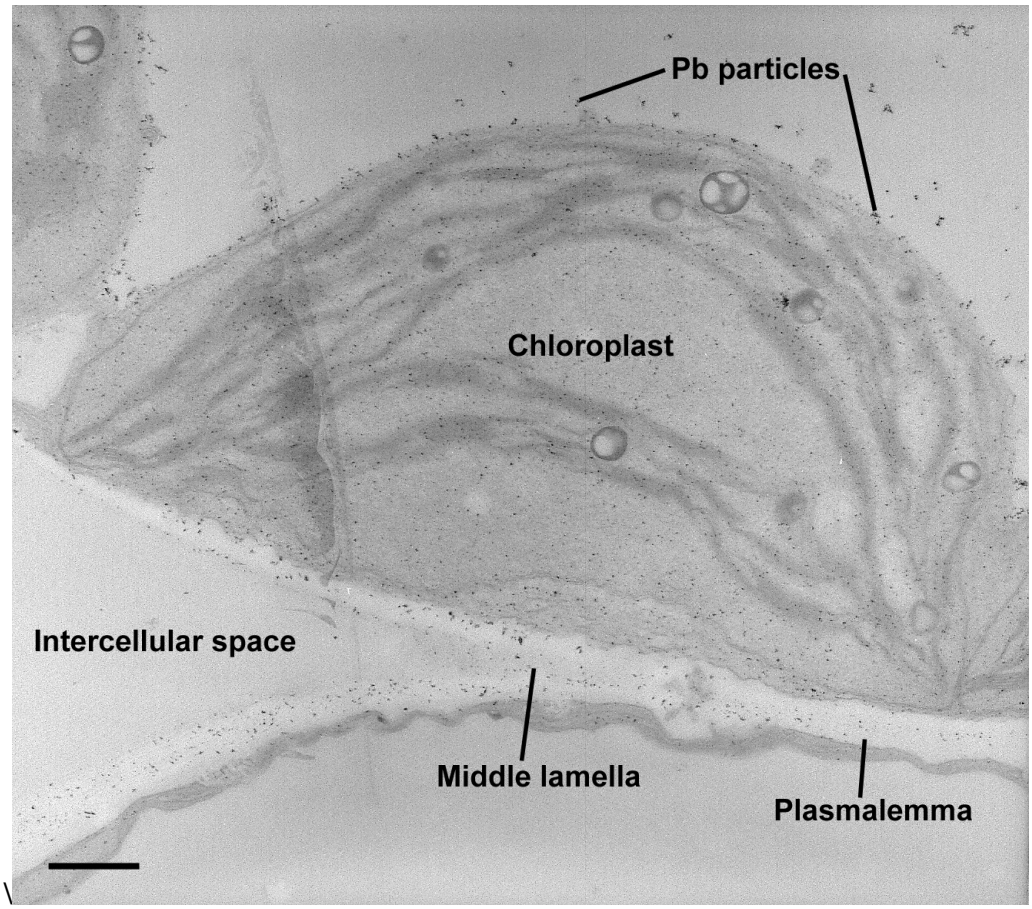

Figure 3.21: Transmission electron micrograph of an unstained ultra-thin section of the cotyledon from a 7-d-old *A. thaliana* seedling grown in medium containing 100 μM $Pb(NO_3)_2$. Magnification of the micrograph was at 15,000 X. Bar = 500 nm.

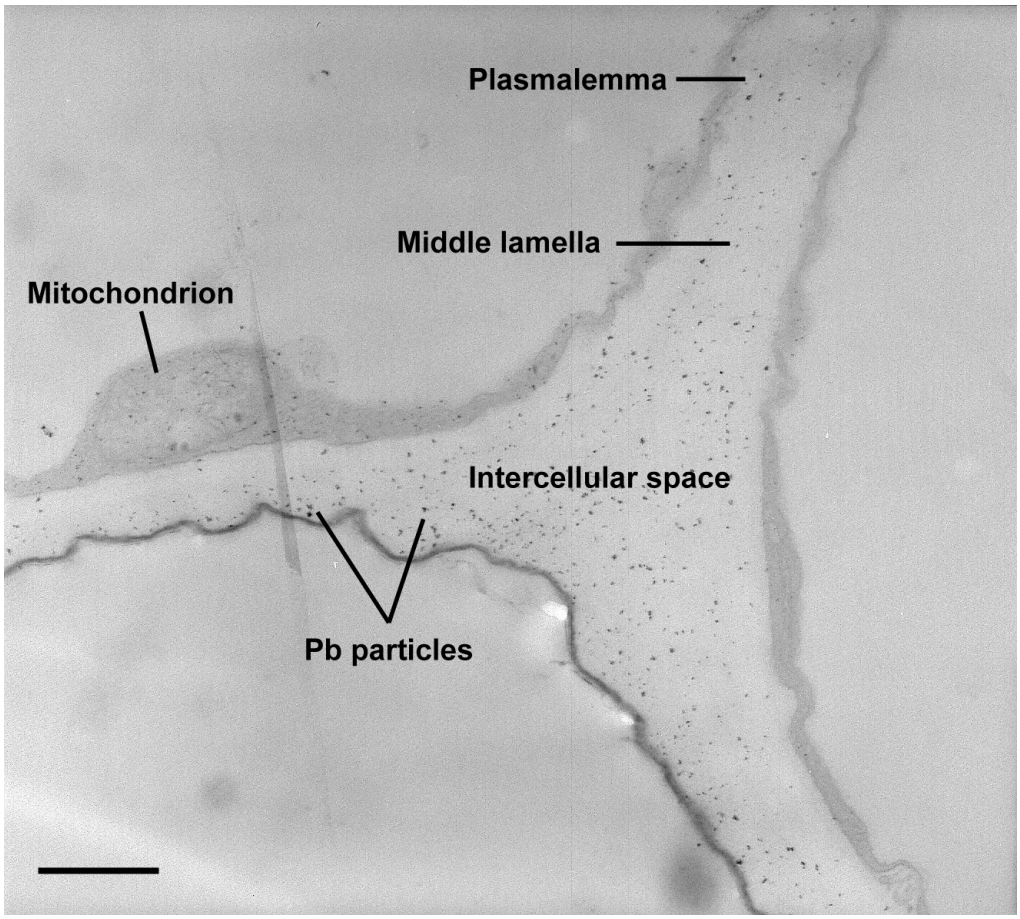

Figure 3.22: Transmission electron micrograph of an unstained ultra-thin section of the cotyledon from a 7-d-old *A. thaliana* seedling grown in medium containing 100 µM $Pb(NO_3)_2$. Magnification of the micrograph was at 20,000 X. Bar = 500 nm.

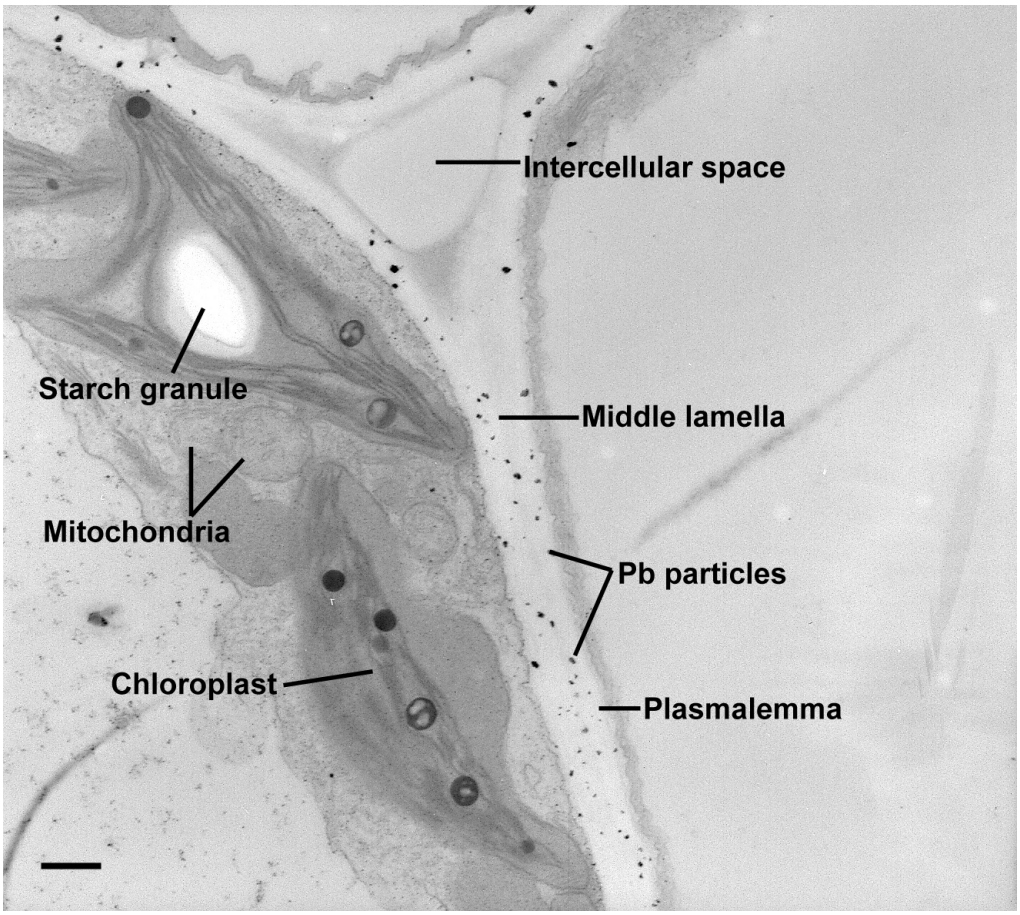

Figure 3.23: Transmission electron micrograph of an unstained ultra-thin section of the cotyledon from a 7-d-old *A. thaliana* seedling grown in medium containing 200 μM $Pb(NO_3)_2$. Magnification of the micrograph was at 10,000 X. Bar = 500 nm.

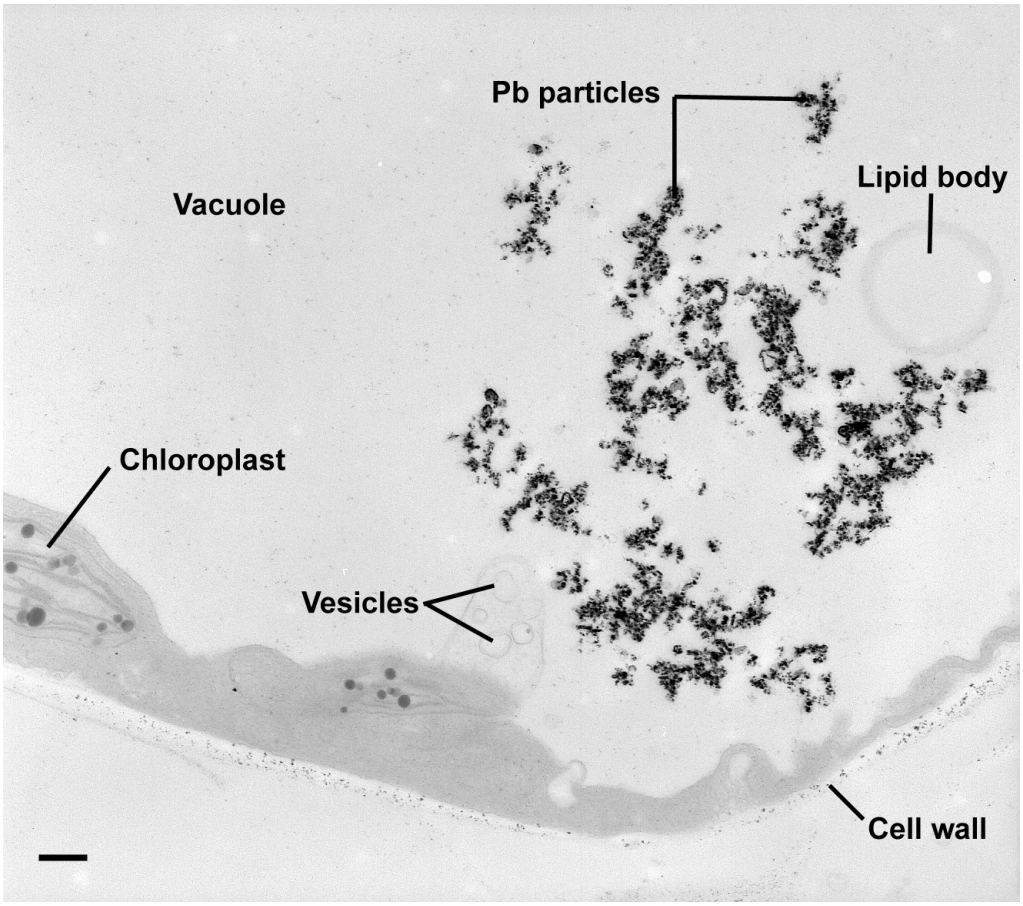

Figure 3.24: Transmission electron micrograph of an unstained ultra-thin section of the cotyledon from a 7-d-old *A. thaliana* seedling grown in medium containing 200 µM $Pb(NO_3)_2$. Magnification of the micrograph was at 8,000 X. Bar = 500 nm.

3.4.2 Effects of Pb on *A. thaliana* seedlings

Pb belongs to a group of elements that are considered to be inessential for life functions. According to Wilkins (1957), the tolerance of plants to Pb can be measured by the tolerance index. *A. thaliana* seedlings were able to tolerate 25 and 50 μM $Pb(NO_3)_2$ in culture media. Changes in the growth patterns of roots and shoots of plants exposed to Pb have previously been shown to be concentration dependent (Xiong, 1998). High levels of $Pb(NO_3)_2$ (100, 150 and 200 μM) were toxic to *A. thaliana* seedlings. Symptoms included browning of the root, inhibition of root elongation, fewer root hairs, and lower biomass of the plants. Similar deleterious effects on the shape and appearance have also been observed in *Zea mays* (Huang & Cunningham, 1996), *Pisum sativum* (Malecka *et al.*, 2008) and plant species of the Fabaceae family (Piechalak *et al.*, 2002). Huang & Cunningham (1996) reported that the inhibition of root growth is an indication of Pb toxicity. It is the first visual symptom of Pb toxicity, since roots accumulated the prevalent quantity of Pb ions. Retarded shoot growth is the consequence of root growth inhibition. The inhibitory effects of Pb on seedling growth presumably arise from the heavy metal interference with normal development and metabolic processes. For example, Pb ions interfered with auxin regulated cell elongation in the wheat coleoptile assay (Lane *et al.*, 1978). Pb treatments were reported to disturb microtubule organization in the root meristem of *Z. mays*, leading to inhibition of cell division in root tips (Eun *et al.*, 2000). Pb damages the microtubules of the mitotic spindle, causing abnormal mitosis to occur. However, the blocking of cells in pro-metaphase is not permanent (Wierzbicka, 1994). Malkowski *et al.* (2002) have shown that Pb caused leakage of K^+ ions from the roots of corn seedlings, thereby disrupting the cell extension processes. Stunted shoot growth, however, was not a consequence of K^+ leakage, but of an unknown Pb-induced signal in roots which was transmitted to shoots. Pb also disturbed the water regime of a plant, causing it to lose cell turgor and cell wall plasticity (Sharma & Dubey, 2005).

Additionally, Pb tends to bind to the sulphydryl (-SH) group of enzymes involved in growth and metabolic processes (Hall, 2002; Sharma & Dubey, 2005). The -SH groups at the active site of an enzyme that is important for its activity and stabilization of tertiary structure were compromised. Pb treatment also caused blockage of carboxyl (-COOH) groups and displaced the essential metals in metalloenzymes (Sharma & Dubey,

2005). Consequently, proteins lost their functions and normal physiological activities of the seedlings would be upset.

The localization of pink lead rhodizonate in the root (especially root tip) and at the edge of cotyledons, is consistent with the morphological observations, suggesting that deposition of Pb caused the discoloration of the root and at the edge of the cotyledons. Pb may have been precipitated on the root surface as lead phosphate, or it may have displaced other essential cations, such as Ca^{2+} or Mg^{+} from specific binding sites (Dietz *et al.*, 1999; Sharma & Dietz, 2009), causing the discolouration to occur.

Seed germination represents the beginning of a new generation and it is an important phase in a plant's life cycle (Atici *et al.*, 2005). As observed in *Raphanus sativus* (Lane & Martin, 1977) and in an earlier study using *A. thaliana* (Li *et al.*, 2005), the germination of *A. thaliana* seeds in the present experiment was insensitive to Pb in the nutrient solutions up to 200 μM $Pb(NO_3)_2$. However, this is different from the findings reported using *Oryza sativa* (Mukherjee & Maitra, 1976; Mukherji & Maitra, 1977), *Sonchus oleraceus* (Xiong, 1997), *Pisum sativum* (Wierzbicka & Obidzinska, 1998), *Brassica pekinensis* (Xiong, 1998), and *Cicer arietinum* (Atici *et al.*, 2005) which showed inhibition of seed germination. Since the seed coats of different species differ in their permeability to Pb (Wierzbicka & Obidzinska, 1998), it is possible that the seed coat of *A. thaliana* could act as an effective barrier to Pb uptake and protect the embryos from Pb contamination. Thus, the important enzymes involved in germination processes were not affected (Singh *et al.*, 1997).

3.4.3 Pb uptake, accumulation and detoxification in *A. thaliana* seedlings

Pb content was expressed as nmol/plant and not as nmol/FW. This is partly because of the technical difficulties and inaccurate data obtained by weighing a discrete amount of plant material. The moisture content was rapidly lost into the surrounding particularly during dissecting the seedlings into the roots and shoots. In a comparison between heavy metal contents in plants on a per-plant and fresh-weight basis, it was shown that the trend for both quantification methods were comparable (Song *et al.*, 2003). The quantity of heavy metals uptake was dependent on the levels of $Pb(NO_3)_2$ treatment, and plant fresh weight was reduced following exposure to $Pb(NO_3)_2$ in a dose-dependent manner. Hence, Pb

contents of plant materials were not normalized by fresh weight.

Sections for TEM were made from approximately similar locations of the primary roots and cotyledons. The purpose of TEM was to localize the deposition of water-insoluble form of Pb within the tissues, and to check if Pb treatment resulted in subcellular disruption or modification of cellular structures. All TEM observations were performed on unstained sections, and Pb particles generally appeared as distinctive dark fine grains or heavy deposits. These dense granules and deposits in Pb-treated tissues that were not present in the non-Pb-treated controls were assumed to be Pb compounds. Identification of Pb deposits in post-osmicated unstained sections was sufficient as they are electron-dense, thus contrast with the tissue (Jarvis & Leung, 2001, 2002; Wierzbicka *et al.*, 2007). For each tissue type the control micrographs are used as a basis for comparison. Micrographs were also taken at a low magnification (e.g. 6,000 X) to allow visualization of the overall pattern of Pb accumulation in cells.

As observed in other studies (Lane & Martin, 1977; Kumar *et al.*, 1995; Huang & Cunningham, 1996; Liu *et al.*, 2000; Jarvis & Leung, 2001, 2002; Piechalak *et al.*, 2002; Malecka *et al.*, 2008), Pb accumulated mainly in the roots and Pb translocation from roots to shoots was low. Pb generally has a low bioavailability because it tends to be bound and immobilized within the soil matrix. It occurs as insoluble precipitates in the form of phosphate, carbonates and hydroxide, which are largely unavailable for plant uptake (Lasat, 2002). In this study, pH was maintained between 4.5 - 5.0 to maximize Pb solubility in modified Huang & Cunningham (1996) nutrient solutions. Low pH has been shown to increase the solubility of Pb (Blaylock *et al.*, 1997; Huang *et al.*, 1997).

The root is the primary source of entry for all inputs of Pb into the plant through ion exchange, and regulation of the Pb^{2+} influx and efflux to plants (Clemens *et al.*, 2002). Roots accumulate more Pb than leaves by trapping to the cation exchange capacity (CEC) of cell wall structure. Lane & Martin (1977) suggested that Pb moves predominantly into the root apoplast across the cortex in a radial manner. Then, Pb accumulates at the endodermis which acts as a partial barrier to Pb movement between the root and shoot. The crossing of metal ions from root apoplast to endodermis and suberised Casparian strips before entering the xylems is a difficult process (Greger, 1999). Translocation of metal ions from roots to shoots requires membrane transport proteins, which have yet to

be identified (Clemens *et al.*, 2002; Pilon-Smits, 2005). The binding of Pb to the cell walls through which it has to pass could also decrease Pb accumulation in the aerial parts of plants (Lane & Martin, 1977). All these have contributed to the apparently low translocation of Pb in *A. thaliana* seedlings, which was similar to the findings of other studies. Pb concentration in the shoots of 7-d-old *A. thaliana* seedlings was generally one- to five-fold less than Pb contents found in the root system.

Under TEM, Pb particles appeared as dark fine grains or dark heavy deposits. The larger particles typically have sharp, angular edges with a very grainy, crystalline appearance. The higher level of Pb found in the plants is highly dependent on sequestration and/or translocation processes. Metal accumulation and distribution patterns vary between species and within genotypes of a species. In general, the concentration of metals decreased from roots to stems, and leaves (Greger, 1999). Inorganics are sequestered in compartments where they are least harmful to cellular processes, such as vacuole, cell wall, epidermis and trichomes. Nevertheless, the size and shapes of Pb deposits, and their distribution in the cellular structures were generally not uniform (Wierzbicka, 1987).

In the present study, Pb sequestration was found to be associated with the binding to cell walls and precipitation in intercellular spaces. This finding is similar to many other studies showing that the cell wall is the main site of Pb accumulation (Antosiewicz, 2005; Jarvis & Leung, 2002; Seregin & Ivanov, 2001; Wierzbicka, 1998; Wierzbicka *et al.*, 2007). Pb has high affinity to negatively charged galacturonic acid, which is the main component of two pectin domains in the cell wall: homogalacturonan and rhamnogalacturonan (Polec-Pawlak *et al.*, 2007). For example, Qureshi *et al.* (1985) and Poulter *et al.* (1985) demonstrated that the high tolerance of Pb in *Anthoxanthum odoratum* is the result of Pb accumulation in the cell wall. By binding of Pb to specific sites in the cell walls of epidermis and mesophyll, the amount that enters into the cells is reduced, and thus cell metabolism might be protected against Pb toxic effects. Pb was also reported to increase polysaccharides in the cell wall and wall thickness of *Allium cepa* (Wierzbicka, 1998).

When the cell walls contain high concentration of metal ions, some could gain entry into the cytoplasm via active and passive transport (Greger, 1999). One of the possible pathways of which Pb cross the plasma membrane is through Ca^{2+}-channels (Huang & Cunningham, 1996). The authors discovered the significant inhibition of voltage-gated

Ca^{2+}-channel activity by Pb in the plasma membrane of wheat roots. Pb may block or compete with the Ca^{2+}-channels for transportation into the cells. Plant cells would then need to detoxify the metals by producing metal-chelating compounds, compartmentalization of the metals into the vacuole, or increasing efflux pumping of metals out of the cells. In this study, Pb was also found in various cellular compartments, particularly in the central vacuole as dense Pb aggregates. Some fine Pb grains were encapsulated in the vesicles, suggesting that specific intracellular mechanisms might be involved in cytosolic Pb transport to specific vacuoles or membranous compartments. Consistent with avoidance mechanisms (Clemens, 2001; Hall, 2002), vacuoles could play a role for toxic metal storage. By efflux of ions or compartmentalization into vacuole, excess metal ions can be removed or isolated from the cytosol, thereby protecting cells from the detrimental effects of Pb. Jarvis & Leung (2001) suggested that the thick Pb residues within the cell walls and around the intercellular spaces are indications of apoplastic transport. The existence of Pb in the cytoplasm of plant cells indicates a symplastic interaction. In response to a very high Pb concentration (200 μM), Pb deposits in *A. thaliana* cotyledons were found in chloroplasts, which may contribute to the higher visually observed symptoms of Pb toxicity at this level. The photosynthetic process of seedlings was likely to be affected by Pb.

The morphology of cellular components, including mitochondria, endoplasmic reticulum, and chloroplast, did not manifest signs of severe impact by the presence of Pb in this study. In *Pinus radiata* plants grown in a medium containing 500 μM $Pb(NO_3)_2$, no morphological change was observed in the cellular components (Jarvis & Leung, 2002). In contrast, the mitochondrial cristae and mitochondrial membranes were adversely affected in *P. sativum* roots exposed to a similar Pb concentration (Malecka *et al.*, 2008). The length of Pb treatment and plant species may account for these differences.

3.5 Conclusion

Pb is a non-essential element and its uptake by 7-d-old *A. thaliana* seedlings brought about changes in the morphology of the seedlings and inhibition of root growth. Their roots appeared to be short, thickened, brown, and with fewer root hairs. Based on the tolerance

index, 75 μM $Pb(NO_3)_2$ and above brought about more than 50% root growth inhibition. Roots and shoots have distinct roles in plant biology and are exposed to different environments. The roots are involved in the absorption of water and nutrients, while the cotyledon of shoots play a role in photosynthesis. Thus, both react differently when being challenged by heavy metal treatments. In response to Pb, *A. thaliana* seedlings primarily appear to undergo avoidance mechanisms. Consistent with previous studies, Pb was found to be retained predominantly in the root, and only a small portion of it was transported to the shoot. Pb was mainly immobilized in the cell walls and intercellular spaces to minimize Pb from entering the cells and interfering with the vital functions of cytosols. Pb that has inevitably entered the cytosols might be efflux-pumped and sequestered into the vacuoles. The rate of Pb translocation from roots to shoots was relatively low (18 - 43%) in *A. thaliana* seedlings, probably due to the binding of Pb to cell walls as it flowed through the xylem. In the present investigation, the morphology of cellular organelles seemed not to be severely affected by Pb. It is known that cytosolic heavy metals can dramatically increase ROS levels associated with membrane damage. The next chapter looks into the biochemical changes in *A. thaliana* seedlings to defend against Pb-induced oxidative stress, assessing the simultaneous tolerance mechanisms where plants repair, limit the excessive level of ROS in the cells, and maintain a healthier cellular environment.

Chapter 4

Pb-induced oxidative stress in *Arabidopsis thaliana* seedlings, monitored by antioxidant systems

4.1 Introduction

Pb has been shown to induce oxidative stress in various plant species by generation of lipid peroxidation and reactive oxygen species (ROS), such as superoxide anion ($\cdot O_2^-$), hydrogen peroxide (H_2O_2) and hydroxyl ($\cdot OH$) radicals (Rucinka *et al.*, 1999; Malecka *et al.*, 2001; Kopyra & Gwozdz, 2003; Verma & Dubey, 2003). However, the extent to which Pb intensity induces ROS greatly depends on Pb concentration, the duration of exposure, plant species and developmental stage (Sharma & Dietz, 2009). As Pb stress intensity is raised, the level of antioxidative enzymes activities might be increased as a defence mechanism against Pb-induced ROS, or decreased as a result of enzyme inactivation.

When Pb enters the cells, the equilibium of ROS is disrupted and becomes toxic to plant cells. Therefore, plants initiate a signal transduction pathway that triggers enzymatic and non-enzymatic antioxidative system to detoxify the cells (Ahmad, 1995; Dalton, 1995). In successive attacks, superoxide dismutase (SOD) destroys superoxide radicals, catalase (CAT) decomposes hydrogen peroxides, glutathione peroxidase (GPX) neutralizes lipid hydroperoxides, and glutathione reductase (GR) regenerates glutathiones.

Non-enzymatic antioxidants including carotenoids, tocopherols, ascorbic acid, and glutathione are also of important components (Ahmad, 1995; Dalton, 1995). On the other hand, Pb ions are capable of binding to the thiol group of several enzymes, lowering the capacity of oxidation-reduction and electron transport system. ROS are overproduced, leading to cell death (Malecka *et al.*, 2001).

Our knowledge of the biochemical basis of Pb-induced responses in early seedlings growth of *A. thaliana* is still sketchy. Early seedling growth is of particular importance because it is the initial stage in the life of a plant which projects its future physiological and biochemical processes (Singh *et al.*, 1997). In this study, we aim to better understand the defence mechanisms of 7-d-old *A. thaliana* exposed to Pb by investigating the following processes: 1) the generation of ROS caused by Pb, 2) oxidative stress as a result of ROS production, 3) the activity of several antioxidant enzymes, and 4) the correlation between intensity of the stress, Pb concentration and antioxidant capacity of plant cells.

4.2 Materials and methods

4.2.1 Plant material and culture conditions

There were three replicate plates in each Pb treatment group, at the concentrations of 0, 25, 50, 75 and 100 µM. Approximately 150 *A. thaliana* seeds (Col-0, Lehle Seeds, USA) were surface-sterilized and sown on modified Huang & Cunningham (1996) agar plate (see Sections 2.1 and 2.2).

4.2.2 Sample collection for biochemical studies

After 7 d of growth, all seedlings from three plates were collected with straight fine point forceps and pooled together into sterilized pre-weighed 1.5 mL Eppendorf tubes placed on ice (see Section 2.10). Liquid nitrogen was used to flash freeze the samples prior to storage at -80˚C.

4.2.3 Extractions and assays for hydrogen peroxide, lipid hydroperoxide and antioxidative enzymes

The extraction and measurement of H_2O_2, lipid hydroperoxide, SOD, CAT, GR, GPX and POD were conducted according to the procedures explained in Sections 2.11 and 2.12. A total of five independent sample extractions were carried out, each using a pool of plant materials from three replicate plates (~150 seedlings x 3 plates = ~450 seedlings per crude extract). Crude extracts from different Pb treatment groups were analyzed using a plate reader.

4.2.4 Statistical analysis

Each crude extract was considered as an independent experimental unit for statistical analysis. The results are the means and standard error of mean from five independent biological samples. Data were transformed for statistical analysis. As described in Section 2.23, one-way analysis of variance (ANOVA) was accomplished using STATISTICA 8 (StatSoft Inc., USA) and tested for homogeneity of variance (Hartley F-max). Significant difference between the means of Pb treatments group were compared using Fisher's LSD test. Different letters in the graphs indicate the results are significant at a probability of 5% ($p < 0.05$).

4.3 Results

4.3.1 Pb stress induced ROS generation

No significant difference in the H_2O_2 content was detected in *A. thaliana* seedlings treated with 25 μM $Pb(NO_3)_2$ compared with the control (Figure 4.1). Generally, a higher amount of H_2O_2 level was found in seedlings treated with higher concentrations of $Pb(NO_3)_2$ ($\geq$ 50 μM) in the medium. In the treatment with 100 μM $Pb(NO_3)_2$, the seedlings contained 2.2-fold more H_2O_2 than the control ($p < 0.05$).

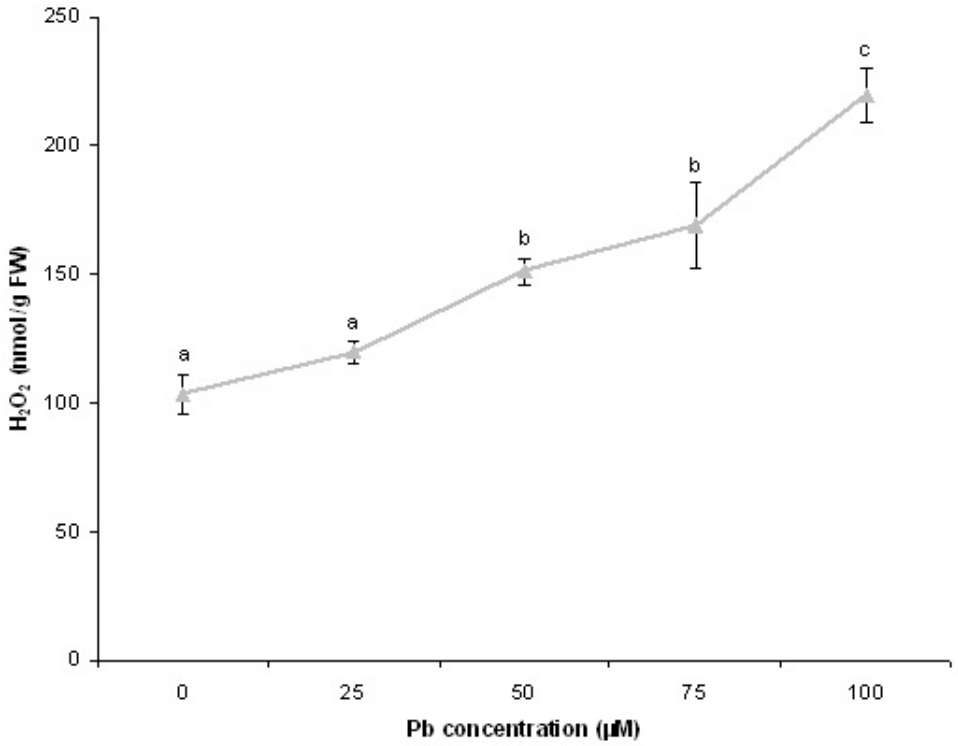

Figure 4.1: Effect of Pb on H_2O_2 level of 7-d-old *A. thaliana* seedlings. Results presented as mean $\pm$ standard error (n = 5). Different letters in the graph represent significant differences at $p < 0.05$, according to one-way ANOVA and multiple comparison using Fisher's LSD test.

4.3.2 Oxidative stress as a consequence of Pb exposure

Lipid hydroperoxide level in seedlings exposed to 25 μM $Pb(NO_3)_2$ was 4.1-fold greater than that of the control ($p < 0.05$, Figure 4.2). Seedlings treated with 50, 75 and 100 μM $Pb(NO_3)_2$ contained 5.4-, 7.6- and 9.6-fold, respectively, more lipid hydroperoxide than that of the control ($p < 0.05$).

4.3.3 Changes of antioxidative enzyme activities

The activities of SOD, CAT, GR, GPX and POD in the extracts of *A. thaliana* seedlings treated with different concentrations of $Pb(NO_3)_2$ and without it (control) were determined. After 1 week of exposure to $Pb(NO_3)_2$, increased activities of these antioxidative enzymes were generally observed, except when seedlings were exposed to 25 μM $Pb(NO_3)_2$, in comparison to the control ($p > 0.05$, Figures 4.3, 4.4, 4.5, 4.6, and 4.7). When the $Pb(NO_3)_2$ concentration in the growth medium was 100 μM, the specific activities of all antioxidative enzymes tested were significantly enhanced by 2.1-, 3.2-, 2.3-, 1.8- and 4.6-fold, respectively, compared with the control ($p < 0.05$). Significant elevations of the activities of these enzymes (except GPX) were also observed at 50 and 75 μM $Pb(NO_3)_2$.

4.4 Discussion

4.4.1 Pb, ROS and oxidative stress

Pb does not participate in plant metabolism. Thus, there is a need to understand the mechanisms behind the ability of plants to survive in Pb contaminated environments. The destructive effects of Pb are visibly morphologically, and ultrastructural studies have already shown that most of the Pb was sequestered in cell walls, intercellular spaces, or vacuole (Chapter 3). Plants also undergo biochemical changes to mitigate against oxidative stress induced by heavy metals (Navari-Izzo & Quartacci, 2001). Under normal conditions, ROS is a by-product of various plant metabolic pathways, including photosynthesis, respiration, fatty acid oxidation, and aging (Liu *et al.*, 2009a). The levels of ROS inside the cells are maintained at their lowest by the relevant protective mechanisms

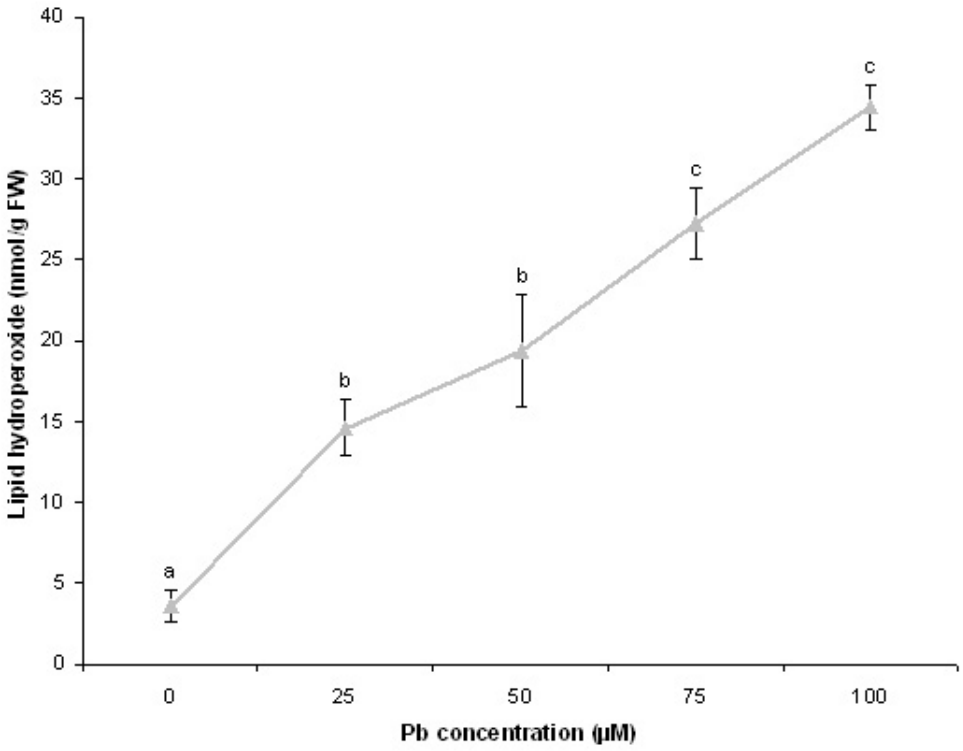

Figure 4.2: Effect of Pb on lipid hydroperoxide level of 7-d-old *A. thaliana* seedlings. Results presented as mean ± standard error (n = 5). Different letters in the graph represent significant differences at $p < 0.05$, according to one-way ANOVA and multiple comparison using Fisher's LSD test.

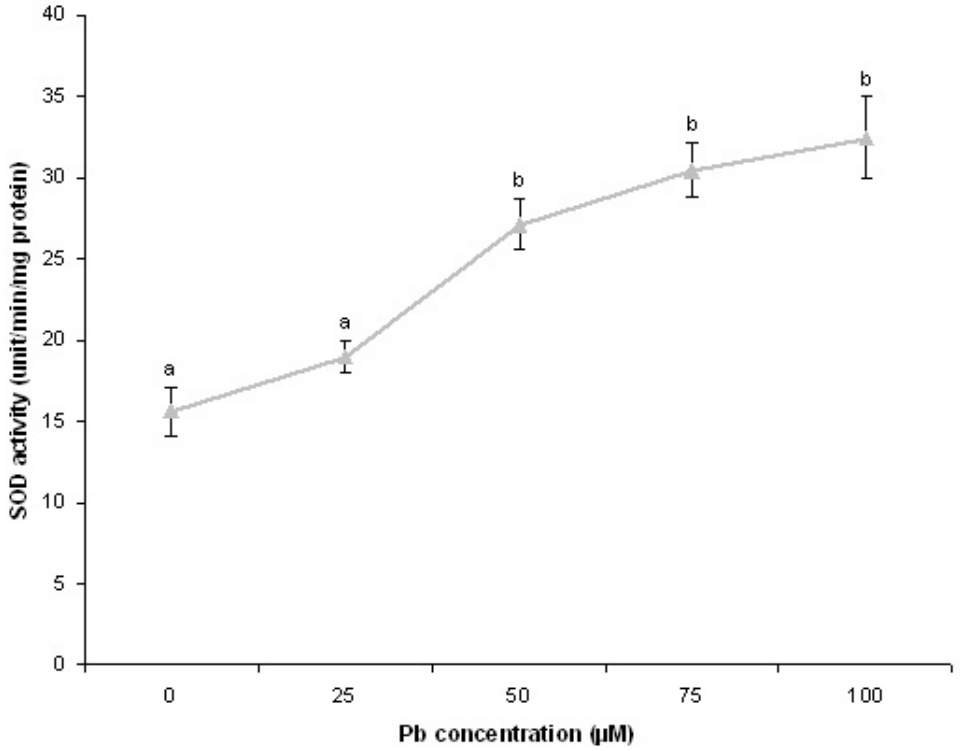

Figure 4.3: Effect of Pb on the specific SOD activity of 7-d-old *A. thaliana* seedlings. Results presented as mean ± standard error (n = 5). Different letters in the graph represent significant differences at $p < 0.05$, according to one-way ANOVA and multiple comparison using Fisher's LSD test.

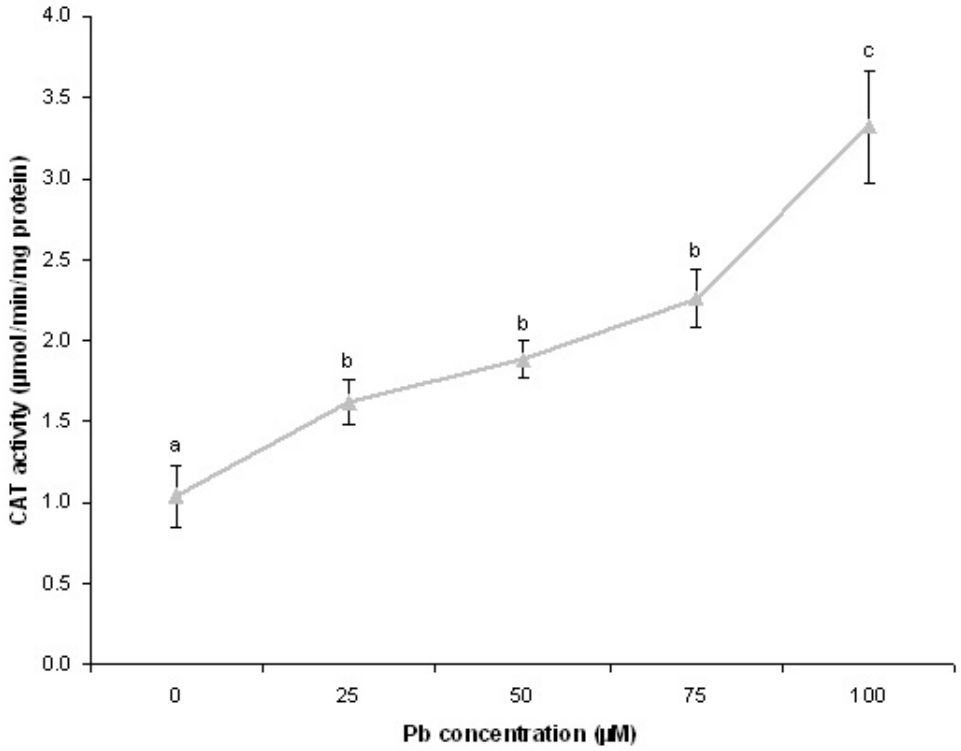

Figure 4.4: Effect of Pb on the specific CAT activity of 7-d-old *A. thaliana* seedlings. Results presented as mean ± standard error (n = 5). Different letters in the graph represent significant differences at $p < 0.05$, according to one-way ANOVA and multiple comparison using Fisher's LSD test.

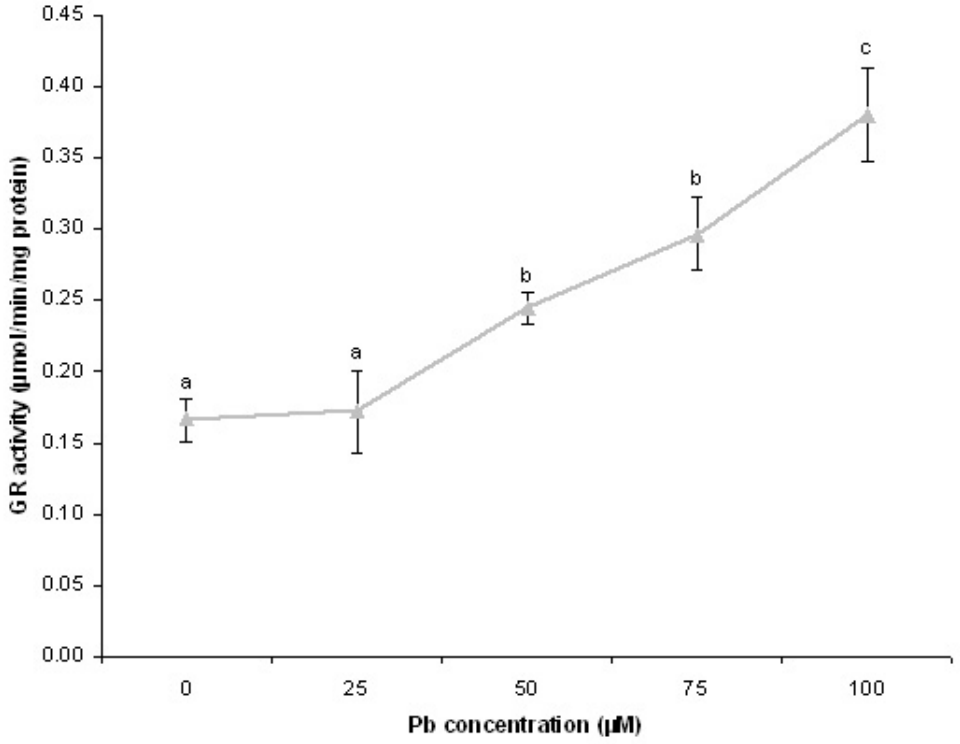

Figure 4.5: Effect of Pb on the specific GR activity of 7-d-old *A. thaliana* seedlings. Results presented as mean ± standard error (n = 5). Different letters in the graph represent significant differences at $p < 0.05$, according to one-way ANOVA and multiple comparison using Fisher's LSD test.

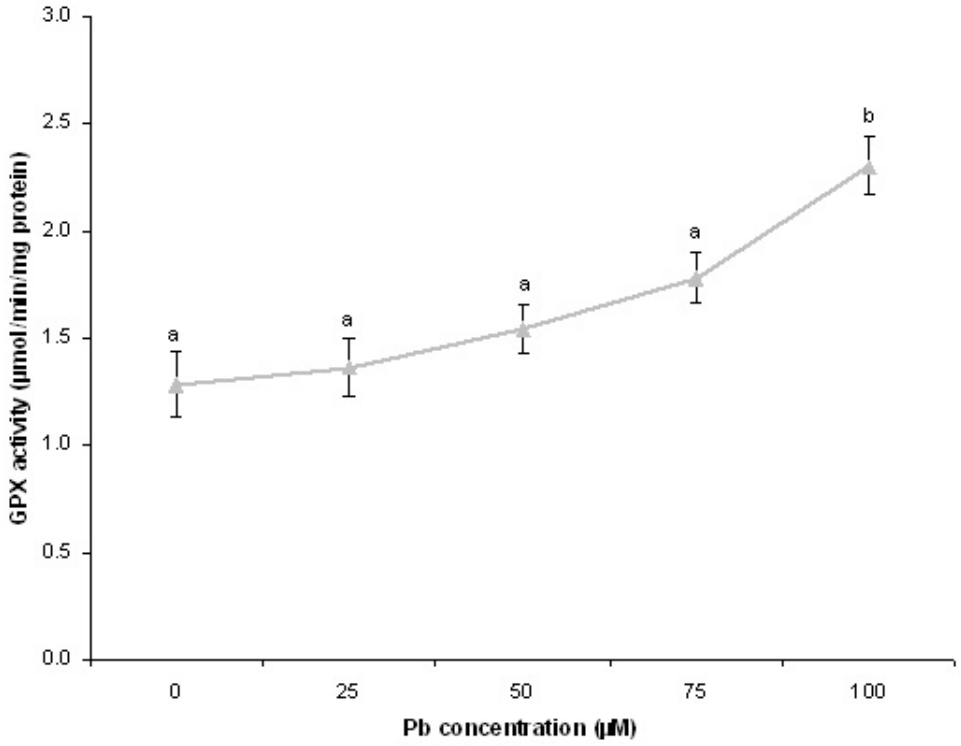

Figure 4.6: Effect of Pb on the specific GPX activity of 7-d-old *A. thaliana* seedlings. Results presented as mean ± standard error (n = 5). Different letters in the graph represent significant differences at $p < 0.05$, according to one-way ANOVA and multiple comparison using Fisher's LSD test.

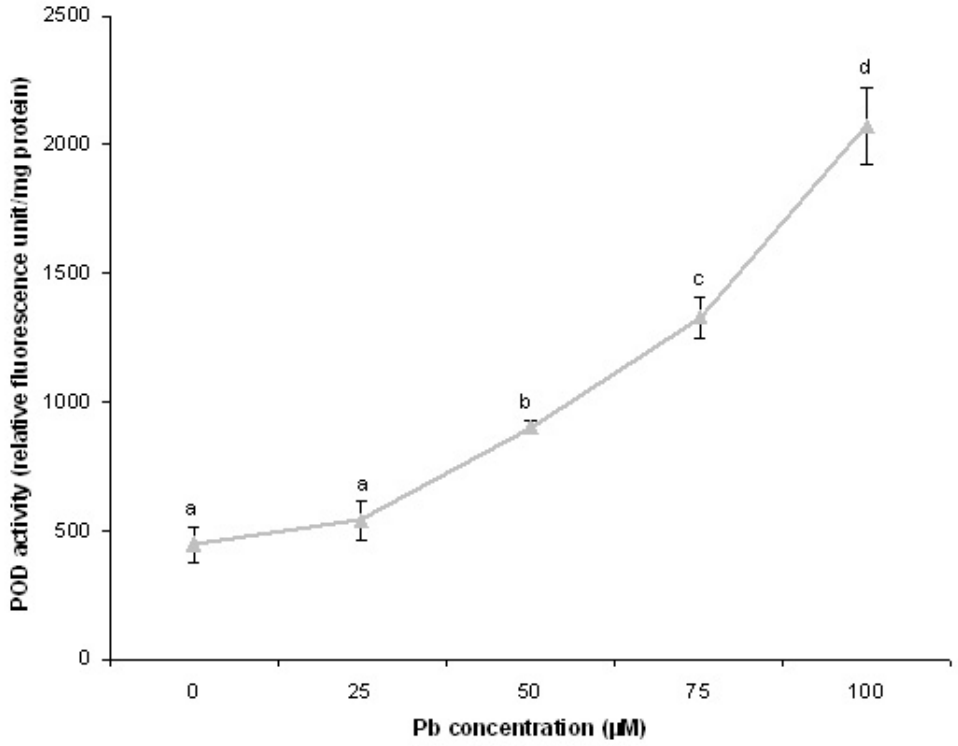

Figure 4.7: Effect of Pb on the specific POD activity of 7-d-old *A. thaliana* seedlings. Results presented as mean ± standard error (n = 5). Different letters in the graph represent significant differences at $p < 0.05$, according to one-way ANOVA and multiple comparison using Fisher's LSD test.

and scavenged by different antioxidative defence components. However, the equilibrium between production and scavenging of ROS is disturbed by adverse environmental factors including heavy metals (Bolwell & Wojtaszek, 1997; Blokhina *et al.*, 2003; Apel & Hirt, 2004). The degree of cell damage under heavy metal stress is greatly influenced by the rate of ROS generation, as well as the efficiency and capacity of cellular detoxification and repair systems (Dietz *et al.*, 1999).

Various studies have reported that Pb accelerates ROS-generating processes (in the form of $^{\cdot}O_2^-$, H_2O_2, or $^{\cdot}OH$) and causes overproduction of ROS in plants, resulting in membrane damage, and leading to oxidative stress (Rucinka *et al.*, 1999; Malecka *et al.*, 2001; Geebelen *et al.*, 2002; Piechalak *et al.*, 2002; Kopyra & Gwozdz, 2003; Verma & Dubey, 2003; Ruley *et al.*, 2004; Reddy *et al.*, 2005; Ruciska-Sobkowiak & Pukacki, 2006; Przymusinski *et al.*, 2007; Qureshi *et al.*, 2007; Liu *et al.*, 2008; Malecka *et al.*, 2009a,b). In the present investigation, Pb was also capable of inducing H_2O_2 and lipid hydroperoxide accumulation in *A. thaliana* seedlings. Pb affects the electron transfer and metabolic activities in the chloroplasts, mitochondria, and peroxisomes, which are the main sources of ROS (Sharma & Dietz, 2009). These events lead to imbalanced cellular redox activities, where excess H_2O_2 triggers the secondary messengers and responses in plants by reacting with amino acids, unsaturated fatty acids and other molecules (Dietz *et al.*, 1999; Sharma & Dietz, 2009). Additionally, Pb can change the fatty acid composition in lipid membranes by decreasing saturated fatty acids level and increasing unsaturated fatty acids content in the membrane (Halliwell & Gutteridge, 1999). Thus, plasma membrane may increase its permeability through K^+ ions leakage and accelerated the senescence rate. Increased lipid peroxidation is considered to be an indication of oxidative stress (Devi & Prasad, 1999).

4.4.2 Effects of Pb on antioxidative defence system in plants

In order to repair the H_2O_2-initiated cell damage, plants have developed a complex antioxidative defence system. The enzymatic and non-enzymatic antioxidants determine the steady-state level of cellular ROS and prevent them from exceeding the toxic thresholds (Choudhury & Panda, 2005; Sharma & Dietz, 2009). However, heavy metal stress disrupts the balance between ROS production and detoxification (Sharma & Dietz, 2009).

In the present study, *A. thaliana* seedlings exhibited an increased antioxidative defence. This would help to remove excess ROS.

As the first line of defence against ROS-mediated toxicity, SOD neutralizes destructive $\cdot O_2^-$ which is converted to H_2O_2 and O_2 (Ahmad, 1995; Dalton, 1995). SOD also functions as an enzymatic protector against Pb-induced peroxidation (Reddy *et al.*, 2005; Ruley *et al.*, 2004). A Pb-dependent increase in the specific activity of SOD was found in the 7-d-old seedlings. Pb seems to initiate SOD synthesis in cells for the removal of $\cdot O_2^-$ radicals. This is consistent with other studies on *Pisum sativum* (Malecka *et al.*, 2001), *Lupinus luteus* (Rucinka *et al.*, 1999; Kopyra & Gwozdz, 2003), *Oryza sativa* (Verma & Dubey, 2003), *Sesbania drummondii* (Ruley *et al.*, 2004), *Macrotyloma uniflorum*, *Cicer arietinum* (Reddy *et al.*, 2005), *Cassia angustifolia* (Qureshi *et al.*, 2007), and *Sedum alfredii* (Liu *et al.*, 2008). In *Hypnum plumaeforme*, SOD activity increased significantly at 0.01 and 0.1 mM Pb, but decreased gradually with higher Pb concentrations. This is because excess ROS may interact with the -SH groups of the enzymes, damaging the SOD structure and deactivating its physiological functions (Sun *et al.*, 2009). Up-regulation of SOD is essential to maintain the overall defence system of plants susceptible to oxidative damage (Qureshi *et al.*, 2007).

CAT, an oxidoreductase, acts sequentially to SOD, converting H_2O_2 to non-toxic H_2O and O_2. An increase in CAT was observed in 7-d-old *A. thaliana* seedlings, suggesting its adaptive feature to combat Pb-mediated oxidative damage. The scavenging mechanism to remove excessive H_2O_2 seems to be effective. Similarly, an increase of CAT activity was found in *S. drummondii* (Ruley *et al.*, 2004), *M. uniflorum*, *C. arietinum* (Reddy *et al.*, 2005), and *C. angustifolia* (Qureshi *et al.*, 2007). When the toxic level of Pb reached a certain threshold, a decline in CAT was observed in *L. luteus* (Rucinka *et al.*, 1999), *P. sativum* (Malecka *et al.*, 2001), and *O. sativa* (Verma & Dubey, 2003), attributed to the inactivation of enzyme proteins, reduction in enzyme synthesis or alteration in the enzyme subunit groups (Verma & Dubey, 2003). The intensity of Pb stress on CAT activity was found to be tissue specific and species dependent (Malecka *et al.*, 2001; Verma & Dubey, 2003).

GR is one of the enzymes of the ascorbate-glutathione cycle, catalyzing the NADPH-dependent reduction of glutathione disulphide (GSSG) to glutathione (GSH). A high

GSH/GSSG ratio is important for maintaining the proper redox conditions in the cells (Ahmad, 1995; Dalton, 1995). The present study showed a gradual increase of GR activity in Pb-treated *A. thaliana* seedlings. GR may help to regenerate GSH from GSSG under Pb stress to increase the GSH/GSSG ratio and total GSH pool. Similarly, induction in GR activity due to Pb treatments have been reported in *O. sativa* (Verma & Dubey, 2003), *M. uniflorum*, *C. arietinum (Reddy* et al.*, 2005)*, *C. angustifolia* (Qureshi *et al.*, 2007), and the roots of *S. alfredii* (Liu *et al.*, 2008).

On the other hand, GPX renders potentially harmful H_2O_2 to harmless H_2O, using GSH as a reducing agent. The GPX cycle is closely associated with the regeneration of GSH from GSSG by GR (Ahmad, 1995). Cytosolic GPX also catalyzes lipid hydroperoxides (Ahmad, 1995) to reduce Pb-mediated oxidative stress. The induction of GPX activities in the present investigation suggests a general strategy adopted by *A. thaliana* seedlings to deal with the oxidative stress imposed by Pb.

POD is also an important enzyme which scavenges H_2O_2. The role of POD in plants under stress has been widely accepted (Verma & Dubey, 2003; Liu *et al.*, 2009a). In the present investigation, elevation of POD activity was evident as the intensity of Pb stress increased. The induction of POD has been reported as a general plant response to toxic concentrations of metal (Sun *et al.*, 2009). The inhibition of plant growth was correlated with the heavy metal dosage. POD isozymes are located in the cell wall, cytosol, vacuole and extracellular spaces (Verma & Dubey, 2003). Hence, the stimulation of POD activity in *A. thaliana* seedlings grown under Pb-containing medium might be a result of the POD released from the cell wall- and vacuole-bound Pb.

4.5 Conclusion

When Pb entered the cytosol and accumulated in 7-d-old *A. thaliana* seedlings, the generation of ROS was induced, and the level of lipid hydroperoxide was intensified. This was accompanied by an up-regulation in the activity of antioxidative enzymes, in a Pb-dependent manner. Pb toxicity caused oxidative stress in *A. thaliana* seedlings, which the seedlings appeared to be capable of activating cell rescue, defending themselves against the harmful oxidative stress and thereby acclimating to Pb. Therefore, a combination

of avoidance (see Chapter 3) and tolerance mechanisms exists in *A. thaliana* seedlings treated with Pb, that maintain the essential cellular metabolism for survival. In these circumstances, there are also common stress-related genes that are involved in ROS detoxification. The next chapter explores the molecular mechanisms focussing on the gene expression of annexin 1, which *A. thaliana* seedlings may invoke to reduce the toxic effects of Pb stress.

Chapter 5

Participation of Annexin 1 in the response of *Arabidopsis thaliana* seedlings to Pb exposure

5.1 Introduction

The lack of genes identified as conferring the capacity for Pb resistance and accumulation has delayed the potential of Pb phytoremediation (Song *et al.*, 2003). Currently, an important research focus is to seek a better understanding of the mechanisms of Pb tolerance by plant cells. This may be useful for genetically engineering plants with improved tolerance to Pb, and hence better phytoremediation capabilities in the near future. By identifying genes or proteins associated with Pb stress, molecular mechanisms governing stress responses can be further comprehended.

Annexins, which are Ca^{2+}-dependent phospholipid- and membrane-binding proteins, have been reported to be structurally related to HSP. They are able to function as chaperones, as well as having several other functions and biochemical properties similar to HSP (Rhee *et al.*, 2000; White *et al.*, 2002). This has led researchers to examine the existence of annexins in higher plants (Smallwood *et al.*, 1990, 1992; Clark & Roux, 1995; Delmer & Potikha, 1997; Gerke & Moss, 2002). The precise functions of annexins in plants are not known. However, annexin from *A. thaliana*, a model experimental plant, has been found to be regulated differently under a variety of abiotic stresses (see Sections 1.8.4.2

and 1.8.4.3). Although it has not been studied before, it would seem that annexins could be involved in the response of plants to heavy metal stress and that they might have a role in protecting the cells from such stress.

Annexin 1 (*AnnAt1*) is the most abundant annexin in *A. thaliana* and it has been subjected to the most detailed study among all plant annexins (Konopka-Postupolska *et al.*, 2009). *AnnAt1* is expressed predominantly in roots (Clark *et al.*, 2001; Lee *et al.*, 2004). The present study aims to obtain new insights into whether *AnnAt1* is involved in Pb tolerance in plant cells. The possible participation of *AnnAt1* in Pb stress was assessed by comparing gene expression between Pb stressed and non-stressed 7-d-old *A. thaliana* seedlings. Study of the change of AnnAt1 protein level under Pb stress was also attempted. A study of the relative contribution of annexin in defence against Pb stress may lead to revelation of molecular mechanisms involved in interactions between toxic metals and plant species.

Prior to qRT-PCR analysis, several strategies, such as ensuring high RNA quality and selecting internal controls for normalization, were performed to optimize the specificity, sensitivity, and reproducibility of qRT-PCR reactions. The considerations which have been incorporated in the present study are explained in this chapter.

5.2 Materials and methods

5.2.1 Plant materials and growth conditions

Approximately 150 cold-treated *A. thaliana* Col-0 seeds were sown on each agar plate containing modified Huang & Cunningham (1996) medium (see Sections 2.1 and 2.2). Each Pb treatment (0, 25, 50, 75 and 100 μM) consisted of three replicate plates.

5.2.2 Sample collection for molecular and protein studies

Seven-d-old *A. thaliana* seedlings were collected from three plates with straight fine point forceps. They were pooled together into a sterilized pre-weighed 1.5 mL Eppendorf tubes placed on ice (see Section 2.10). The weight of the plant materials for RNA extraction

was less than 100 mg (Qiagen, 2006). The samples were flash frozen in liquid nitrogen before storage at -80˚C.

5.2.3 RNA isolation and cDNA synthesis

Total RNA was extracted from the whole seedlings ($\leq$ 100 mg) by the RNeasy Plant Mini Kit (Qiagen) according to the manufacturer's procedure with slight modification (see Section 2.15.1). The RNA was treated with RNase-Free DNase kit (Qiagen) to eliminate the possible influence of genomic DNA contamination. Nucleic acid concentration was quantified using a NanoDrop® ND-100 Spectrophotometer (BioLab Nanodrop Technologies), as explained in Section 2.15.2. Purity of the total isolated RNA was ascertained by the 260/280 nm ratio and the RNA integrity was checked with 1% (w/v) agarose gel electrophoresis (see Section 2.15.3). cDNA synthesis was carried out using two-step RT-PCR according to the instructions from Transcriptor Reverse Transcriptase (Roche), as explained in Section 2.15.4.

5.2.4 Primer design

5.2.4.1 Housekeeping genes

A housekeeping gene, also known as an internal endogenous standard, should be a stable and secure unregulated transcript. Primer sequences for reference genes were chosen based on Cantero *et al.* (2006) and Remans *et al.* (2008). Candidate genes and their primer ID given in this thesis are listed in Table 5.1. PCR primers were designed using web Primer3 (Rozen & Skaletsky, 2000) and BLAST search, as explained in Section 2.16.1.

All combinations of the candidate reference genes were tested in real-time PCR. A dissociation curve was generated to check for specificity of the amplification product, and further confirmed by direct agarose gel electrophoresis (see Section 2.17). All primers were ordered from Invitrogen.

Candidate gene	**Primer ID given in this thesis**	**Forward primer**	**Reverse primer**	**GenBank accession number**	**Start location**	**Stop location**
Adenosine phosphoribosyl transferase 1	*APT1*	TTGGATCGAGTGTTGATGCT	CGGGGATTTTAAGTGGAACA	AF325045	627	786
SAND family protein	*SAND*	GCGTTAAGGCAAGCTACAGG	TTTCTGTGCACCAGCAAGAC	NM_128399.3	1063	1173
Mitosis protein YLS8	*YLS8*	TCCCGTGAACTGGTTTCATT	CAACGGCTTCCAAATTTCAT	NM_120912.2	564	706
F-box protein	*FBOX*	GCACTTCTGAGACTTTCGGC	GGCTGTTGCATGACTGAAGA	NM_121575.4	1446	1602

Table 5.1: Reference genes and their primer sequences.

5.2.4.2 The target gene

Primer sequences specific for *AnnAt1* were designed by Dr. Gregory B. Clark (Department of Molecular Cell and Developmental Biology, University of Texas, Austin, Texas, USA) using web Primer3 (Rozen & Skaletsky, 2000) based on the cDNA sequences deposited in NCBI (http://www.ncbi.nlm.nih.gov/Entrez/). The 3'-untranslated region was used to generate primer specific for *AnnAt1* as it is normally more unique than coding sequence (van Pelt-Verkuil *et al.*, 2008e). In a preliminary study, two forward and two reverse primers were designed. A dissociation curve was generated to check for specificity of amplification product, and confirmed by direct agarose gel electrophoresis. Upon verification, a primer pair with the best PCR efficiency was chosen for real-time PCR analysis (Table 5.2).

5.2.5 Evaluation and selection of stable housekeeping genes

Since the prerequisite for normalization of target gene transcript is to have a stable gene expression, it is crucial to select a proper internal control gene under the applied experimental conditions. Bestkeeper (Pfaffl *et al.*, 2004), NormFinder (Andersen *et al.*, 2004) and geNorm (Vandesompele *et al.*, 2002b) were used to validate the expression stability of candidate housekeeping genes (Table 5.1).

5.2.6 Real-time PCR conditions and assay optimization

Real-time PCR was performed to test reference genes and target gene in preliminary experiments. Annexin 1 gene expression was quantified relatively with mitosis protein YLS8 as an internal control (Section 5.3.1.2). The PCR mix was prepared according to the procedure for FastStart SYBR Green Master (Roche) as described in Section 2.16.2. "No template control" (NTC) contained 1 µL DEPC-water instead of diluted cDNA.

In the initial experiment, optimization of real-time PCR was performed by evaluating the optimum amount of cDNA template, and annealing temperature (T_a), across a range of concentrations. This included the use of a standard curve, or a linear dilution series of starting material (Section 5.2.7). PCR condition is crucial to produce reliable data (van Pelt-Verkuil *et al.*, 2008e). cDNA templates from different Pb treatment groups were

Candidate gene	**Primer ID given in this thesis**	**Forward primer**	**Reverse primer**	**GenBank accession number**	**Start location**	**Stop location**
Annexin 1	*AnnAt1*	GGAACAGCATTCCTTTGGAG	GCAGCTTATGTTTCTCTGTGGA	AF083913	893	1020

Table 5.2: Target gene and its primer sequences.

pooled, and then serial dilution of the templates into 1:1, 1:10 and 1:100 were carried out for real-time PCR tests. A 10-fold dilution of the cDNA was selected as the optimal condition for further real-time PCR experiments. Generally, the annealing temperature (T_a) of a primers pair is ± 5˚C lower than its melting temperature (T_m). Hence, T_a range between 52˚C to 55˚C was evaluated. 54˚C was selected as the annealing temperature for further real-time PCR experiments (Section 5.3.1.3).

Technical errors in real-time PCR were reduced by reducing the number of pipetting steps (see Section 2.16.2). Diluted cDNA was mixed with real-time PCR reagents, before aliquoting into each reaction well that had been preloaded with 1 µL each of the forward and reverse primers (6 µM working solution). All aliquots for target and housekeeping genes were carried out in parallel to minimize variation between PCR runs. Real-time PCR was performed in a 96-well reaction plate with a thermal cycler (Stratagene Mx3005P™) following a brief centrifugation to collect the samples at the bottom of the tubes.

The following thermal cycling conditions were used in real-time PCR: 50˚C for 2 min to prevent carry-over contamination; 95˚C for 10 min to activate FastStart Taq DNA Polymerase; and 40 cycles of denaturation at 95˚C for 15 s; annealing of primers at 54˚C for 60 s; extension at 72˚C for 30 s (see Section 2.16.3). Fluorescent data were acquired at the end of the extension phase. Automated melting curve analysis (95˚C for 60 s; 55˚C for 30 s; 95˚C for 30 s) with a heating rate of 0.1˚C per second was generated to check for specificity of amplification (see Section 2.17.1).

Gel electrophoresis was also conducted at the end of each PCR run as an additional control of specificity to confirm that only one single product of the expected length was yielded (see Section 2.17.2).

5.2.7 Standard curve for PCR amplification check

A standard curve was generated using a 4-fold dilution series over at least 4 dilution points to assessed the accuracy of pipetting, reproducibility, and sensitivity of a PCR assay. Three technical replicates comprising triplicates were independently performed. A linear regression line was plotted by taking the logarithm of the template concentration against the corresponding threshold cycle using Microsoft Office Excel 2003 (Microsoft

Corporation, USA). Graphical trendlines represent linear fits. R^2, slope and intercept were generated.

The slope value and correlation coefficient (R^2) of the standard curve will show if a linear relation is observed. Generally, a good standard curve gave high efficiency (90% - 110%), good linear fit ($R^2 > 0.985$), and low replicate variability for individual standards ($SD_{rep}/mean_{rep}$ x 100 = %CV < 1%) (Muller, 2007; Stratagene, 2007; Vandesompele, 2009).

5.2.8 Efficiency of the PCR reaction

PCR efficiency can be obtained conveniently from REST software (Pfaffl *et al.*, 2002). Alternatively, the slope of the line of best fit drawn to the standard curve was used to determine reaction efficiency. Typically, a linear fit with a slope between -3.1 and -3.6 is equivalent to calculated 90 - 110% reaction efficiency (Stratagene, 2007). The following equation was also used to calculate the corresponding real-time PCR efficiency:

$$\text{Efficiency}=10^{(-1/\text{slope})}-1$$

(Slope = slope of the standard curve)(Peirson *et al.*, 2003)

The efficiency and accuracy of a PCR assay determined the quality of a standard curve, and vice versa. Theoretically, for 100% PCR amplification efficiency, the amount of DNA is expected to double with each cycle.

5.2.9 Quantification of gene expression and statistical analysis

The relative expression of *AnnAt1* gene was normalized against the expression of *YLS8* which is the most consistently expressed reference gene transcript. The fold differences of *AnnAt1* in response to different Pb concentrations were quantified and analyzed in REST 2008 (Pfaffl *et al.*, 2002), using pair-wise randomization test (see Section 2.18). *P*-values which were less or equal to 0.05 showed that there was significant difference between the Pb treatments. This experiment was performed three times, each with an independent biological sample.

5.2.10 Protein analysis

The total protein was extracted from frozen whole seedlings (~100 mg) according to Weigel & Glazebrook (2002) with modification (see Section 2.19). The protein contents of the crude extracts were quantified following the method of Bradford (1976) (see Section 2.20), and 35 µg protein was used for one-dimensional discontinuous SDS-PAGE according to Laemmli (1970) using 12% acrylamide (see Section 2.21). As described in Section 2.22, western blot analysis was performed following the work of Clark *et al.* (2005) and NBT-BCIP was used to detect the alkaline phosphatase activity.

5.3 Results

5.3.1 Gene expression of *AnnAt1*

5.3.1.1 Quality of isolated RNA

Isolated total RNA was visually observed on 1% (w/v) agarose gel (Figure 5.1). In each lane loaded with RNA samples, only two distinct bands can be seen. The bands appeared to be sharp showing no degradation. The 28S:18S rRNA ratio was relatively high ($\geq$1.0) and a A_{260}/A_{280} ratio of 1.9 - 2.1 was obtained from the spectrophotometer, indicating high quality, intact RNA. No extra high molecular weight band was seen, confirming the efficient removal of genomic DNA with DNase I.

5.3.1.2 Expression stability and selection of the housekeeping gene

In order to select the best housekeeping gene for determination of *AnnAt1* transcript level, all Ct data obtained over the entire study were compared. Each of the three independent experiments consisted of triplicates of the control and each of the Pb treatment groups (0, 25, 50, 75 and 100 µM). Therefore, four candidate housekeeping genes, each of n = 45, were evaluated.

The software Bestkeeper help with the choice of the optimal housekeeping genes based on pairwise Pearson correlation coefficient (Pfaffl *et al.*, 2004). The results were directly obtained from standard deviation (SD) and coefficient of variance (CV) values. The lower the SD and CV values, the more suitable is the housekeeping gene for the

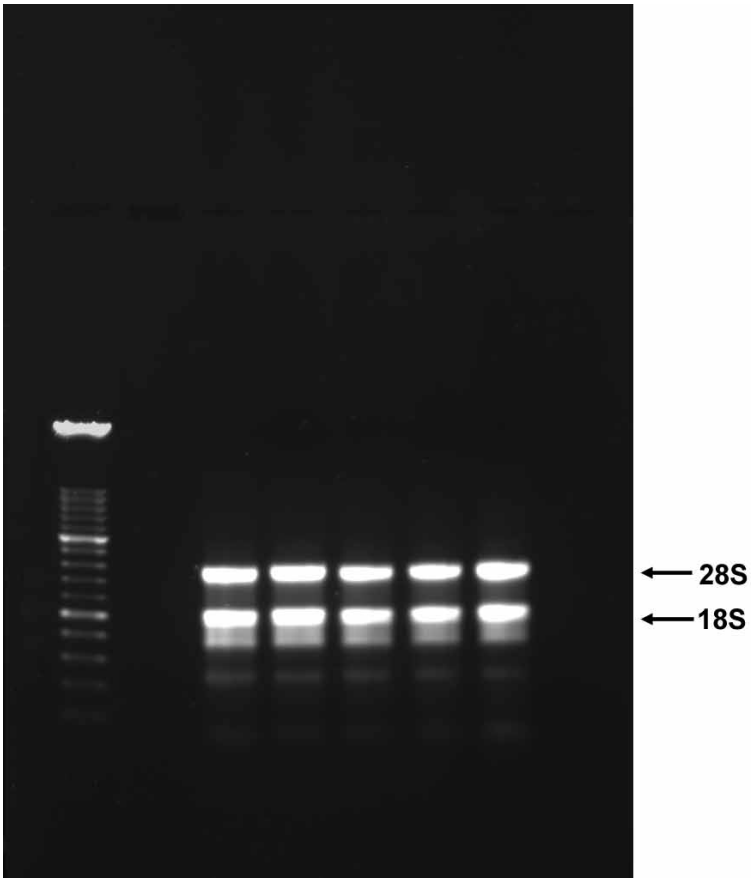

Figure 5.1: Integrity and size distribution of isolated total RNA. Sharpness of bands and ratio of 28S rRNA to 18S rRNA was observed after performing 1% (w/v) agarose gel electrophoresis. The image shown is a representative from three independent experiments with similar results. From left lane: DNA marker; RNA isolated from seedlings treated with 0; 25; 50; 75; and 100 µM $Pb(NO_3)_2$.

Data of candidate housekeeping genes (n = 4)				
Factor	***APT1***	***SAND***	***YLS8***	***FBOX***
N	45	45	45	45
GM [Ct]	24.61	27.37	23.48	27.72
AM [Ct]	24.62	27.39	23.39	27.73
Min [Ct]	23.19	25.70	22.37	26.58
Max [Ct]	26.37	29.02	24.90	29.44
SD [±Ct]	**0.57**	**0.82**	**0.53**	**0.67**
CV [% Ct]	2.30	3.00	2.26	2.42
Min [x-fold]	-2.65	-3.33	-2.10	-2.29
Max [x-fold]	3.35	3.26	2.58	3.47
SD [±x-fold]	1.48	1.76	1.44	1.59

Table 5.3: Descriptive statistics of four candidate housekeeping genes (*APT1*, *SAND*, *YLS8* and *FBOX*) obtained from Bestkeeper (Pfaffl *et al.*, 2004). Ct: cycle threshold values, N: number of samples, GM [Ct]: geometric mean of Ct, AM [Ct]: arithmetic mean of Ct, Min [Ct] and Max [Ct]: the extreme values of Ct, SD [±Ct]: standard deviation of Ct, CV [% Ct]: Ct's coefficient of variance as expressed in percentage, Min [x-fold] and Max [x-fold]: the extreme values of absolute regulation cooefficient, SD [±x-fold]: standard deviation of the absolute regulation coefficients.

present study. According to the variability observed, mitosis protein YLS8 has the lowest value among the four candidate housekeeping genes (Table 5.3), it appeared to be the most stably expressed internal control.

The average expression stability value (M) for each candidate housekeeping gene was calculated automatically by NormFinder using a model-based approach (Andersen *et al.*, 2004). The M of *APT1*, *SAND*, *YLS8* and *FBOX* is 0.006, 0.006, 0.002 and 0.004 respectively (Table 5.4). The top ranked gene, *YLS8*, has the smallest stability value, demonstrated that it is the most stably expressed candidate housekeeping gene.

Similar to NormFinder, the gene with the lowest M calculated automatically by geNorm is the most stably expressed control gene (Vandesompele *et al.*, 2002b). geNorm ranked *YLS8* as the most stable gene (M = 0.020; Table 5.5). This was followed by *FBOX*, *APT1* and *SAND*.

Data of candidate housekeeping genes (n = 4)				
Factor	***APT1***	***SAND***	***YLS8***	***FBOX***
N	45	45	45	45
M	0.006	0.006	0.002	0.004
SE	0.001	0.001	0.001	0.001
Best gene	**YLS8**			

Table 5.4: Stability values of four candidate housekeeping genes (*APT1*, *SAND*, *YLS8* and *FBOX*) obtained from NormFinder (Andersen *et al.*, 2004). The top ranked gene, YLS8, which has the smallest stability value, is the candidate gene most stably expressed. N: number of samples, M: average expression stability values, SE: standard error.

Data of candidate housekeeping genes (n = 4)				
Factor	***APT1***	***SAND***	***YLS8***	***FBOX***
N	45	45	45	45
M	0.023	0.026	0.020	0.022
Most stable gene	**YLS8**			

Table 5.5: Stability values of four candidate housekeeping genes (*APT1*, *SAND*, *YLS8* and *FBOX*) obtained from geNorm (Vandesompele *et al.*, 2002a). Gene with the lowest M values, YLS8, has the most stable expression. N: number of samples, M: average expression stability values, SE: standard error.

5.3.1.3 Optimization of PCR condition and assay

Since the known amount of a standard template for calculation of the initial amounts of unknown target samples was not available in the present molecular study, it is necessary to find out the optimum amount of cDNA template required for qPCR analysis. In a preliminary experiment, a serial dilution of pooled cDNA template was performed using the recommended final concentration of primers at 300 nM (Figure 5.2). A sigmoid-shaped amplification curve was observed. Although it is recommended that the lowest Ct value possible should be obtained (Stratagene, 2007), insufficient undiluted cDNA template was available to perform all the needed qPCR run. Hence, 10-fold diluted cDNA concentration was selected for subsequent qPCR assays.

The T_a ranges between 52˚C to 55˚C during the PCR reaction run gave similar results. Only one discrete peak was generated from the melting curve data and a single band was observed on the agarose gel, indicating the amplification was specific. Typically, the annealing temperature of primers pair is ± 5˚C lower than its melting temperature (van Pelt-Verkuil *et al.*, 2008c). Therefore, 54˚C was selected as the annealing temperature for all real-time PCR reaction experiments.

5.3.1.4 Real-time PCR efficiency

High PCR efficiency allows accurate quantification in real-time PCR. All available cDNAs were pooled into triplicates of varying dilutions, in order to determine the PCR efficiency of each transcript and achieve the best estimation of PCR efficiency. Logarithms of 4-fold serially diluted cDNA samples were plotted against threshold cycle (Ct) value. Standard curve of four candidate housekeeping genes: *APT1* (Figure 5.3) gave a slope of -3.3487 and R^2= 0.9992; *SAND* (Figure 5.4) gave a slope of -3.2046 and R^2 = 0.9911; *YLS8* (Figure 5.5) gave a slope of -3.4443 and R^2 = 0.9998; and *FBOX* (Figure 5.6) gave a slope of -3.1777 and R^2 = 0.9979. Slope for the target gene, *AnnAt1* is -3.4236 and its R^2 = 0.9999 (Figure 5.7). The high linearity of standard curves (R^2 > 0.985) indicates that the data points fit nicely to a straight line, meeting the correlation between replicates and the linear range of detection for PCR assay. PCR assays were reproducible. Ct value decreased with increasing cDNA input in control and Pb-treated groups.

The efficiency and accuracy of PCR determined the quality of a standard curve. The

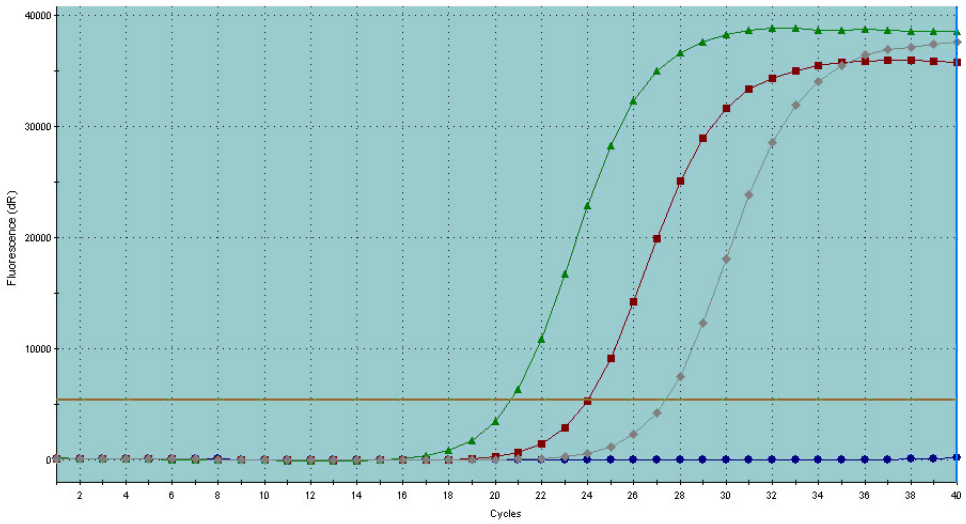

Figure 5.2: Amplification plot of *AnnAt1* using a linear dilution series of cDNA templates. cDNA templates from different Pb treatments group were pooled, serial dilution of 1:1, 1:10 and 1:100 were carried out in parallel. Blue line: blank, Green line: undiluted cDNA, Red line: 10x diluted cDNA, Grey line: 100x diluted cDNA.

corresponding real-time PCR efficiency was calculated according to the equation: efficiency = $10^{-1/\text{slope}}$-1, as shown in Table 5.6. Herein, the PCR efficiency for each candidate housekeeping gene is: *APT1* = 98.89%, *SAND* = 105.14%, *YLS8* = 95.13%, and *FBOX* = 106.39%. Real-time PCR efficiency for the gene of interest, *AnnAt1*, is 95.93%. The present study verifies that the real-time PCR assays were efficient (90 - 110%), allowing reliable gene quantification.

5.3.1.5 Verification of the amplification product

An automated melting curve analysis (also known as dissociation curve) was performed at the end of amplification reaction to ensure that only the gene of interest was amplified in the qPCR assay. A single distinct peak was observed in the 10-fold diluted cDNA sample in both the selected housekeeping (Figure 5.8) and target genes (Figure 5.9), at ~75˚C and ~77.5˚C, respectively. Only a small shift was observed in the no template control (NTC) of *YLS8* gene, probably due to contamination of the well.

Agarose gel electrophoresis was carried out to further verify the specificity of ampli-

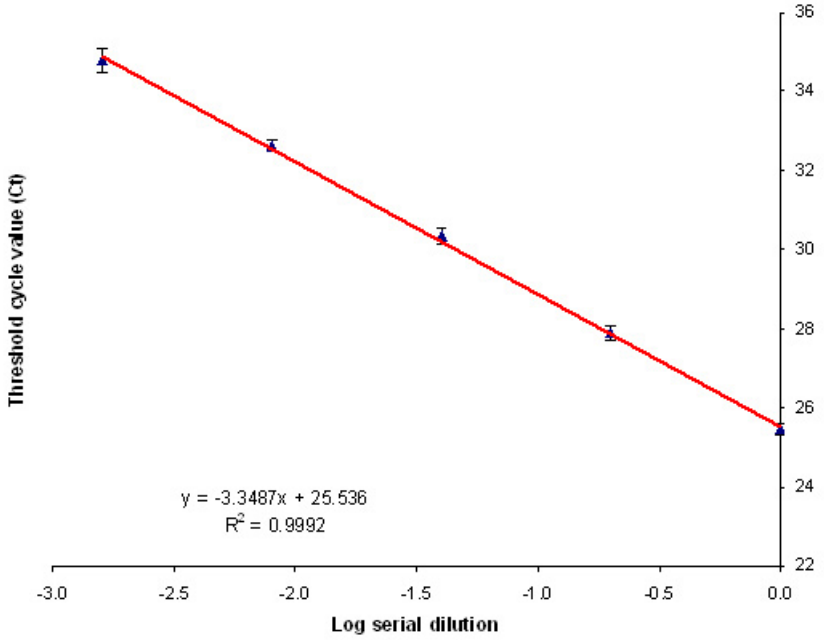

Figure 5.3: Standard curve of candidate housekeeping gene, adenosine phosphoribosyl transferase 1 (*APT1*), constructed from logarithm of 4-fold serially diluted cDNA samples and plotted against threshold cycle (Ct) value. Results presented as mean ± standard error from three independent experiments in triplicate (n = 9). Linear regression analysis of the standard curve shows near perfect linearity (R^2 = 0.9992).

Gene	**Slope of standard curve**	**PCR efficiency (%)**
Candidate reference genes		
APT1	-3.3487	98.89
SAND	-3.2046	105.14
YLS8	-3.4443	95.13
FBOX	-3.1777	106.39
Target gene		
AnnAt1	-3.4236	95.93

Table 5.6: Real-time PCR efficiency calculated from the slope of standard curve (Figure 5.3, 5.4, 5.5, 5.6 and 5.7), according to the equation E = $10^{(-1/slope)}$-1.

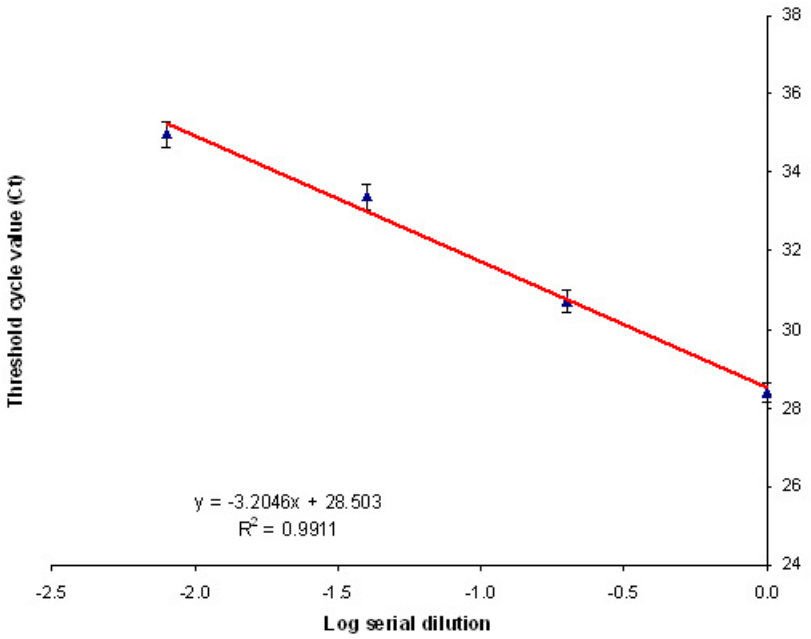

Figure 5.4: Standard curve of candidate housekeeping gene, SAND family protein, constructed from logarithm of 4-fold serially diluted cDNA samples and plotted against threshold cycle (Ct) value. Results presented as mean $\pm$ standard error from three independent experiments in triplicate (n = 9). Linear regression analysis of the standard curve shows near perfect linearity ($R^2 = 0.9911$).

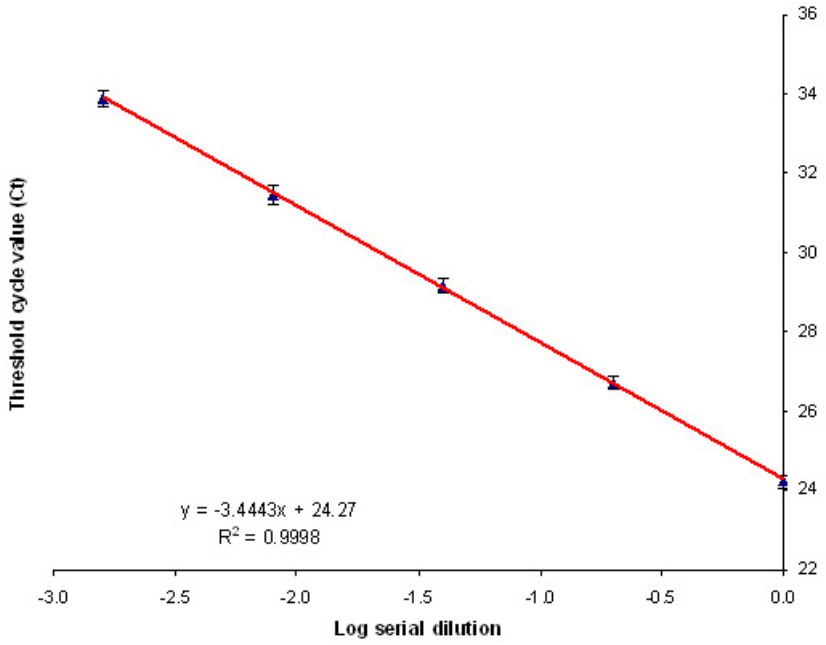

Figure 5.5: Standard curve of candidate housekeeping gene, mitosis protein YLS8, constructed from logarithm of 4-fold serially diluted cDNA samples and plotted against threshold cycle (Ct) value. Results presented as mean $\pm$ standard error from three independent experiments in triplicate (n = 9). Linear regression analysis of the standard curve shows near perfect linearity ($R^2 = 0.9998$).

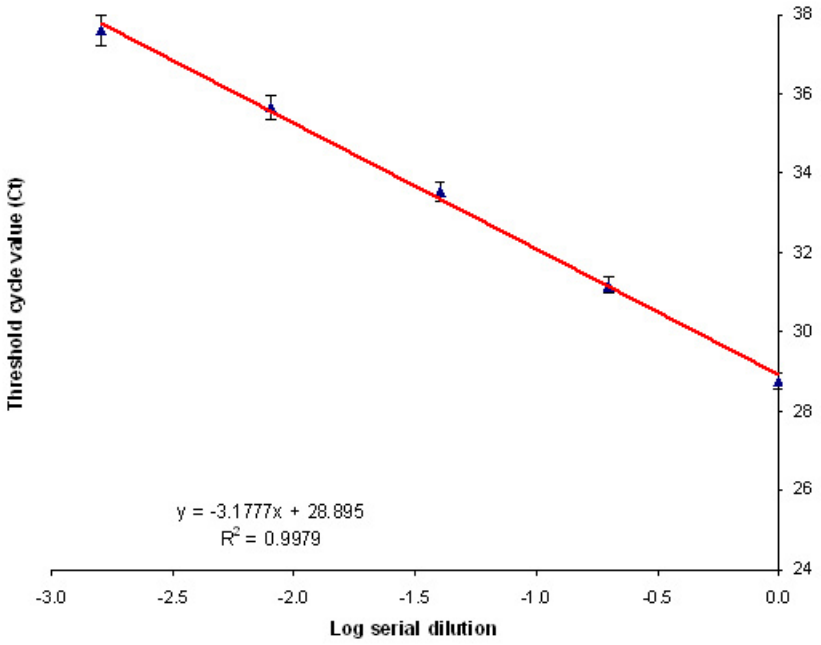

Figure 5.6: Standard curve of candidate housekeeping gene, F-box protein, constructed from logarithm of 4-fold serially diluted cDNA samples and plotted against threshold cycle (Ct) value. Results presented as mean $\pm$ standard error from three independent experiments in triplicate (n = 9). Linear regression analysis of the standard curve shows near perfect linearity ($R^2 = 0.9979$).

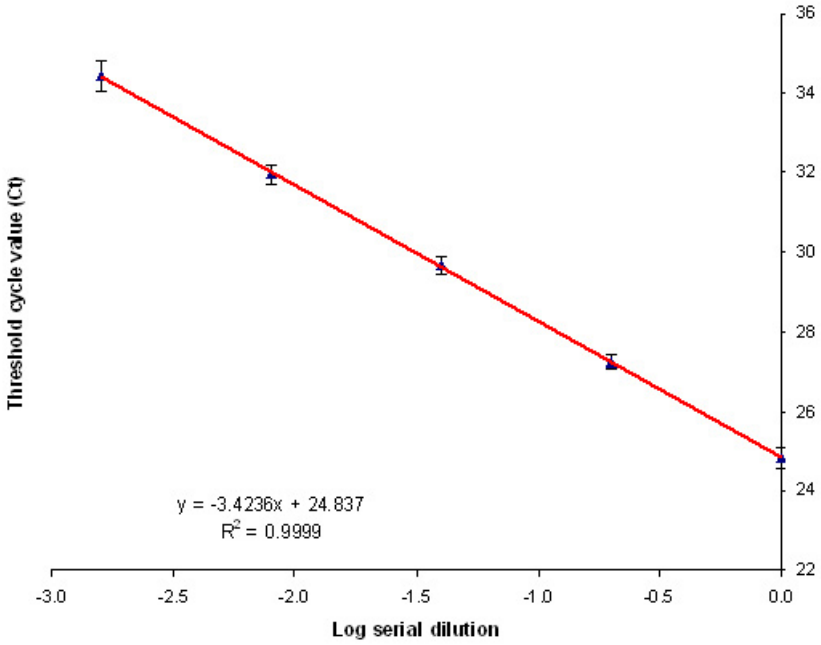

Figure 5.7: Standard curve of target gene, Annexin 1 (*AnnAt1*), constructed from logarithm of 4-fold serially diluted cDNA samples and plotted against threshold cycle (Ct) value. Results presented as mean $\pm$ standard error from three independent experiments in triplicate (n = 9). Linear regression analysis of the standard curve shows near perfect linearity ($R^2 = 0.9999$).

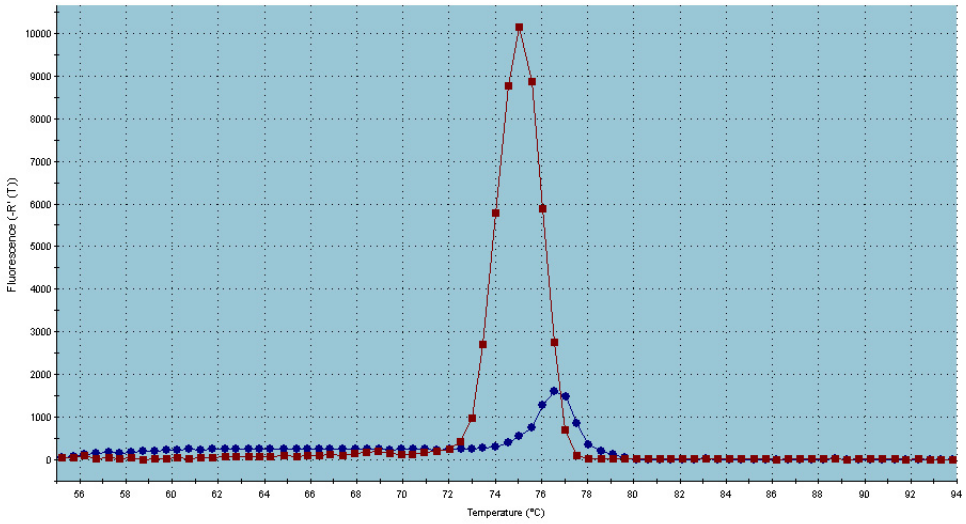

Figure 5.8: Dissociation curve of the selected housekeeping gene, mitosis protein YLS8. A representative image from three independent experiments with similar results is shown. Blue: NTC, Red: 10x diluted cDNA template.

cation products. As shown in Figure 5.10, a single PCR amplicon of the expected size was observed on the agarose gel. The length of amplicon for *APT1*, *SAND*, *YLS8*, *FBOX* and *AnnAt1* is 160, 111, 143, 157 and 128 bp, respectively. No band was observed in NTC.

5.3.1.6 Transcript level of *AnnAt1* in response to Pb

The relative quantification of *AnnAt1* gene expression normalizing against mitosis protein YLS8 was accomplished by REST 2008 software, based on the PCR efficiency and Ct deviation of Pb-treated sample to non-Pb treated sample (Pfaffl *et al.*, 2002). Significant difference between the relative expressions was evaluated by the software via a randomization test. As shown in Table 5.7, Pb effect on *AnnAt1* expression in plants exposed to lower $Pb(NO_3)_2$ concentrations (25, 50 and 75 µM) was not significantly different from the control ($p > 0.05$). However, *AnnAt1* message levels were doubled (2.12-fold, $p < 0.001$) in seedlings treated with 100 µM Pb, in comparison to the control.

Pb concentration (µM)	**Relative fold differences**	**SE**	**95% CI**	***P*-value**	**Interpretation**
0	1.000	-	-	-	-
25	1.022	0.844 - 1.260	0.651 - 1.497	0.767	-
50	0.967	0.777 - 1.284	0.453 - 1.487	0.802	-
75	1.069	0.679 - 1.489	0.489 - 1.668	0.581	-
100	2.115	1.769 - 2.614	1.265 - 3.029	0.000	Up-regulation

Table 5.7: Relative fold differences of *AnnAt1* in response to different Pb concentrations. The expression level of *AnnAt1* gene was normalized against mitosis protein YLS8 using REST 2008 software (Pfaffl *et al.*, 2002). Results from three independent experiments in triplicate (n = 9) were presented.

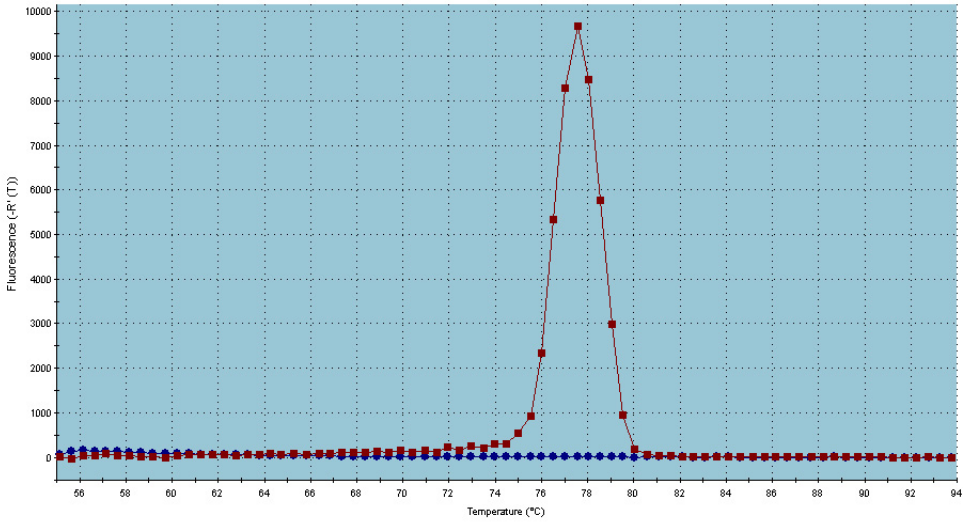

Figure 5.9: Dissociation curve of the target gene, Annexin 1. A representative image from three independent experiments with similar results is shown. Blue: NTC, Red: 10x diluted cDNA template.

5.3.2 AnnAt1 protein

5.3.2.1 Quality of protein extract

The qualitative characteristics of protein extracts obtained were evaluated using one dimension SDS-PAGE and Coomassie blue staining. A representative gel from many replicated experiments is shown in Figure 5.11. Well-resolved bands appeared on the gel and smearing was almost not visually observed suggesting good electrophorestic separation. The large subunit of Rubisco was clearly seen in all protein yields of 7-d-old *A. thaliana* seedlings exposed to different Pb treatments. However, despite more than 10 attempts to detect AnnAt1 protein (using antibody for this protein) after transfer of proteins from SDS-PAGE gel to nitrocellulose membrane, no signal was found.

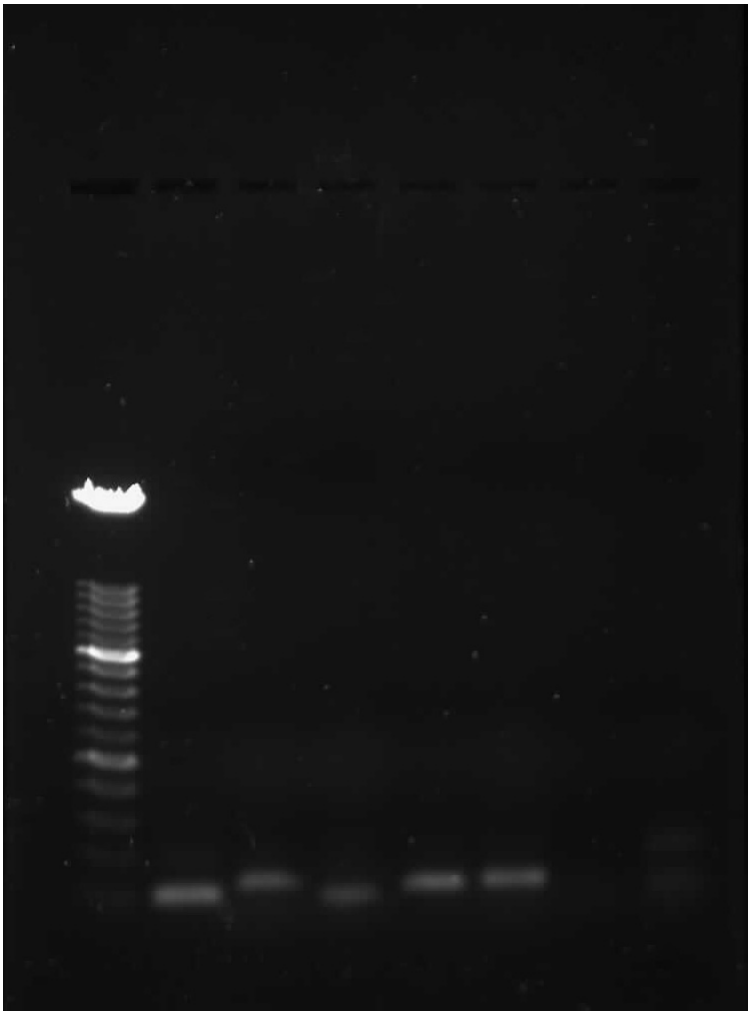

Figure 5.10: Specificity of the real-time PCR product documented with 1% (w/v) agarose gel electrophoresis. A single PCR product of the expected length was observed. From left: DNA marker; amplicon of *AnnAt1* (128 bp); *APT1* (160 bp); *SAND* (111 bp); *YLS8* (143 bp); and *FBOX* (157 bp); NTC.

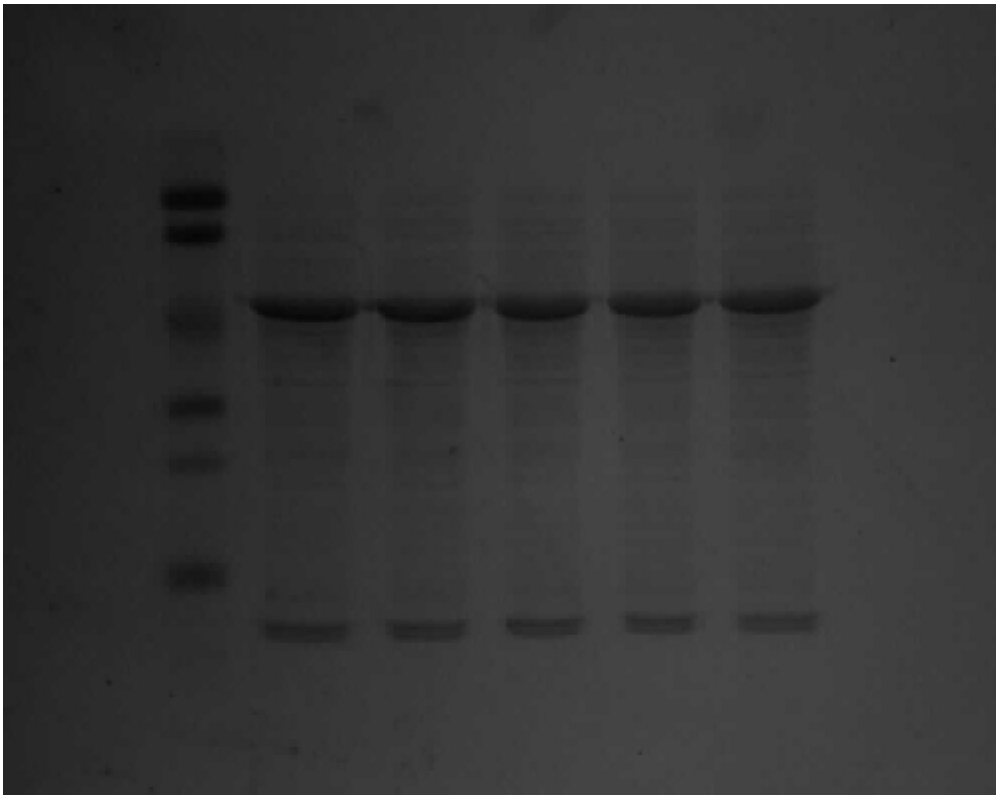

Figure 5.11: SDS-PAGE gel of proteins extracted from 7-d-old *A. thaliana* seedlings. Gel was stained with Coomassie-brilliant blue. From left lane: low-range Prestained SDS-PAGE standards (Bio-Rad); protein extracts from seedlings treated with 0; 25; 50; 75; and 100 μM $Pb(NO_3)_2$.

5.4 Discussion

5.4.1 Integrity of RNA and its effect on qRT-PCR

The quality of isolated RNA is of extreme importance in order to obtain a biologically meaningful study of changes in gene expression level (Fleige & Pfaffl, 2006). Degraded RNA samples greatly affect qRT-PCR data and the selection of proper housekeeping genes for normalization. By evaluating the impact of RNA quality on expression stability of a reference gene, Perez-Novo *et al.* (2005) found that the highly stable genes in intact RNA samples were among the most unstable genes in degraded samples. Consequently, the accuracy and reliability in the interpretation of gene expression results could be compromised.

It is well known that RNA is sensitive to degradation, a problem also encountered earlier on in the present study. By taking precautions in handling sample materials and elimination of RNase contamination (see Section 2.14), the integrity of total RNA isolated was apparently retained. Conventionally, RNA can be isolated via guanidine isothiocyanate or phenol/chloroform/isoamylalcohol method (van Pelt-Verkuil *et al.*, 2008a). In the present study, a commercial RNA isolation kit based on the chemistry of guanidine isothiocyanate and the denaturing activity of β-mercaptoethanol (van Pelt-Verkuil *et al.*, 2008a) was used for RNA extraction. It has the advantages of using only a small quantity of hazardous chemicals, as well as enabling efficient isolation of pure and intact RNA. DNase treatment was necessary in eliminating any contaminating genomic DNA template that may produce false positive amplification signals (van Pelt-Verkuil *et al.*, 2008c).

5.4.2 Ensuring PCR quality - reliability, sensitivity and specificity

5.4.2.1 PCR condition

Optimization of PCR condition was conducted in preliminary experiments to allow reliable detection of up- and down-regulation of gene expression. The primer anealing temperature and time were optimized to maximize the amplification efficiency and minimize incompletely amplified, non-specific, or extraneous primer-dimer originate from the self- or cross- homologies of primer-primer (Lowe *et al.*, 1990; van Pelt-Verkuil *et al.*,

2008c). Careful experimental procedures were instigated to reduce the technical errors in PCR reaction setup and minimize inter-variation of PCR runs (see Section 2.16.3). For example, the number of pipetting steps was standardized by preparing a master mix before aliquoting a standard volume into each reaction well. NTC was incorporated in all PCR reactions to check for contaminations (Udvardi *et al.*, 2008). The results obtained via the melting curve analysis (a single distinct peak) and agarose gel electrophoresis (a single PCR product of the expected size) verified the specificity of PCR amplification products in the present study.

5.4.2.2 PCR efficiency

PCR efficiency is closely associated with the sensitivity and specificity of the PCR amplification reaction (van Pelt-Verkuil *et al.*, 2008b). Low PCR efficiency may decrease the amount of specific amplification products by generating unintended non-specific amplification products. This may lead to over-estimation of gene expression level (Peirson *et al.*, 2003). Thus, PCR efficiency has a significant impact on the accuracy of gene expression calculations, and it is an essential marker in the quantification of a target gene (Tichopad *et al.*, 2003). The efficiency of PCR may be affected by the presence of inhibitors in the RNA samples, size of the amplification product, formation of the secondary structure, and quality of the primer (Fleige & Pfaffl, 2006). With proper primer pairs, RNA quality, and cDNA synthesis protocol, PCR efficiency can be optimized (Yuan *et al.*, 2006). The high reaction efficiency of 90 - 110% and linearity of standard curves ($R^2 > 0.985$) obtained in the present study add confidence to the reproducibility of gene expression results acquired.

5.4.2.3 Primer designs

The primers designs were based on the publicly available sequences and were tested using BLAST to minimize the influence of non-target binding sites. Whenever possible, care was taken in designing the primer pairs, as explained in Section 1.10.3.5. By minimizing the possibility of primer-dimer formation, amplification efficiency can be maximized (Bustin *et al.*, 2005). All housekeeping and *AnnAt1* primer pairs yielded a single product with equal efficiency, suggesting that the primer pairs selected were appropriate and

working properly.

5.4.3 Selection of a stably expressed housekeeping gene

Accurate quantification by qRT-PCR depends on the normalisation of the measured gene expression data with a stably expressed reference gene (Bustin, 2002; Vandesompele *et al.*, 2002b; Andersen *et al.*, 2004; Brunner *et al.*, 2004; Pfaffl *et al.*, 2004; Radonic *et al.*, 2004; Huggett *et al.*, 2005; Nicot *et al.*, 2005; Remans *et al.*, 2008; Guenin *et al.*, 2009). Since the expression of a commonly used housekeeping gene is not always stable (Thellin *et al.*, 1999; Czechowski *et al.*, 2005), three reference genes (*SAND*, *YLS8*, *FBOX*) suitable for studying gene expression in *A. thaliana* to Cd and Cu have been identified by Remans *et al.* (2008). *APT1* has been used by Cantero *et al.* (2006) as an internal control to normalize the transcript level of *AnnAt1* in response to abiotic stresses. These four candidate housekeeping genes were included in the present investigation, eliminating the need to search for new stably expressed reference genes subjected to Pb treatments.

In the present investigation, *YLS8* was identified as the best candidate reference gene for normalization by BestKeeper, geNorm, and NormFinder. This suggests that *YLS8* is suitable for studying the effect of $Pb(NO_3)_2$ on the gene expression of 7-d-old *A. thaliana* seedlings. The subsequent ranking of the candidate housekeeping genes (according to their stability values) generated by these softwares vary. The different algorithms used by the three reference gene validation softwares in evaluating the relative expression stability of these four candidate housekeeping genes may explain the variations.

5.4.4 The role of *AnnAt1* in Pb stress

Annexins are characterized by their potential to bind to negatively charged membrane phospholipids and calcium in a reversible manner. Transcriptome studies in *A. thaliana* have uncovered changes in stress-regulated genes in response to different environmental stimuli (Kreps *et al.*, 2002). *AnnAt1* gene expression may be up-regulated or down-regulated. Cantero *et al.* (2006) reported that the message levels of *AnnAt1* were increased 42-fold in response to NaCl, 39-fold in response to drought, and 13-fold in response to low temperature (4˚C). Under high temperature at 37˚C for 2 h, the message levels of *An-*

nAt1 were only increased marginally (less than 2-fold). In *Medicago sativa*, the annexin gene was induced by osmotic stress, abscisic acid (ABA, a stress hormone) and water deficiency (Kovacs *et al.*, 1998). In *Brassica juncea*, an annexin gene, *AnnBj1*, was regulated by ABA, ethephon, salicylic acid, methyl jasmonate, NaCl, Mannitol, PEG, $CdCl_2$, methyl viologen, and H_2O_2 (Jami *et al.*, 2008). In *Medicago truncatula*, an annexin-like gene was up-regulated by approximately 7-fold in response to Al treatment (Chandran *et al.*, 2008). In the leaves of 6-week-old *A. thaliana*, the mRNA level of *AnnAt1* was significantly stimulated after 24 h of ABA treatment (Konopka-Postupolska *et al.*, 2009). The transcript level of *AnnAt1* increased significantly within 2 h of drought treatment, and declined after that. A similar situation was observed in the *AnnAt1* transcript level subjected to 24 h of wounding and NaCl treatment before declining after 48 h. In contrast, Lee *et al.* (2004) reported that the *AnnAt1* expression level was not affected by treatment with NaCl. All these discrepancies suggest that the regulation of *AnnAt1* is dependent on the developmental stage, tissues, type of stress, and length of exposure.

The present study demonstrated that *AnnAt1* is possibly involved in the Pb stress response during early seedling growth. When *A. thaliana* seedlings were exposed to 100 μM $Pb(NO_3)_2$, the *AnnAt1* message level was enhanced marginally by 2.12-fold. Konopka-Postupolska *et al.* (2009) has shown a slight increase in *AnnAt1* mRNA levels prior to 100 mM Cd^{2+} treatment. At high level of heavy metal concentrations, the equilibrium between production and scavenging of ROS was disrupted, leading to the overproduction of ROS. As explained in Chapter 4, Pb may decrease the efficiency of oxidation-reduction enzymes in electron transport system by binding to the thiol groups. Subsequently, ROS such as H_2O_2 may act as signal molecules to trigger the signal transduction machinery, involving protein kinases, phosphatases, and Ca^{2+}-binding regulatory proteins (Grover *et al.*, 2001). The level of free Ca^{2+} in the cytoplasm may be induced as a result of increasing Ca^{2+} from the extracellular space and vacuole via Ca^{2+} channel (Clark *et al.*, 2005). These stress signallings and/or elevated Ca^{2+} influx might regulate gene expression of *AnnAt1*, in order to initiate a biochemical change in plants.

AnnAt1 may act as a peroxidase (Gorecka *et al.*, 2005) in neutralizing ROS and providing tolerance to H_2O_2. By up-regulating *AnnAt1* gene expression, plants can adapt, or defend against Pb-induced oxidative damage. The first results suggesting the involvement

of *AnnAt1* in oxidative stress responses was carried out in △*oxyR* mutant of *Escherichia coli* (Gidrol *et al.*, 1996). The insertion of an *AnnAt1* gene in the △*oxyR* mutant enhanced the its survivability in the presence of H_2O_2. The authors hypothesized that the ability of *AnnAt1* in complementing △*oxyR* bacteria during the oxidative stress is by reducing H_2O_2 level and displaying higher peroxidase activity. Further studies carried out by Kush & Sabapathy (2001) supported the role of annexin in protecting mammalian cells against oxidative cellular damage via modulation of Ca^{2+} signalling. As a result, superoxide production and protein kinase C activity were reduced. In plants, annexin 1 has been shown to play a role as a redox sensor to limit the excessive levels of ROS during oxidative burst (Gorecka *et al.*, 2005). By detoxifying ROS, *AnnAt1* may protect membranes from oxidation. Furthermore, *AnnAt1* may assist transport of Pb into the vacuoles and cell walls for sequestration (see Chapter 3), thus reducing the harmful effect of heavy metals in the cytosol.

At lower levels of Pb concentration (25, 50 and 75 μM), the toxic effect of Pb is lessened. As a result, the transcript level of *AnnAt1* may not be significantly triggered.

5.4.5 Changes of AnnAt1 protein level in Pb tolerance

Since the transcript level of *AnnAt1* was marginally induced when the seedlings were grown in 100 μM $Pb(NO_3)_2$ for 7 d, the functional significance of AnnAt1 protein in response to Pb stress is unclear. Although proteins are translated from the mRNA samples, protein levels may not necessarily correlate with the mRNA levels (Hassinen *et al.*, 2007; Ahsan *et al.*, 2009; Taylor *et al.*, 2009). Proteins may undergo post-translational modification when seedlings were exposed to unfavorable environmental conditions. For example, Lee *et al.* (2004) found that the mRNA level of *AnnAt1* was not affected upon adding NaCl into the medium, but the AnnAt1 protein level was significantly changed. The authors suggested that the alteration of AnnAt1 protein level in response to salinity stress was a result of proteasomal protein degradation. Besides, the activation of post-translational modification or binding partner may be necessary for ROS-scavenging systems to function at the physiological level (Konopka-Postupolska *et al.*, 2009). Plants overexpressing AnnAt1 protein were more tolerant to drought, compared to the knockout plants. However, during normal growth and development, post-translational regulation of

AnnAt1 expression did not take place (Cantero *et al.*, 2006).

In the preliminary experiments, the conditions for protein expression have been enhanced by modifying the method of Weigel & Glazebrook (2002). By increasing the concentrations of protease inhibitors and carefully suspending the ground frozen whole seedlings in the ice-cold protein extraction buffer with the aid of a mini plastic pestle, the quality of protein samples was improved. Evaluation using one dimensional SDS-PAGE and Coomassie blue staining showed the extracted protein samples were of high quality. The improved conditions may have minimized the degradation of protein samples by protease activity. However, western blot experiments were unable to produce any useful results. An alternative protein extraction method by Conlon & Salter (2007) was performed, yielding good quality protein samples. A lot of time has been devoted to western blot analysis without obtaining useful results. The AnnAt1 antibodies sent from University of Texas, Austin (USA) was unexpectedly held up in quarantine by the New Zealand biosecurity border control for a prolonged period (more than 3 months). Improper storage conditions might have affected the quality of the antibodies. Although new batches of the antibodies were ordered, time constraints have restricted further progress in this aspect of the study.

5.5 Conclusion

The present investigation suggests the involvement of *AnnAt1* in the response of 7-d-old *A. thaliana* seedlings to a high threshold concentration of Pb. The expression of *AnnAt1* was doubled when exposed to 100 μM $Pb(NO_3)_2$, suggesting that *A. thaliana* seedlings were likely to repair, or defend themselves against Pb-mediated stress. *AnnAt1* may act as ROS and/or Ca^{2+} signals, as a membrane protector, in detoxification of excessive ROS, or in sequestration of Pb. This finding opens a new area of investigation into the roles played by annexin in plant stress responses and particularly its potential involvement in Pb tolerance.

Chapter 6

Evaluation of the protective effect of nitric oxide on Pb-induced toxicity of *Arabidopsis thaliana* seedlings

6.1 Introduction

Nitric oxide (NO) is a gaseous molecule that has many biological functions. In recent years, many studies have obtained evidence that supports a role for exogenous NO in ameliorating heavy metal toxicity in plants. Pre-treatment with SNP ameliorated the Cd-induced toxic effects on yellow lupin (Kopyra & Gwozdz, 2003), rice (Hsu & Kao, 2004), sunflower (Laspina *et al.*, 2005), soybean (Kopyra *et al.*, 2006), and wheat (Singh *et al.*, 2008). SNP also improved seed germination and reduced the detrimental effect of Pb on root growth and morphology of yellow lupin (Kopyra & Gwozdz, 2003). Inhibition by Al of root elongation in indian herbs (Wang & Yang, 2005) and hibiscus (Tian *et al.*, 2007) was alleviated by pre-treatment with SNP. When subjected to Cu treatments, exogenous NO enhanced the antioxidative capacity of wheat (Hu *et al.*, 2007) and scavenged the excess ROS in rice (Yu *et al.*, 2005). In rice, pre-treatment with SNP increased certain antioxidant enzyme activities of As- (Singh *et al.*, 2009) and La- (Qiang *et al.*, 2007) treated plants. All these findings are consistent with the hypothesis that exogenous NO can protect plants against the detrimental effects of heavy metals.

The mechanisms by which NO helps plants to resist heavy metal stress are subjects

of numerous studies, especially in relation to the possible involvement of antioxidative enzyme activities. For example, pre-incubation with SNP before treatment with Cd has resulted in reduced of SOD activity in wheat roots (Singh *et al.*, 2008), and increased activity in yellow lupin roots (Kopyra & Gwozdz, 2003). NO may also alter the expression level of certain genes (Grun *et al.*, 2006; Arasimowicz & Floryszak-Wieczorek, 2007). Therefore, the protective effects of NO in plants are dependent on the species, type of tissues or cells, external conditions and activation of the signalling pathway in plants (Neill *et al.*, 2003; Palavan-Unsal & Arisan, 2009). Thus far, the role of exogenous NO in ameliorating Pb-induced oxidative stress has only been reported in *Lupinus luteus* (Kopyra & Gwozdz, 2003). Depending on the concentration of applied Pb, SNP pre-treatment may or may not alter the antioxidant enzyme activities, including those of SOD, CAT and POD.

The present study aims to contribute to a better understanding of the defence mechanisms by which exogenously supply NO is beneficial to Pb tolerance in *A. thaliana* seedlings. The effect of NO on plant growth and development, physiological, biochemical responses and altered gene expression of *AnnAt1* was studied.

6.2 Materials and methods

An outline of the pre-treatments and subsequent experimental work carried out and presented in this chapter is shown in Figure 6.1.

6.2.1 Preparation of seeds for pre-treatments

Seeds of wild-type *A. thaliana* Col-0 purchased from Lehle Seeds were surface-sterilized and cold-treated as described in Section 2.1.

6.2.2 Preparation of SNP

Sodium nitroprusside (SNP), purchased from BDH, was used as a nitric oxide donor. SNP stock solution (20 mM) was prepared in a beaker, and filtered through a 0.22 µm Sterile Syringe Driven Filter (Millipore Corporation, Bedford, MA, USA) into a 10 mL sterilized

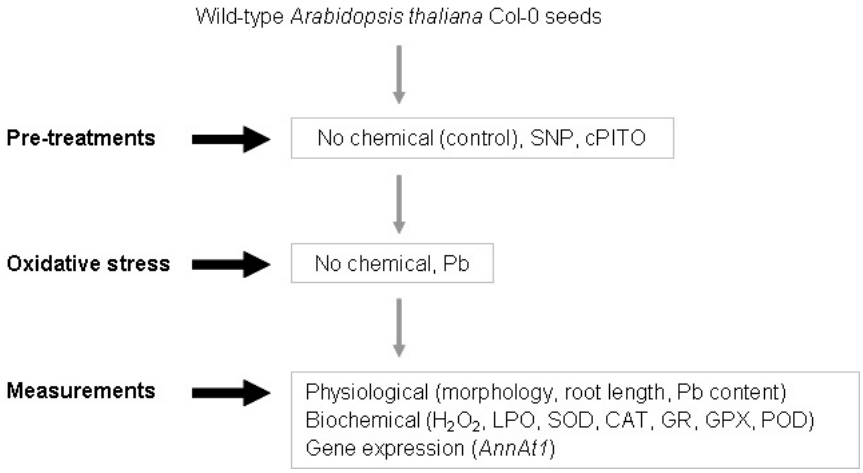

Figure 6.1: Overall protocol for pre-treatment with SNP ± cPTIO and grown on modified HC medium for further analysis.

glass bottle prior storage at 4˚C in the dark. A preliminary experiment with SNP at 0.5, 1, 2.5, 5 and 10 mM was carried out to determine SNP concentration showing the most potent effect. Based on the root length measurements, pre-treatment with the SNP at 0.5 mM had the greatest counteracting effect on Pb-mediated inhibition of root elongation. Hence, this concentration was chosen to pre-treat seeds in the experiments described in this chapter.

6.2.3 Preparation of cPTIO

To confirm the protective effect observed after pre-treatments with SNP was due specifically to NO and not other components in SNP, in a parallel experiment an NO-specific scavenger, 2-(4-carboxyphenyl)- 4,4,5,5-tetramethylimidazoline-1-oxyl-3-oxide (cPTIO) was simultaneously supplied with SNP. cPTIO was purchased from Sigma. A 2 mM cPTIO stock solution was prepared, filtered through a 0.22 µm Sterile Syringe Driven Filter (Millipore Corporation, Bedford, MA, USA) into 1.5 mL sterilized Eppendorf tube, and kept at -80˚C.

Plate (in triplicate)	0.5 mM SNP	1.0 mM cPTIO	100 µM $Pb(NO_3)_2$
A	-	-	-
B	+	-	-
C	+	+	-
D	-	+	-
E	-	-	+
F	+	-	+
G	+	+	+
H	-	+	+

Table 6.1: Different combinations of 0.5 mM SNP and 1.0 mM cPTIO pre-treatments, and an oxidative stress treatment (100 µM $Pb(NO_3)_2$). Each plate was in triplicate.

6.2.4 Pre-treatment with SNP and/or cPTIO

Sterile dH_2O used for stratification was removed with a sterile pasteur pipette. To examine the possible protective roles of NO on Pb-induced toxicity, wild-type *A. thaliana* seeds were suspended in ~1 mL 0.5 mM SNP $\pm$ 1 mM cPTIO at 4˚C in the dark for 3 h. Sterile dH_2O was used as control.

6.2.5 Oxidative stress

Approximately 150 seeds were placed on modified HC medium in the presence or absence of 100 µM $Pb(NO_3)_2$ using a sterile Pasteur pipette (see Sections 2.1 and 2.2). A general overview of the different treatments is summarized in Table 6.1. All agar plates were placed on the bench in the growth room with continuous lighting (24 h photoperiod at 26.5 µE/sec/m^2, 22˚C) in a completely randomized design.

6.2.6 Appearance and morphology

After sowing the cold-stratified seeds for 7 d, 15 seedlings were randomly selected (see Section 2.5). Digital photos were taken for a morphological study of SNP pre-treated *A. thaliana* seedlings to 100 µM $Pb(NO_3)_2$ treatment, including changes in the shape,

appearance and colour of roots and cotyledons.

6.2.7 Root length measurement

Ten seedlings were randomly collected and photographed using a Nikon D1x camera fitted with a Nikon 60 mm Macro lens (see Section 2.6). The mean of ten measurements was considered as one replicate to compensate for the variation in root length. There are two independent experimental series comprising of three replicates for each treatment (Table 6.1).

6.2.8 Graphite furnace atomic absorption spectroscopy

Acid digestion was carried out to determine the total concentration of Pb in plant materials from different pre-treatments grown in medium containing 100 μM $Pb(NO_3)_2$. Non-Pb exposed seedlings were included as controls. Ten 7-d-old seedlings were randomly selected and desorbed in 1 mM Na_2EDTA for 1 min, washed thoroughly 5 times with nanopure H_2O, and excised into roots and shoots (see Section 2.8). Three independent experiments consisting of five replicates were performed. Duplicate absorbance readings were taken and interpolated against calibration curves. The Pb contents of plant materials were expressed as nmol/plant.

6.2.9 Collection of plant materials for biochemical and genetic studies

One-week-old *A. thaliana* seedlings from three replicate plates were pooled and collected with straight fine point forceps (see Section 2.10). The plant materials were flash frozen in liquid nitrogen, and stored at -80˚C until analysis.

6.2.10 Extractions and assays for hydrogen peroxide, lipid hydroperoxide and antioxidative enzymes

Methods for extraction and measurement of H_2O_2, lipid hydroperoxide, SOD, CAT, GR, GPX and POD were performed according to Sections 2.11 and 2.12. There are five in-

dependent biological samples; each was based on a pool of plant materials from three replicate plates. Each independent biological sample was considered as an experimental unit for statistical analysis. Crude extracts were analyzed using a plate reader.

6.2.11 Gene expression of *AnnAt1*

The isolation of total RNA, cDNA synthesis and real-time PCR were explained in Sections 2.15 and 2.16. The specificity of amplification product was checked according to Section 2.17 and the transcript level of *AnnAt1* was quantified according to Section 2.18. There are two independent experiments in this study.

6.2.12 Statistical analysis

The significant differences between the means of treatment groups (Table 6.1) were detected using factorial ANOVA and then compared through post-hoc Fisher's LSD test (see Section 2.23). Data were transformed when necessary and tested for homogeneity of variance (Hartley's F-max) prior to statistical analysis. Different letters in the graphs or tables indicate the results are significant at a probability of 5% ($p < 0.05$).

6.3 Results

6.3.1 SNP application methods: Challenges of adding SNP directly into the medium

In preliminary experiments, 1 µM SNP $\pm$ 1 µM cPTIO was added into autoclaved modified HC medium containing 100 µM $Pb(NO_3)_2$. As shown in Figure 6.2, results obtained from three independent experiments were variable. Pb accumulation in the roots of 7-d-old *A. thaliana* seedlings grown on medium containing chemicals (Pb $\pm$ SNP $\pm$ cPTIO) in comparison to the control (Pb only) were as follows: (a) Pb + SNP: 60.5% and 26.7% reduction in experiment 1 and 2, respectively; but no significant difference in experiment 3. (b) Pb + cPTIO: 25.1% reduction in experiment 2; but no significant difference in experiment 1 and 3. (c) Pb + SNP + cPTIO: 52.4% and 23.7% reduction in experiment 1 and 2, respectively; but no significant difference in experiment 3.

TEM was performed to determine if the addition of SNP into the modified HC medium might affect the pattern of Pb uptake and subcellular structures of plant cells, causing the dissimilar data obtained via GF-AAS. As explained in Chapter 3, in the root of *A. thaliana* seedlings exposed to a 100 μM $Pb(NO_3)_2$, Pb depositions were mainly localized in the vacuole, intercellular spaces, and cell wall regions (Figures 6.3 and 6.4). In the presence of 1 μM SNP, fewer Pb particles seemed to be localized in the root cells (Figure 6.5).

Similarly, only minimal amount of very fine Pb grains were detected in the intercellular spaces and cell wall regions of *A. thaliana* cotyledon (Figure 6.6). In the presence of 1 μM SNP in Pb-containing medium, Pb depositions appeared to be almost absent from the cotyledonary cells (Figure 6.7).

The presence of SNP in Pb-containing medium did not appear to change the pattern of Pb uptake and ultrastructure of cellular organelles, but appeared to reduce or minimize Pb accumulation in the root and cotyledonary cells of 7-d-old *A. thaliana* seedlings.

6.3.2 Concentrations of SNP pre-treatment on Pb-induced root growth inhibition

Root growth inhibition is the most obvious effect of Pb toxicity. Therefore, the SNP concentration required for the pre-treatment of *A. thaliana* seeds to alleviate the effect of Pb-induced morphological change was determined. As shown in Figure 6.8, a change in root elongation due to SNP concentration was observed in Pb-exposed seedlings. A concentration of 0.5 mM SNP was chosen to further investigate the role of NO in Pb toxicity. This appeared to be the most effective concentration to oppose Pb-mediated inhibition of root elongation. Root growth increased by 35.2% in Pb-exposed seedlings pre-treated with 0.5 mM SNP, compared to the Pb-treated controls without SNP pre-treatment. Pre-treatment with 1.0 mM SNP before subjecting to 100 μM $Pb(NO_3)_2$ recovered the root inhibition by only 24.0%.

By contrast, the root length of seedlings pre-treated with 2.5 mM SNP was reduced by 13.1%, in comparison to the Pb control. A further increase in SNP concentration had a deleterious effect on the root growth. Pre-treatment with high concentrations of SNP (5 mM and 10 mM) severely magnified Pb-inhibition of root growth, whereby the roots

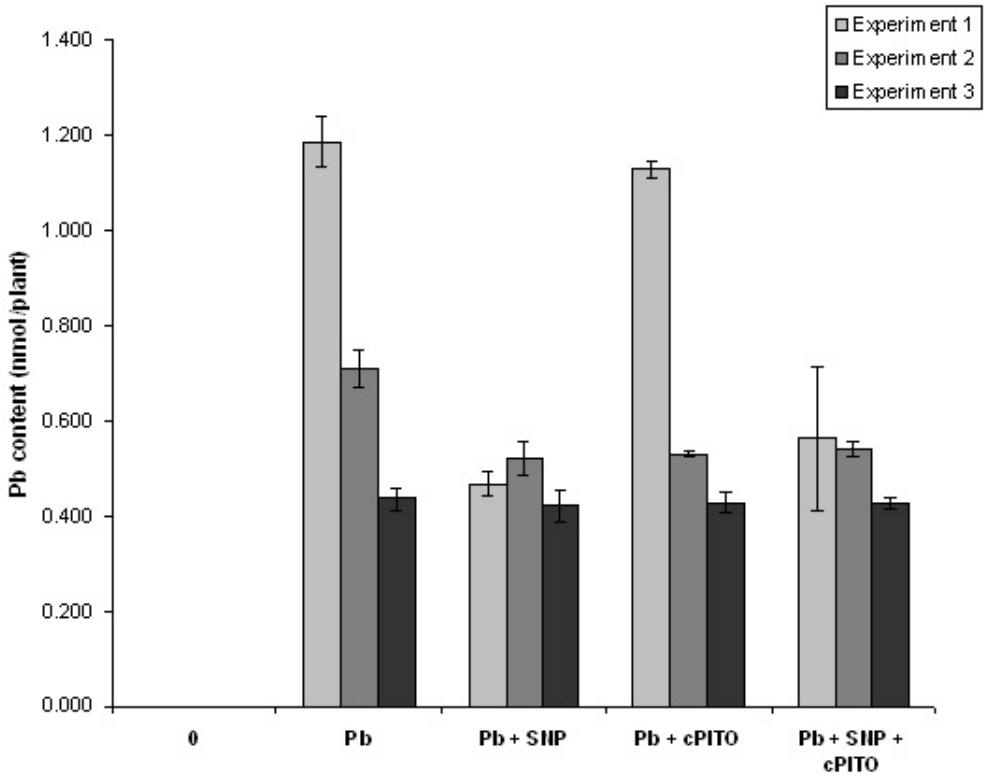

Figure 6.2: Effects of direct application of SNP ± cPTIO in modified HC medium to Pb uptake of 7-d-old *A. thaliana* roots. 1 µM sterilized SNP ± 1 µM sterilized cPTIO was supplemented into modified HC medium containing 100 µM $Pb(NO_3)_2$ after the autoclaved medium was cooled down to ±50˚C. Seeds were then plated on the agar. Results from three independent experimental series are presented as means ± SE (n = 3).

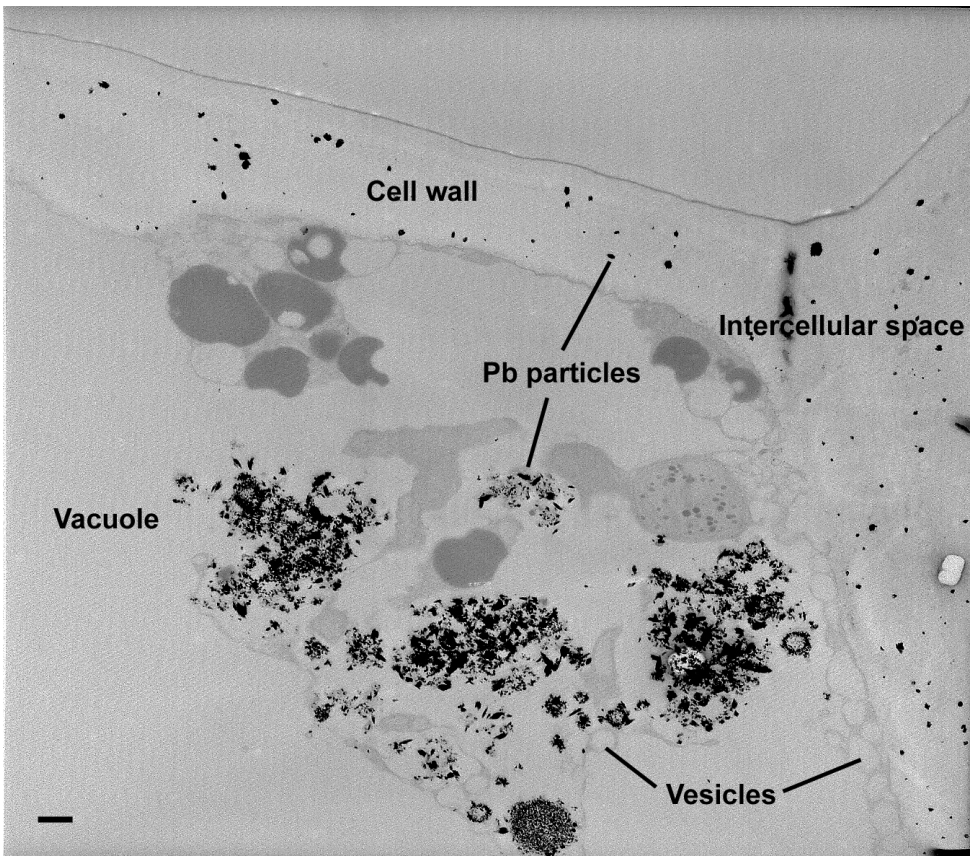

Figure 6.3: Transmission electron micrograph of an unstained ultra-thin section of the root from a 7-d-old *A. thaliana* seedling grown in medium containing 100 μM $Pb(NO_3)_2$ in the absence of SNP. Magnification of the micrograph was at 6,000 X. Bar = 500 nm.

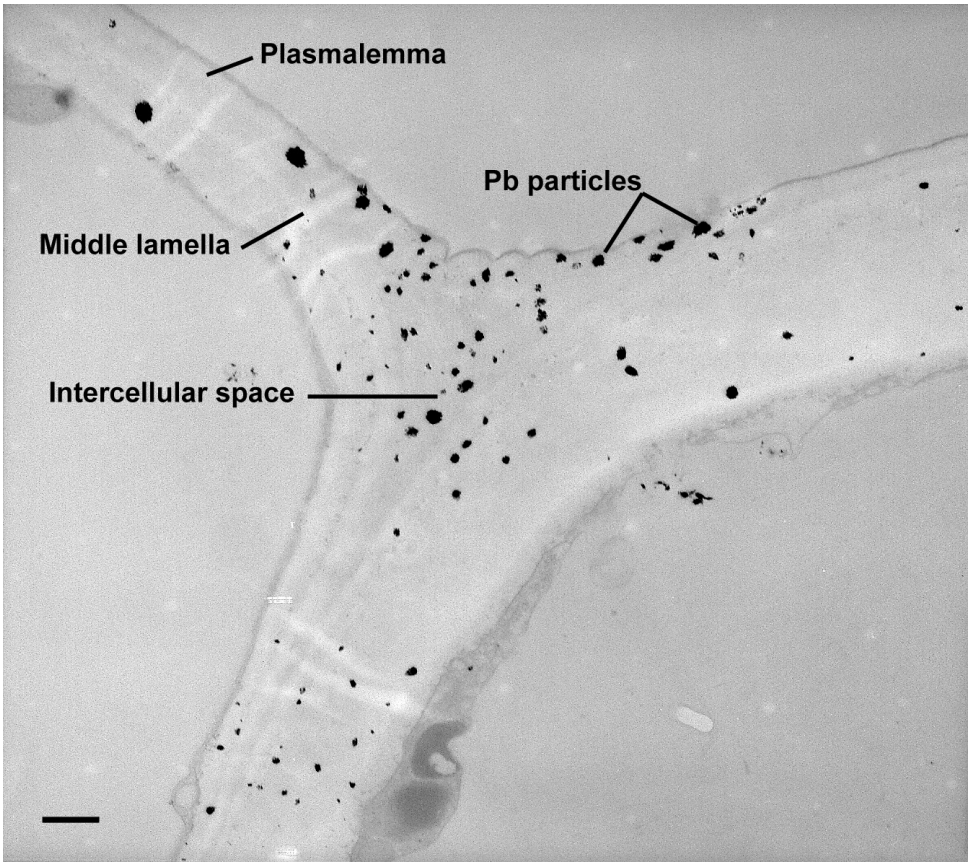

Figure 6.4: Transmission electron micrograph of an unstained ultra-thin section of the root from a 7-d-old *A. thaliana* seedling grown in medium containing 100 μM $Pb(NO_3)_2$ in the absence of SNP. Magnification of the micrograph was at 20,000 X. Bar = 500 nm.

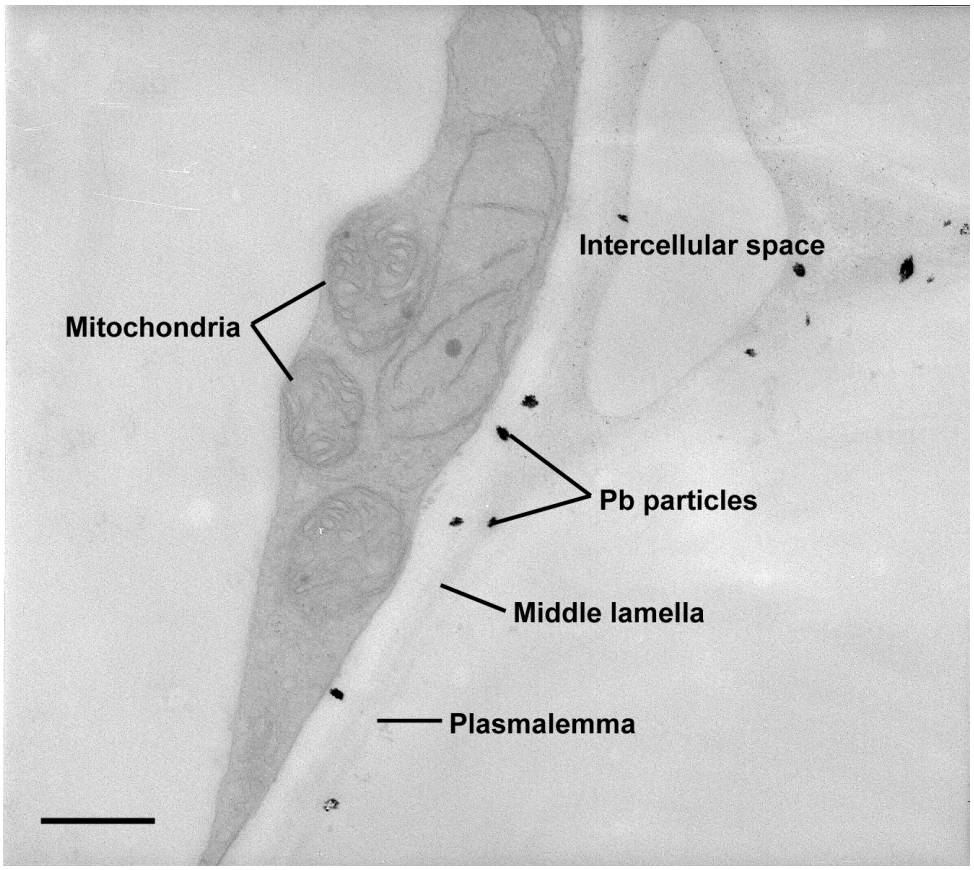

Figure 6.5: Transmission electron micrograph of an unstained ultra-thin section of the root from a 7-d-old *A. thaliana* seedling grown in medium containing 100 μM $Pb(NO_3)_2$ in the presence of 1 μM SNP. Magnification of the micrograph was at 20,000 X. Bar = 500 nm.

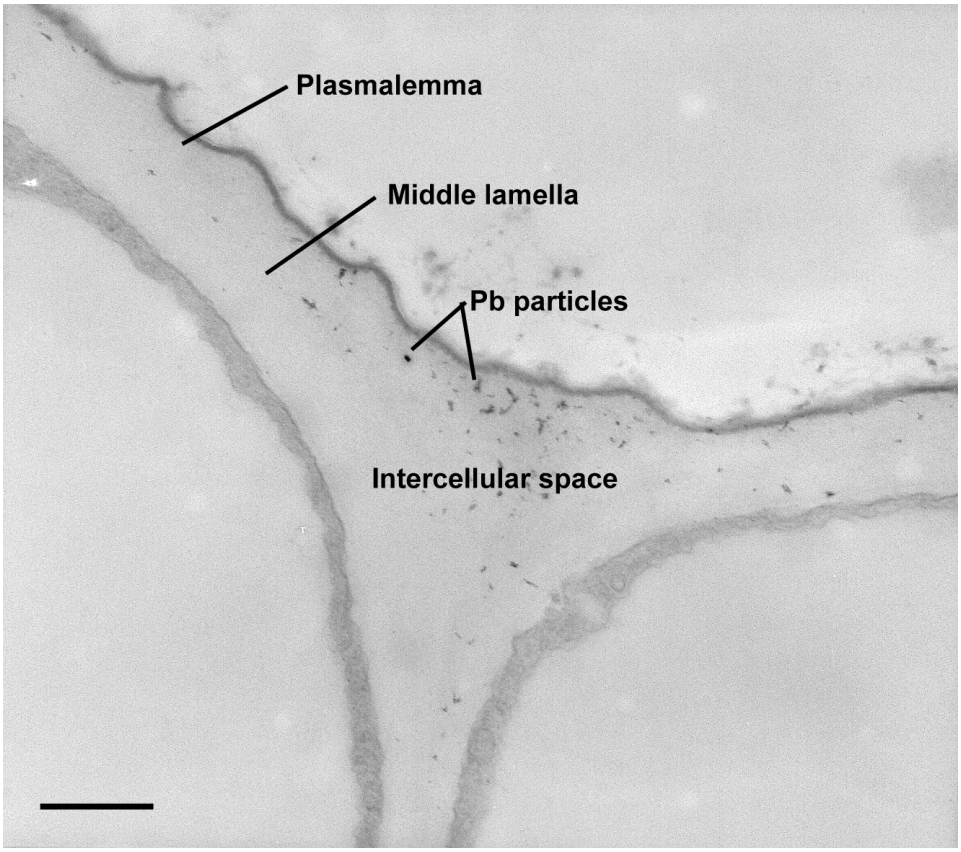

Figure 6.6: Transmission electron micrograph of an unstained ultra-thin section of the cotyledon from a 7-d-old *A. thaliana* seedling grown in medium containing 100 μM $Pb(NO_3)_2$ in the absence of SNP. Magnification of the micrograph was at 20,000 X. Bar = 500 nm.

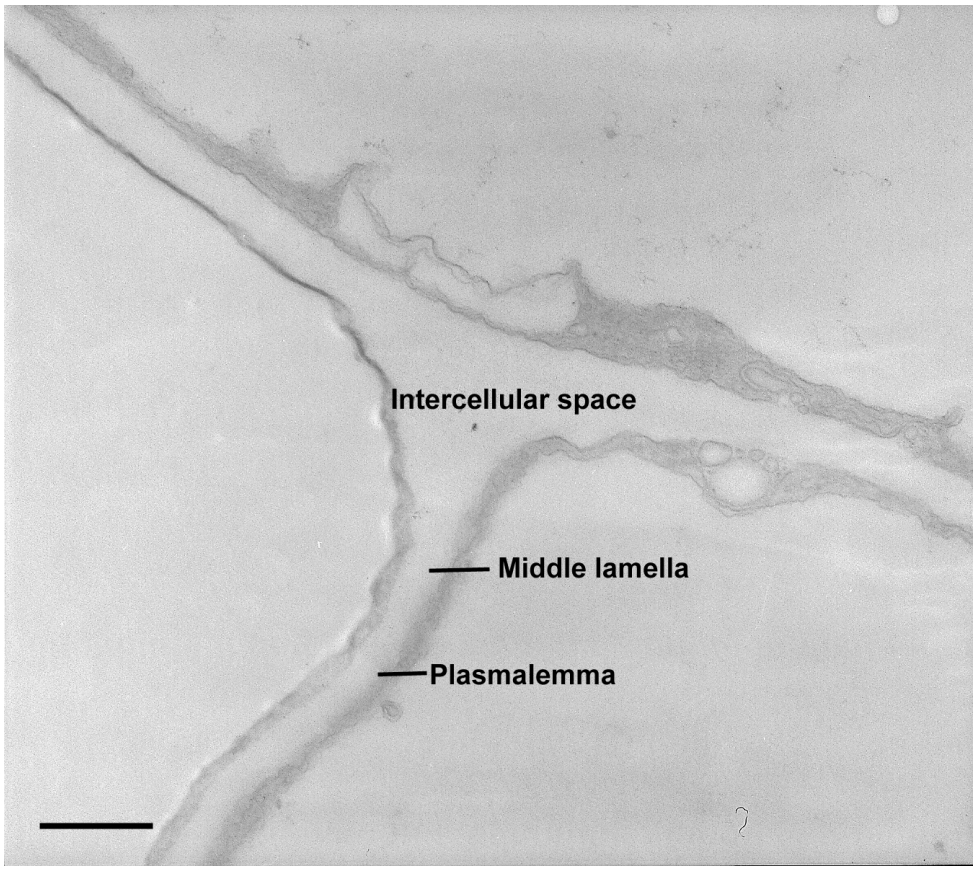

Figure 6.7: Transmission electron micrograph of an unstained ultra-thin section of the cotyledon from a 7-d-old *A. thaliana* seedling grown in medium containing 100 µM $Pb(NO_3)_2$ in the presence of 1 µM SNP. Magnification of the micrograph was at 20,000 X. Bar = 500 nm.

were 40.3% and 64.0%, respectively, shorter than Pb-treated seedlings.

6.3.3 cPTIO as a NO scavenger

According to the procedure reported in Hu *et al.* (2007), the concentration of cPTIO used was twice the concentration of SNP. In a preliminary experiment, 1 mM cPTIO was found to be able to counteract the possitive effect of 0.5 mM SNP on Pb-inhibited root elongation. Hence, this concentration of cPTIO was used as a NO scavenger throughout this study.

6.3.4 SNP pre-treatment reduced the effect of Pb-stressed symptoms in *A. thaliana*

Generally, Pb stress symptoms (shorter and thickened roots, browning at the edge of the cotyledons) following exposure to a high level of Pb as described in Section 3.3.1 were less evident in *A. thaliana* seedlings pre-treated with SNP (Figure 6.9).

6.3.5 Exogenous NO alleviates Pb-induced inhibition of root elongation

To determine the potential physiological effect of additives (SNP and/or cPTIO) in the absence of Pb on *A. thaliana* seedlings, the effects of these additives were evaluated by measuring the root growth of seedlings grown on nutrient agar without Pb. In the absence of Pb, root elongation of seedlings pre-treated with SNP and/or cPTIO was not significantly different ($p > 0.05$) from the controls (no chemical additive).

After growing *A. thaliana* on Pb-containing nutrient agar for 7 d, reduction in root elongation was less when seeds were pre-treated with 0.5 mM SNP (Figure 6.10). cPTIO was able to counteract this effect of SNP.

6.3.6 Effect of SNP pre-treatment on Pb uptake and accumulation

SNP pre-treatment did not significantly reduce Pb uptake and accumulation in the roots and shoots of *A. thaliana* seedlings ($p > 0.05$, Figure 6.11). The percentage of Pb translo-

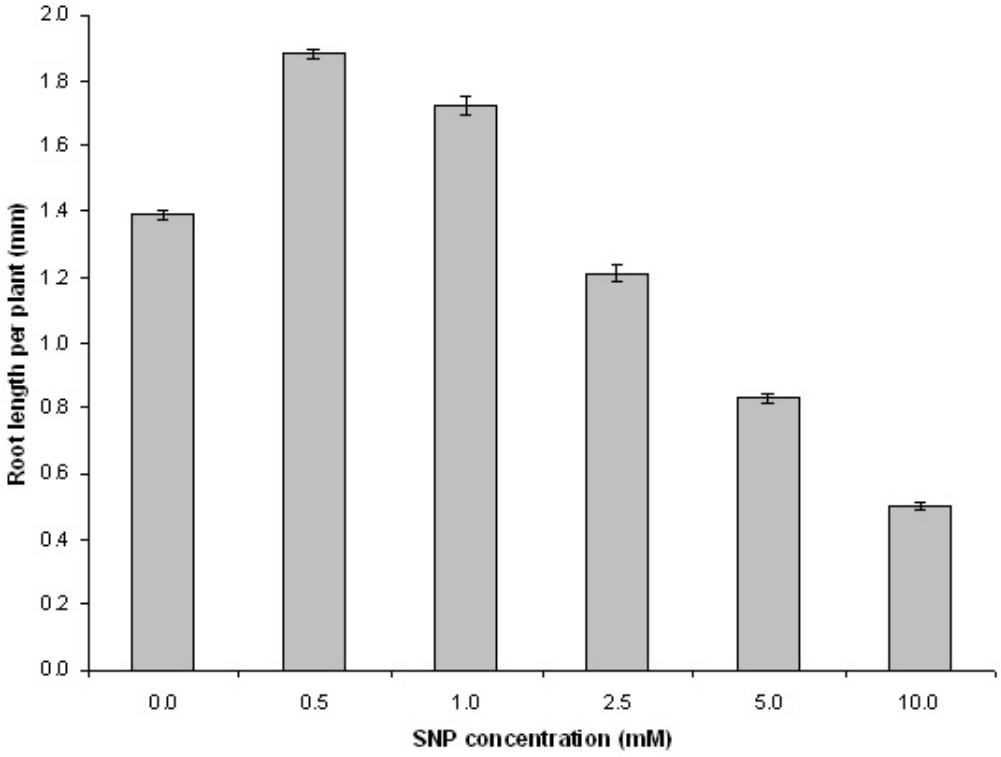

Figure 6.8: Effect of varying concentrations of SNP on Pb-induced root growth inhibition of 7-d-old *A. thaliana* seedlings. Seeds were incubated in SNP for 3 h prior to sowing in modified HC medium containing 100 μM $Pb(NO_3)_2$. A representative result from two independent experiments with three replicates is presented (n = 3). Each replicate (n) is derived from the average of root length measurements calculated from ten seedlings. The bars indicate standard error of the means. The root length for control seedlings without any pre-treat or post-treat chemical was 7.0 $\pm$ 0.03 mm.

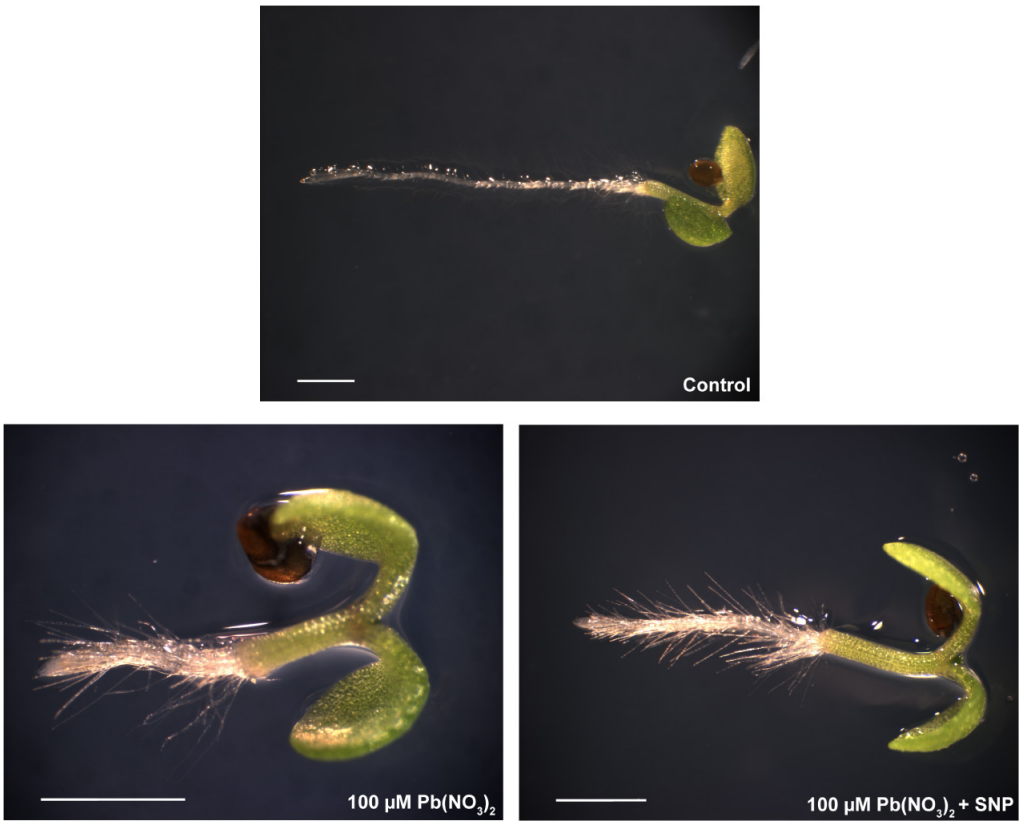

Figure 6.9: Effects of SNP pre-treatment on *A. thaliana* seedlings grown on modified HC medium in the presence of 100 µM $Pb(NO_3)_2$. The changes in the shape, appearance and colour of roots and cotyledons were observed. The scale bars indicate 1 mm.

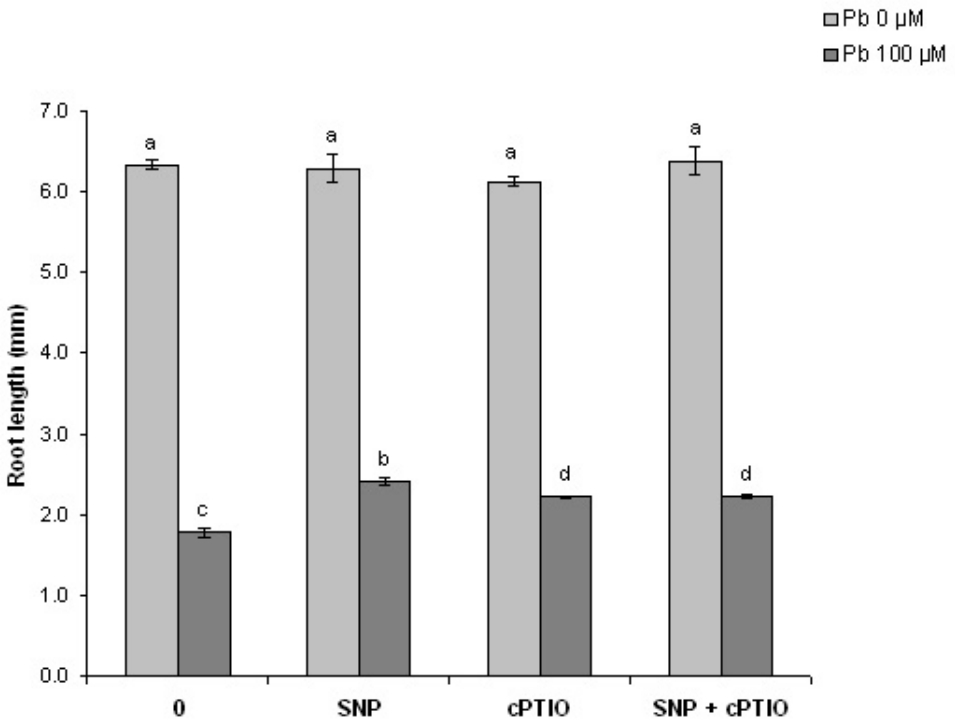

Figure 6.10: Effects of SNP ± cPTIO pre-treatment on the length of *A. thaliana* roots under Pb stress conditions. Seeds were pre-treated with 0.5 mM SNP ± 1 mM cPTIO or sterile H_2O for 3 h, and grown on modified HC medium in the presence or absence of 100 µM $Pb(NO_3)_2$. A representative result from two independent experiments is shown (n = 3). The bars indicate standard error of the means. Different letters represent significant differences at $p < 0.05$, according to factorial ANOVA and multiple comparison using Fisher's LSD test.

cation from roots to shoots was only between 17 to 21%. Pre-treatment with cPTIO alone slightly reduced Pb accumulation in the shoots.

6.3.7 NO donor ameliorates Pb-induced generation of ROS

In the modified HC medium without $Pb(NO_3)_2$, no significant difference ($p > 0.05$) in the H_2O_2 content was detected in *A. thaliana* seedlings pre-incubated with SNP and/or cPTIO, in comparison to the controls (sterile dH_2O, Figure 6.12). Seven-d-old seedlings exposed to 100 µM $Pb(NO_3)_2$ contained 2.5-fold more H_2O_2 than the control. Upon pre-treatment with SNP, the level of H_2O_2 decreased markedly ($p < 0.05$) to its original content. cPTIO reversed the SNP action. cPTIO pre-treatment alone had no effect on Pb-induced H_2O_2 content ($p > 0.05$).

6.3.8 NO donor repairs Pb-induced oxidative damage

In normal growth and development (no Pb treatment), exogenous NO supply did not alter the lipid hydroperoxide level in *A. thaliana* seedlings (Figure 6.13). However, the lipid hydroperoxide content was markedly higher (by 3.2-fold) in seedlings pre-treated with cPTIO. This suggests that seedlings could be subjected to more oxidative stress following pre-treatment with the NO scavenger. When the seedlings were exposed to 100 µM $Pb(NO_3)_2$, the level of lipid hydroperoxide decreased by 50% following SNP pre-incubation. cPTIO did not significantly affect Pb-induced oxidative stress ($p > 0.05$).

6.3.9 NO and antioxidative enzyme activities

The effects of exogenous NO on the activities of SOD, CAT, GR, GPX and POD were assessed in *A. thaliana* treated without (control) and with 100 µM $Pb(NO_3)_2$. There was a sharp increase in activities of these antioxidative enzymes in seedlings exposed to $Pb(NO_3)_2$. Generally, the induction of these enzymes after $Pb(NO_3)_2$ treatment was 1.9- to 4.7-fold more than the untreated control. However, seedlings pre-incubated with SNP before imposition of Pb stress exhibited a significant decrease ($p < 0.05$) in the levels of these scavenging enzymes (Figures 6.14, 6.15, 6.16, 6.17 and 6.18). After exposing *A. thaliana* seedlings to $Pb(NO_3)_2$ for 7 d, the level of SOD, CAT, GR, GPX and POD

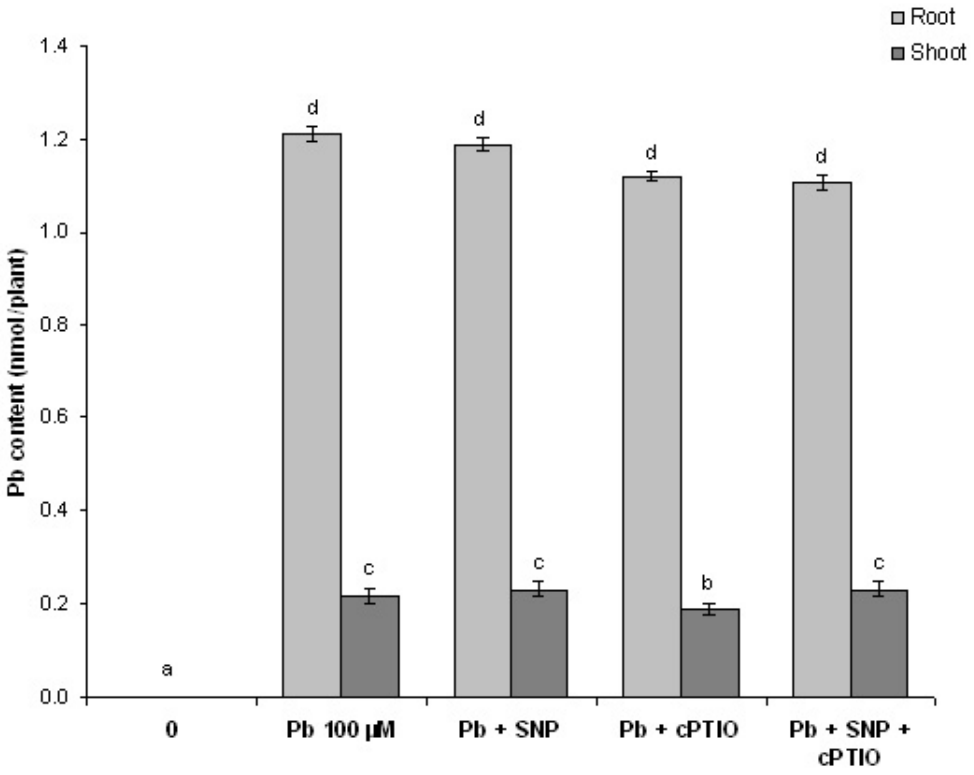

Figure 6.11: Effects of SNP ± cPTIO pre-treatment on Pb uptake and accumulation in 7-d-old *A. thaliana* seedlings. Seeds were pre-treated with 0.5 mM SNP ± 1 mM cPTIO or sterile H_2O for 3 h, and grown on modified HC medium in the presence or absence of 100 µM $Pb(NO_3)_2$. Values are means from three independent experiments with five replicates (n = 15). The bars indicate standard error of the means. Different letters represent significant differences at $p < 0.05$, according to factorial ANOVA and multiple comparison using Fisher's LSD test.

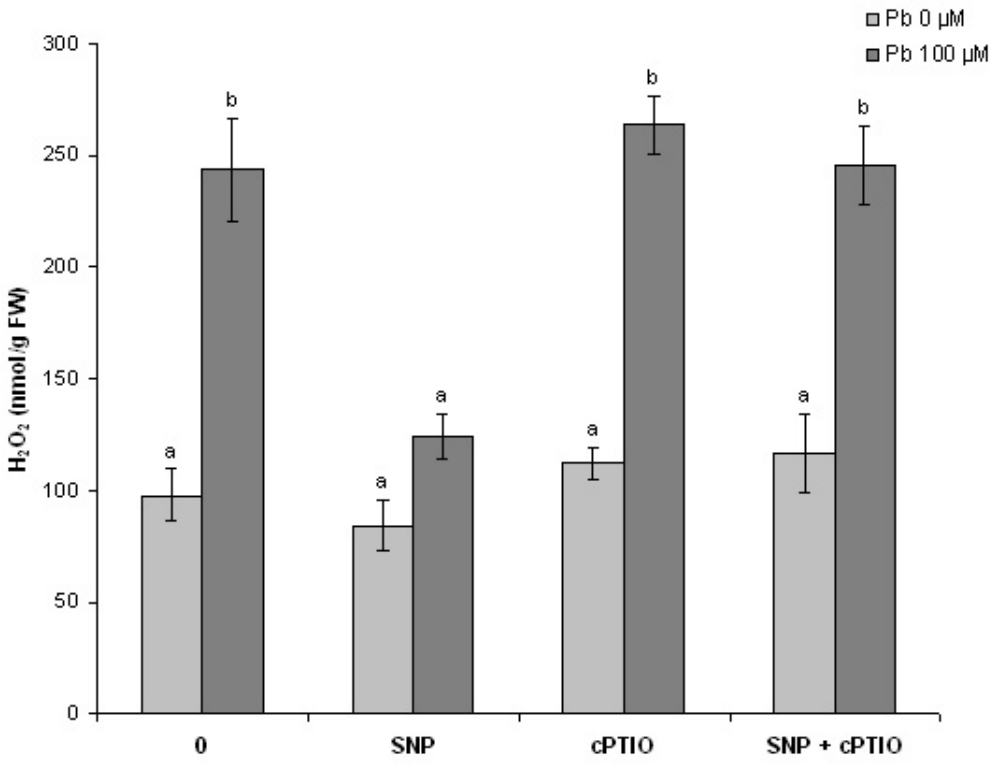

Figure 6.12: Effect of SNP ± cPTIO pre-treatment on H_2O_2 level of 7-d-old *A. thaliana* seedlings under Pb stress condition. Seeds were pre-treated with 0.5 mM SNP ± 1 mM cPTIO or sterile H_2O for 3 h, and grown on modified HC medium in the presence or absence of 100 µM $Pb(NO_3)_2$. Results presented as mean ± standard error (n = 5). Different letters represent significant differences at $p < 0.05$, according to factorial ANOVA and multiple comparison using Fisher's LSD test.

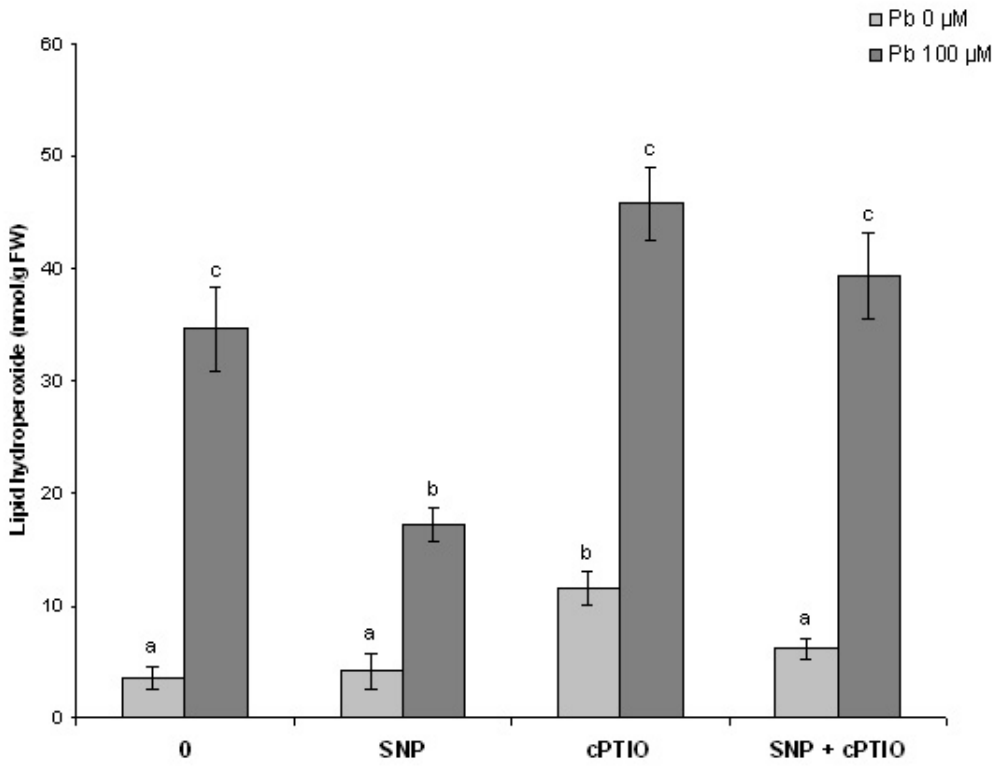

Figure 6.13: Effect of SNP ± cPTIO pre-treatment on lipid hydroperoxide level of 7-d-old *A. thaliana* seedlings under Pb stress condition. Seeds were pre-treated with 0.5 mM SNP ± 1 mM cPTIO or sterile H_2O for 3 h, and grown on modified HC medium in the presence or absence of 100 µM $Pb(NO_3)_2$. Results presented as mean ± standard error (n = 5). Different letters represent significant differences at $p < 0.05$, according to factorial ANOVA and multiple comparison using Fisher's LSD test.

were 23 - 45% lower in comparison to those without SNP pre-treatment. This observed trend of changes in antioxidative enzymes upon SNP pre-treatment paralleled the changes in ROS species (H_2O_2 and lipid hydroperoxide). Similarly, the positive effect of SNP in decreasing the specific activity of SOD, CAT, GR, GPX and POD was reversed by cPTIO.

Depending on the type of antioxidative enzymes, pre-treatment with SNP and/or cPTIO either enhanced, diminished or had no effect on the specific enzyme activities in *A. thaliana* in the absence of Pb. For example, the specific activity of CAT and GPX were reduced following SNP pre-incubation. On the other hand, the specific activity of SOD and GR were increased following cPTIO pre-treatment.

6.3.10 NO and the regulation of *AnnAt1*

Similar to the findings in Section 5.3.1.1, sharp and non-smearing bands were observed in isolated total RNA samples (Figure 6.19), showing no sign of degradation. A 28S:18S rRNA ratio of ≥ 1.0, and a A_{260}/A_{280} ratio of 1.9 - 2.1 was acquired, showing high quality and intact RNA.

The relative quantification of *AnnAt1* gene expression was normalized against mitosis protein YLS8 using REST 2008 software (Table 6.2). In non-Pb treated samples, SNP pre-treatment did not significantly change the message level of *AnnAt1* ($p > 0.05$). In Pb-treated samples, SNP pre-treatment up-regulated *AnnAt1* message level by 1.194-fold ($p < 0.05$). Pre-incubation with both SNP and cPTIO, or cPTIO alone slightly down-regulated *AnnAt1* expression by 0.798- and 0.769-fold, respectively, in seedlings grown without $Pb(NO_3)_2$. When *A. thaliana* were pre-treated with SNP and cPTIO before exposing to $Pb(NO_3)_2$, the transcript level of *AnnAt1* was enhanced by 1.266-fold ($p < 0.05$). In contrast to the findings in Chapter 5, *AnnAt1* gene expression was not significantly changed when seedlings (without pre-treatment) were exposed to 100 μM $Pb(NO_3)_2$ treatment ($p > 0.05$).

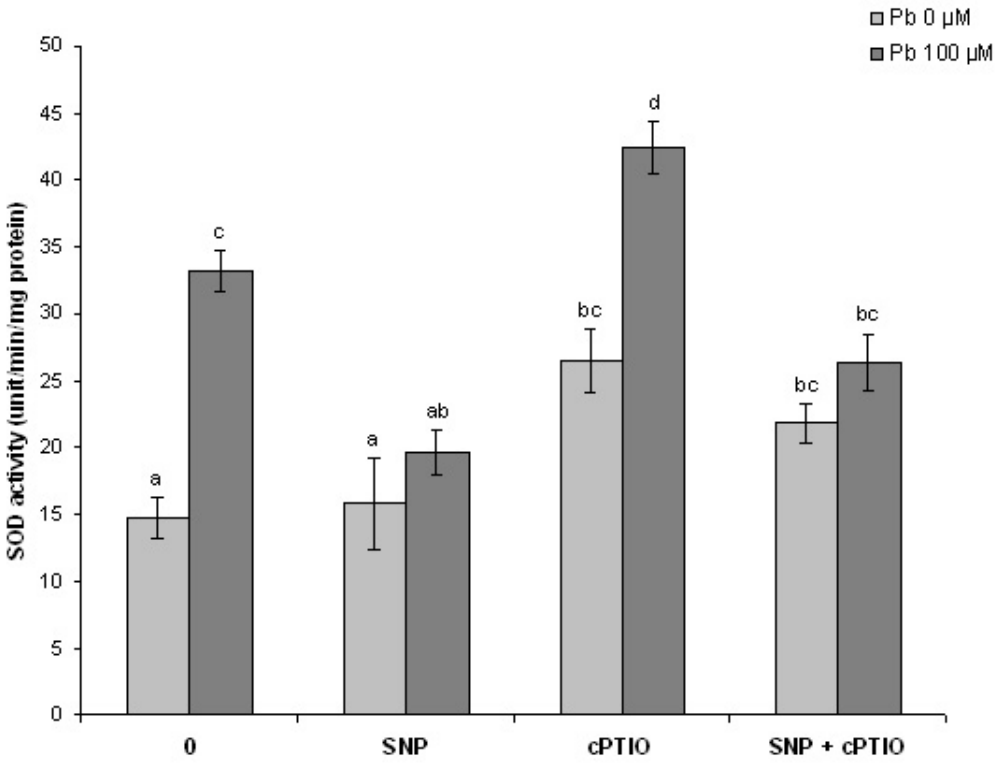

Figure 6.14: Effect of SNP ± cPTIO pre-treatment on the specific activity of SOD level of 7-d-old *A. thaliana* seedlings under Pb stress condition. Seeds were pre-treated with 0.5 mM SNP ± 1 mM cPTIO or sterile H_2O for 3 h, and grown on modified HC medium in the presence or absence of 100 µM $Pb(NO_3)_2$. Results presented as mean ± standard error (n = 5). Different letters represent significant differences at $p < 0.05$, according to factorial ANOVA and multiple comparison using Fisher's LSD test.

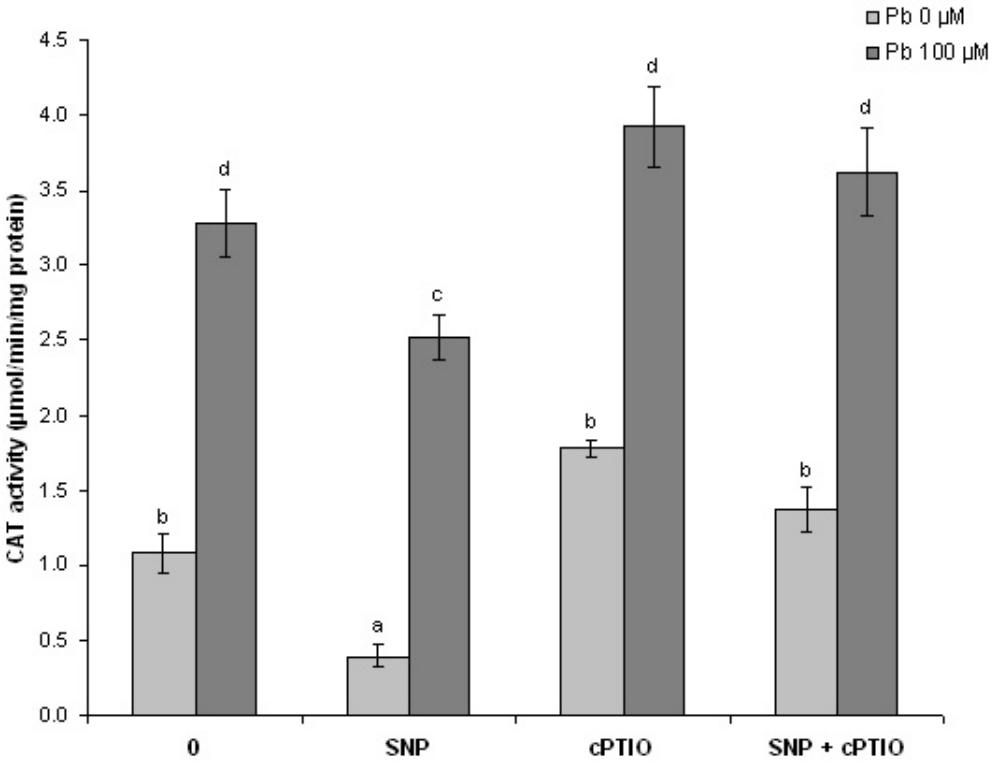

Figure 6.15: Effect of SNP ± cPTIO pre-treatment on the specific activity of CAT level of 7-d-old *A. thaliana* seedlings under Pb stress condition. Seeds were pre-treated with 0.5 mM SNP ± 1 mM cPTIO or sterile H_2O for 3 h, and grown on modified HC medium in the presence or absence of 100 µM $Pb(NO_3)_2$. Results presented as mean ± standard error (n = 5). Different letters represent significant differences at $p < 0.05$, according to factorial ANOVA and multiple comparison using Fisher's LSD test.

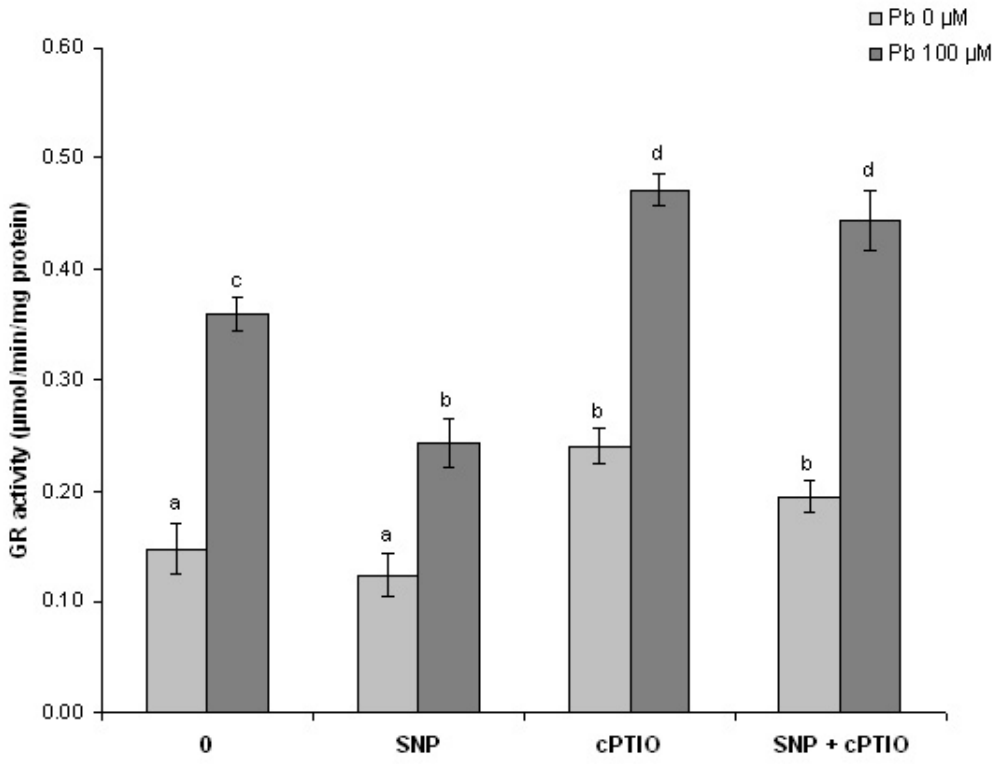

Figure 6.16: Effect of SNP ± cPTIO pre-treatment on the specific activity of GR level of 7-d-old *A. thaliana* seedlings under Pb stress condition. Seeds were pre-treated with 0.5 mM SNP ± 1 mM cPTIO or sterile H_2O for 3 h, and grown on modified HC medium in the presence or absence of 100 µM $Pb(NO_3)_2$. Results presented as mean ± standard error (n = 5). Different letters represent significant differences at $p < 0.05$, according to factorial ANOVA and multiple comparison using Fisher's LSD test.

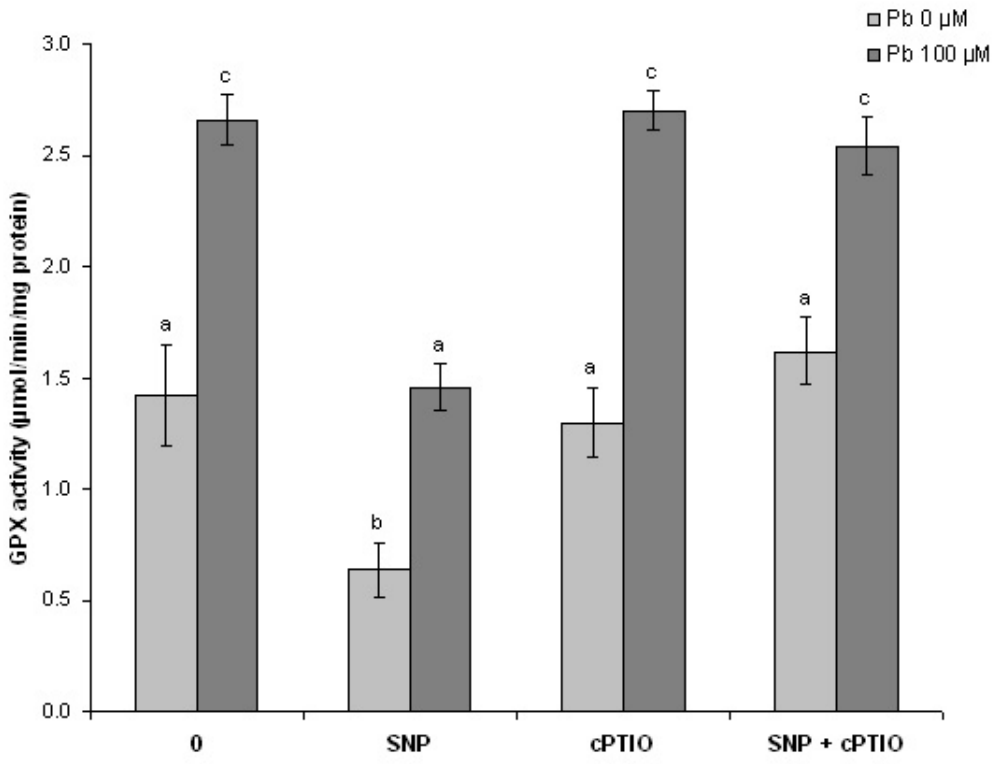

Figure 6.17: Effect of SNP ± cPTIO pre-treatment on the specific activity of GPX level of 7-d-old *A. thaliana* seedlings under Pb stress condition. Seeds were pre-treated with 0.5 mM SNP ± 1 mM cPTIO or sterile H_2O for 3 h, and grown on modified HC medium in the presence or absence of 100 µM $Pb(NO_3)_2$. Results presented as mean ± standard error (n = 5). Different letters represent significant differences at $p < 0.05$, according to factorial ANOVA and multiple comparison using Fisher's LSD test.

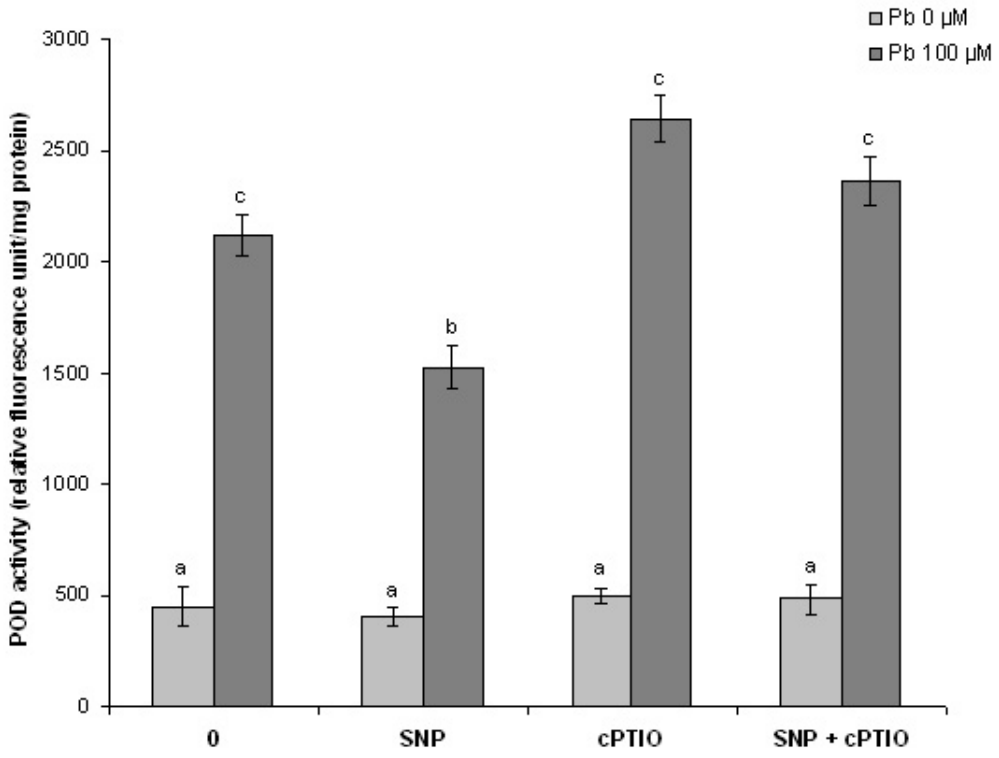

Figure 6.18: Effect of SNP ± cPTIO pre-treatment on the specific activity of POD level of 7-d-old *A. thaliana* seedlings under Pb stress condition. Seeds were pre-treated with 0.5 mM SNP ± 1 mM cPTIO or sterile H_2O for 3 h, and grown on modified HC medium in the presence or absence of 100 µM $Pb(NO_3)_2$. Results presented as mean ± standard error (n = 5). Different letters represent significant differences at $p < 0.05$, according to factorial ANOVA and multiple comparison using Fisher's LSD test.

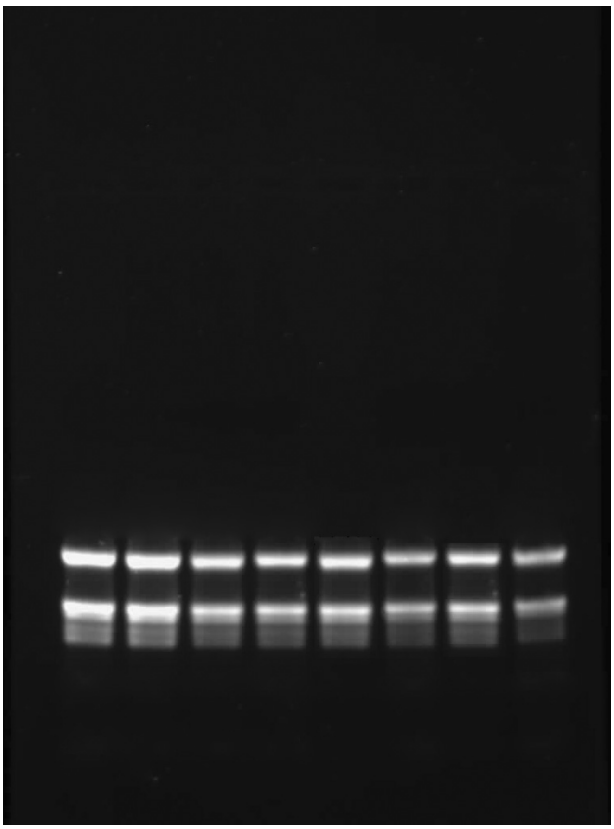

Figure 6.19: Integrity and size distribution of isolated total RNA from seedlings pretreated with SNP ± cPTIO or sterile sterile H_2O for 3 h. Sharpness of bands and ratio of 28S rRNA to 18S rRNA was observed after performing 1% (w/v) agarose gel electrophoresis. Image shown is that of a representative gel from two independent experiments with similar results.

Pre-treatment		Oxidative stress	Gene expression of *AnnAt1*				
0.5 mM SNP	**1 mM cPTIO**	**100 µM $Pb(NO_3)_2$**	**Relative fold differences**	**SE**	**95% CI**	**P-value**	**Interpretation**
-	-	-	1.000	-	-	-	-
+	-	-	0.917	0.772 - 1.081	0.724 - 1.256	0.274	-
+	+	-	0.798	0.634 - 0.977	0.599 - 1.137	0.030	Down-regulation
-	+	-	0.769	0.681 - 0.880	0.619 - 0.966	0.001	Down-regulation
-	-	+	1.033	0.898 - 1.192	0.755 - 1.328	0.628	-
+	-	+	1.194	1.013 - 1.365	0.880 - 1.510	0.025	Up-regulation
+	+	+	1.030	0.849 - 1.249	0.760 - 1.422	0.761	Up-regulation
-	+	+	1.266	1.124 - 1.426	1.048 - 1.574	0.004	-

Table 6.2: Effect of SNP $\pm$ cPTIO pre-treatment on the transcript level of *AnnAt1* under Pb stress condition. Relative fold differences of *AnnAt1* was normalized against mitosis protein YLS8 using REST 2008 software (Pfaffl *et al.*, 2002). Results from two independent experiments in triplicate (n = 6) were presented.

6.4 Discussion

6.4.1 SNP chelates Pb^{2+} in the modified HC medium

It is possible that Pb^{2+} chelation by SNP could occur during treatment. In solutions, SNP is a short-lived and unstable compound (Sigma-Aldrich, 1996). Aqueous solutions of SNP are temperature, light and acidic-pH sensitive. When the SNP solutions were exposed to environmental light source or acidic condition (the pH of modified HC medium is 4.5 - 5.0), SNP may decompose, producing cyanide ions (Figure 6.20). These cyanide ions may react and chelate Pb^{2+} in the medium, thereby reducing Pb bioavailability in the medium and/or rendering Pb^{2+} non-toxic.

By comparing the results of SNP and Al on root elongation, Tian *et al.* (2007) concluded that the alleviation of Al-inhibition of root growth by SNP was not the result of metal-SNP complexation in the media. Similarly, the reduction in root elongation was modulated whether *A. thaliana* seedlings were grown on the modified HC medium containing both 1 μM SNP and 100 μM $Pb(NO_3)_2$, or were pre-incubated with SNP before subjecting to Pb-stress treatments. However, when both SNP and $Pb(NO_3)_2$ were present together in the medium, inconsistent Pb accumulation results were obtained via GF-AAS. This raises the possibility of interactions of NO-releasing compound (SNP) with the metal ions, and the instability of SNP.

When studying Pb accumulation and uptake in *A. thaliana* seedlings, the unstable SNP and/or cPTIO may have decomposed before sowing *A. thaliana* seeds on the modified HC medium. This might result in variations between experiments. SNP and/or cPTIO might also contain other components which could affect the metal uptake. Cations, for example, in the medium can compete with Pb^{2+}. Thus, the uptake of Pb^{2+} decreases with decreasing metal:nutrient ratio. Competitions between hydrogen ions and Pb^{2+} at the uptake sites in the roots also affect a plant's ability to accumulate metals. As a result, effects of SNP on the responses of seedlings to Pb stress were inconsistent.

The initial experiments identified problems of adding SNP and $Pb(NO_3)_2$ together in the medium. Pre-treatment of seeds with SNP for 3 h in the dark before subjecting to Pb stress was found to be more suitable. This allows SNP to exert its effect before being chelated.

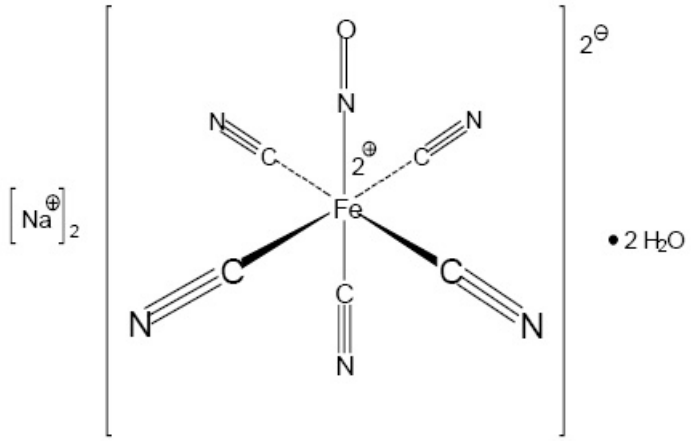

Figure 6.20: Structure of sodium nitroprusside (Sigma-Aldrich, 1996).

6.4.2 Selection of SNP pre-treatment concentration

The beneficial and harmful effects of NO reactivity with ROS is concentration dependent (Beligni & Lamattina, 1999a, 2001). At low concentration of SNP (0.5 mM), ROS could react with NO to form peroxynitrite. This will then subsequently react with H_2O_2 to yield non-toxic NO_2^- and O_2 (Hsu & Kao, 2004). Therefore, the toxic effect of Pb was counteracted by low NO concentration, keeping a balance redox state in seedlings. The inhibitory effect of Pb on root growth was minimized. In contrast, $OONO^-$ tends to be overproduced at high SNP concentrations, such as 5 and 10 mM (Beligni & Lamattina, 2001). They have toxic effects on plant cells, leading to more profound inhibition of root growth on *A. thaliana* seedlings.

6.4.3 Effect of NO on seedlings growth

The inhibitory effect of Pb on the growth of 7-d-old *A. thaliana* seedlings has been explained in Section 3.4.2, where Pb induced morphological change of the seedlings and inhibited root elongation. However, exogenous supply of NO (0.5 mM SNP) was found to protect 7-d-old *A. thaliana* seedlings under Pb stress conditions, resulting in better root and shoot growth. The benefits of NO-releasing compounds were specific because a NO

scavenger, cPTIO, reversed this ameliorating effect of SNP on the root growth. NO was discovered to be involved in the regulation of root growth and development via auxin signalling transduction pathway (Kopyra & Gwozdz, 2003; Correa-Aragunde *et al.*, 2004).

The roots of seedlings pre-treated with cPTIO were 24 - 25% longer than those of seedlings without pre-treatment. Correa-Aragunde *et al.* (2004) have also reported that the depletion of endogenous NO with cPTIO caused 40% increase in primary root length of tomato plants. NO scavenger may play a role in the regulation of root growth, or triggering a secondary response in seedlings.

Consistent with the present findings, Singh *et al.* (2009) showed the amelioration of As-induced inhibition of root and coleoptile growth by the application of 50 µM SNP in *Oryza sativa*. Pre-treatment of *Lupinus luteus* seedlings with 10 µM SNP efficiently attenuated the detrimental effect of Pb and Cd on root growth (Kopyra & Gwozdz, 2003). By recovering the NOS activity to produce endogenous NO, SNP is able to arrest Al-induced inhibition of root growth in *Hibiscus moscheutos* (Tian *et al.*, 2007). By decreasing Al accumulation in root tips, SNP counteracted the inhibitory effect of Al on the root of *Cassia tora* (Wang & Yang, 2005).

There is one exception to the majority of reports on the protective effects of NO on root elongation. Besson-Bard *et al.* (2009) claimed that NO contributes to Cd-inhibition of root growth by decreasing Ca^{2+} content in roots, and this effect was reversed when Cd-treated rice seedlings were supplemented with cPTIO. The differences in NO functions may be related to the metal speciation, type of plants and tissues, as well as concentration and source of NO. More experiments are needed to clarify the relationship between NO and root elongation under heavy metal stress.

6.4.4 Effect of NO on Pb uptake, accumulation and detoxification in *A. thaliana*

The influence of exogenously provided NO on metal uptake and translocation is not well understood. In *O. sativa* (Hsu & Kao, 2004) and *Triticum aestivum* (Hu *et al.*, 2007), the protective roles of NO were not due to the reduction of Cd and Cu contents in the plant tissues. However, in *C. tora*, the Al content in the SNP-treated root tip was 20%

lower than the control (Wang & Yang, 2005). Additionally, SNP inhibited the uptake and translocation of La from root to shoot by 21% in rice seedlings (Qiang *et al.*, 2007). SNP seems to prevent metal uptake in both of the latter studies, implying the differential responses of plants under different conditions.

In *A. thaliana* seedlings, although exogenous NO appeared to protect seedlings against Pb-induced stress, SNP pre-treatment did not significantly reduce Pb uptake and accumulation. It is likely that exogenous NO did not alter pumping of metals at the plasma membrane. Hence, pre-treated seeds do not tolerate Pb toxicity by Pb exclusion, but by tolerance mechanisms.

6.4.5 Effect of NO on Pb-induced oxidative stress and antioxidative defence system

Pb treatment resulted in an increased of lipid hydroperoxide and H_2O_2 levels in 7-d-old *A. thaliana* seedlings, indicating Pb-induced oxidative stress (see Section 4.4.1). Pre-treatment of *A. thaliana* seeds with SNP resulted in efficient reduction of H_2O_2 level, suggesting NO might act as an antioxidant or signal actions to scavenge ROS. Several previous studies have demonstrated the ability of NO to scavenge metal-induced ROS and to participate in the antioxidant cellular system (Kopyra & Gwozdz, 2003; Hsu & Kao, 2004; Laspina *et al.*, 2005; Wang & Yang, 2005; Yu *et al.*, 2005; Kopyra *et al.*, 2006; Hu *et al.*, 2007; Qiang *et al.*, 2007; Singh *et al.*, 2008; Zhang *et al.*, 2008; Singh *et al.*, 2009).

In addition, heavy metals could reduce the production of NO in plants, which could result in $^{\cdot}O_2^-$ accumulation, leading to an oxidative burst (Rodriguez-Serrano *et al.*, 2009). For example, Al inhibited NOS activity and reduced endogenous NO concentrations in *Hibiscus moscheutos* (Tian *et al.*, 2007) and in the transition zone of *A. thaliana* (Illes *et al.*, 2006). However, Cd increased endogenous NO production in *Glycine max* (Kopyra *et al.*, 2006) and *A. thaliana* (Besson-Bard *et al.*, 2009). These inconsistent results might be attributed to the method of application, the length of exposure to NO donors, or to heavy metal speciation. The present investigation seems to suggest that Pb mediated the inhibition of endogenous NO, because pre-treatment with cPTIO alone markly increased

the lipid hydroperoxide content in seedlings grown on Pb-containing medium. It is likely that such cPTIO application further depleted the endogenous NO in *A. thaliana* seedlings, and severely magnified the Pb-triggered oxidative stress. On the other hand, SNP applications restored the Pb-induced reduction of NO in *A. thaliana* seedlings, and thus limited excessive ROS accumulation.

Accumulation of lipid hydroperoxide is a consequence of ROS overproduction (Verma & Dubey, 2003). When ROS under Pb stress was scavenged, the lipid hydroperoxide chain was significantly attenuated in the seedlings of NO and Pb-treatment. NO may also act as a membrane stabilizer (Laspina *et al.*, 2005) that could resist Pb-induced ion leakage, thereby lowering the oxidative stress in Pb-exposed *A. thaliana*.

Besides initiating oxidatively destructive processes in plants, ROS may trigger various signaling pathways to maintain the equilibrium between ROS generation and detoxification (Neill *et al.*, 2003). In such cases, plants initiate a signal transduction pathway that triggers enzymatic and non-enzymatic antioxidative system to detoxify the cells (Ahmad, 1995; Dalton, 1995). In a series of primary enzymatic antioxidative reactions, SOD destroys $^{\cdot}O_2^-$, CAT and POD decompose H_2O_2, GPX dismutates lipid hydroperoxides, and GR regenerates glutathiones (see Section 4.4.2).

Under Pb stress conditions, a general trend was observed: the antioxidative enzyme activities were significantly decreased in 7-d-old seedlings supplied with exogenous NO. This could be due to reduction of excessive ROS level in *A. thaliana* seedlings. In contrast, the specific activities of SOD, CAT and GR were significantly increased in seedlings of cPTIO and Pb-treatment, likely in response to the high level of ROS level. The alleviation effect of NO is specific, because cPTIO reversed the effect of NO in the presence of Pb.

Under control conditions, a reduction of CAT and GPX was observed in seedlings pre-treated with SNP. NO may regulate ROS metabolism by affecting CAT activity that contains hemachrome iron, and GPX activity that contains non-hemachrome iron (Qiang *et al.*, 2007). In seedlings pre-incubated with cPTIO in the presence or absence of SNP, the activities of SOD and GR were enhanced. This is because cPTIO may scavenge the endogenous NO in *A. thaliana* seedlings, and elicit a mild or severe oxidative stress. SOD may be upregulated to counteract with the excess $^{\cdot}O_2^-$ accumulation, whereas GR maintained the total GSH pool. *A. thaliana* seedlings seem to have evolved a complex

antioxidant defence system to acclimatize to the stressors and environmental conditions.

6.4.6 Effect of NO on *AnnAt1* gene expression

It has been found that NO can regulate gene expression in plants, including under conditions of wounding, plant-pathogen interaction, signal affecting plant cell organelles, sexual reproduction, plant growth and development, stomatal closure, and iron homeostasis (Grun *et al.*, 2006). The formation of S-nitrosylated proteins by NO, consisting an S-NO bond, is the most important mechanism that affects the function of many cellular proteins (see Section 1.9.4). Under control conditions, SNP pre-treatment does not seem to affect the regulation of *AnnAt1*. When *A. thaliana* seeds were pre-treated with cPTIO and/or SNP, *AnnAt1* seemed to decrease slightly. The action of NO scavenger may elicit a mild response on the regulation of *AnnAt1*. There is a possibility that the scavenging of endogenous NO reduced the transcript level of *AnnAt1*.

Under Pb treatment, the endogenous NO levels in 7-d-old seedlings was disturbed. SNP pre-treatment may alleviate the effect of ROS over-accumulation and restore the NO level in *A. thaliana* seedlings. However, there is little information concerning the molecular mechanisms underlying the beneficial effects of NO. The imbalances of ROS and NO levels could interfere with the transcript level of *AnnAt1*. Although REST 2008 program detected the up-regulation of *AnnAt1* in seedlings pre-treated with SNP and/or cPTIO, the present study cannot rule out the possibility whereby NO did not regulate the gene expression of *AnnAt1*. This is because the relative fold-change in comparison to the control was minimal (< 2-fold). NO may also trigger different defence responses in different cell types. However, in this study, gene expression in whole seedlings was investigated and may not be specific to certain type of cells.

In the previous chapter, the gene expression of *AnnAt1* was found to be doubled at a high threshold concentration of Pb. However, it was not statistically significant in the present chapter. The limited control over the way seeds were pooled (since a new batch of *A. thaliana* seeds commercially purchased was used for work in this chapter) may have contributed to the discrepancy in data interpretation. It is also likely that the storage or aging of seeds have affected their biological properties (Hay *et al.*, 2003; Clerkx *et al.*, 2004; Niedzielski *et al.*, 2009).

6.5 Conclusion

At the physiological level, Pb stress symptoms were less evident in seedlings pre-treated with the NO donor, SNP. However, exogenous NO did not seem to alter Pb transport into the plant materials or efflux pumping of Pb at the plasma membrane. Pb disturbed the antioxidant defences in *A. thaliana* seedlings, leading to oxidative stress. Exogenous application of SNP was capable of counteracting the Pb-induced toxicity by reducing the H_2O_2 and lipid hydroperoxide contents efficiently. NO might confer protection to seedlings mainly by acting as an antioxidant or as a signal for actions to scavenge the excessive ROS level. Subsequently, antioxidative enzyme activites were reduced. The protective effect of NO was specific in *A. thaliana* seedlings, because cPTIO overturned the effect of NO in the presence of Pb.

Chapter 7

Isolation of a putative Pb mutant from EMS-mutagenized M_2 population

7.1 Introduction

To date, an ideal plant capable of Pb phytoremediation is non-existent (see Section 1.4.3), mainly due to the scarcity of genes that specially confer Pb tolerance and accumulation. Although genetic engineering may be applied to develop transgenic plants that exhibit a desired trait for Pb phytoremediation (see Section 1.4.1), the use of genetically modified plants in the field has not been publicly accepted in New Zealand (see Section 1.7.1.2). An alternative approach is conventional mutagenesis techniques.

Ethyl methane sulfonate (EMS) has been used successfully to induce new mutant variants of *A. thaliana* (Delhaize, 1996; Chen *et al.*, 1997; Navarro *et al.*, 1999), *Brassica juncea* (Schulman *et al.*, 1999), *Helianthus annuus* (Nehnevajova *et al.*, 2007), *Hordeum vulgare* (Zhu *et al.*, 2003), *Medicago truncatula* (Ellis *et al.*, 2003) and *Pisum sativum* (Tsyganov *et al.*, 2007) with enhanced heavy metal tolerance, resistance and accumulation. This chemical mutagen introduces random point mutations in the genome. Metal sensitive mutants have also been isolated in *A. thaliana* (Howden & Cobbett, 1992; Howden *et al.*, 1995b; Vliet *et al.*, 1995; Larsen *et al.*, 1996; Larkin *et al.*, 1999). They have been used to better understand the mechanisms of heavy metal regulation in plant. For example, *cup1* mutant is sensitive to Cu because it was unable to sequester excess intracellular Cu level effectively, leading to as much as 3-fold increase of Cu accumulation in

roots (Vliet *et al.*, 1995).

In the present study, a commercially available EMS-mutagenized M_2 population from the ecotype Columbia of *A. thaliana* was used to screen for Pb tolerant mutant. This small crucifer is particularly useful for conducting mutation experiments attributing to its small size, short life cycle, ability to produce a large number of small seeds, and its natural tendency to self-fertilize (Estelle & Somerville, 1986; Chen *et al.*, 1997; Meinke *et al.*, 1998). Chen *et al.* (1997) has recommended utilizing *A. thaliana* as a model system to study Pb tolerance and accumulation in plants. To the best of my knowledge, Chen *et al.* (1997) and Schulman *et al.* (1999) are the only two reports of Pb-related mutation screening study in plants (see Section 1.7.2.3).

To further seek for Pb tolerant mutants, the present research was initiated. Hence, the goals of this study were: 1) to isolate Pb tolerant mutants of *A. thaliana*; and 2) to determine if the (putative) mutation would affect the regulation of *AnnAt1*.

7.2 Materials and methods

7.2.1 Plant material and growth conditions

Surface-sterilized M_2 populations from the ecotype Columbia of *A. thaliana* treated with ethyl methanesulfonate (EMS) as the mutagen (Lehle Seeds, USA) were grown on modified Huang & Cunningham (1996) agar plates containing 150 μM $Pb(NO_3)_2$, according to the experimental procedures in Sections 2.1 and 2.2. The Pb concentration in modified HC medium chosen for germination and mutant screening was 150 μM $Pb(NO_3)_2$ because: 1) it brought about more than 75% root growth inhibition; and 2) Pb stress symptoms were more pronounced, and putative mutants could be revealed based on visual inspection of plates for those *A. thaliana* seedlings that remained green among bleached ones. Hence, this would shorten screening time and use fewer resources.

7.2.2 Screening of the the M_2 population and isolation of a putative Pb mutant

In total, over 5,000 seeds were screened. After 1 month from sowing on modified HC medium containing 150 μM $Pb(NO_3)_2$, the number of living plants, which were not wilted, formed roots and had purple-green leaves, was recorded. After a further 2 months (3 months from the first sowing on plates), individuals that displayed the ability to survive on 150 μM $Pb(NO_3)_2$ were rescued and transferred to MS medium (see Section 7.2.8) without $Pb(NO_3)_2$ in a tissue culture jar. From these plants, five were randomly selected for TEM analysis (see Section 2.9) to study the pattern of Pb accumulation and the possible mechanism of Pb tolerance in the plants. The plants (approximately 25) selected for recovery were based on a few qualitative morphological features, including no sign of wilting, roots penetrated into the medium, and the presence of purple-green leaves, a well-known symptom of Pb stress. After the plants grew on the MS medium to maturity, they were transferred to seedling soil mix for seed production in a light room (16/8 h photoperiod at 26.5 μE/sec/m^2, 22˚C). Only one plant survived and produced seeds. This plant was identified as a putative Pb-tolerant mutant (M_3-1).

7.2.3 Production of M_4 progeny

The isolated putative mutant seeds (M_3-1) were plated on Pb-free MS medium (pH 5.8), according to the methods described previously (Section 2.1). After 2 weeks of growing on MS medium, the seedlings were transplanted onto seedling soil mix for self-pollination to obtain a sufficient amount of M_4 generation seeds for use in all experiments. The putative Pb mutant seeds of this M_4 progeny were kept in an Eppendorf tube and stored at 4˚C.

7.2.4 Germination rate

The ability of M_4 seedlings counteracting Pb toxicity was rescreened and visually assessed for phenotypic confirmation alongside with wild-type *A. thaliana* ecotype Columbia Col-0 (WT), and EMS-mutagenized *A. thaliana* (M_2). Seeds were surface sterilized, cold-treated for 2 - 4 d, and plated on modified HC medium with and without 150 μM $Pb(NO_3)_2$, as described in Section 2.1. After 7 d of growth, the germination rate was

scored as a percentage of seeds sown according to Section 3.2.2.1. In this experiment, there were five replicates and it was repeated twice.

7.2.5 Survival rate

Since prolonged exposure to high concentration of Pb caused lethality in plants, the plates were evaluated after 2 months (8 weeks). Appearance of the three populations were visually observed, and the number of plants (with roots and purple-green leaves) which survived on the Pb-containing medium was recorded. The survival rate of the three populations were calculated as the following:

$$\text{Survival rate (\%)} = \frac{\text{Number of plants survived after 8 weeks}}{\text{Number of seedlings germinated after 1 week}} \text{x } 100\%$$

7.2.6 Gene expression of *AnnAt1*

After 7 d of growth, WT, M_2 and M_4 seedlings were collected for gene expression studies (see Section 2.10). Total RNA isolation, cDNA synthesis and real-time PCR were carried out according to Section 2.15 and 2.16. After checking the specificity of amplification product (see Section 2.17), the transcript level of *AnnAt1* was quantified as described in Section 2.18. Two independent experiments were carried out for gene expression analysis.

7.2.7 Statistical analysis

Statistical analysis was accomplished according to Section 2.23. All values presented are means and standard error or the means, where significant differences at $p < 0.05$ were indicated by different letters in the graphs.

7.2.8 Preparation of MS medium

A well-known plant growth medium used in laboratories, Murashige & Skoog (1962), was used for the recovery of isolated putative mutant (Section 7.2.2). This medium is enriched with nutrients necessary for plant cultivation and development, and is referred to

as MS medium. The composition of MS medium containing 0.8% (w/v) agar is shown in Appendix A.1.2.

The major salt stock (50 mL, 10x concentrate), minor salt stock (5 mL, 100x concentrate), organic stock (5 mL, 100x concentrate) and iron stock (5mL, 100x concentrate) were mixed with 375 mL nanopure H_2O in a 500 mL glass bottle. After pH adjustment to 5.8 with 0.1 M HCl using a pH meter (E350B, Metrohm, Herisau, Switzerland), 4 g bacteriological grade agar (Danisco, Copenhagen, Denmark) was added to the mixture. The medium was autoclaved (121˚C for 20 min) and then cooled to ~50˚C, before it was poured into sterile tissue culture jars, each containing about 25 mL in a laminar flow cabinet. Upon solidification, the tissue culture jars were capped and kept at room temperature until use.

7.3 Results

7.3.1 Isolation of a putative mutant with enhanced Pb tolerance

A selection process was designed to screen an EMS-mutagenized M_2 population of *A. thaliana* seeds where point mutations have been induced. After 1 month of cultivation, 10 - 15% of unwilted plants of this population were found on minimal media supplemented with 150 µM $Pb(NO_3)_2$ (Figure 7.1a). After another 2 months, the number of unwilted plants dropped to 7 - 10%. However, the plants appeared to be severely stunted, resembled the size that of a 1-month-old, and looked dormant. It is interesting to note that near 50% of these plants had roots growing on top, curled up, or did not penetrate into the agar to minimize root-Pb contact. Purple leaves, indicating Pb stress, were also observed.

Plants with roots penetrated into the Pb-containing medium and ability to maintain green (or purple-green) leaves were selected as putative Pb tolerant mutants for recovery. In the absence of $Pb(NO_3)_2$, 20 - 25% of these *A. thaliana* plants slowly re-growed on MS media (Figure 7.1b). Some of these plants began to grow taller, producing longer roots and leaves, while others did not grow and became wilted. When the putative Pb mutants began to form a bud (Figure 7.1c), they were placed in seedling soil mix (Figure 7.1d) and allowed to set seeds (Figure 7.1e).

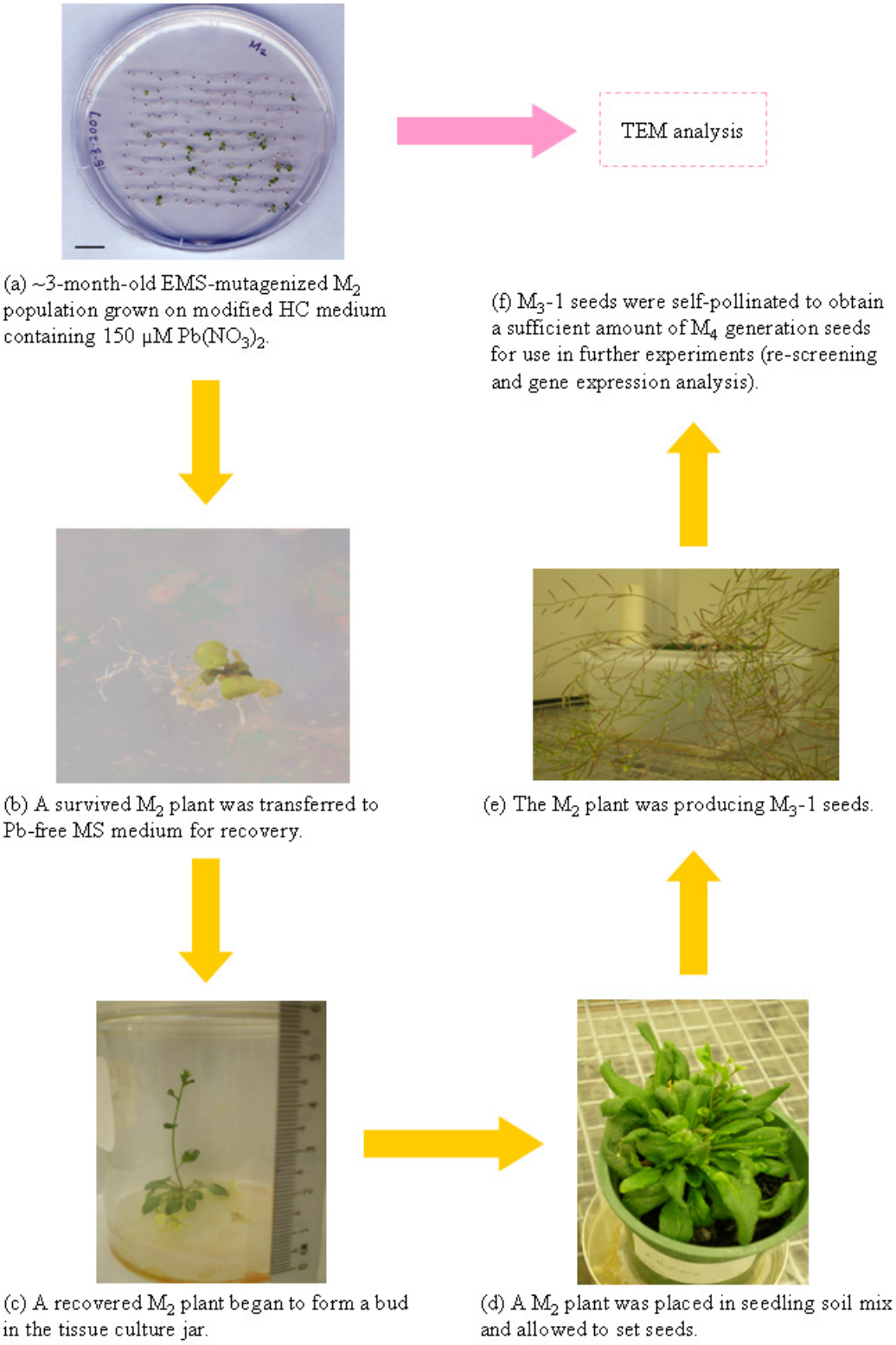

Figure 7.1: Isolation of a putative Pb tolerant mutant.

7.3.2 Germination rate of WT, M_2 and M_4

During the rescreening process, the appearance of the putative Pb tolerant mutant was visually observed. Phenotypically, the appearance and size of 7-d-old rescreened M_4 seedlings seems bigger, nearly similar to a wild-type seedling exposed to 50 μM $Pb(NO_3)_2$ (see Figure 3.2). Pb stress symptom seems less evident, in comparison to a EMS-mutagenized M_2 seedling.

Although Pb-treated 7-d-old seedlings displayed symptoms of toxicity (see Section 3.3.1), no significant inhibition of germination was found between seedlings exposed to Pb or without Pb within the same population (e.g. Pb-treated WT seedlings to non Pb-treated WT seedlings; Figure 3.1). Generally, the number of seeds germinated from EMS-mutagenized M_2 population is 10 - 16% lower than the wild-type and M_4 population.

7.3.3 Further exposure of WT, M_2 and M_4 to Pb

After 2 months of sowing on Pb-containing medium, the number of M_4 *A. thaliana* plants which were able to grow without wilting was 3-fold higher than the M_2 population (Figure 7.3). However, it was only 1.2-fold higher than the wild-type plants. From visual observation, the size of all plants were not much different than that of the 1-month-old.

7.3.4 Ultrastructural localizaton of Pb in a putative Pb mutant

The appearance of 3-month-old, Pb-exposed, EMS-mutagenized M_2 *A. thaliana* plants suggested that they were stressed. Interestingly, at the ultrastructural level, the cellular organelles of *A. thaliana* appeared to be healthy and normal. No destructive changes were observed. In roots of *A. thaliana* plants exposed to 150 μM $Pb(NO_3)_2$, Pb deposited in a relatively high density at a certain region (unknown) outside the Casparian strip (Figure 7.4). TEM revealed that the vacuoles were free from Pb (Figure 7.5). At 25k magnification, a small number of very fine Pb grains were observed in the intercellular space (Figure 7.6). No Pb particles were found in the leaf (Figures 7.7, 7.8 and 7.9).

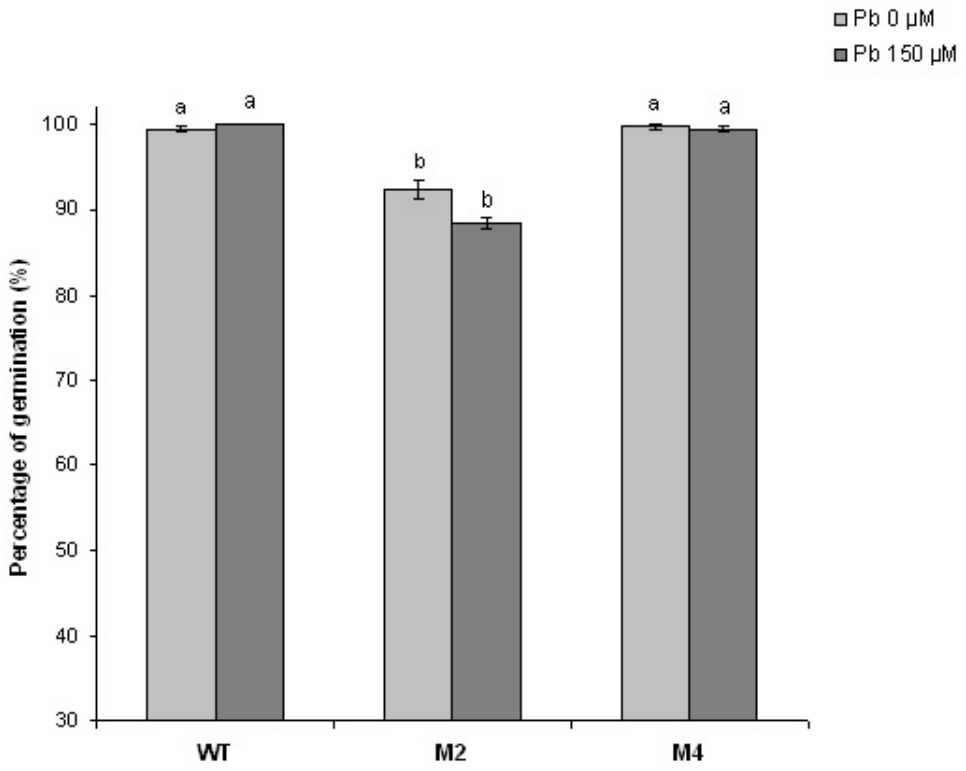

Figure 7.2: Effect of Pb treatment on the germination of different generations of *A. thaliana* seeds. The germination rate was scored as a percentage of seeds sown. A representative result from two independent experiments with five replicates is shown (n = 5). The bars indicate standard error of the means. Different letters represent significant differences at $p < 0.05$, according to one-way ANOVA and then multiple comparison using Fisher's LSD test.

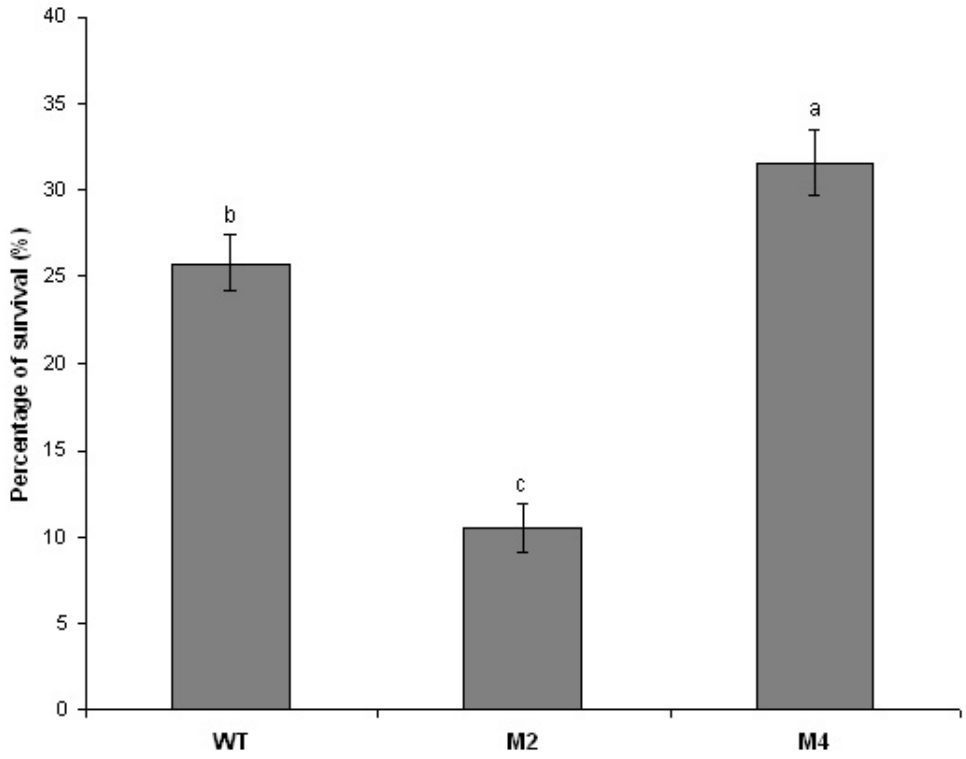

Figure 7.3: Percentage of surviving *A. thaliana* plants grown on modified HC medium containing 150 µM $Pb(NO_3)_2$ after 2 months of planting. The survival rate of plants grown in the absence of $Pb(NO_3)_2$ was between 97 - 100% ($p > 0.05$) and was not plotted. Data presented as mean ± S.E. of three replicates (n = 3). Different letters represent significant differences at $p < 0.05$, according to one-way ANOVA and then multiple comparison using Fisher's LSD test.

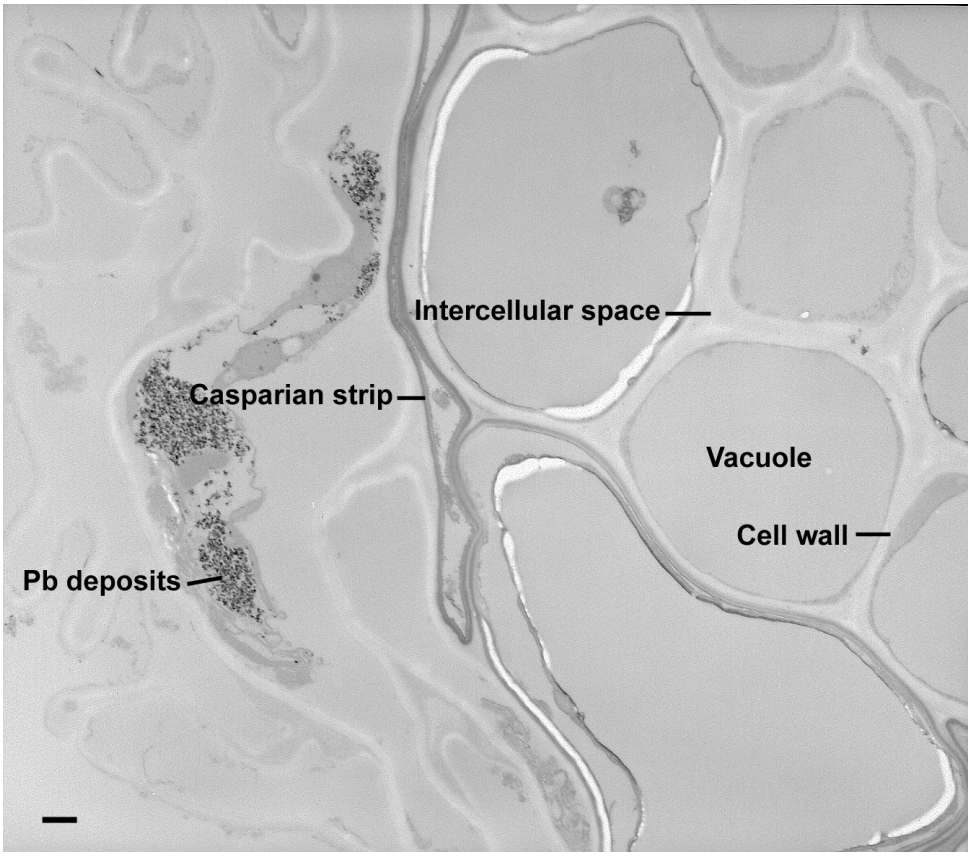

Figure 7.4: Transmission electron micrograph of an unstained ultra-thin section of the root from a EMS-mutagenized M_2 *Arabidopsis thaliana* grown in the medium containing 150 µM $Pb(NO_3)_2$. Magnification of the micrograph was at 6,000 X. Bar = 500 nm.

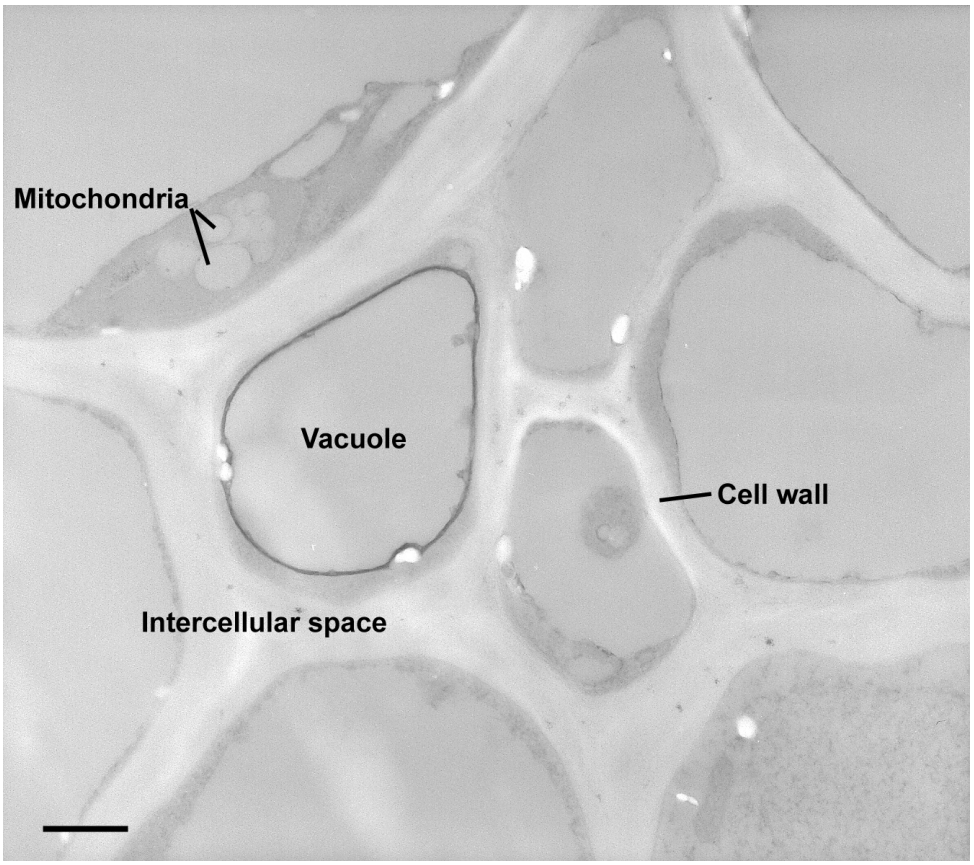

Figure 7.5: Transmission electron micrograph of an unstained ultra-thin section of the root from a EMS-mutagenized M_2 *Arabidopsis thaliana* grown in the medium containing 150 µM $Pb(NO_3)_2$. Magnification of the micrograph was at 15,000 X. Bar = 500 nm.

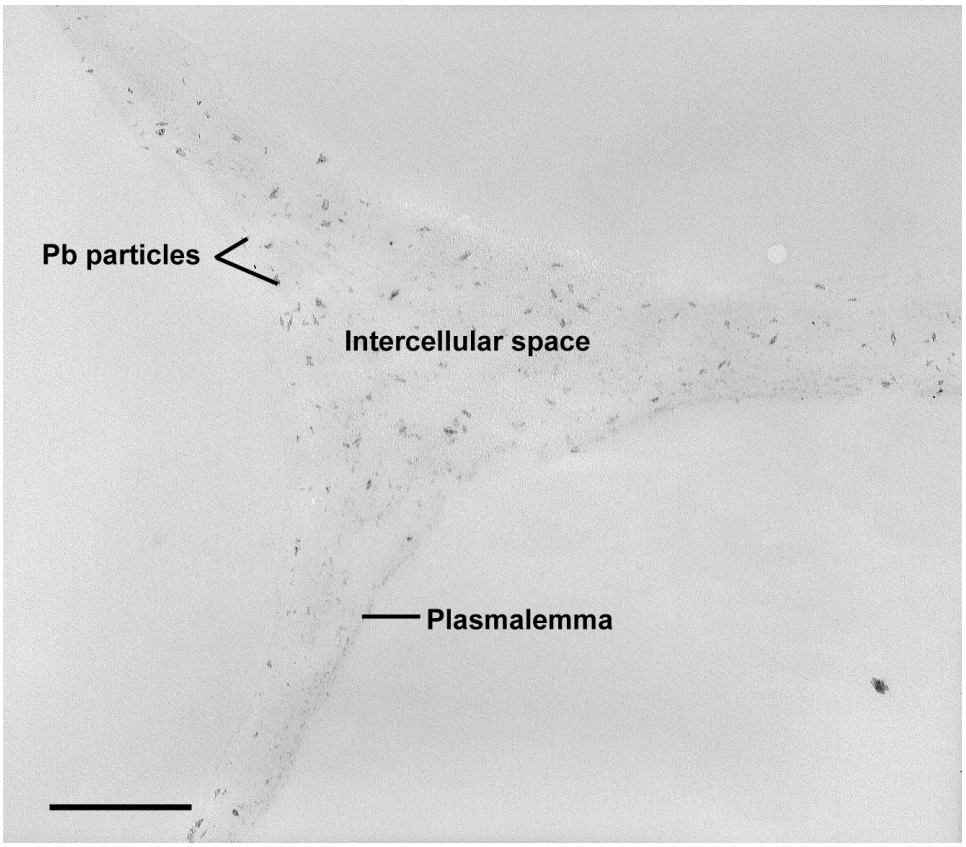

Figure 7.6: Transmission electron micrograph of an unstained ultra-thin section of the root from a EMS-mutagenized M_2 *Arabidopsis thaliana* grown in the medium containing 150 µM $Pb(NO_3)_2$. Magnification of the micrograph was at 25,000 X. Bar = 500 nm.

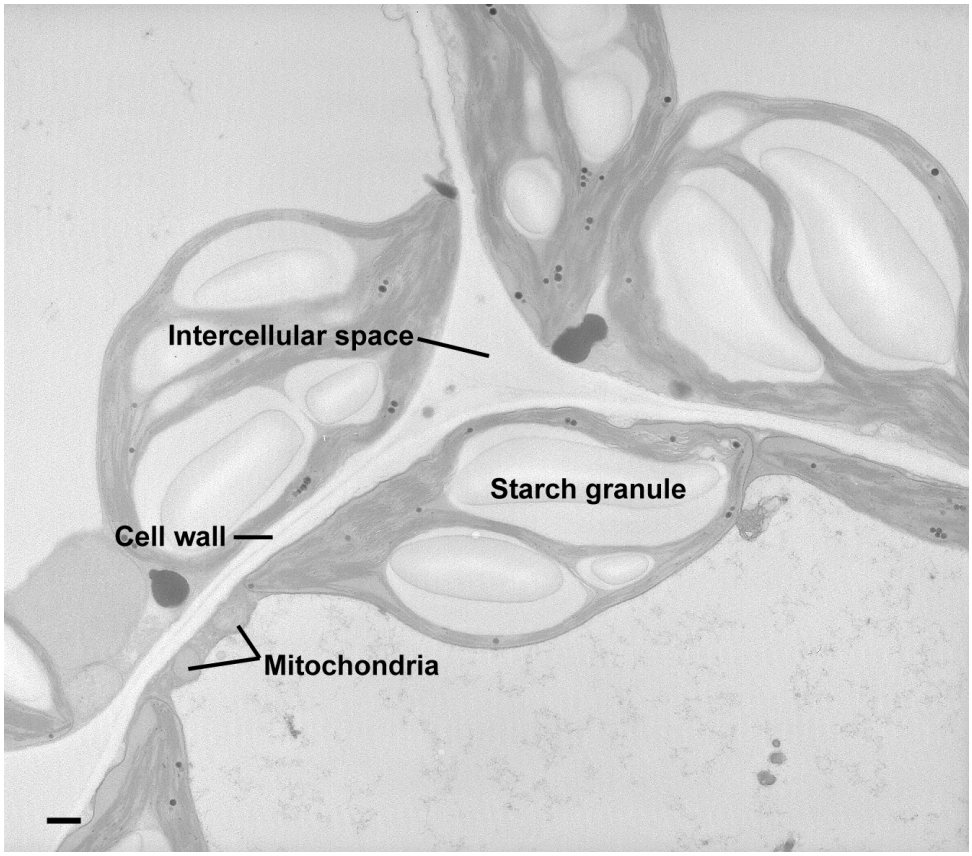

Figure 7.7: Transmission electron micrograph of an unstained ultra-thin section of the leaf from a EMS-mutagenized M_2 *Arabidopsis thaliana* grown in the medium containing 150 µM $Pb(NO_3)_2$. Magnification of the micrograph was at 6,000 X. Bar = 500 nm.

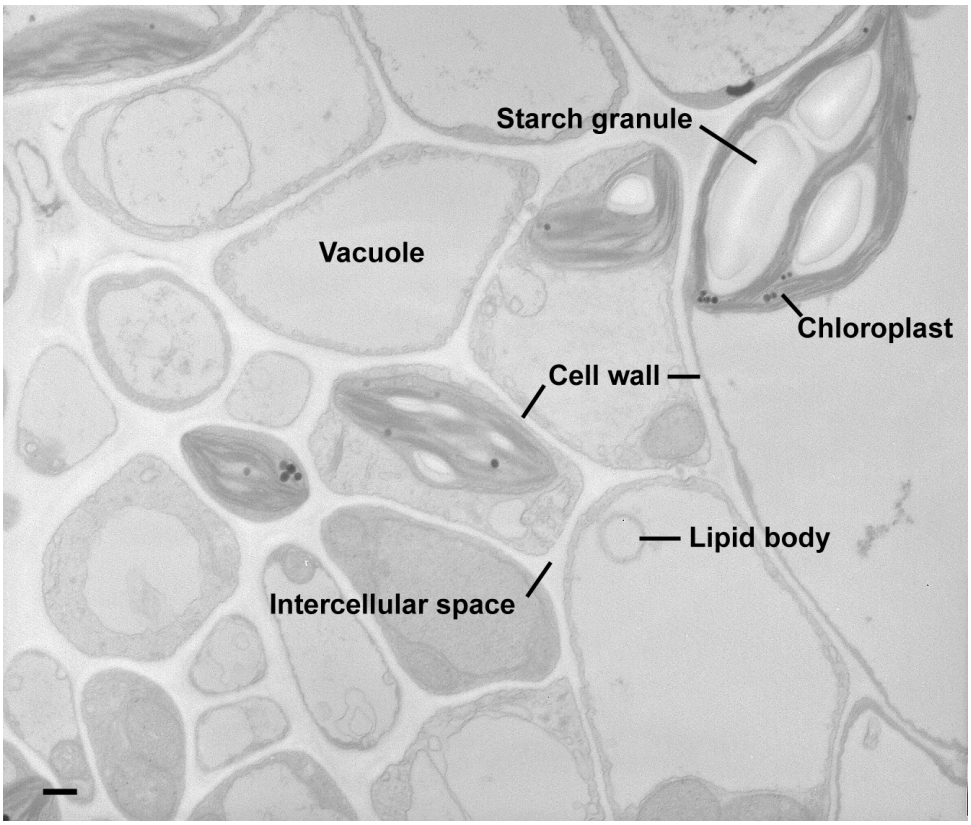

Figure 7.8: Transmission electron micrograph of an unstained ultra-thin section of the leaf from a EMS-mutagenized M_2 *Arabidopsis thaliana* grown in the medium containing 150 μM $Pb(NO_3)_2$. Magnification of the micrograph was at 6,000 X. Bar = 500 nm.

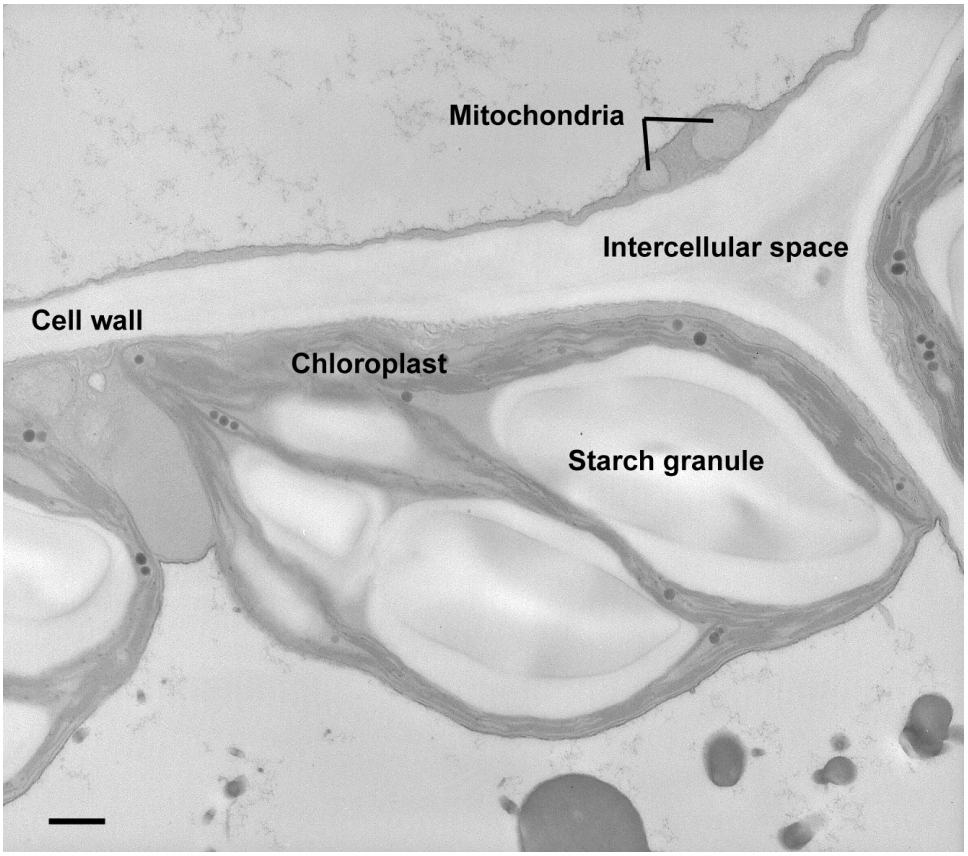

Figure 7.9: Transmission electron micrograph of an unstained ultra-thin section of the leaf from a EMS-mutagenized M_2 *Arabidopsis thaliana* grown in the medium containing 150 µM $Pb(NO_3)_2$. Magnification of the micrograph was at 10,000 X. Bar = 500 nm.

7.3.5 Gene expression of *AnnAt1*

In comparison to the non Pb-treated 7-d-old WT *A. thaliana* seedlings, the relative expression of *AnnAt1* in M_2 population grown in the absence of $Pb(NO_3)_2$ was down-regulated by 0.821-fold ($p < 0.05$; Table 7.1). However, no significant difference between WT and M_4 seedlings grown in the absence of $Pb(NO_3)_2$ was detected as far as *AnnAt1* expression is concerned ($p > 0.05$). With a 150 µM $Pb(NO_3)_2$ treatment, the transcript levels of the WT, M_2 and M_4 population were up-regulated by 2.282-, 1.183- and 1.949-fold ($p < 0.05$), respectively.

If the M_2 seedlings grown in the absence of Pb was used as a normalizer (Table 7.2), the transcript levels of *AnnAt1* in M_2 and M_4 seedlings subjected to 150 µM $Pb(NO_3)_2$ treatment were up-regulated by a mean factor of 1.442 and 1.375 ($p < 0.05$), respectively. No significant difference was detected between M_2 and M_4 population grown in the absence of $Pb(NO_3)_2$ ($p > 0.05$).

Within the M_4 population, *AnnAt1* message levels were doubled (2.186-fold, $p < 0.05$) in seedlings treated with 150 µM $Pb(NO_3)_2$, in comparison to the seedlings without Pb exposure (Table 7.3).

7.4 Discussion

7.4.1 Isolation of a putative Pb tolerant mutant

Mutants can be identified phenotypically by investigating root growth, hypocotyl length, flowering time, germination rate, fresh weight gain, and water loss (Weigel & Glazebrook, 2002). To minimize the tedious technical procedure especially from the original root growth assay to identify Pb-tolerant mutants, a post-germination screen, which involved long term exposure of the mutagenized population of *Arabidopsis*, was developed. As high concentrations of Pb normally inhibit growth and cause lethality in plants, plants that were able to maintain relatively green leaves with its roots penetrated into the medium, after approximately 3 months, were selected as putative Pb tolerant mutants. Hence, this method allows simple visual screening of a relatively large EMS-mutagenized M_2 population to isolate mutants with a high tolerance to Pb.

150 µM $Pb(NO_3)_2$	Type of *A. thaliana*	Relative fold differences	SE	95% CI	P-value	Interpretation
-	WT	1.000	-	-	-	-
-	M_2	0.821	0.749 - 0.901	0.655 - 0.966	0.002	Down-regulation
-	M_4	0.892	0.746 - 1.052	0.689 - 1.138	0.152	-
+	WT	2.282	2.105 - 2.482	2.011 - 2.727	0.002	Up-regulation
+	M_2	1.183	1.011 - 1.382	0.927 - 1.479	0.028	Up-regulation
+	M_4	1.949	1.755 - 2.196	1.609 - 2.497	0.002	Up-regulation

Table 7.1: Relative fold differences of *AnnAt1* in WT, M_2 and M_4 *A. thaliana* seedlings in response to 150 µM $Pb(NO_3)_2$. Relative fold differences of *AnnAt1* was normalized against mitosis protein YLS8 using REST 2008 software (Pfaffl *et al.*, 2002), and compared to the non Pb-treated WT seedlings. Results from two independent experiments in triplicate (n = 6) were presented.

150 µM $Pb(NO_3)_2$	Type of *A. thaliana*	Relative fold differences	SE	95% CI	P-value	Interpretation
-	M_2	1.000	-	-	-	-
-	M_4	1.087	0.900 - 1.277	0.830 - 1.492	0.304	-
+	M_2	1.442	1.219 - 1.656	1.118 - 1.940	0.002	Up- regulation
+	M_4	2.375	2.114 - 2.777	1.939 - 3.060	0.001	Up-regulation

Table 7.2: Relative fold differences of *AnnAt1* of M_2 and M_4 *A. thaliana* seedlings in response to 150 µM $Pb(NO_3)_2$. Relative fold differences of *AnnAt1* was normalized against mitosis protein YLS8 using REST 2008 software (Pfaffl *et al.*, 2002), and compared to the non Pb-treated M_2 seedlings. Results from two independent experiments in triplicate (n = 6) were presented.

150 µM $Pb(NO_3)_2$	Type of *A. thaliana*	Relative fold differences	SE	95% CI	P-value	Interpretation
-	M_4	1.000	-	-	-	-
+	M_4	2.186	1.823 - 2.579	1.647 - 3.066	0.002	Up-regulation

Table 7.3: Relative fold differences of *AnnAt1* of M_4 *A. thaliana* seedlings in response to 150 µM $Pb(NO_3)_2$. Relative fold differences of *AnnAt1* was normalized against mitosis protein YLS8 using REST 2008 software (Pfaffl *et al.*, 2002), and compared to the non Pb-treated M_4 seedlings. Results from two independent experiments in triplicate (n = 6) were presented.

Of the over 5,000 M_2 seedlings screened, only 1 putative Pb-tolerant mutant was recovered and set seeds. The mutation frequency produced from EMS is approximately 1% (Howden & Cobbett, 1992). Up to 50 putative Pb mutants were expected from 5,000 seeds. However, this was not the case. The death and infertility of other putative mutants may be due to mutations in the developmental pathway. Some putative mutants were not isolated because a mutation may have no morphological effect on plants, or only cause slight changes in phenotype that may not be detectable.

Due to the genetic variability between individual seedlings, a small percentage of wild-type and EMS-mutagenized M_2 populations were able to thrive on the Pb-containing medium. It was also interesting to note that plants were able to survive on Pb-containing medium for more than 3 months by minimizing root-agar contact (e.g. curling up the roots), possibly due to an altered physiological response to Pb. Plants are also likely to become dormant, or go into a resting stage in a Pb-stressed environment and re-generate again under favorable environment (Baker, A.J.M., personal communication). Pb may block the entry of various ions, such as K^+, Ca^{2+}, Mg^{2+}, Zn^{2+}, Cu^{2+}, Fe^{3+} and NO_3^-, causing nutrient imbalance or malnutrition in plants (Sharma & Dubey, 2005). These plants have the ability to recover in MS medium without Pb.

During the rescreening processes, putative Pb mutants were initially bigger in size, in comparison to wild-type and M_2 seedlings. However, exposure to Pb for 2 months eventually resulted in more than 50% lethality in the M_4 population. Hence, two of the key issues arising from this technique were: 1) the accuracy in identification and selection of putative mutants, and 2) the length of exposure to Pb. In order to resolve these issues and identify more useful mutants, it is necessary to compare all of the parameters for phenotypic measurements. However, more resources would be required than was allowed in the present study. Whether the putative Pb tolerant mutant was a true mutant or not was not determined.

7.4.2 Pb uptake and detoxification in putative Pb mutant

The pattern of Pb accumulation in putative Pb mutants is useful for providing insights into the mechanisms of Pb tolerance. Because the number of EMS-mutagenized M_2 plants which survived on Pb-containing medium were insufficient for GF-AAS analysis, TEM

analysis was carried out. The putative Pb tolerant mutants showed a noticeably lower Pb accumulation level in comparison to 7-d-old wild-type seedlings as shown in Sections 3.3.5 and 3.3.6. Pb has high affinity for galacturonic acids of the cell wall and can bind tightly to them (Polec-Pawlak *et al.*, 2007). Although the age of *A. thaliana* was different (7-d-old vs 3-month-old), it is reasonable to expect that if the sequestration pathway was similar, the cell wall and vacuole remained the sites for Pb accumulation as the plants grew.

In the roots of a mature plant, Casparian strips may restrict Pb from entering the xylem (Greger, 1999). Consequently, translocation of Pb from root to shoot became more difficult as the Pb concentration gradient decreased. Hence, Pb particles were not detected in the leaves. At 150 μM $Pb(NO_3)_2$, wild-type *A. thaliana* seedlings predominantly accumulate Pb in the cell wall, intercellular space and vacuole (see Section 3.4.3). In the present chapter, it is reasonable to detect a small amount of Pb grains in the intercellular space of a putative mutant.

The putative mutants may be able to produce and/or exudate certain metal chelating compounds to precipitate Pb as a non-toxic form, such as Pb-carbonate, -sulphate and -phosphate (Salt *et al.*, 1998), outside the Casparian strips. Binding of exudate to heavy metals prevents the circulation of Pb ions as free Pb^{2+}, thereby decreasing the bioavailability of Pb. For example, an Al-tolerant barley mutant secreted more citrate and malate exudate as part of its detoxification mechanism to reduce Al accumulation (Zhu *et al.*, 2003).

Inorganics including Pb are taken up into the root cytoplasm via membrane transporter proteins (Pilon-Smits, 2005), such as Ca^{2+}-channel proteins and H^{+}-ATPases (Clemens *et al.*, 2002). It is possible that a transporter at the plasma membrane and/or vacuole of Pb tolerant mutants was changed, thereby preventing the transport of Pb into the cells. Similarly, Pb tolerant mutants may have a greater number of efflux transporter in the plasma membrane to pump the metals out of the cells. Since Pb tolerant mutants seem to go into a resting stage, the former explanation seems more likely.

7.4.3 *AnnAt1* gene expression

Gene expression of *AnnAt1* was studied in the isolated putative mutants through the M_4 generation. Generally, stress-related proteins, or heat shock proteins (HSP) are synthesized in response to abiotic stresses, including heavy metals (Vierling, 1991; Aarts & Fiers, 2003). It was found that HSP protects cells from stress and maintains normal cellular functions (Rhee *et al.*, 2000; Grover *et al.*, 2001; Hall, 2002). Although *AnnAt1* has several functions and biochemical properties similar to HSP (Rhee *et al.*, 2000; White *et al.*, 2002), the exact mechanisms of HSP in relation to heavy metal toxicity is not well known.

Differences between genotypes of seeds used may have resulted in differential responses to Pb, leading to data discrepancy. This could be because wild-type and EMS-mutagenized M_2 seeds were purchased from a commercial source (Lehle Seeds, USA), and the present study had limited control over the grouping of seeds. Therefore, the transcript level of *AnnAt1* was compared within the same population (e.g. Pb-treated M_4 seedlings to non Pb-treated M_4 seedlings).

As observed in Section 5.3.1.6, the *AnnAt1* message level was up-regulated by 2.2-fold when putative Pb mutants were exposed to 150 μM $Pb(NO_3)_2$ for 7 d. Since GFS-AAS and TEM analysis of M_4 seedlings were not conducted for the determination of Pb uptake due to the time constraint, the following explanation is speculative. If the putative Pb-tolerant mutants of M_4 generation accumulated high level of Pb concentrations, it is likely that ROS was overproduced and free Ca^{2+} in the cytoplasm increased. *AnnAt1* was induced to initiate a biochemical change in plants. *AnnAt1* may aid in refolding proteins that were denatured by Pb exposure.

However, if the 7-d-old M_4 seedlings accumulated similarly low levels of Pb as the matured EMS-mutagenized M_2 population of *A. thaliana* (Section 7.3.4), the gene expression of *AnnAt1* is expected to be down-regulated. One possible exception to this expectation might be because the membrane transporter proteins regulating Pb have been altered. Less transporters or ion channels were available to transport the high amount of Pb ions across the plasma membrane. Ca^{2+}-signalling/channel was modulated, leading to the initiation of a different stress response which subsequently enhances the transcript level of *AnnAt1*.

7.5 Conclusion

A post-germination procedure to isolate putative Pb-tolerant mutants is described. *A. thaliana* population mutagenized with the chemical EMS was screened. After exposure to 150 μM $Pb(NO_3)_2$ for approximately 3 months, potential Pb tolerant mutants were selected based on the ability to grow with their roots penetrating into the medium and maintaining purple-green leaves without wilting. Only one putative Pb mutant recovered from the rescue and set seeds. The 7-d-old putative Pb mutant seemed to display enhanced shoot and root growth in the presence of 150 μM $Pb(NO_3)_2$ than the wild-type seedlings. The expression of *AnnAt1* in putative Pb tolerant mutants was doubled when exposed to 150 μM $Pb(NO_3)_2$. However, prolonged Pb treatment for 2 months was lethal to many putative Pb mutants, and their survival rate was only 1.2-fold higher than the wild-type plants. Due to the limited resources, the present study could not determine if this is a true mutant or merely caused by genetic variability. More phenotypic measurements are required for future study and improvements are recommended in the next chapter.

Chapter 8

General discussion and future directions

8.1 Pb phytoremediation

Because of increasing anthropogenic outputs, Pb has gained attention as a potent environmental and health hazard. The metal is responsible for a deterioration in soil quality, leading to a sharp decline in crop productivity. In a case study in Ghana, Pb caused a reduction of 13.7 - 43.2% in crop yield (Mensah *et al.*, 2008). Pb, a non-essential element, is persistent and cannot be degraded from the environment. In the last decade, phytoremediation has emerged as a potential remediation tool to remove heavy metal pollutants from the environment. The concept of plant-based environmental remediation is technically and economically attractive, compared to the conventional remediation methods.

The application of Pb phytoremediation in the field is hampered by inadequate knowledge of the associated biological processes, including Pb uptake, accumulation, tolerance and detoxification in plants. Hence, a model plant system, *Arabidopsis thaliana*, was selected as the experimental plant in this study. Its small size, short life cycle, ability to produce a large number of small seeds, and natural tendency to self-fertilize (Estelle & Somerville, 1986; Chen *et al.*, 1997; Meinke *et al.*, 1998), makes *A. thaliana* an attractive plant to study Pb-plant interactions in a laboratory environment. Although *A. thaliana* is widely used for genetic modification studies with the aim to develop novel plants with improved performance, research publications on the biological responses of plants to Pb are

relatively rare. A basic understanding of the mechanisms underpinning physiological and biochemical responses of *A. thaliana* seedlings to Pb may help to advance phytoremediation using molecular genetic and transgenic approaches. Additionally, classical breeding and exploitation of genetic variation in plants (Memon & Schroder, 2009), can also play a role in the development of phytoremediation. A multi-experimental approach involving GF-AAS, TEM, enzyme assay, and qRT-PCR analysis (see Section 1.10) was used in this thesis to further investigate the physiological, biochemical and molecular responses of *A. thaliana* seedlings to Pb exposure.

8.2 How did *A. thaliana* seedlings respond to Pb exposure in this study?

In the seeds of *A. thaliana*, the testa (seed coat) could prevent Pb uptake and protect the internal tissues from Pb contamination until it is ruptured by the germinating radicle. In the *A. thaliana* seedlings, Pb was mainly taken up through the root system and much of it remained there. This is consistent with similar studies on many other species reported to date. Only part of Pb in the root was translocated to the shoots because generally the bioavailability of Pb from soil solution is very low, making it less mobile (Blaylock *et al.*, 1997; Huang *et al.*, 1997). Since Pb has high affinity to negatively charged polygalacturonic acids in the cell wall (Ernst *et al.*, 1992; Greger, 1999), heavy depositions of Pb were found around the intercellular spaces and within the cell walls. Jarvis & Leung (2001) referred to this as apoplastic transport. Translocation of Pb from roots to shoots requires metal transporter proteins (Clemens *et al.*, 2002; Pilon-Smits, 2005) to cross the endodermis, which functions as a partial barrier to Pb movement between the root and shoot, and suberised Casparian strips before entering xylem. These might have contributed to the observed restricted movement of Pb from roots to the aerial parts of *A. thaliana* seedlings.

As the external concentration of Pb in the treatment solution used in the present study became higher, the barrier function and permeability of plasma membrane of root cells was modulated (Verkleij & Schat, 1990; Hall, 2002). A greater amount of Pb entered the cytoplasm, which has been referred to as symplastic transport (Jarvis & Leung, 2001). Dense Pb particles were detected in the central vacuole of a cell in 7-d-old seedlings. This

would mainly compartmentalize Pb and protect cells from the toxic effects of Pb. There was a small amount of fine Pb grains encapsulated in vesicles, which were likely to be involved in transporting cytotosolic Pb into the vacuole or membranous compartments.

Pb inside the cells exerted adverse effects on the physiological processes of *A. thaliana* seedlings. Visual symptoms of Pb toxicity, including browning of the root and the edge of cotyledon, inhibition of root elongation, fewer root hairs, stunted shoot growth, and wilting of the seedlings, were observed. It is known that Pb could inhibit enzymes which are essential to physiological processes of a cell by binding with their -SH and -COOH groups at the active site, and by displacing the essential metals in metalloenzymes with Pb (Dietz *et al.*, 1999; Malecka *et al.*, 2001; Hall, 2002; Sharma & Dubey, 2005; Sharma & Dietz, 2009). The efficiency of oxidation-reduction enzymes in electron transport system might be interrupted, leading to alteration of water potential, hormonal status, mineral nutrition, membrane structure, and an unbalanced cellular redox status (Sharma & Dubey, 2005).

In *A. thaliana* seedlings, the ROS, including $^{\cdot}O_2^-$, H_2O_2, and $^{\cdot}OH$, rose rapidly. The damaging effects of ROS on lipids, proteins, carbohydrates and nucleic acids were inevitable (Gratao *et al.*, 2005). Moreover, Pb changed the fatty acid composition of the membrane, causing peroxidation of essential lipids and electron leakage (Dietz *et al.*, 1999; Halliwell & Gutteridge, 1999). This situation is generally known as oxidative stress (Devi & Prasad, 1999).

In order to remove excess ROS, avoid a build-up of ROS, and repair the cell damage inaugurated by Pb-induced ROS, *A. thaliana* seedlings developed a range of antioxidative cellular defence activities. Enzymatic antioxidants of interest in this study, including SOD, CAT, GR, GPX and POD of seedlings treated with as much as 100 μM $Pb(NO_3)_2$ were enhanced to counteract Pb-increased oxidative stress. These antioxidative enzymes could work together to attack and neutralize ROS, producing non-toxic H_2O and O_2 (Moller *et al.*, 2007). Additionally, ROS may also act as signalling molecules in triggering gene expression and secondary responses in plants (Dietz *et al.*, 1999; Sharma & Dubey, 2005). The rapid and intricate signalling cascades which initiated biochemical changes may enable the 7-d-old *A. thaliana* seedlings to mitigate against Pb-induced oxidative stress and acclimate to the short-term exposure of Pb for survival. It is important

to note that this is not the trend in all reported cases. Pb-induced ROS is greatly dependent on Pb concentration, the length of exposure, plant species and developmental stage (Sharma & Dietz, 2009). A lethal Pb concentration may completely inhibit the antioxidative defence systems of plants, or a prolonged exposure to Pb may subsequently inactivate antioxidative enzyme activities. Both would lead to cell death.

Generally, the tolerance of plants to Pb contaminants is based on several mechanisms. A network of avoidance and tolerance mechanisms take place simultaneously, in order to control cell metabolic homeostasis and stress tolerance in plants. In response to Pb stress, enzymes, genes, and metabolites work together to maintain the essential cellular processes in plants. A series of possible events involving Pb uptake and detoxification in the present study is illustrated in Figure 8.1.

8.3 *AnnAt1* in Pb stress

Although the response of different plants to different stressors varies, there are common stress-related genes that are involved in the detoxification of ROS (Aarts & Fiers, 2003). This experiment was undertaken to further understand the molecular mechanisms plants employ to deal with Pb stress, focussing on the possible role of *AnnAt1* in Pb tolerance. Annexins are reported to be related to heat shock proteins, which are the most extensively characterized stress-response genes (Rhee *et al.*, 2000; Grover *et al.*, 2001; White *et al.*, 2002). Additionally, annexins have emerged as a key player in abiotic stresses, and are likely to play a role in Pb exposure. The present study detected up-regulation of *AnnAt1* in seedlings exposed to 100 μM $Pb(NO_3)_2$, by 2.12-fold. Pb-induced oxidative stress may be a component of *AnnAt1* gene expression. It is likely that at a certain threshold of Pb concentration or ROS level, *AnnAt1* expression is activated to participate in defence against Pb-mediated stress.

The link between *AnnAt1* gene expression, Pb levels, Ca^{2+}- and ROS-mediated signalling pathway appears to be a more complex subject than originally envisaged. The up-regulation of *AnnAt1*-mediated protection may not be fully elucidated through quantitative real-time PCR alone, as the relative fold differences were minimal. Nevertheless, it cannot be dismissed that annexins might be involved in Pb tolerance. *AnnAt1* is multi-

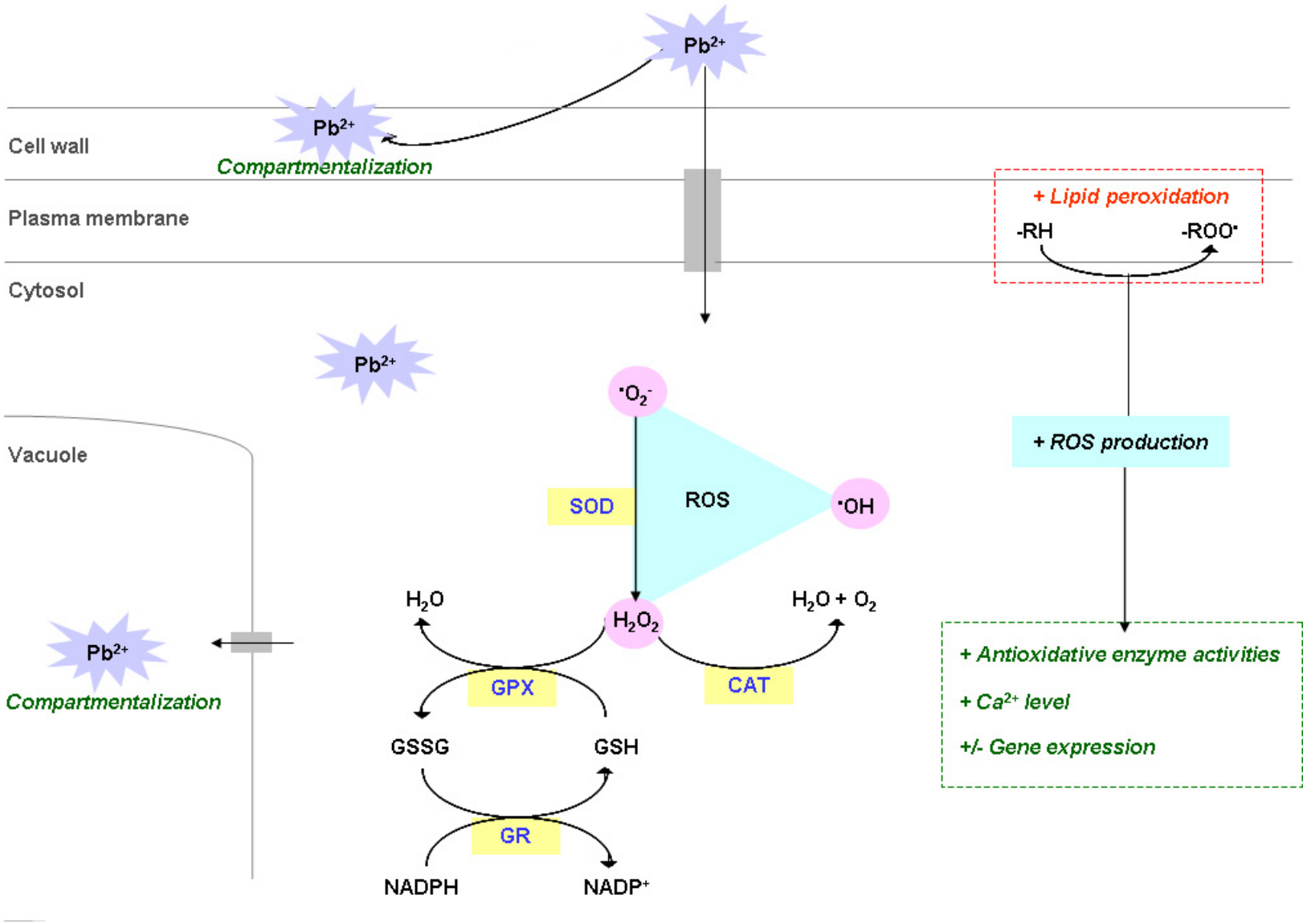

Figure 8.1: Mechanisms of Pb uptake and detoxification in 7-d-old *A. thaliana* seedlings. +: increase, -: decrease, pink circle: ROS, yellow box: antioxidative enzyme, grey box: transporter protein.

functional, and may act as a ROS signal, Ca^{2+} channel, membrane protector and Pb transport (Figure 8.2). There are eight annexin genes in *A. thaliana*, which have been shown to be regulated differentially to different stress treatments (Clark *et al.*, 2001). The responses of these annexin genes to Pb may vary in different tissues. Therefore, the roles of each annexin gene to Pb stress in different tissues at different developmental stages need to be examined in future studies.

8.4 How would nitric oxide protect *A. thaliana* seedlings from Pb toxicity?

NO-generating systems are inducible by environmental stress. Many studies have shown a role for exogenous NO in alleviating heavy metal toxicity in plants. To the best of my knowledge, the protective effect of exogenous NO in Pb-induced oxidative stress was only demonstrated in *Lupinus luteus* (Kopyra & Gwozdz, 2003). Clearly, more studies are needed to further address the functions of nitric oxide in Pb stress. The action of exogenous NO may vary in different plant species. Exogenous NO was found to reduce the negative impact of Pb stress on seedling growth. Consistent with previous studies, data from the present experiments suggest that exogenous NO conferred protection to *A. thaliana* seedlings primarily by acting as an antioxidant to scavenge the excessive ROS level. In contrast to Kopyra & Gwozdz (2003), the antioxidative enzyme activities in *A. thaliana* seedlings were reduced. It is likely that exogenous NO resulted in efficient reduction of H_2O_2 level and attenuated Pb-induced lipid hydroperoxide chain reaction. Subsequently, less antioxidative enzyme activities were activated.

It is interesting that exogenous NO did not significantly alter Pb uptake and accumulation. Unlike Al (Wang & Yang, 2005) and La (Qiang *et al.*, 2007), reduction of the deleterious effect of Pb stress in 7-d-old *A. thaliana* seedlings seemed to be mainly through tolerance mechanisms. Probably due to the confounding effects of mixed, pooled populations of seeds from a commercial source and storage of seeds, the precise reason for the inability to detect the previously observed relative fold differences in *AnnAt1* gene expression is not clear. The imbalances of ROS and NO levels may also interfere with the transcript level of *AnnAt1*. Nevertheless, this experiment is intriguing, leading to further

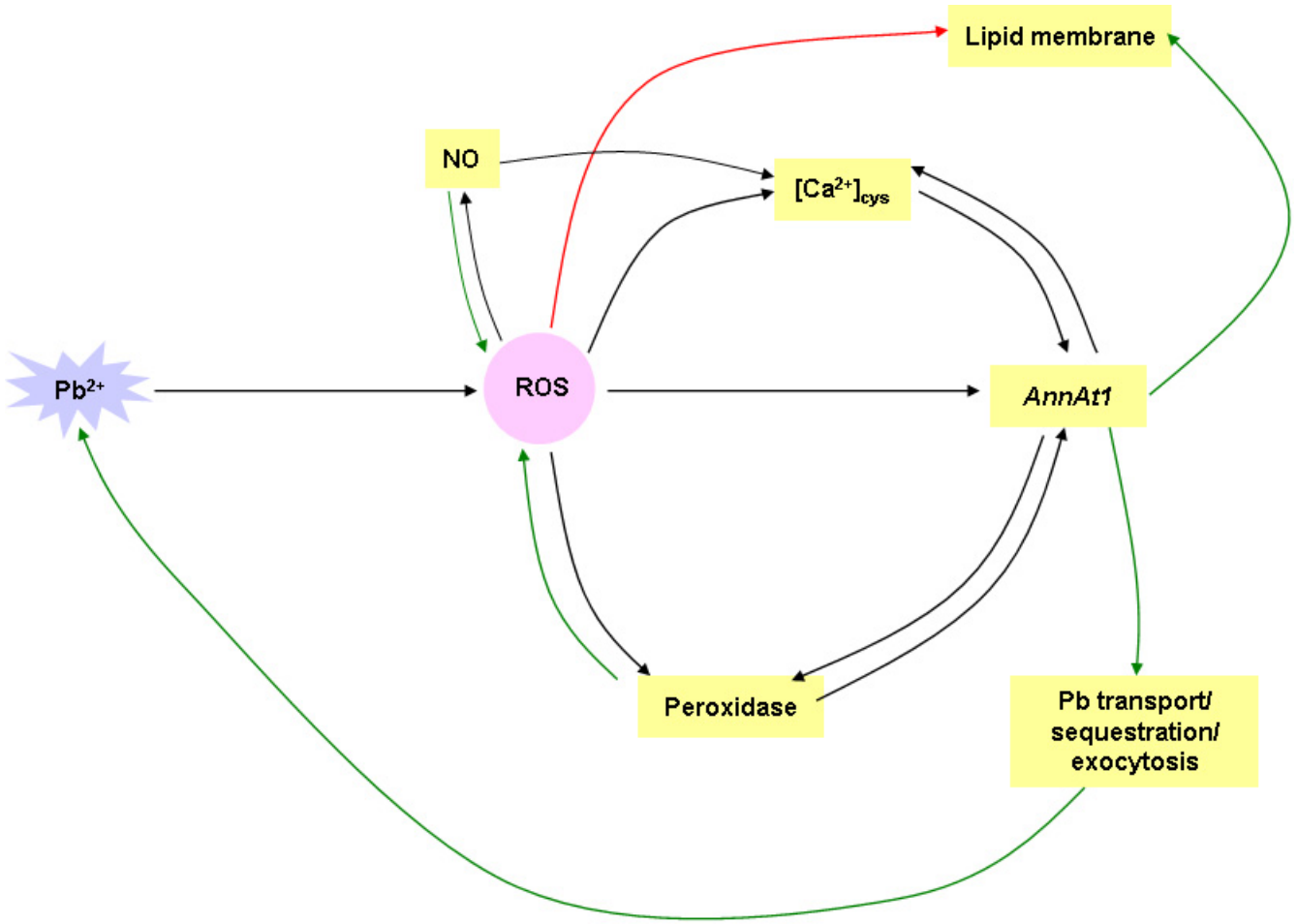

Figure 8.2: Possible mechanisms of *AnnAt1* in response to Pb. Black line: triggering the response, green line: protective effect, red line: damaging effect.

questions to be addressed and considered in association with Ca^{2+} signaling and *AnnAt1* regulation.

8.5 Screening of a putative Pb tolerant mutant

As described earlier, there are a few reports of genes that specifically confer Pb tolerance and accumulation. Only two studies of genetic screens have been performed to identify new mutant variants with enhanced tolerance to Pb (Chen *et al.*, 1997; Schulman *et al.*, 1999). Hence, the present research sought to isolate Pb tolerant mutants from EMS-mutagenized M_2 population of *A. thaliana*. A post-germination screen involving prolonged Pb exposure was developed for this purpose. A minority of the survivors appeared to go into a resting stage. The TEM analysis suggests Pb uptake into the plants was prevented. One putative Pb mutant was recovered to set seeds. The 7-d-old putative Pb mutants of M_4 generation showed greater root and shoot development in the presence of 150 μM $Pb(NO_3)_2$, in comparison to wild-type and EMS-mutagenized M_2 seedlings. In M_4 seedlings, gene expression of *AnnAt1* subjected to Pb treatment was twice that of the non-Pb-treated control. During the re-screening process, the relatively high mortality rate after 2 months of Pb treatment casts doubts about the efficacy of this mutant isolation technique. Limited resources have restricted further phenotypic measurements, and thus whether the putative Pb tolerant mutant is a true mutant was not determined further. However, the present investigation was valuable. It serves as a pilot experiment to guide further development of Pb mutant screening methods.

8.6 Limitations of the study

The present study was designed to probe Pb accumulation and tolerance mechanisms of *A. thaliana* seedlings under laboratory conditions. The objectives of the thesis were highlighted in Section 1.12. However, certain basic limitations of the study should be noted.

1. *Application in the field*: All of the experiments were conducted in a controlled environment. Hence it was not designed to evaluate the utility of phytoremedia-

tion in the field. The sample size may not be large enough to definitely assess Pb phytoremediation in a field application. Furthermore, because of its small size, *A. thaliana* is not a plant of choice for implementation as a phytotechnology system at contaminated sites.

2. *Nutrient medium*: Although modified Huang & Cunningham (1996) nutrient solution has been formulated specifically for use in Pb accumulation experiments, it may not reflect the actual nutrient contents at the contaminated sites. The minimal medium was mainly designed to allow plant growth, to reduce the nutrient contents that can form complexes with Pb, and to minimize Pb-nutrient uptake competition.

3. *Pb concentrations*: Several $Pb(NO_3)_2$ treatments were carried out to stimultaneously test the phytoremediation ability of *A. thaliana* seedlings in modified HC nutrient solution. Based on the morphological observation and tolerance index, 100 µM $Pb(NO_3)_2$ was chosen for comparing antioxidative defence system and gene expression between Pb stressed and non-stressed seedlings. This concentration may not be the lethal level in 7-d-old seedlings because otherwise, the antioxidative enzymes and gene expression level may have been completely inhibited. This could complicate the interpretation of experimental data. The Pb concentration chosen in the present study may not resemble the bioavailability of Pb in contaminated fields.

4. *Pb exposure*: Cold-stratified seeds were plated on modified HC medium (with or without Pb), and seedlings were harvested for analysis after a week. This is not the time limit of phytoremediation, but using 7-d-old seedlings is more realistic for this thesis research. While seedlings were used here, it may not refect the physiological, biochemical and molecular mechanisms in older plants.

5. *SNP pre-treatment*: Based on the procedure reported in Hu *et al.* (2007), seeds were pre-treated with SNP for 3 h before initiation of stress treatment, and the amount of cPTIO to scavenge exogenously supplied NO was twice the concentration of SNP. From a preliminary experiment, 0.5 mM SNP was chosen to pre-treat *A. thaliana* seeds because it had the greatest effect on Pb-inhibition of root elongation (see Section 6.3.2), while 1 mM cPTIO was used as a NO scavenger (see Section 6.3.3). However, the quantity of NO released by SNP, the amount of NO produced naturally

in the seeds/plants, and the portion of exogenous/internal NO scavenged by cPTIO were not measured in this study.

6. *Genotype and storage of seeds*: Individual genotypes of a similar population may vary from one another. This natural genetic variability allows a population to adapt to environmental changes. This phenomenon was particularly evident in the gene expression data in Chapter 5 and 6 (as described in the last paragraph of Section 6.4.6). Since *A. thaliana* seeds were commercially purchased, the grouping of seeds was beyond this researcher's control. The length of storage of seeds may also affect the quality and response of *A. thaliana* (Hay *et al.*, 2003; Clerkx *et al.*, 2004; Niedzielski *et al.*, 2009).

7. *Plant materials for analysis*: Biochemical and gene expression analysis were investigated in whole seedlings. Since roots and shoots play distinctly different roles in plant biology and are exposed to very different environments, the data may not be specific to certain type of cells.

8.7 Future directions

Although phytoremediation is a promising technology to remediate heavy metal contaminants, fundamental studies are needed to improve its effectiveness. The potential research areas include basic science, design, implementation and economics, assessments of ecological and health risks, regulatory acceptance, and biodiversity considerations (McIntyre, 2003). Multiple challenges and opportunities are awaiting to be explored in order to fully establish phytoremediation as a viable phytotechnology. This study has only begun to elucidate our current understanding of plant responses to Pb contaminants. It has: 1) identified the physiological and biochemical responses to Pb of 7-d-old *A. thaliana* seedlings, 2) examined the gene expression level of *AnnAt1* to Pb, 3) assessed the protective effect of NO in Pb-induced oxidative damage, and 4) tried to isolate putative Pb tolerant mutants. Since a knowledge of the basic science crucially underpins the success of phytoremediation applications, the present study can be considered as a positive step in advancing Pb tolerance research. However, the outcomes of the current work also leave

many questions to be investigated. Future research and techniques that can be considered are outlined in the following sections.

8.7.1 Plant physiology and basic mechanisms of Pb phytoremediation

It is believed that older plants are more resistant to heavy metal stress and have greater adaptation ability than seedlings or young plants (Mleczek *et al.*, 2009). These authors have shown that 2- and 3-year-old *Salix viminalis* are more capable of acclimating to heavy metal-contaminated environments and are able to accumulate a higher metal content in the roots, in comparison to the 1-year-old. It would be interesting to study the mechanisms of Pb uptake, tolerance and detoxification of plants at different ages. Older plants may develop better root systems to absorb, or exclude metals from entering the cells. This also raises a remarkable question for phytoremediators: Would older plants later introduced to a polluted area have better adaptability to heavy metal pollutions than younger plants grown on a metal contaminated site (Macnair, 2002; Lefebvre *et al.*, 2009)? The cellular structure of plants may be affected by natural variation of heavy metal concentrations in soil and this requires further investigation. Hence, there is a need to have a better understanding of evolution and adaptation of plants to unfavorable environments.

It has been shown that the accumulation of Pb in shoots increased as the duration of Pb exposure increased (Huang & Cunningham, 1996). However, in Chapter 7, longer duration of Pb exposure seemed to cause *A. thaliana* plants to go into a resting stage and Pb deposits were absent from the leaves (see Section 7.3.4). It would also be interesting to test if a different period of treatment can affect the translocation of Pb in wild-type *A. thaliana* shoots, or if a mutation exists in the mutagenized population. Lower concentrations of Pb that are less inhibitory to plant growth for a long term study may need to be applied.

Historically, transmission electron microscopy is the most widely used technique to determine the cellular distribution of Pb within plant cells. Electron-dense Pb particles which are absent from the non Pb-treated control are assumed to be Pb. As described in Section 1.10.2, TEM has been applied to study ultrastructural localization of Pb in many

plant species. Recently, TEM with energy dispersive X-ray spectrometer (EDX), also known as X-ray microanalysis, was employed to distinguish Pb particles from artifacts or other electron-dense materials that may be present in the samples (Sahi *et al.*, 2002; Fritz, 2007). This technique allows direct confirmation of electron-dense deposits as Pb.

Pb movements in plants are normally restricted to cell walls that contain high cation exchange capacity, CEC (Raskin *et al.*, 1997). It would be useful to find out the major form of Pb immobilization in *A. thaliana* seedlings. From the peaks of X-ray spectra in TEM-EDX, Sahi *et al.* (2002) revealed that Pb was mainly sequestered as Pb phosphate in the cell wall, plasma membrane and vacuole of *Sesbania drummondii*. Using a similar technique, Fritz (2007) characterized CEC in *Picea abies* and found that CEC values were different in different tissue types. High CEC in cortical cells subsequently reduced metal transport into the xylem. On the other hand, X-ray absorption spectroscopic analysis (XANES and EXAFS) suggests the importance of carboxyl ligands in binding of Pb^{2+} in *Medicago sativa* (Tiemann *et al.*, 2002). The binding of Pb^{2+} did not change the oxidation state of alfalfa biomass, but was through coordination with oxygen atoms via carboxyl groups. These studies suggest that revealing the complexation of Pb with different functional groups of transport proteins, organic acid chelators, and cell walls, as well as its oxidation state may provide further clues on Pb transport pathway and retention in the roots.

A very recent paper challenged the binding of Pb to pectin compounds in cell wall as an initial tolerance reaction in plants (Krzeslowska *et al.*, 2010). The research group from Poland demonstrated the remobilization of cell wall-bound Pb, which later entered plant cell protoplast by endocytosis. Vesicle trafficking was involved in transportation of Pb into and within protoplast via the endocytotic/secretion pathway. Compartmentalization of Pb to cell wall was demonstrated as a final Pb sequestration strategy. In the present investigation, Pb particles were seen in vesicles. Vesicles were thought to be involved in cytosolic Pb transport to specific vacuoles or membranous compartments, after Pb was taken up by metal transporters into the cells. It is unclear if internalization by endocytosis occured in Pb uptake or long distance transport. Further clarification is eagerly awaited.

In order to speed up the development of phytotechnologies, analyis of heavy metal uptake should be non-destructive, fast, cheap, applicable to a large number of samples,

accurate, and reproducible (Necemer *et al.*, 2008). Three multi-elemental analytical techniques that require only one simple sample preparation are recommended by the authors: 1) energy dispersive X-ray fluorescence spectrometry (EDXRF), 2) total reflection X-ray fluorescence spectrometry (TXRF), and 3) micro-proton induced X-ray emission (micro-PIXE). These X-ray fluorescence-based techniques are also capable of detecting non-metal elements, such as phosphate, sulfur, clorine and bromine. Thus, the biological processes of plant-Pb interaction, uptake of macro- and micronutrients in *A. thaliana*, and its distribution in different plant tissues are appealing areas for further investigation.

Other newly developed techniques that have been used to map Pb accumulation, transport and disposal strategy in plants are, grazing exit micro X-ray fluorescence analysis (GE-μ-XRF) (Awane *et al.*, 2009), laser ablation inductively coupled plasma mass spectrometry (LA-ICP-MS) (Hanc *et al.*, 2009), synchrotron X-ray fluorescence spectroscopy (SRXRF) (Lei *et al.*, 2008), and synchrotron-radiation micro X-ray fluorescence analysis (SR-μ-XRF) (Kodera *et al.*, 2008). In the selection for an appropriate modern approach, issues such as the type of tissues, site of Pb of interest (e.g. on surface of a plant) and cost need to be taken into account.

8.7.2 Studies on annexins of *A. thaliana*

By looking at the low up-regulation of *AnnAt1* gene expression level, one may argue that this gene does not have a possible role in Pb tolerance. Therefore, the incomplete experiment involving AnnAt1 protein analysis should be prioritized (see Section 5.4.5). This is because under Pb stress, AnnAt1 protein may change post-translationally to function at the physiological level. Proteomics could be a potential platform to gain more insight into Pb stress response in plants (Ahsan *et al.*, 2009). It would also be particularly interesting to study the mode of action of annexin 1 through gene knockouts, its over-expression in transgenic plants and complementation tests.

Annexins are thought to be involved in ion channel activity, exocytosis, cell wall synthesis, and binding to membrane, actin and GTP (Clark *et al.*, 2001, 2005). The authors demonstrated that AnnAt1 is mainly located in secretory cell types with *in situ* RNA localization and protein localization. In addition, it has been found that salt treatment caused AnnAt1 protein lost from cytoplasmic fraction and redistributed to membrane fraction

(Lee *et al.*, 2004). Under Pb treatment, it is also likely for AnnAt1 to redistribute and translocate in the cells as a defence, or repair mechanism. Since AnnAt1 is a Ca^{2+}-binding protein, a Ca^{2+} chelator such as EGTA could be used as a verification tool. Determination of the tissue and cellular localization of the AnnAt1 gene and protein may help to elucidate its functions as a defence system to cope with toxic Pb.

To date, it is still unclear how ROS or elevated cytosolic Ca^{2+} might trigger *AnnAt1* responses. Any change of the peroxidase activity of *AnnAt1* to Pb treatment remains to be further experimentally demonstrated. Using a confocal laser scanning microscopy, Rodriguez-Serrano *et al.* (2009) has proposed a model consisting of cross-talk among Ca^{2+}, ROS and NO of *Pisum sativum* in response to Cd. These molecules work together, acting as a cell signalling and regulation network in plant response to Cd toxicity. The development of fluorescence probes enables researchers to visualize and quantify many dynamic events in the living plants, using a confocal laser scanning microscope (Fricker & Meyer, 2001; Sandalio *et al.*, 2008). A similar *in vivo*, non-destructive technique would be a useful tool to better understand the role of *AnnAt1*, Ca^{2+}, ROS and NO play in plant cells under Pb treatment. Subsequently, plant cross tolerance to abiotic stresses can be better understood.

AnnAt1 has multiple functions to protect plants against abiotic stresses. It is important to note that there are eight *Arabidopsis* annexin genes (Clark *et al.*, 2001), and the response of individual annexin to Pb stress may vary. Research is needed to test the cellular localization pattern and expression level of each individual annexin in different tissues and cell types. This could provide more information about Pb tolerance mechanisms not outlined in this thesis.

8.7.3 Mutagenesis studies

The experimental design for isolation of a Pb mutant may need to be reconsidered. In a study by Chen (2005), a germination screen was unsuccessful to isolate Cd tolerant mutants. After modification to a post-germination screen that involved germinating seeds on Cd-free media plates for 4 days before transferring to Cd-containing plates, 19 putative mutants (seedlings that were able to maintain green cotyledons) were isolated from 8,400 EMS-mutagenized seeds. It is likely that this screening method could also be used for Pb

tolerant mutant isolation. A fine nylon mesh, which contains pores to separate the seeds from the agar, can be used to transfer a large number of seedlings between the plates. Due to the limited time frame of this project, the procedure according to Chen (2005) has not been used.

Additionally, a non-destructive and highly sensitive screening technique has been developed by Schulman *et al.* (1999) to isolate Cd and Pb hyperaccumulators in *B. juncea*. Seedlings were submerged in a solution incorporated with radioactive isotopes of the metals of interest. Then, metal accumulation in these seedlings was visualized with a phosphorimager. An alternative technique known as X-ray fluorescence spectrometry has been developed by Delhaize *et al.* (1993). The authors have successfully isolated Al-, P- and Mn-mutants in *A. thaliana*. In the future, these techniques can be applied in screening EMS-mutagenized M_2 population, allowing rapid isolation of Pb mutant plants. Besides screening EMS-mutagenized M_2 population, discovery of new genes can be performed by identifying mutants in the collections of T-DNA lines of *A. thaliana*.

It would also be interesting to isolate Pb-hypersensitive mutants in EMS-mutagenized *A. thaliana* lines to assist studies on Pb response in plants. A comparative analysis of the responses of Pb-tolerant and -sensitive mutants allows a researcher to identify new genes that play a role in phytoremediation. Cd-, Cu- and Al-sensitive *A. thaliana* mutants have been successfully isolated. In designing an experiment, however, it is important to detect a sensitive phenotype after a short period of exposure to a toxic metal (Howden & Cobbett, 1992).

8.7.4 Searching for Pb tolerance genes or proteins

One of the rapid ways to identify genes associated with regulated response to Pb exposure is microarray analysis. This method enables the expression levels of thousands of genes to be studied at the same time. After that, quantitative real-time PCR can be used to validate the results from microarray analysis. For example, Liu *et al.* (2009b) screened 6,210 *A. thaliana* genes using microarray analysis, and detected changes in the expression profile of 1,310 genes. The similarity of 18 randomly selected gene expression data between microarrays and quantitative real-time RT-PCR was 86.1%, verifying the reliability of the data. Under Pb stress, the up-regulated genes were those that are commonly

involved in stress, anti-oxidation systems, and biosynthetic pathway (e.g. sulfur assimilation, auxin and jasmonic acid biosynthesis, signalling and transcription factor families) (Liu *et al.*, 2009b). Characterization of these abundantly expressed genes will complement the molecular basis of Pb detoxification.

It is vital to investigate protein complexes from the membranes of chloroplasts, mitochondria, and plasma membranes (Ahsan *et al.*, 2009). Chloroplasts and mitochondria are targets for ROS because these organelles play a role in photosynthesis and photorespiration. Plasma membranes perceive stress, and contain proteins that are involved in transportation, trafficking and signal transduction (Ahsan *et al.*, 2009).

8.7.5 Genetic modification of promising plant species

Environment Canada has compiled a database of terrestrial and aquatic plants that have the potential to decontaminate metal-polluted sites (McIntyre, 2003). Plants capable of hyperaccumulating Pb are: *Eichhornia crassipes*, *Hydrilla verticillata*, *Lemna minor*, *Salvinia olesta*, *Spirodela polyrrhiza*, *Vallisneria americana*, *Brassica juncea*, *Helianthus annuus*, *Thlaspi caerulescens*, and *Anthyrium yokoscense*. However, not all of these plants poss the ideal traits as a metal phytoremediator (see Section 1.4.1). Further evaluation and identification of the most effective Pb tolerance mechanism(s) from these species are eagerly awaited. Isolation of the hyperaccumulating genes may serve as a template for genetic engineering of plants with improved tolerance to Pb. In an experiment, it is important to treat a plant with a metal concentration at which hyperaccumulation genes will be expressed without clouding the data with global, general, or unspecific stress responses.

Bibliography

Aarts, M.G.M. & Fiers, M.W.E.J. (2003). What drives plant stress genes? *Trends in Plant Science*, **8**, 99–102.

Agency For Toxic Substances & Disease Registry, A.T.S.D.R. (2007a). Priority list of hazardous substances. [Online] http://www.atsdr.cdc.gov/.

Agency For Toxic Substances & Disease Registry, A.T.S.D.R. (2007b). Toxicological profile for lead. [Online] http://www.atsdr.cdc.gov/tfacts13.html.

Ahmad, S. (1995). Antioxidant mechanisms of enzymes and proteins. In S. Ahmad, ed., *Oxidative stress and antioxidant defenses in biology*, 238–272, Chapman & Hall, New York.

Ahsan, N., Renaut, J. & Komatsu, S. (2009). Recent developments in the application of proteomics to the analysis of plant responses to heavy metals. *Proteomics*, **9**, 2602–2621.

Alloway, B.J. (1995). The origin of heavy metals in soils. In B.J. Alloway, ed., *Heavy metals in soils*, chap. 3, 38–57, Blackie Academic and Professional, Glosgow, UK.

American Elements, A.E. (2009). Pb. [Online] http://www.americanelements.com/pb.html.

Andersen, C.L., Jensen, J.L. & Orntoft, T.F. (2004). Normalization of real-time quantitative reverse transcription-PCR data: a model-based variance estimation approach to identify genes suited for normalization, applied to bladder and colon cancer data sets. *Cancer Research*, **64**, 5245–5250.

Antosiewicz, D. & Wierzbicka, M. (1999). Localization of lead in *Allium cepa* L. cells by electron microscopy. *Journal of Microscopy*, **195**, 139–146.

Antosiewicz, D.M. (2005). Study of calcium-dependent lead-tolerance on plants differing in their level of ca-deficiency tolerance. *Environmental Pollution*, **134**, 23–34.

Apel, K. & Hirt, H. (2004). Reactive oxygen species: metabolism, oxidative stress, and signal transduction. *Annual Review of Plant Biology*, **55**, 373–399.

Arasimowicz, M. & Floryszak-Wieczorek, J. (2007). Nitric oxide as a bioactive signalling molecule in plant stress responses. *Plant Science*, **172**, 876–887.

Arthur, E.L., Rice, P.J., Rice, P.J., Anderson, T.A., Baladi, S.M., Henderson, K.L.D. & Coats, J.R. (2005). Phytoremediation - an overview. *Critical Reviews in Plant Sciences*, **24**, 109–122.

Atici, O., Agar, G. & Battal, P. (2005). Changes in phytohormone contents in chickpea seeds germinating under lead or zinc stress. *Biologia Plantarum*, **49**, 215–222.

Awane, T., Fukuoka, S., Nakamachi, K. & Tsuji, K. (2009). Grazing exit micro X-ray fluorescence analysis of a hazardous metal attached to a plant leaf surface using an X-ray absorber method. *Analytical Chemistry*, **81**, 3356–3364, doi: 10.1021/ac802599x.

Baker, A.J.M. (1981). Accumulators and excluders -strategies in the response of plants to heavy metals. *Journal of Plant Nutrition*, **3**, 643–654.

Baker, A.J.M. & Walker, P.L. (1990). Ecophysiology of metal uptake by tolerance plants. In A.J. Shaw, ed., *Heavy metal tolerance in plants: evolutionary aspects*, 155–177, CRC Press, Boca Raton.

Baker, A.J.M., McGrath, S.P., Reeves, R.D. & Smith, J.A.C. (2000). Metal hyperaccumulator plants: a review of the ecology and physiology of a biological resource for phytoremediation of metal-polluted soils. In N. Terry & G.S. Banuelos, eds., *Phytoremediation of contaminated soil and water*, 85–108, Lewis Publishers, Boca Raton, FL.

Banowetz, G.M., Dierksen, K.P., Azevedo, M.D. & Stout, R. (2004). Microplate quantification of plant leaf superoxide dismutases. *Analytical Biochemistry*, **332**, 314–320.

Beligni, M.V. & Lamattina, L. (1999a). Is nitric oxide toxic or protective? *Trends in Plant Science*, **4**, 299–300.

Beligni, M.V. & Lamattina, L. (1999b). Nitric oxide counteracts cytotoxic processes mediated by reactive oxygen species in plant tissues. *Planta*, **208**, 337–344.

Beligni, M.V. & Lamattina, L. (2000). Nitric oxide stimulates seed germination and deetiolation, and inhibits hypocotyl elongation, three light-inducible responses in plants. *Planta*, **210**, 215–221.

Beligni, M.V. & Lamattina, L. (2001). Nitric oxide in plants: the history is just beginning. *Plant, Cell & Environment*, **24**, 267–278.

Beligni, M.V., Fath, A., Bethke, P.C., Lamattina, L. & Jones, R.L. (2002). Nitric oxide acts as an antioxidant and delays programmed cell death in barley *Aleurone layers*. *Plant Physiology*, **129**, 1642–1650.

Bert, V., Macnair, M.R., Laguerie, P.d., Saumitou-Laprade, P. & Petit, D. (2000). Zinc tolerance and accumulation in metallicolous and nonmetallicolous populations of *Arabidopsis halleri* (Brassicaceae). *New Phytologist*, **146**, 225–233.

Besson-Bard, A., Gravot, A., Richaud, P., Auroy, P., Duc, C., Gaymard, F., Taconnat, L., Renou, J., Pugin, A. & Wendehenne, D. (2009). Nitric oxide contributes to cadmium toxicity in *Arabidopsis* by promoting cadmium accumulation in roots and by up-regulating genes related to iron uptake. *Plant Physiology*, **149**, 1302–1315.

Blaylock, M.J., Salt, D.E., Dushenkov, S., Zakharova, O., Gussman, C., Kapulnik, Y., Ensley, B.D. & Raskin, I. (1997). Enhanced accumulation of pb in indian mustard by soil-applied chelating agents. *Environmental Science & Technology*, **31**, 860–865.

Blokhina, O., Virolainen, E. & Fagerstedt, K.V. (2003). Antioxidants, oxidative damage and oxygen deprivation stress: a review. *Annals of Botany*, **91**, 179–194.

Bolwell, G.P. & Wojtaszek, P. (1997). Mechanisms for the generation of reactive oxygen species in plant defence - a broad perspective. *Physiological and Molecular Plant Pathology*, **51**, 347–366.

Boopathy, R. (2000). Factors limiting bioremediation technologies. *Bioresource Technology*, **74**, 63–67.

Boustead, C.M., Smallwood, M., Small, H., Bowles, D.J. & Walker, J.H. (1989). Identification of calcium-dependent phospholipid-binding proteins in higher plant cells. *FEBS Letters*, **244**, 456–460.

Bradford, M.M. (1976). A rapid and sensitive method for the quantitation of microgram quantities of protein utilizing the principle of protein-dye binding. *Analytical Biochemistry*, **72**, 248–254.

Brunner, A., Yakovlev, I. & Strauss, S. (2004). Validating internal controls for quantitative plant gene expression studies. *BMC Plant Biology*, **4**, 1–7.

Bustin, S.A. (2000). Absolute quantification of mRNA using real-time reverse transcription polymerase chain reaction assays. *Journal of Molecular Endocrinology*, **25**, 169 – 93.

Bustin, S.A. (2002). Quantification of mrna using real-time reverse transcription PCR (RT-PCR): trends and problems. *Journal of Molecular Endocrinology*, **29**, 23 – 39.

Bustin, S.A., Benes, V., Nolan, T. & Pfaffl, M.W. (2005). Quantitative real-time RT-PCR - a perspective. *Journal of Molecular Endocrinology*, **34**, 597–601.

Cantero, A., Barthakur, S., Bushart, T.J., Chou, S., Morgan, R.O., Fernandez, M.P., Clark, G.B. & Roux, S.J. (2006). Expression profiling of *Arabidopsis* annexin gene family during germination, de-etiolation and abiotic stress. *Plant Physiology and Biochemistry*, **44**, 13–24.

Chandran, D., Sharopova, N., Ivashuta, S., Gantt, J., VandenBosch, K. & Samac, D. (2008). Transcriptome profiling identified novel genes associated with aluminum toxicity, resistance and tolerance in *Medicago truncatula*. *Planta*, **228**, 151–166.

Cheeseman, J.M. (2006). Hydrogen peroxide concentrations in leaves under natural conditions. *Journal of Experimental Botany*, **57**, 2435–2444.

Chen, A. (2005). *Long distance transport of phytochelatins in Arabidopsis and the isolation and characterization of cadmium tolerant mutants in Arabidopsis*. Ph.D. thesis, University of California, San Diego.

Chen, J., Huang, J., Caspar, T. & Cunningham, S.D. (1997). *Arabidopsis thaliana* as a model system for studying lead accumulation and tolerance in plants. In E.L. Kruger, T.A. Anderson & J.R. Coats, eds., *Phytoremediation of Soil and Water Contaminants*, 264–273, American Chemical Society, Washington, D.C.

Chin, L. (2007). *Investigations into lead (Pb) accumulation in Symphytum officinale L. : a phytoremediation study*. Ph.D. thesis, School of Biological Sciences, University of Canterbury, Christchurch, New Zealand.

Cho, M., Chardonnens, A.N. & Dietz, K.J. (2003). Differential heavy metal tolerance of *Arabidopsis halleri* and *Arabidopsis thaliana*: a leaf slice test. *New Phytologist*, **158**, 287–293.

Cho, U.H. & Seo, N.H. (2005). Oxidative stress in *Arabidopsis thaliana* exposed to cadmium is due to hydrogen peroxide accumulation. *Plant Science*, **168**, 113–120.

Choudhury, S. & Panda, S. (2005). Toxic effects, oxidative stress and ultrastructural changes in moss *Taxithelium nepalense* (Schwaegr.) broth. under chromium and lead phytotoxicity. *Water, Air, & Soil Pollution*, **167**, 73–90.

Clark, G.B. & Roux, S.J. (1995). Annexins of plant cells. *Plant Physiology*, **109**, 1133–1139.

Clark, G.B., Sessions, A., Eastburn, D.J. & Roux, S.J. (2001). Differential expression of members of the annexin multigene family in *Arabidopsis*. *Plant Physiology*, **126**, 1072–1084.

Clark, G.B., Lee, D., Dauwalder, M. & Roux, S.J. (2005). Immunolocalization and histochemical evidence for the association of two different *Arabidopsis* annexins with secretion during early seedling growth and development. *Planta*, **220**, 621–631.

Clemens, S. (2001). Molecular mechanisms of plant metal tolerance and homeostasis. *Planta*, **212**, 475–486.

Clemens, S., Palmgren, M.G. & Kramer, U. (2002). A long way ahead: understanding and engineering plant metal accumulation. *Trends in Plant Science*, **7**, 309–315.

Clerkx, E.J.M., El-Lithy, M.E., Vierling, E., Ruys, G.J., Vries, H.B.D., Groot, S.P.C., Vreugdenhil, D. & Koornneef, M. (2004). Analysis of natural allelic variation of *Arabidopsis* seed germination and seed longevity traits between the accessions Landsberg *erecta* and Shakdara, using a new recombinant inbred line population. *Plant Physiology*, **135**, 432–443.

Cobbett, C.S. (2003). Heavy metals and plants: model systems and hyperaccumulators. *New Phytologist*, **159**, 289–293.

Conlon, H.E. & Salter, M.G. (2007). Plant protein extraction. In E. Rosato, ed., *Circadian rhythms: methods and protocols*, vol. 362 of *Methods in molecular biology*, 379–383, Humana Press Inc., Totowa, NJ.

Correa-Aragunde, N., Graziano, M. & Lamattina, L. (2004). Nitric oxide plays a central role in determining lateral root development in tomato. *Planta*, **218**, 900–905.

Cribb, A.E., Leeder, J.S. & Spielberg, S.P. (1989). Use of a microplate reader in an assay of glutathione reductase using 5,5'-dithiobis(2-nitrobenzoic acid). *Analytical Biochemistry*, **183**, 195–196.

Csuros, M. & Csuros, C. (2002). Graphite furnace atomic absorption spectrometry. In M. Csuros & C. Csuros, eds., *Environmental sampling and analysis for metals*, 129–142, Lewis Publishers, Boca Raton.

Cunningham, S.D. & Ow, D.W. (1996). Promises and prospects of phytoremediation. *Plant Physiology*, **110**, 715–719.

Cunningham, S.D., Berti, W.R. & Huang, J.W. (1995). Phytoremediation of contaminated soils. *Trends in Biotechnology*, **13**, 393–397.

Cunningham, S.D., Shann, J.R., Crowley, D.E. & Anderson, T.A. (1997). Phytoremediation of contaminated water and soil. In E.L. Kruger, T.A. Anderson & J.R. Coats, eds., *Phytoremediation of soil and water contaminants*, vol. 664 of *ACS symposium series*, 2–19, American Chemical Society, Washington, DC.

Czechowski, T., Stitt, M., Altmann, T., Udvardi, M.K. & Scheible, W.R. (2005). Genome-wide identification and testing of superior reference genes for transcript normalization in *Arabidopsis*. *Plant Physiology*, **139**, 5–17.

Dalton, D.A. (1995). Antioxidant defenses of plants and fungi. In A. Sami, ed., *Oxidative stress and antioxidant defenses in biology*, 298–354, Chapman & Hall, New York.

Davies, B.E. (1995). Lead. In B.J. Alloway, ed., *Heavy metals in soils*, Blackie Academic and Professional, Glosgow, UK.

Davison, J. (2005). Risk mitigation of genetically modified bacteria and plants designed for bioremediation. *Journal of Industrial Microbiology and Biotechnology*, **32**, 639–650.

Delhaize, E. (1996). A metal-accumulator mutant of *Arabidopsis thaliana*. *Plant Physiology*, **111**, 849–855.

Delhaize, E., Craig, S., Beaton, C.D., Bennet, R.J., Jagadish, V.C. & Randall, P.J. (1993). Aluminum tolerance in wheat (*Triticum aestivum* L.) (i. uptake and distribution of aluminum in root apices). *Plant Physiology*, **103**, 685–693.

Delledonne, M., Yiji, X., Richard, A.D. & Chris, L. (1998). Nitric oxide functions as a signal in plant disease resistance. *Nature*, **394**, 585–588.

Delledonne, M., Murgia, I., Ederle, D., Sbicego, P.F., Biondani, A., Polverari, A. & Lamb, C. (2002). Reactive oxygen intermediates modulate nitric oxide signaling in the plant hypersensitive disease-resistance response. *Plant Physiology and Biochemistry*, **40**, 605–610.

Delmer, D.P. & Potikha, T.S. (1997). Structures and functions of annexins in plants. *Cellular and Molecular Life Sciences*, **53**, 546–553.

Devi, S.R. & Prasad, M.N.V. (1999). Membrane lipid alterations in heavy metal exposed plants. In M.N.V. Prasad & J. Hagemeyer, eds., *Heavy metal stress in plants : from molecules to ecosystems*, 99–116, Springer-Verlag, Berlin, Germany.

di Toppi, S.L. & Gabbrielli, R. (1999). Response to cadmium in higher plants. *Environmental and Experimental Botany*, **41**, 105–130.

Dietz, K., Baier, M. & Kramer, U. (1999). Free radicals and reactive oxygen species as mediator of heavy metal toxicity in plants. In M. Prasad & J. Hagemeyer, eds., *Heavy metal stress in plants : from molecules to ecosystems*, 73–97, Springer-Verlag, Berlin Heidelberg New York.

Drazkiewicz, M., Skorzynska-Polit, E. & Krupa, Z. (2004). Copper-induced oxidative stress and antioxidant defence in *Arabidopsis thaliana*. *BioMetals*, **17**, 379–387.

Drazkiewicz, M., Skorzynska-Polit, E. & Krupa, Z. (2006). The redox state and activity of superoxide dismutase classes in *Arabidopsis thaliana* under cadmium or copper stress. *Chemosphere*, **67**, 188–193.

Dubovskaya, L., Kolesneva, E., Knyazev, D. & Volotovskii, I. (2007). Protective role of nitric oxide during hydrogen peroxide-induced oxidative stress in tobacco plants. *Russian Journal of Plant Physiology*, **54**, 755–762.

Duffus, J.H. (2002). "Heavy metals" - a meaningless term? *Pure and Applied Chemistry*, **74**, 793–807.

Durner, J., Wendehenne, D. & Klessig, D.F. (1998). Defense gene induction in tobacco by nitric oxide, cyclic GMP, and cyclic ADP-ribose. *Proceedings of the National Academy of Sciences*, **95**, 10328–10333.

Eapen, S. & D'Souza, S.F. (2005). Prospects of genetic engineering of plants for phytoremediation of toxic metals. *Biotechnology Advances*, **23**, 97–114.

Ellis, D.R., Lopez-Millan, A.F. & Grusak, M.A. (2003). Metal physiology and accumulation in a *Medicago truncatula* mutant exhibiting an elevated requirement for zinc. *New Phytologist*, **158**, 207–218.

Ernst, W.H.O., Verkleij, J.A.C. & Schat, H. (1992). Metal tolerance in plants. *Acta Botanica Neerlandica*, **41**, 229–248.

Estelle, M.A. & Somerville, C.R. (1986). The mutants of *Arabidopsis*. *Trends in Genetics*, **2**, 89–93.

Eun, S.O., Shik Youn, H. & Lee, Y. (2000). Lead disturbs microtubule organization in the root meristem of *Zea mays*. *Physiologia Plantarum*, **110**, 357–365.

Fischerova, Z., Tlustos, P., Jirina, S. & Kornelie, S. (2006). A comparison of phytoremediation capability of selected plant species for given trace elements. *Environmental Pollution*, **144**, 93–100.

Fleige, S. & Pfaffl, M.W. (2006). Rna integrity and the effect on the real-time qRT-PCR performance. *Molecular Aspects of Medicine*, **27**, 126 – 139, real-time Polymerase Chain Reaction.

Freeman, W.M., Walker, S.J. & Vrana, K.E. (1999). Quantitative RT-PCR: pitfalls and potential. *BioTechniques*, **26**, 112–125.

Fricker, M. & Meyer, A. (2001). Confocal imaging of metabolism *in vivo*: pitfalls and possibilities. *J. Exp. Bot.*, **52**, 631–640.

Fritz, E. (2007). Measurement of cation exchange capacity (CEC) of plant cell walls by X-ray microanalysis (EDX) in the transmission electron microscope. *Microscopy and Microanalysis*, **13**, 233–244.

Gachon, C., Mingam, A. & Charrier, B. (2004). Real-time PCR: what relevance to plant studies? *Journal of Analytical Atomic Spectrometry*, **55**, 1445–1454.

Geebelen, W., Vangronsveld, J., Adriano, D.C., Van Poucke, L.C. & Clijsters, H. (2002). Effects of Pb-EDTA and EDTA on oxidative stress reactions and mineral uptake in *Phaseolus vulgaris*. *Physiologia Plantarum*, **115**, 377–384.

Gerke, V. & Moss, S.E. (2002). Annexins: from structure to function. *Physiological Reviews*, **82**, 331–371.

Gidrol, X., Sabelli, P.A., Fern, Y.S. & Kush, A.K. (1996). Annexin-like protein from *Arabidopsis thaliana* rescues $\triangle$*oxyR* mutant of *Escherichia coli* from H_2O_2 stress. *PNAS*, **93**, 11268–11273.

Gorecka, K.M., Konopka-Postupolska, D., Hennig, J., Buchet, R. & Pikula, S. (2005). Peroxidase activity of annexin 1 from *Arabidopsis thaliana*. *Biochemical and Biophysical Research Communications*, **336**, 868–875.

Gorecka, K.M., Thouverey, C., Buchet, R. & Pikula, S. (2007). Potential role of annexin annat1 from *Arabidopsis thaliana* in pH-mediated cellular response to environmental stimuli. *Plant and Cell Physiology*, **48**, 792–803.

Gratao, P., Polle, A., Lea, P. & Azevedo, R. (2005). Making the life of heavy metal-stressed plants a little easier. *Functional Plant Biology*, **32**, 481–494.

Greger, M. (1999). Metal availability and bioconcentration in plants. In M.N.V. Prasad & J. Hagemeyer, eds., *Heavy metal stress in plants : from molecules to ecosystems*, 1–28, Springer-Verlag, Berlin, Germany, Berlin, Germany.

Greman, H., Velikonja-Bolta, S., Vodnik, D., Kos, B. & Lestan, D. (2001). EDTA enhanced heavy metal phytoextraction: metal accumulation, leaching and toxicity. *Plant and Soil*, **235**, 105–114.

Grene, R. (2008). Oxidative stress and acclimation mechanisms in plants. The Arabidopsis Book.

Grill, E., Winnacker, E.L. & Zenk, M.H. (1987). Phytochelatins, a class of heavy-metal-binding peptides from plants, are functionally analogous to metallothioneins. *Proceedings of the National Academy of Sciences of the United States of America*, **84**, 439–443.

Grover, A., Kapoor, A., Lakshmi, O.S., Agarwal, S., Sahi, C., Katiyar-Agarwal, S., Agarwal, M. & Dubey, H. (2001). Understanding molecular alphabets of the plant abiotic stress responses. *Curent Science*, **80**, 206–216.

Grun, S., Lindermayr, C., Sell, S. & Durner, J. (2006). Nitric oxide and gene regulation in plants. *Journal of Experimental Botany*, **57**, 507–516.

Guenin, S., Mauriat, M., Pelloux, J., Van Wuytswinkel, O., Bellini, C. & Gutierrez, L. (2009). Normalization of qRT-PCR data: the necessity of adopting a systematic, experimental conditions-specific, validation of references. *Journal of Experimental Botany*, **60**, 487–493.

Hagemeyer, J. (1999). Ecophysiology of plant growth under heavy metal stress. In M. Prasad & J. Hagemeyer, eds., *Heavy metal stress in plants : from molecules to ecosystems*, 157–182, Springer-Verlag, Berlin Heidelberg New York.

Hall, J.L. (2002). Cellular mechanisms for heavy metal detoxification and tolerance. *Journal of Experimental Botany*, **53**, 1–11.

Halliwell, B. & Gutteridge, J.M.C. (1999). *Free radicals in biology and medicine*. Oxford University Press, Oxford, 3rd edn.

Hanc, A., Baralkiewicz, D., Piechalak, A., Tomaszewska, B., Wagner, B. & Bulska, E. (2009). An analysis of long-distance root to leaf transport of lead in *Pisum sativum* plants by laser ablation-ICP-MS. *International Journal of Environmental Analytical Chemistry*, **89**, 651–659.

Hassinen, V.H., Tervahauta, A.I. & Karenlampi, S.O. (2007). Searching for genes involved in metal tolerance, uptake, and transport. In *Phytoremediation*, 265–289, Humana Press.

Hay, F.R., Mead, A., Manger, K. & Wilson, F.J. (2003). One-step analysis of seed storage data and the longevity of *Arabidopsis thaliana* seeds. *Journal of Experimental Botany*, **54**, 993–1011.

Heid, C.A., Stevens, J., Livak, K.J. & Williams, P.M. (1996). Real time quantitative PCR. *Genome Res*, **6**, 986–994.

Hellemans, J., Mortier, G., De Paepe, A., Speleman, F. & Vandesompele, J. (2007). qBase relative quantification framework and software for management and automated analysis of real-time quantitative PCR data. *Genome Biology*, **8**, 1–14.

Hettiarachchi, G.M. & Pierzynski, G.M. (2004). Soil lead bioavailability and *in situ* remediation of lead-contaminated soils: a review. *Environmental Progress*, **23**, 78–93.

Hogg, N. & Kalyanaraman, B. (1999). Nitric oxide and lipid peroxidation. *Biochimica et Biophysica Acta (BBA) - Bioenergetics*, **1411**, 378–384.

Hong, J.K., Yun, B.W., Kang, J.G., Raja, M.U., Kwon, E., Sorhagen, K., Chu, C., Wang, Y. & Loake, G.J. (2008). Nitric oxide function and signalling in plant disease resistance. *Journal of Experimental Botany*, **59**, 147–154.

Hoshino, D., Hayashi, A., Temmei, Y., Kanzawa, N. & Tsuchiya, T. (2004). Biochemical and immunohistochemical characterization of *Mimosa* annexin. *Planta*, **219**, 867–875.

Howden, R. & Cobbett, C.S. (1992). Cadmium-sensitive mutants of *Arabidopsis thaliana*. *Plant Physiology*, **100**, 100–107.

Howden, R., Andersen, C.R., Goldsbrough, P.B. & Cobbett, C.S. (1995a). A cadmium-sensitive, glutathione-deficient mutant of *Arabidopsis thaliana*. *Plant Physiology*, **107**, 1067–1073.

Howden, R., Goldsbrough, P.B., Andersen, C.R. & Cobbett, C.S. (1995b). Cadmium-sensitive, *cad1* mutants of *Arabidopsis thaliana* are phytochelatin deficient. *Plant Physiology*, **107**, 1059–1066.

Hsu, Y. & Kao, C. (2004). Cadmium toxicity is reduced by nitric oxide in rice leaves. *Plant Growth Regulation*, **42**, 227–238.

Hu, K.D., Hu, L.Y., Li, Y.H., Zhang, F.Q. & Zhang, H. (2007). Protective roles of nitric oxide on germination and antioxidant metabolism in wheat seeds under copper stress. *Plant Growth Regulation*, **53**, 173–183.

Huang, D., Ou, B. & Prior, R.L. (2005). The chemistry behind antioxidant capacity assays. *Journal of Agricultural and Food Chemistry*, **53**, 1841–1856.

Huang, J.W. & Cunningham, S.D. (1996). Lead phytoextraction: species variation in lead uptake and translocation. *New Phytologist*, **134**, 75–84.

Huang, J.W., Chen, J., Berti, W.R. & Cunningham, S.D. (1997). Phytoremediation of lead-contaminated soils: role of synthetic chelates in lead phytoextraction. *Environmental Science Technology*, **31**, 800–805.

Huggett, J., Dheda, K., Bustin, S. & Zumla, A. (2005). Real-time RT-PCR normalisation; strategies and considerations. *Genes and Immunity*, **6**, 279–284.

Illes, P., Schlicht, M., Pavlovkin, J., Lichtscheidl, I., Baluska, F. & Ovecka, M. (2006). Aluminium toxicity in plants: internalization of aluminium into cells of the transition zone in *Arabidopsis* root apices related to changes in plasma membrane potential, endosomal behaviour, and nitric oxide production. *Journal of Experimental Botany*, **57**, 4201–4213.

Iwamoto, T. & Nasu, M. (2001). Current bioremediation practice and perspective. *Journal of Bioscience and Bioengineering*, **92**, 1–8.

Jami, S.K., Clark, G.B., Turlapati, S.A., Handley, C., Roux, S.J. & Kirti, P.B. (2008). Ectopic expression of an annexin from *Brassica juncea* confers tolerance to abiotic and biotic stress treatments in transgenic tobacco. *Plant Physiology and Biochemistry*, **46**, 1019–1030.

Janssens, B.J., Childress, J.J., Baguet, F. & Rees, J.F. (2000). Reduced enzymatic antioxidative defense in deep-sea fish. *Journal of Experimental Biology*, **203**, 3717–3725.

Jarvis, M.D. (2001). *An investigation into some aspects related to the phytoremediation potential of Pinus Radiata (D. Don) & Chamaecytisus proliferus (L.f.) Link ssp. proliferus var. palmensis (H. Christ.)*. Ph.D. thesis, University of Canterbury, Christchurch.

Jarvis, M.D. & Leung, D.W.M. (2001). Chelated lead transport in *Chamaecytisus proliferus* (L.f.) link ssp. *proliferus* var. *palmensis* (H. Christ): an ultrastructural study. *Plant Science*, **161**, 433–441.

Jarvis, M.D. & Leung, D.W.M. (2002). Chelated lead transport in *Pinus radiata*: an ultrastructural study. *Environmental and Experimental Botany*, **48**, 21–32.

John, D.A. & Leventhal, J.S. (1995). Bioavailability of metals. U.S. Geological Survey Open-File Rep. 95-831.

Jurkiewicz, A., Turnau, K., Mesjasz-Przyblowicz, J., Przybylowicz, W. & Godzik, B. (2001). Heavy metal localisation in mycorrhizas of *Epipactis atrorubens* (Hoffm.) Besser (Orchidaceae) from zinc mine tailings. *Protoplasma*, **218**, 117–124.

Karenlampi, S., Schat, H., Vangronsveld, J., Verkleij, J.A.C., van der Lelie, D., Mergeay, M. & Tervahauta, A.I. (2000). Genetic engineering in the improvement of plants for phytoremediation of metal polluted soils. *Environmental Pollution*, **107**, 225–231.

Klein, D. (2002). Quantification using real-time PCR technology: applications and limitations. *Trends in Molecular Medicine*, **8**, 257–260.

Kodera, H., Nishioka, H., Muramatsu, Y. & Terada, Y. (2008). Distribution of lead in lead-accumulating pteridophyte *Blechnum niponicum*, measured by synchrotron radiation micro X-ray fluorescence. *Analytical Sciences*, **24**, 1545–1549.

Koeppe, D.E. (1981). Lead: understanding the minimal toxicity of lead in plants. In N.W. Lepp, ed., *Effect of heavy metal pollution on plants: Effects of trace metals on plant function*, vol. 1 of *Pollution monitoring series*, 55–76, Applied Science Publishers, London.

Konopka-Postupolska, D., Clark, G., Goch, G., Debski, J., Floras, K., Cantero, A., Fijolek, B., Roux, S. & Hennig, J. (2009). The role of annexin 1 in drought stress in *Arabidopsis*. *Plant Physiology*, **150**, 1394–1410.

Kopyra, M. & Gwozdz, E.A. (2003). Nitric oxide stimulates seed germination and counteracts the inhibitory effect of heavy metals and salinity on root growth of *Lupinus luteus*. *Plant Physiology and Biochemistry*, **41**, 1011–1017.

Kopyra, M., Stachon-Wilk, M. & Gwozdz, E. (2006). Effects of exogenous nitric oxide on the antioxidant capacity of cadmium-treated soybean cell suspension. *Acta Physiologiae Plantarum*, **28**, 525–536.

Kotrba, P., Najmanova, J., Macek, T., Ruml, T. & Mackova, M. (2009). Genetically modified plants in phytoremediation of heavy metal and metalloid soil and sediment pollution. *Biotechnology Advances*, **27**, 799–810.

Kovacs, I., Ayaydin, F., Oberschall, A., Ipacs, I., Bottka, S., Pongor, S., Dudits, D. & Toth, E.C. (1998). Immunolocalization of a novel annexin like protein encoded by a stress and abscisic acid responsive gene in alfalfa. *The Plant Journal*, **15**, 185–197.

Kramer, U. (2005). Phytoremediation: novel approaches to cleaning up polluted soils. *Current Opinion in Biotechnology*, **16**, 133–141.

Kramer, U. & Chardonnens, A.N. (2001). The use of transgenic plants in the bioremediation of soils contaminated with trace elements. *Applied Microbiology and Biotechnology*, **55**, 661–672.

Kreps, J.A., Wu, Y., Chang, H.S., Zhu, T., Wang, X. & Harper, J.F. (2002). Transcriptome changes for *Arabidopsis* in response to salt, osmotic, and cold stress. *Plant Physiology*, **130**, 2129–2141.

Krzeslowska, M., Lenartowska, M., Samardakiewicz, S., Bilski, H. & Wozny, A. (2010). Lead deposited in the cell wall of *Funaria hygrometrica* protonemata is not stable - a remobilization can occur. *Environmental Pollution*, **158**, 325–338.

Kubista, M., Andrade, J.M., Bengtsson, M., Forootan, A., Jonak, J., Lind, K., Sindelka, R., Sjoback, R., Sjogreen, B., Strombom, L., Stahlberg, A. & Zoric, N. (2006). The real-time polymerase chain reaction. *Molecular Aspects of Medicine*, **27**, 95–125.

Kumar, P.B.A.N., Dushenkov, V., Motto, H. & Raskin, I. (1995). Phytoextraction: the use of plants to remove heavy metals from soils. *Environmental Science & Technology*, **29**, 1232–1238.

Kush, A. & Sabapathy, K. (2001). Oxy5, a novel protein from *Arabidopsis thaliana*, protects mammalian cells from oxidative stress. *The International Journal of Biochemistry & Cell Biology*, **33**, 591–602.

Laemmli, U.K. (1970). Cleavage of structural proteins during assembly of head of bacteriophage-t4. *Nature*, **227**, 680–685.

Lamattina, L., Garcia-Mata, C., Graziano, M. & Pagnussat, G. (2003). Nitric oxide: the versatility of an extensive signal molecule. *Annual Review of Plant Biology*, **54**, 109–136.

Lane, S. & Martin, E.S. (1977). A histochemical investigation of lead uptake in *Raphanus sativus*. *New Phytologist*, **79**, 281–286.

Lane, S., Margin, E. & Carrod, J. (1978). Lead toxic effect on indole-3-acetic acid induced cell elongation. *Planta*, **144**, 7984.

Larkin, E., Dunaway, S., Ellini, K., Rubio, M., Sanchez, C., Sehorn, M. & Weiss, L. (1999). An *Arabidopsis thaliana* copper-sensitive mutant. *Bios*, **70**, 147–157.

Larsen, P.B., Tai, C.Y., Kochian, L.V. & Howell, S.H. (1996). *Arabidopsis* mutants with increased sensitivity to aluminum. *Plant Physiology*, **110**, 743–751.

Lasat, M.M. (2002). Phytoextraction of toxic metals: a review of biological mechanisms. *Journal of Environmental Quality*, **31**, 109–120.

Laspina, N.V., Groppa, M.D., Tomaro, M.L. & Benavides, M.P. (2005). Nitric oxide protects sunflower leaves against Cd-induced oxidative stress. *Plant Science*, **169**, 323–330.

Lee, C. (2007). Western blotting. In E. Rosato, ed., *Circadian Rhythms: Methods & Protocols*, vol. 362 of *Methods in Molecular Biology*, 391–399, Humana Press Inc., Totowa, NJ.

Lee, M., Lee, K., Lee, J., Noh, E.W. & Lee, Y. (2005). AtPDR12 contributes to lead resistance in *Arabidopsis*. *Plant Physiology*, **138**, 827–836.

Lee, S., Lee, E.J., Yang, E.J., Lee, J.E., Park, A.R., Song, W.H. & Park, O.K. (2004). Proteomic identification of annexins, calcium-dependent membrane binding proteins that mediate osmotic stress and abscisic acid signal transduction in *Arabidopsis*. *Plant Cell*, **16**, 1378–1391.

Lefebvre, V., Kiani, S.P. & Durand-Tardif, M. (2009). A focus on natural variation for abiotic constraints response in the model species *Arabidopsis thaliana*. *International Journal of Molecular Sciences*, **10**, 3547–3582.

Lei, M., Chen, T.B., Huang, Z.C., Wang, Y.D. & Huang, Y.Y. (2008). Simultaneous compartmentalization of lead and arsenic in co-hyperaccumulator *Viola principis* H. de Boiss.: An application of SRXRF microprobe. *Chemosphere*, **72**, 1491–1496.

Lei, Y., Yin, C. & Li, C. (2007). Adaptive responses of *Populus przewalskii* to drought stress and SNP application. *Acta Physiologiae Plantarum*, **29**, 519–526.

Li, Q.Y., Niu, H.B., Yin, J., Wang, M.B., Shao, H.B., Deng, D.Z., Chen, X.X., Ren, J.P. & Li, Y.C. (2008). Protective role of exogenous nitric oxide against oxidative-stress induced by salt stress in barley (*Hordeum vulgare*). *Colloids and Surfaces B: Biointerfaces*, **65**, 220–225.

Li, W., Khan, M.A., Yamaguchi, S. & Kamiya, Y. (2005). Effects of heavy metals on seed germination and early seedling growth of *Arabidopsis thaliana*. *Plant Growth Regulation*, **46**, 45–50.

Liemann, S. & Lewit-Bentley, A. (1995). Annexins: a novel family of calcium-and membrane-binding proteins in search of a function. *Structure*, **3**, 233–237.

Lightner, J. & Caspar, T. (1998). Seed mutagenesis in *Arabidopsis*. In J.M. Martinez-Zapater & J. Salinas, eds., *Arabidopsis protocols*, 91–104, Humana Press, Totowa, N.J.

Liu, D., Jiang, W., Liu, C., Xin, C. & Hou, W. (2000). Uptake and accumulation of lead by roots, hypocotyls and shoots of indian mustard [*Brassica juncea* (L.)]. *Bioresource Technology*, **71**, 273–277.

Liu, D., Li, T.Q., Jin, X.F., Yang, X.E., Islam, E. & Mahmood, Q. (2008). Lead induced changes in the growth and antioxidant metabolism of the lead accumulating and non-accumulating ecotypes of *Sedum alfredii*. *Journal of Integrative Plant Biology*, **50**, 129–140.

Liu, D., Zou, J., Meng, Q., Zou, J. & Jiang, W. (2009a). Uptake and accumulation and oxidative stress in garlic (*Allium sativum* L.) under lead phytotoxicity. *Ecotoxicology*, **18**, 134–143.

Liu, T., Liu, S., Guan, H., Ma, L., Chen, Z., Gu, H. & Qu, L.J. (2009b). Transcriptional profiling of *Arabidopsis* seedlings in response to heavy metal lead (Pb). *Environmental and Experimental Botany*, **67**, 377–386.

Livak, K.J. & Schmittgen, T.D. (2001). Analysis of relative gene expression data using real-time quantitative PCR and the 2-△△CT method. *Methods*, **25**, 402–408.

Lowe, T., Sharefkin, J., Yang, S.Q. & Dieffenbach, C.W. (1990). A computer program for selection of oligonucleotide primers for polymerase chain reactions. *Nucleic Acids Research*, **18**, 1757–1761.

Macnair, M.R. (2002). Within and between population genetic variation for zinc accumulation in *Arabidopsis halleri*. *New Phytologist*, **155**, 59–66.

Maksymiec, W. & Krupa, Z. (2006). The effects of short-term exposition to Cd, excess Cu ions and jasmonate on oxidative stress appearing in *Arabidopsis thaliana*. *Environmental and Experimental Botany*, **57**, 187–194.

Malecka, A., Jarmuszkiewicz, W. & Tomaszewska, B. (2001). Antioxidative defense to lead stress in subcellular compartments of pea root cells. *Acta Biochimica Polonica*, **48**, 687–698.

Malecka, A., Piechalak, A., Morkunas, I. & Tomaszewska, B. (2008). Accumulation of lead in root cells of *Pisum sativum*. *Acta Physiologiae Plantarum*, **30**, 629–637.

Malecka, A., Derba-Maceluch, M., Kaczorowska, K., Piechalak, A. & Tomaszewska, B. (2009a). Reactive oxygen species production and antioxidative defense system in pea root tissues treated with lead ions: mitochondrial and peroxisomal level. *Acta Physiologiae Plantarum*, **31**, 1065–1075.

Malecka, A., Piechalak, A. & Tomaszewska, B. (2009b). Reactive oxygen species production and antioxidative defense system in pea root tissues treated with lead ions: the whole roots level. *Acta Physiologiae Plantarum*, **31**, 1053–1063.

Malkowski, E., Kita, A., Galas, W., Karcz, W. & Kuperberg, J.M. (2002). Lead distribution in corn seedlings (*Zea mays* L.) and its effect on growth and the concentrations of potassium and calcium. *Plant Growth Regulation*, **37**, 69–76.

Mallick, N. & Rai, L.C. (2002). Physiological responses of non-vascular plants to heavy metal. In M.N.V. Prasad & K. Strzalka, eds., *Physiology and biochemistry of metal toxicity and tolerance in plants*, 111–148, Kluwer Academic Publisher, Dordrecht, Boston.

Malone, C., Koeppe, D.E. & Miller, R.J. (1974). Localization of lead accumulated by corn plants. *Plant Physiology*, **53**, 388–394.

Maple, J. & Moller, S.G. (2007). Mutagenesis in *Arabidopsis*. In E. Rosato, ed., *Circadian Rhythms*, vol. 362 of *Methods in Molecular Biology*, 197–206, Humana Press.

Maral, J., Puget, K. & Michelson, A.M. (1977). Comparative study of superoxide dismutase, catalase and glutathione peroxidase levels in erythrocytes of different animals. *Biochemical and Biophysical Research Communications*, **77**, 1525–1535.

Martinez, M., Bernal, P., Almela, C., Velez, D., Garcia-Agustin, P., Serrano, R. & Navarro-Avino, J. (2006). An engineered plant that accumulates higher levels of heavy metals than *Thlaspi caerulescens*, with yields of 100 times more biomass in mine soils. *Chemosphere*, **64**, 478–485.

McIntyre, T. (2003). Phytoremediation of heavy metals from soils. In *Phytoremediation*, vol. 78 of *Advances in Biochemical Engineering/Biotechnology*, 97–123, Springer Berlin, Heidelberg.

Meagher, R.B. (2000). Phytoremediation of toxic elemental and organic pollutants. *Current Opinion in Plant Biology*, **3**, 153–162.

Meinke, D.W., Cherry, J.M., Dean, C., Rounsley, S.D. & Koorneef, M. (1998). *Arabidopsis thaliana*: a model plant for genome analysis. *Science*, **282**, 662–682.

Memon, A. & Schroder, P. (2009). Implications of metal accumulation mechanisms to phytoremediation. *Environmental Science and Pollution Research*, **16**, 162–175.

Mensah, E., Allen, H., Shoji, R., Odai, S., Kyei-Baffour, N., Ofori, E. & Mezler, D. (2008). Cadmium (Cd) and lead (Pb) concentrations effects on yields of some vegetables due to uptake from irrigation water in Ghana. *International Journal of Agricultural Research*, **3**, 243–251.

Mihaljevic, B., Katusin-Razem, B. & Razem, D. (1996). The reevaluation of the ferric thiocyanate assay for lipid hydroperoxides with special considerations of the mechanistic aspects of the response. *Free Radical Biology and Medicine*, **21**, 53–63.

Mittler, R. (2002). Oxidative stress, antioxidants and stress tolerance. *Trends in Plant Science*, **7**, 405–410.

Mleczek, M., Lukaszewski, M., Kaczmarek, Z., Rissmann, I. & Golinski, P. (2009). Efficiency of selected heavy metals accumulation by *Salix viminalis* roots. *Environmental and Experimental Botany*, **65**, 48–53.

Moller, I.M., Jensen, P.E. & Hansson, A. (2007). Oxidative modifications to cellular components in plants. *Annual Review of Plant Biology*, **58**, 459–481.

Morel, M., Crouzet, J., Gravot, A., Auroy, P., Leonhardt, N., Vavasseur, A. & Richaud, P. (2009). AtHMA3, a P1B-ATPase allowing Cd/Zn/Co/Pb vacuolar storage in *Arabidopsis*. *Plant Physiology*, **149**, 894–904.

Mortimer, J.C., Laohavisit, A., Macpherson, N., Webb, A., Brownlee, C., Battey, N.H. & Davies, J.M. (2008). Annexins: multifunctional components of growth and adaptation. *Journal of Experimental Botany*, **59**, 533–544.

Mukherjee, S. & Maitra, P. (1976). The effect of lead on growth and metabolism of germinating rice seeds and on mitosis of onion root tips. *Indian Journal of Experimental Biology*, **14**, 519–521.

Mukherji, S. & Maitra, P. (1977). Growth and metabolism of germinating rice (*Oryza sativa* L.) seeds as influcned by toxic concentrations of lead. *Z. Pflanzenphysiol. Bd.*, **81**, 26–33.

Muller, S. (2007). Real time quantitative PCR. [Online] http://www.gene-quantification.org/AssayOpt-Stratagene.pdf.

Murashige, T. & Skoog, F. (1962). A revise medium for rapid growth and bio assays with tobacco tissue cultures. *Physiologia Plantarum*, **14**, 473–497.

Navari-Izzo, F. & Quartacci, F., Mike (2001). Phytoremediation of metals: tolerance mechanisms against oxidative stress. *Minerva Biotecnologica*, **13**, 73–83.

Navarro, S.X., Dziewatkoski, M.P. & Enyedi, A.J. (1999). Isolation of cadmium excluding mutants of *Arabidopsis thaliana* using a vertical mesh transfer system and ICP-MS. *Journal of Environmental Science and Health, Part A: Toxic/Hazardous Substances and Environmental Engineering*, **34**, 1797–1813.

Nawrot, M., Szarejko, I. & Maluszynski, M. (2001). Barley mutants with increased tolerance to aluminium toxicity. *Euphytica*, **120**, 345–356.

Necemer, M., Kump, P., Scancar, J., Jacimovic, R., Simcic, J., Pelicon, P., Budnar, M., Jeran, Z., Pongrac, P., Regvar, M. & Vogel-Mikus, K. (2008). Application of X-ray fluorescence analytical techniques in phytoremediation and plant biology studies. *Spectrochimica Acta Part B: Atomic Spectroscopy*, **63**, 1240–1247.

Nehnevajova, E., Herzig, R., Federer, G., Erismann, K.H. & Schwitzguebel, J.P. (2007). Chemical mutagenesis:a promising technique to increase metal concentration and extraction in sunflowers. *International Journal of Phytoremediation*, **9**, 149–165.

Nehnevajova, E., Herzig, R., Bourigault, C., Bangerter, S. & Schwitzguebel, J.P. (2009). Sability of enhanced yield and metal uptake by sunflower mutants for improved phytoremediation. *International Journal of Phytoremediation*, **11**, 329–346.

Neill, S., Bright, J., Desikan, R., Hancock, J., Harrison, J. & Wilson, I. (2008). Nitric oxide evolution and perception. *Journal of Experimental Botany*, **59**, 25–35.

Neill, S.J., Desikan, R. & Hancock, J.T. (2003). Nitric oxide signalling in plants. *New Phytologist*, **159**, 11–35.

Nicot, N., Hausman, J.F., Hoffmann, L. & Evers, D. (2005). Housekeeping gene selection for real-time RT-PCR normalization in potato during biotic and abiotic stress. *Journal of Experimental Botany*, **56**, 2907–2914.

Niedzielski, M., Walters, C., Luczak, W., Hill, L.M., Wheeler, L.J. & Puchalski, J. (2009). Assessment of variation in seed longevity within rye, wheat and the intergeneric hybrid triticale. *Seed Science Research*, **19**, 213–224.

Paglia, D. & Valentine, W. (1967). Studies on the quantitative and qualitative characterization of erythrocyte glutathione peroxidase. *Journal of Laboratory and Clinical Medicine*, **70**, 158–168.

Palavan-Unsal, N. & Arisan, D. (2009). Nitric oxide signalling in plants. *The Botanical Review*, **75**, 203–229.

Peer, W.A., Mamoudian, M., Lahner, B., Reeves, R.D., Murphy, A.S. & Salt, D.E. (2003). Identifying model metal hyperaccumulating plants: germplasm analysis of 20 Brassicaceae accessions from a wide geographical area. *New Phytologist*, **159**, 421–430.

Peirson, S.N. & Butler, J.N. (2007). Quantitative polymerase chain reaction. In E. Rosato, ed., *Circadian Rhythms: Methods & Protocols*, vol. 362 of *Methods in Molecular Biology*, 349–362, Humana Press Inc., Totowa, NJ.

Peirson, S.N., Butler, J.N. & Foster, R.G. (2003). Experimental validation of novel and conventional approaches to quantitative real-time PCR data analysis. *Nucleic Acids Research*, **31**, e73.

Perez-Novo, C.A., Claeys, C., Speleman, F., Van Cauwenberge, P., Bachert, C. & Vandesompele, J. (2005). Impact of rna quality on reference gene expression stability. *BioTechniques*, **39**, 52–56.

Pfaffl, M.W. (2001). A new mathematical model for relative quantification in real-time RT-PCR. *Nucleic Acids Research*, **29**, 2002–2007.

Pfaffl, M.W., Horgan, G.W. & Dempfle, L. (2002). Relative expression software tool (REST©) for group-wise comparison and statistical analysis of relative expression results in real-time PCR. *Nucleic Acids Research*, **30**, 1–10.

Pfaffl, M.W., Tichopad, A., Prgomet, C. & Neuvians, T. (2004). Determination of stable housekeeping genes, differentially regulated target genes and sample integrity: BestKeeper - Excel-based tool using pair-wise correlations. *Biotechnology Letters*, **26**, 509–515.

Phipps, D.A. (1981). Chemistry and biochemistry of trace metals in biological system. In N.W. Lepp, ed., *Effect of heavy metal pollution on plants: Effect of trace metals on plant function*, vol. 1 of *Pollution monitoring series*, 1–54, Applied Science Publishers, London.

Piechalak, A., Tomaszewska, B., Baralkiewicz, D. & Malecka, A. (2002). Accumulation and detoxification of lead ions in legumes. *Phytochemistry*, **60**, 153–162.

Pilon-Smits, E. (2005). Phytoremediation. *Annual Review of Plant Biology*, **56**, 15–39.

Pilon-Smits, E. & Pilon, M. (2002). Phytoremediation of metals using transgenic plants. *Critical Reviews in Plant Sciences*, **21**, 439–456.

Polec-Pawlak, K., Ruzik, R., Lipiec, E., Ciurzynska, M. & Gawronska, H. (2007). Investigation of Pb(II) binding to pectin in *Arabidopsis thaliana*. *Journal of Analytical Atomic Spectrometry*, **22**, 968–972.

Poulter, A., Collin, H.A., Thurman, D.A. & Hardwick, K. (1985). The role of the cell wall in the mechanism of lead and zinc tolerance in *Anthoxanthum odoratum* L. *Plant Science*, **42**, 61–66.

Proust, J., Houlne, G., Schantz, M.L. & Schantz, R. (1996). Characterization and gene expression of an annexin during fruit development in *Capsicum annuum*. *FEBS Letters*, **383**, 208–212.

Przymusinski, R., Rucinska-Sobkowiak, R., Ilska, B. & Gwozdz, E. (2007). Organospecific responses of lupin seedlings to lead localization of hydrogen peroxide and peroxidase activity. *Acta Physiologiae Plantarum*, **29**, 411–416.

Puig, S., Andres-Colas, N., Garcia-Molina, A. & Penarrubia, L. (2007). Copper and iron homeostasis in *Arabidopsis*: responses to metal deficiencies, interactions and biotechnological applications. *Plant, Cell & Environment*, **30**, 271–290.

Qiagen, G. (2006). *RNeasy ®Mini Handbook*. Qiagen GmbH, Hilden, Germany, 4th edn.

Qiang, X., Qiaomei, R., Feihua, W., Xuan, H., Zhenming, P. & Hailei, Z. (2007). Nitric oxide alleviates oxidative stress caused by lanthanum in rice leaves. *Journal of Rare Earths*, **25**, 631–636.

Qiao, W., Xiao, S., Yu, L. & Fan, L.M. (2009). Expression of a rice gene OsNOA1 reestablishes nitric oxide synthesis and stress-related gene expression for salt tolerance in *Arabidopsis nitric oxide-associated 1* mutant *Atnoa1*. *Environmental and Experimental Botany*, **65**, 90–98.

Qureshi, J.A., Thurman, D.A., Hardwick, K. & Collin, H.A. (1985). Uptake and accumulation of zinc, lead and copper in zinc and lead tolerant *Anthoxanthum odoratum* L. *New Phytologist*, **100**, 429–434.

Qureshi, M., Abdin, M., Qadir, S. & Iqbal, M. (2007). Lead-induced oxidative stress and metabolic alterations in *Cassia angustifolia* Vahl. *Biologia Plantarum*, **51**, 121–128.

Radonic, A., Thulke, S., Mackay, I.M., Landt, O., Siegert, W. & Nitsche, A. (2004). Guideline to reference gene selection for quantitative real-time PCR. *Biochemical and Biophysical Research Communications*, **313**, 856–862.

Ramakers, C., Ruijter, J.M., Deprez, R.H.L. & Moorman, A.F.M. (2003). Assumption-free analysis of quantitative real-time polymerase chain reaction (PCR) data. *Neuroscience Letters*, **339**, 62–66.

Raskin, I., Smith, R.D. & Salt, D.E. (1997). Phytoremediation of metals: using plants to remove pollutants from the environment. *Current Opinion in Biotechnology*, **8**, 221–226.

Reddy, A.M., Kumar, S.G., Jyothsnakumari, G., Thimmanaik, S. & Sudhakar, C. (2005). Lead induced changes in antioxidant metabolism of horsegram (*Macrotyloma uniflorum* (Lam.) Verdc.) and bengalgram (*Cicer arietinum* L.). *Chemosphere*, **60**, 97–104.

Redei, G.P. (1992). Classical mutagenesis. In C. Koncz, N.H. Chua & J. Schell, eds., *Methods in Arabidopsis research*, 16–82, World Scientific, Singapore ; River Edge, N.J.

Remans, T., Smeets, K., Opdenakker, K., Mathijsen, D., Vangronsveld, J. & Cuypers, A. (2008). Normalisation of real-time RT-PCR gene expression measurements in *Arabidopsis thaliana* exposed to increased metal concentrations. *Planta*, **227**, 1343–1349.

Rescher, U. & Gerke, V. (2004). Annexins - unique membrane binding proteins with diverse functions. *Journal of Cell Science*, **117**, 2631–2639.

Rhee, H.J., Kim, G.Y., Huh, J.W., Kim, S.W. & Na, D.S. (2000). Annexin I is a stress protein induced by heat, oxidative stress and a sulfhydryl-reactive agent. *European Journal of Biochemistry*, **267**, 3220–3225.

Richards, K.D., Schott, E.J., Sharma, Y.K., Davis, K.R. & Gardner, R.C. (1998). Aluminum induces oxidative stress genes in *Arabidopsis thaliana*. *Plant Physiology*, **116**, 409–418.

Robinson, B. & Anderson, C. (2007). Phytoremediation in New Zealand and Australia. In N. Willey, ed., *Phytoremediation : methods and reviews*, Methods in biotechnology, 455–468, Humana Press, Totowa, N.J.

Rodriguez-Serrano, M., Romero-Puertas, M.C., Zabalza, A.N.A., Corpas, F.J., Gomez, M., Del Rio, L.A. & Sandalio, L.M. (2006). Cadmium effect on oxidative metabolism of pea (*Pisum sativum* L.) roots. Imaging of reactive oxygen species and nitric oxide accumulation *in vivo*. *Plant, Cell & Environment*, **29**, 1532–1544.

Rodriguez-Serrano, M., Romero-Puertas, M.C., Pazmino, D.M., Testillano, P.S., Risueno, M.C., del Rio, L.A. & Sandalio, L.M. (2009). Cellular response of pea plants to cadmium toxicity: cross talk between reactive oxygen species, nitric oxide, and calcium. *Plant Physiology*, **150**, 229–243.

Rozen, S. & Skaletsky, H.J. (2000). Primer3 on the www for general users and for biologist programmers. In S. Krawetz & S. Misener, eds., *Bioinformatics Methods and Protocols: Methods in Molecular Biology*, 365–386, Humana Press, Totowa, NJ.

Rucinka, R., Waplak, S. & Gwozdz, E.A. (1999). Free radical formation and activity of antioxidant enzymes in lupin roots exposed to lead. *Plant Physiology and Biochemistry*, **37**, 187–194.

Ruciska-Sobkowiak, R. & Pukacki, P.M. (2006). Antioxidative defense system in lupin roots exposed to increasing concentrations of lead. *Acta Physiologiae Plantarum*, **28**, 357–364.

Ruley, A.T., Sharma, N.C. & Sahi, S.V. (2004). Antioxidant defense in a lead accumulating plant, *Sesbania drummondii*. *Plant Physiology and Biochemistry*, **42**, 899–906.

Saffar, A., Bagherich Najjar, M.B. & Mianabadi, M. (2009). Activity of antioxidant enzymes in response to cadmium in *Arabidopsis thaliana*. *Journal of Biological Sciences*, **9**, 44–50.

Sahi, S.V., Bryant, N.L., Sharma, N.C. & Singh, S.R. (2002). Characterization of a lead hyperaccumulator shrub, *Sesbania drummondii*. *Environmental Science & Technology*, **36**, 4676–4680.

Salt, D.E., Smith, R.D. & Raskin, I. (1998). Phytoremediation. *Annual Review of Plant Physiology and Plant Molecular Biology*, **49**, 643–668.

Sambrook, J., Russell, D.W. & Maniatis, T. (2001). *Molecular cloning : a laboratory manual*. Cold Spring Harbor Laboratory Press, Cold Spring Harbor, N.Y., 3rd edn.

Sandalio, L.M., Rodriguez-Serrano, M., Romero-Puertas, M.C. & del Rio, L.A. (2008). Imaging of reactive oxygen species and nitric oxide *in vivo* in plant tissues. In E. Cadenas & L. Packer, eds., *Nitric Oxide, Part F*, vol. 440 of *Methods in Enzymology*, 397–409, Academic Press.

Sanders, D., Brownlee, C. & Harper, J.F. (1999). Communicating with calcium. *Plant Cell*, **11**, 691–706.

Saxena, P.K., KrishnaRaj, S., Dan, T., Perras, M.R. & Vettakkorumakankav, N.N. (1999). Phytoremediation of heavy metal contaminated and polluted soils. In M. Prasad & J. Hagemeyer, eds., *Heavy metal stress in plants : from molecules to ecosystems*, 305–329, Springer-Verlag, Berlin Heidelberg New York.

Schlemmer, G., Radziuk, B. & Schiemmer, G. (1999). *Analytical graphite furnace atomic absorption spectrometry: a laboratory guide*. Birkhauser Verlag AG, Switzerland.

Schulman, R.N., Salt, D.E. & Raskin, I. (1999). Isolation and partial characterization of a lead-accumulating *Brassica juncea* mutant. *TAG Theoretical and Applied Genetics*, **99**, 398–404.

Semane, B., Cuypers, A., Smeets, K., Van Belleghem, F., Horemans, N., Schat, H. & Vangronsveld, J. (2007). Cadmium responses in *Arabidopsis thaliana*: glutathione metabolism and antioxidative defence system. *Physiologia Plantarum*, **129**, 519–528.

Seregin, I.V. & Ivanov, V.B. (2001). Physiological aspects of cadmium and lead toxic effects on higher plants. *Russian Journal of Plant Physiology*, **48**, 523–544.

Sharma, P. & Dubey, R.S. (2005). Lead toxicity in plants. *Brazilian Journal of Plant Physiology*, **17**, 35–52.

Sharma, S.S. & Dietz, K.J. (2009). The relationship between metal toxicity and cellular redox imbalance. *Trends in Plant Science*, **14**, 43–50.

Shi, Q., Ding, F., Wang, X. & Wei, M. (2007). Exogenous nitric oxide protect cucumber roots against oxidative stress induced by salt stress. *Plant Physiology and Biochemistry*, **45**, 542–550.

Sigma-Aldrich, S. (1996). Sodium nitroprusside dihydrate. [Online] http://www.sigmaaldrich.com.

Singh, H.P., Batish, D.R., Kaur, G., Arora, K. & Kohli, R.K. (2008). Nitric oxide (as sodium nitroprusside) supplementation ameliorates Cd toxicity in hydroponically grown wheat roots. *Environmental and Experimental Botany*, **63**, 15–167.

Singh, H.P., Kaur, S., Batish, D.R., Sharma, V.P., Sharma, N. & Kohli, R.K. (2009). Nitric oxide alleviates arsenic toxicity by reducing oxidative damage in the roots of *Oryza sativa* (rice). *Nitric Oxide*, **20**, 289–297.

Singh, R.P., Tripathi, R.D., Sinha, S.K., Maheshwari, R. & Srivastava, H.S. (1997). Response of higher plants to lead contaminated environment. *Chemosphere*, **34**, 2467–2493.

Smallwood, M.F., Keen, J.N. & Bowles, D.J. (1990). Purification and partial sequence analysis of plant annexins. *The Biochemical Journal*, **270**, 157–161.

Smallwood, M.F., Gurr, S.J., McPherson, M.J., Roberts, K. & Bowles, D.J. (1992). The pattern of plant annexin gene expression. *The Biochemical Journal*, **281**, 501–505.

Song, W.Y., Sohn, E.J., Martinoia, E., Lee, Y.J., Yang, Y.Y., Jasinski, M., Forestier, C., Hwang, I. & Lee, Y. (2003). Engineering tolerance and accumulation of lead and cadmium in transgenic plants. *Nature Biotechnology*, **21**, 914–919.

Stohs, S.J. & Bagchi, D. (1995). Oxidative mechanisms in the toxicity of metal ions. *Free Radical Biology and Medicine*, **18**, 321–336.

Stratagene, A.T.C. (2007). Introduction to quantitative PCR: methods and applications guide. [Online] http://www.stratagene.com.

Sudha, G. & Ravishankar, G.A. (2002). Involvement and interaction of various signaling compounds on the plant metabolic events during defense response, resistance to stress factors, formation of secondary metabolites and their molecular aspects. *Plant Cell, Tissue and Organ Culture*, **71**, 181–212.

Sun, S.Q., He, M., Cao, T., Zhang, Y.C. & Han, W. (2009). Response mechanisms of antioxidants in bryophyte (*Hypnum plumaeforme*) under the stress of single or combined Pb and/or Ni. *Environmental Monitoring and Assessment*, **149**, 291–302.

Suresh, B. & Ravishankar, G.A. (2004). Phytoremediation- a novel and promising approach for environmental clean-up. *Critical Reviews in Biotechnology*, **24**, 97–124.

Suthersan, S.S. (1997). *Remediation engineering : design concepts*. CRC-Lewis Publishers, Boca Raton, Fl.

Taylor, N.L., Tan, Y.F., Jacoby, R.P. & Millar, A.H. (2009). Abiotic environmental stress induced changes in the *Arabidopsis thaliana* chloroplast, mitochondria and peroxisome proteomes. *Journal of Proteomics*, **72**, 367–378.

The Arabidopsis Information Resource, T.A.I.R. (2009). The *Arabidopsis* information resource. [Online] http://www.arabidopsis.org/portals/education/aboutarabidopsis.jsp.

The National Science Foundation, N.S.F. (2009). *Arabidopsis*: The model plant. [Online] http://www.nsf.gov/pubs/2002/bio0202/model.htm.

Thellin, O., Zorzi, W., Lakaye, B., De Borman, B., Coumans, B., Hennen, G., Grisar, T., Igout, A. & Heinen, E. (1999). Housekeeping genes as internal standards: use and limits. *Journal of Biotechnology*, **75**, 291–295.

Thornton, I. (1981). Geochemical aspects of the distribution and forms of heavy metals in soils. In N.W. Lepp, ed., *Effect of heavy metal pollution on plants: Metals in the environment*, Pollution monitoring series, 1–34, Applied Science Publishers, London.

Tian, Q.Y., Sun, D.H., Zhao, M.G. & Zhang, W.H. (2007). Inhibition of nitric oxide synthase (NOS) underlies aluminum-induced inhibition of root elongation in *Hibiscus moscheutos*. *New Phytologist*, **174**, 322–331.

Tichopad, A., Dilger, M., Schwarz, G. & Pfaffl, M.W. (2003). Standardized determination of real-time PCR efficiency from a single reaction set-up. *Nucleic Acids Research*, **31**, e122.

Tiemann, K.J., Gamez, G., Dokken, K., Parsons, J.G. & Gardea-Torresdey, J.L. (2002). Chemical modification and X-ray absorption studies for lead(II) binding by *Medicago sativa* (alfalfa) biomass. *Microchemical Journal*, **71**, 287–293.

Tong, Y.P., Kneer, R. & Zhu, Y.G. (2004). Vacuolar compartmentalization: a second-generation approach to engineering plants for phytoremediation. *Trends in Plant Science*, **9**, 7–9.

Tsyganov, V.E., Belimov, A.A., Borisov, A.Y., Safronova, V.I., Georgi, M., Dietz, K.J. & Tikhonovich, I.A. (2007). A chemically induced new pea (*Pisum sativum*) mutant sgecdt with increased tolerance to, and accumulation of, cadmium. *Annals of Botany*, **99**, 227–237.

Udvardi, M.K., Czechowski, T. & Scheible, W.R. (2008). Eleven golden rules of quantitative RT-PCR. *Plant Cell*, **20**, 1736–1737.

Vaerman, J.L., Saussoy, P. & Ingargiola, I. (2004). Evaluation of real-time PCR data. *Journal of Biological Regulators and Homeostatic Agents*, **18**, 212–214.

van Pelt-Verkuil, E., van Belkum, A. & Hays, J.P. (2008a). The different types and varieties of nucleic acid target molecules. In *Principles and Technical Aspects of PCR Amplification*, 25–62, Springer, Netherlands.

van Pelt-Verkuil, E., van Belkum, A. & Hays, J.P. (2008b). Ensuring PCR quality - quality criteria and quality assurance. In *Principles and Technical Aspects of PCR Amplification*, 213–230, Springer, Netherlands.

van Pelt-Verkuil, E., van Belkum, A. & Hays, J.P. (2008c). Important considerations for typical, quantitative and real-time PCR protocols. In *Principles and Technical Aspects of PCR Amplification*, 119–140, Springer, Netherlands.

van Pelt-Verkuil, E., van Belkum, A. & Hays, J.P. (2008d). PCR primers. In *Principles and Technical Aspects of PCR Amplification*, 63–90, Springer, Netherlands.

van Pelt-Verkuil, E., van Belkum, A. & Hays, J.P. (2008e). The polymerase chain reaction. In *Principles and Technical Aspects of PCR Amplification*, 1–7, Springer, Netherlands.

Vandesompele, J. (2009). qPCR guide. [Online] http://www.eurogentec.com.

Vandesompele, J., De Paepe, A. & Speleman, F. (2002a). Elimination of primer-dimer artifacts and genomic coamplification using a two-step SYBR Green I real-time RT-PCR. *Analytical Biochemistry*, **303**, 95–98.

Vandesompele, J., De Preter, K., Pattyn, F., Poppe, B., Van Roy, N., De Paepe, A. & Speleman, F. (2002b). Accurate normalization of real-time quantitative RT-PCR data by geometric averaging of multiple internal control genes. *Genome Biology*, **3**, 1–12.

Vandesompele, J., Kubista, M. & Pfaffl, M.W. (2009). Real-time PCR: current technology and applications. In J. Logan, K. Edwards & N. Saunders, eds., *Reference gene validation software for improved normalization*, vol. 2, 47–64, Caister Academic Press.

Verkleij, J.A.C. & Schat, H. (1990). Metal tolerance in higher plants. In A.J. Shaw, ed., *Heavy metal tolerance in plants: evolutionary aspects*, 180–195, CRC Press, Boca Raton.

Verma, S. & Dubey, R.S. (2003). Lead toxicity induces lipid peroxidation and alters the activities of antioxidant enzymes in growing rice plants. *Plant Science*, **164**, 645–655.

Vierling, E. (1991). The roles of heat shock proteins in plants. *Annual Review of Plant Physiology and Plant Molecular Biology*, **42**, 579–620.

Vliet, C.v., Andersen, C.R. & Cobbett, C.S. (1995). Copper-sensitive mutant of *Arabidopsis thaliana*. *Plant Physiology*, **109**, 871–878.

Wang, H., Liang, X., Wan, Q., Wang, X. & Bi, Y. (2009). Ethylene and nitric oxide are involved in maintaining ion homeostasis in *Arabidopsis* callus under salt stress. *Planta*, **230**, 293–307.

Wang, Y.S. & Yang, Z.M. (2005). Nitric oxide reduces aluminum toxicity by preventing oxidative stress in the roots of *Cassia tora* L. *Plant Cell Physiology*, **46**, 1915–1923.

Weigel, D. & Glazebrook, J. (2002). *Arabidopsis: a laboratory manual*. Cold Spring Harbor Laboratory Press, New York.

Wendehenne, D., Durner, J. & Klessig, D.F. (2004). Nitric oxide: a new player in plant signalling and defence responses. *Current Opinion in Plant Biology*, **7**, 449–455.

White, P.J., Bowen, H.C., Demidchik, V., Nichols, C. & Davies, J.M. (2002). Genes for calcium-permeable channels in the plasma membrane of plant root cells. *Biochimica et Biophysica Acta (BBA) - Biomembranes*, **1564**, 299–309.

Wierzbicka, M. (1987). Lead translocation and localization in *Allium cepa* roots. *Canadian Journal of Botany*, **65**, 1851–1860.

Wierzbicka, M. (1994). Resumption of mitotic activity in *Allium cepa* L. root tips during treatment with lead salts. *Environmental and Experimental Botany*, **34**, 173–180.

Wierzbicka, M. (1998). Lead in the apoplast of *Allium cepa* L. root tips - ultrastructural studies. *Plant Science*, **133**, 105–119.

Wierzbicka, M. (1999a). Comparison of lead tolerance in *Allium cepa* with other plant species. *Environmental Pollution*, **104**, 41–52.

Wierzbicka, M. (1999b). The effect of lead on the cell cycle in the root meristem of *Allium cepa* L. *Protoplasma*, **207**, 186–194.

Wierzbicka, M. & Obidzinska, J. (1998). The effect of lead on seed imbibition and germination in different plant species. *Plant Science*, **137**, 155–171.

Wierzbicka, M.H., Przedpelska, E., Ruzik, R., Ouerdane, L., Polec-Pawlak, K., Jarosz, M., Szpunar, J. & Szakiel, A. (2007). Comparison of the toxicity and distribution of cadmium and lead in plant cells. *Protoplasma*, **231**, 99–111.

Wilkins, D. (1957). A technique for the measurement of lead tolerance in plants. *Nature*, **180**, 37–38.

Wink, D.A., Hanbauer, I., Krishna, M.C., DeGraff, W., Gamson, J. & Mitchell, J.B. (1993). Nitric oxide protects against cellular damage and cytotoxicity from reactive oxygen species. *Proceedings of the National Academy of Sciences*, **90**, 9813–9817.

Wojtaszek, P. (1997). Oxidative burst: an early plant response to pathogen infection. *Biochemical Journal*, **322**, 681–692.

World Health Organisation, W.H.O. (2001). Lead. [Online] http://www.euro.who.int.

Wu, J., Hsu, F.C. & Cunningham, S.D. (1999). Chelate-assisted Pb phytoextraction: Pb availability, uptake, and translocation constraints. *Environmental Science & Technology*, **33**, 1898–1904.

Xiao, S., Gao, W., Chen, Q.F., Ramalingam, S. & Chye, M.L. (2008). Overexpression of membrane-associated acyl-CoA-binding protein ACBP1 enhances lead tolerance in *Arabidopsis*. *Plant Journal*, **54**, 141–151.

Xiong, Z.T. (1997). Bioaccumulation and physiological effects of excess lead in a roadside pioneer species *Sonchus oleraceus* L. *Environmental Pollution*, **97**, 275–279.

Xiong, Z.T. (1998). Lead uptake and effects on seed germination and plant growth in a Pb hyperaccumulator *Brassica pekinensis* Rupr. *Bulletin of Environmental Contamination and Toxicology*, **60**, 285–291.

Yang, X., Feng, Y., He, Z. & Stoffella, P.J. (2005). Molecular mechanisms of heavy metal hyperaccumulation and phytoremediation. *Journal of Trace Elements in Medicine and Biology*, **18**, 339–353.

Yu, C.C., Hung, K.T. & Kao, C.H. (2005). Nitric oxide reduces Cu toxicity and Cu-induced NH_4^+ accumulation in rice leaves. *Journal of Plant Physiology*, **162**, 1319–1330.

Yuan, J., Reed, A., Chen, F. & Stewart, C.N. (2006). Statistical analysis of real-time PCR data. *BMC Bioinformatics*, **7**, 1–12.

Zhang, L., Zhou, S., Xuan, Y., Sun, M. & Zhao, L. (2009). Protective effect of nitric oxide against oxidative damage in *Arabidopsis* leaves under ultraviolet-b irradiation. *Journal of Plant Biology*, **52**, 135–140.

Zhang, L.P., Mehta, S.K., Liu, Z.P. & Yang, Z.M. (2008). Copper-induced proline synthesis is associated with nitric oxide generation in *Chlamydomonas reinhardtii*. *Plant Cell Physiology*, **49**, 411–419.

Zhao, M., Zhao, X., Wu, Y. & Zhang, L. (2007). Enhanced sensitivity to oxidative stress in an *Arabidopsis* nitric oxide synthase mutant. *Journal of Plant Physiology*, **164**, 737–745.

Zhu, M.Y., Pan, J., Wang, L., Gu, Q. & Huang, C. (2003). Mutation induced enhancement of al tolerance in barley cell lines. *Plant Science*, **164**, 17–23.

Appendices

A.1 Preparation of culture medium

A.1.1 Modified HC medium

Throughout this thesis, Huang & Cunningham (1996) nutrient solution modified by Chin (2007) was used. The composition of modified HC medium containing 0.8% (w/v) agar is shown in Table A.1.

A.1.2 MS medium

For the recovery of isolated putative mutant, Murashige & Skoog (1962) nutrient solution was used. The composition of MS medium containing 0.8% (w/v) agar is shown in Table A.2.

Major salt stock (10x)

Salts	Stock solution concentration (mM)	Final working concentration (µM)
KNO_3	2.0	200
$Ca(NO_3)_2$	0.5	50
$MgSO_4.7H_2O$	0.2	20
NH_4NO_3	0.1	10
KH_2PO_4	0.005	0.5

Minor salt stock (100x)

Salts	Stock solution concentration (µM)	Final working concentration (nM)
KCl	50	500
Fe-EDTA	20	200
H_3BO_3	12	120
$MnSO_4.4H_2O$	2	20
$ZnSO_4.7H_2O$	0.5	5
$CuSO_4.5H_2O$	0.2	2
$Na_2MoO_4.2H_2O$	0.1	1
$NiSO_4$	0.1	1

Full strength HC medium

Composition	Total volume of 500 mL	Total volume of 1 L
Major salt stock (10x)	50 mL	100 mL
Minor salt stock (100x)	5 mL	10 mL
Agar	4 g	8 g
Nanopure H_2O	to 500 mL	to 1 L
Adjusted to pH 4.5 - 5.0 with 0.1 M HCl		

Table A.1: Composition of modified Huang & Cunningham (1996) nutrient solution. Stock solutions were stored at 4˚C.

Major salt stock (10x)

Salts	Amount of chemical (g)
NH_4NO_3	16.5
KNO_3	19.0
$CaCl_2.2H_2O$	4.4
$MgSO_4.7H_2O$	3.7
KH_2PO_4	1.7
Nanopure H_2O	to 1 L

Minor salt stock (100x)

Salts	Amount of chemical (mg)
KI	83
H_3BO_3	620
$MnSO_4.4H_2O$	2230
$ZnSO_4.7H_2O$	860
$CuSO_4.5H_2O$	2.5
$CoCl_2.6H_2O$	2.5
$Na_2MoO_4.2H_2O$	25
Nanopure H_2O	to 1 L

Organic supplement (100x)

Salts	Amount of chemical (mg)
myo-inositol	5000
Nicotinic acid	25
pyridoxine-HCl	25
thiamine-HCL	5
glycine	100
Nanopure H_2O	to 500 mL

Table A.2: Composition of Murashige & Skoog (1962) nutrient solution. Stock solutions were stored at 4˚C.

Iron stock	
Solution A : $FeSO_4.7H_2O$	1.390 g in 200 mL nanopure H_2O
Solution B : $Na_2EDTA.2H_2O$	1.865 g in 200 mL nanopure H_2O
Mix solution A and solution B	
Adjust volume to 500 mL with nanopure H_2O	
Store at 4˚C in the dark	

Full strength MS medium

Composition	**Total volume of 500 mL**	**Total volume of 1 L**
Nanopure H_2O	375 mL	750 mL
Major salt stock (10x)	50 mL	100 mL
Minor salt stock (100x)	5 mL	10 mL
Organic stock (100x)	5 mL	10 mL
Iron stock	5 mL	10 mL
Mix the solution		
Adjusted to pH 5.6 - 5.8 with 0.1 M HCl		
Agar	4 g	8 g
Nanopure H_2O	to 500 mL	to 1 L

Table A.2: Composition of Murashige & Skoog (1962) nutrient solution (continued from the previous page).

A.2 Preparation of buffer and reagents

A.2.1 Sodium phosphate buffer (pH 7.2)

Sodium phosphate buffer (0.075 M, pH 7.2) was prepared according to Table A.3.

0.2 M Na_2HPO_4 stock solution

17.8 g $Na_2HPO_4.2H_2O$

Make to 500 mL with nanopure H_2O

0.2 M $Na_2H_2PO_4$ stock solution

15.6 g $Na_2H_2PO_4.2H_2O$

Make to 500 mL with nanopure H_2O

0.075 M sodium phosphate buffer (pH 7.2)

Composition	Volume (mL)
0.2 M Na_2HPO_4	36
0.2 M $Na_2H_2PO_4$	14
Nanopure H_2O	83

Table A.3: Preparation of 0.075 M sodium phosphate buffer (pH 7.2).

A.2.2 Potassium phosphate buffer

Potassium phosphate buffer (0.1 M) was prepared following methods from Sambrook *et al.* (2001), as shown in Table A.4.

1 M K_2HPO_4 stock solution

87.1 g K_2HPO_4

Make to 500 mL with nanopure H_2O and store at 4˚C

1 M KH_2PO_4 stock solution

68.05 g KH_2PO_4

Make to 500 mL with nanopure H_2O and store at 4˚C

0.1 M potassium phosphate buffer

pH	Volume of 1 M K_2HPO_4 (mL)	Volume of 1 M KH_2PO_4 (mL)
5.8	7.9	92.1
6.0	12.0	88.0
6.2	17.8	82.2
6.4	25.5	74.2
6.6	35.2	64.8
6.8	46.3	53.7
7.0	57.7	42.3
7.2	68.4	31.6
7.4	77.4	22.6
7.6	84.5	15.5
7.8	89.6	10.4
8.0	93.2	6.8

Bring the volume to 1 L with nanopure H_2O

Table A.4: Preparation of 0.1 M potassium phosphate buffer at 25˚C.

A.2.3 TAE buffer

The working solution of 1x TAE buffer was prepared in a 250 mL volumetric flask each time it was used. TAE buffer stock (5 mL 50x concentrate) that was kept at 4˚C was diluted with 245 mL nanopure H_2O. The method is summarized in Table A.5.

50x TAE buffer stock

12.1 g Tris-base
1.86 g Na_2EDTA
2.855 mL Acetic acid*
Bring the volume to 50 mL with nanopure H_2O
Keep at 4˚C
** performed in a fumehood*

1x TAE buffer

5 mL TAE buffer stock (50x)
Make to 250 mL with nanopure H_2O

Table A.5: Preparation of TAE buffer.

A.2.4 DEPC-H_2O

DEPC-H_2O (0.1%, v/v) was prepared by adding 100 µL DEPC (Sigma-Aldrich, St. Louis, MO, USA) to nanopure H_2O in a 100 mL glass bottle in a fume hood. Nanopure H_2O was topped up to 100 mL total volume. The bottle was shaked vigorously to mix DEPC into solution. The solution in the bottle was left overnight at room temperature. It was autoclaved the next day to deactivate DEPC in the water. DEPC-H_2O was aliquoted into RNase-free microcentrifuge tubes and kept at -20˚C. The remaining DEPC-H_2O in the same bottle was stored in an RNA-free container.

A.2.5 RNase-free DNase

RNase-free DNase (Qiagen GmbH, Hilden, Germany) was prepared according to the manufacturer's instructions accompanying the kit purchased. DNase I stock solution was prepared by injecting 550 µL RNase-free H_2O into a vial containing lyophilized DNase I using a sterile needle and 1 mL syringe. The solution was mixed by gently inverting the vial. Then DNase I stock solution was aliquoted into RNase-free microcentrifuge tubes (10 µL single-use aliquot for each tube). The aliquots were stored at -20˚C until use.

A.2.6 Protein extraction buffer

The total protein extraction buffer was modified from Weigel & Glazebrook (2002), as shown in Table A.6.

0.5 M Tris-acetate (pH 7.9)

0.6057 g Tris-base

8 mL nanopure H_2O

Adjust to pH 7.9 with concentrated acetic acid

Make to 10 mL with nanopure H_2O and store at -20°C

1 M potassium acetate

0.9814 g CH_3COOK

Make to 10 mL with nanopure H_2O and store at -20°C

10 mM Na_2EDTA

0.0372 g Na_2EDTA

Make to 10 mL with nanopure H_2O and store at -20°C

10 mM DTT

0.0154 g DTT

Make to 10 mL with nanopure H_2O and store at -20°C

Protein extraction buffer

Component	**Amount**
0.5 M Tris-acetate (pH 7.9)	0.5 mL
1 M CH_3COOK	0.5 mL
10 mM Na_2EDTA	0.5 mL
10 mM DTT	0.5 mL
Glycerol	1.0 mL
Protease cocktail inhibitor	1 tablet
PMSF*	

Make to 5 mL with nanopure H_2O and put on ice

** prepare just before use; dissolve 0.0017 g PMSF in 100 µL methanol*

Table A.6: Reagents for protein extraction.

A.2.7 Reagents for SDS-PAGE

Preparation of the stock solutions for the Laemmli buffer system (Laemmli, 1970), according to the instruction manual for the Mini-PROTEAN III gel apparatus (Bio-Rad Laboratories Inc., Hercules, CA, USA) was outlined in Table A.7.

Acrylamide/bis (30% T, 2.67% C)
87.6 g acrylamide
2,4 g N'N'-bis-methylene-acrylamide
Make to 300 mLl with nanopure H_2O
Filter and store at 4°C in the dark (30 d maximum)

1.5 M Tris-HCl (pH 8.8)
27.23 g Tris-base
80 mL nanopure H_2O
Adjust to pH 8.8 with 1 M HCl
Make to 150 mL with nanopure H_2O and store at 4°C

0.5 M Tris-HCl (pH 6.8)
6 g Tris-base
60 mL nanopure H_2O
Adjust to pH 6.8 with 1 M HCl
Make to 100 mL with nanopure H_2O and store at 4°C

10% (w/v) SDS
10 g SDS
90 mL nanopure H_2O
Stir gently and bring to 100 mL with nanopure H_2O, store at room temperature

Table A.7: Reagents for SDS-PAGE.

5x electrode (running) buffer, pH 8.3

9 g Tris-base

43.2 g glycine

3 g SDS

Make to 600 mL with nanopure H_2O and store at 4°C

1x running buffer

60 mL running buffer (5x)

240 mL nanopure H_2O

4x Laemmli sample buffer (SDS reducing buffer)

Component	**Amount**
Nanopure H_2O	1.2 mL
1 M Tris-HCl (pH 6.8)	2.0 mL
Glycerol	3.2 mL
10% (w/v) SDS	0.64 g
2-mercaptoethanol	1.6 mL
1% (w/v) bromophenol blue	0.016 g
Total volume	*8.0 mL*

Aliquot into 1 mL in Eppendorf tube and store at -20°C

Warm to room temperature before use

Dilute the sample at least 1:4 with sample buffer, and boil for 4 min

Table A.7: Reagents for SDS-PAGE (continued from the previous page).

A.2.8 Reagents for western blot

Reagents in Table A.8 were made for western blot analysis.

2 M Tris

24.2 g Tris-base

Make to 100 mL with nanopure H_2O and store at room temperature

2.5 M NaCl

14.61 g NaCl

Make to 100 mL with nanopure H_2O and store at room temperature

TBS

10 mL Tris (2 M)

60 mL NaCl (2.5 M)

900 mL nanopure H_2O

Adjust to pH 7.5 with concentrated HCl

Make to 1 L with nanopure H_2O and store at room temperature

TBST

200 µL Tween-20

Make to 400 mL with TBS and store at room temperaturee

Blotting buffer (pH 8.3)

0.966 g Tris-base

4.1 g glycine

Dissolve in 200 mL nanopure H_2O

80 mL distilled methanol

Make to 400 mL with nanopure H_2O and store at room temperature

Table A.8: Reagents for western blot.

0.1 M Tris-HCl (pH 9.5)

25 mL Tris (2 M)

450 mL nanopure H_2O

Adjust to pH 9.5 with concentrated HCl

Make to 500 mL with nanopure H_2O and store at room temperature

1 M $MgCl_2$

2.033 g $MgCl_2$

Make to 10 mL with 0.1 M Tris-HCl (pH 9.5) and store at room temperature

Blocking solution*

2 g BSA

Make to 200 mL with TBST

** to be prepared just before use*

NBT

2 mg NBT

2 mL Tris-HCl (0.1 M, pH 9.5)

Store at 4°C in the dark

Table A.8: Reagents for western blot (continued from the previous page).

A.3 GF-AAS calibration curve for Pb

The GF-AAS machine was calibrated with a freshly prepared 200 µmol/L $Pb(NO_3)_2$ standard solution in 1% (v/v) HNO_3 before the analysis for Pb levels in each batch of experimental materials. The stock solution was serially diluted to 20, 50, 100, and 200 nmol/L $Pb(NO_3)_2$ working standard solutions with 1% (v/v) HNO_3. After zeroing the machine with 1% (v/v) HNO_3, a calibration curve was generated automatically by the GBC Avanta software, from the mean absorbance values of two duplicate readings. A representative data comprising of Pb concentration, absorbance readings and mean were shown in Table A.9. The data were used to plot the calibration curve (Figure A.3) along with its equation and coefficient of variance.

Pb concentration (nmol/L)	Reading 1	Reading 2	Mean
0	-0.0001	-0.0007	-0.0004
20	0.0411	0.0418	0.0415
50	0.0887	0.0905	0.0896
100	0.1761	0.1783	0.1772
200	0.2959	0.3158	0.3059

Table A.9: A representative data for the calculation of GF-AAS calibration curve for Pb.

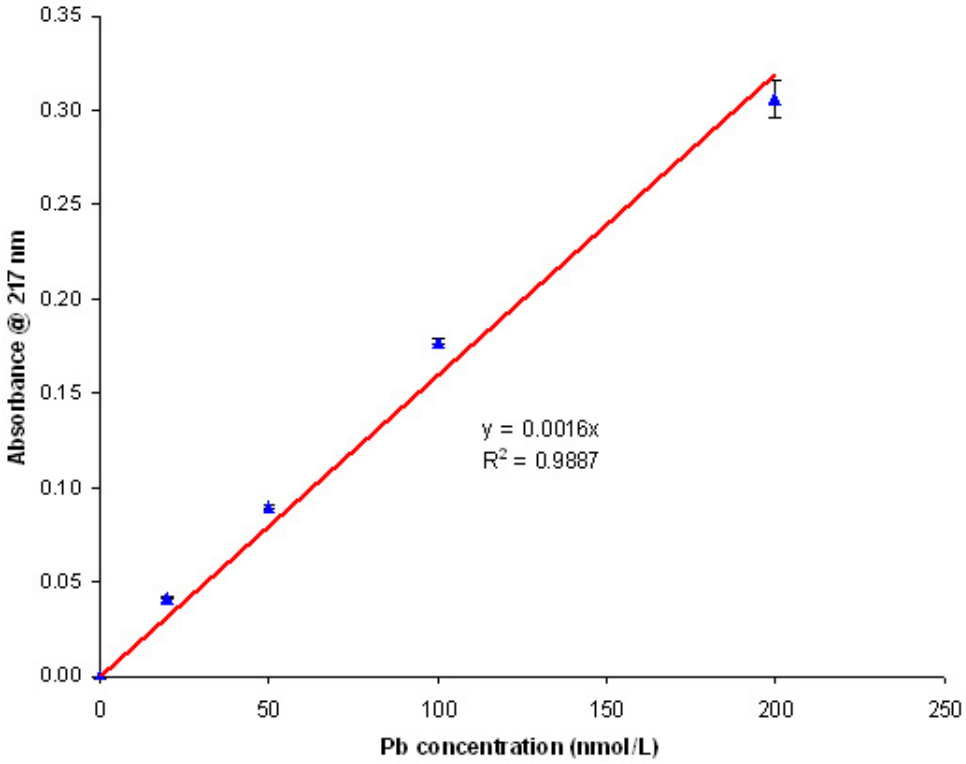

Figure A.3: GF-AAS calibration curve for Pb, constructed from a serial dilution of $Pb(NO_3)_2$ stock solution at 20, 50, 100, and 200 nmol/L. The scale bars indicate standard error of the means.

A.4 Nucleotide sequences for reference and target genes

All sequences used in this thesis were obtained from NCBI in FASTA format.

A.4.1 Adenosine phosphoribosyl transferase 1

>gi|13358234|gb|AF325045.2| *Arabidopsis thaliana* At1g27450

(At1g27450/F17L21_25) mRNA, complete cds

AAATCTGACGCCGAGTATTTTGCTAAAGCAGCAGCCAGTCGGGACAGTGAAATGGCGACTGAAGATGTGC
AAGATCCCAGAATCGCTAAGATTGCCTCTTCCATTAGAGTCATCCCCGACTTCCCTAAACCAGGAATCAT
GTTTCAGGACATAACGACGCTTCTTCTCGACACTGAGGCCTTTAAGGATACTATTGCTTTGTTTGTTGAT
AGATACAAAGATAAAGGCATATCTGTTGTTGCAGGTGTTGAAGCTAGAGGTTTCATTTTTGGCCCTCCTA
TTGCGTTGGCTATTGGTGCCAAATTTGTTCCCATGAGGAAGCCCAAGAAGCTACCTGGGAAGGTTATTTC
GGAGGAGTATTCGTTGGAGTATGGAACAGATACGATTGAGATGCACGTAGGTGCAGTAGAGCCTGGTGAG
CGTGCTATTATTATTGATGACCTCATTGCCACGGGTGGGACTCTCGCTGCTGCAATCCGACTACTTGAAC
GAGTAGGAGTGAAGATTGTTGAATGTGCTTGCGTAATTGAGTTACCAGAGCTTAAGGGAAAGGAGAAACT
AGGAGAGACGTCGCTATTTGTTCTTGTAAAGTCGGCTGCTTAACAAGAAACTGGAAGAGAAGGTTATTGG
ATCGAGTGTTGATGCTATTTTTCATGTATGGTGAGACATTTTGCGTGGGATTTGATCCTTGTTGTTTCAA
CTTATCATAATTGGTTCAGACTAGAAAATGGCATTTGAATGTCAGGATTCGATTGCAGTTTCCTATTGTT
CCACTTAAAATCCCCGATTAATAAGGTGTTATGGGTTTTATTTATAGAATCAAGTTGTAATAGTAGACTC
CAACAGGGGCTAAAGTCTTGGTAACGCAATTCTTCTTTT

A.4.2 SAND family protein

>gi|186503781|ref|NM_128399.3| *Arabidopsis thaliana* SAND family protein

(AT2G28390) mRNA, complete cds

AGCAGAGAGAATCAATGAACACGTCTTGCCATTAGAGGAGACCAACCATTTCTCTCCTCTCTCTTGAAAA
ATCTATAACCGATTTCTGCAATGGCGACTTCAGATTCGAGGTCTTCTCCTTCATCATCCGACACCGAATT
CGCCGATCCAAATCCTAGCTCCGATCCAGAGACGAATTCGGAGCGTGTTCAAAGTCAATTAGAGTCAATG
AATTTATCTCAACCTAGCGAAGTCTCTGATGGTAGCCACACCGAATTTAGCGGTGGCGGCGATGATAATG
ATGATGAGGTTGCATCGGCTAACGGGAACGAAGGCGGAGTTAGCAATGGAGGTTTATTGCGTGAAGGTGT
GGCGGGAACTAGCGGAGGAGAGGTTTTGTTAAGGGCGGAAAATCCGGTGGAAATGGAAGCAGGTGAAGAA
CCACCGAGTCCGACTAGTAGCGGTTACGATGGAGAGAGAGGAAGTAGCGGCGGAGCTACTTCTACTTATA
AAGCTGATGATGGAAGCGAGGATGAGATTAGGGAAGCTAATGTGGATGGTGACACTGCCTCGCAGCATGA
AGCTGCGTGGTTGCCTGGAAAACGCCATGTTGATGAGGATGATGCTTCTACGTCATGGAGAAAGAGGAAG
AAGCATTTCTTCATACTGAGTAACTCAGGCAAACCGATATATTCCAGATATGGAGATGAACATAAGCTTG
CTGGATTTTCAGCTACTCTTCAAGCTATTATTTCTTTTGTGGAGAATGGTGGTGACCGTGTCAACTTAGT
CAAGGCAGGAAATCACCAGGTTGTCTTTCTCGTTAAGGGGCCAATATATCTGGTCTGCATCAGCTGTACA
GATGAAACATATGAGTATTTAAGGGGGCAGTTGGATCTTCTATATGGTCAGATGATACTAATTTTAACAA
AATCAATAGACAGATGTTTTGAAAAGAATGCAAAGTTCGATATGACACCCTTGCTTGGAGGGACAGATGC
TGTCTTCTCATCTCTTGTCCATTCATTTAGCTGGAACCCAGCTACATTTCTTCATGCCTATACTTGTCTT
CCCCTTCCATATGCGTTAAGGCAAGCTACAGGAACCATATTGCAAGAAGTTTGCGCGTCTGGTGTCTTAT
TCTCACTACTAATGTGCAGACACAAGGTTGTCAGTCTTGCTGGTGCACAGAAAGCGTCTCTCCATCCCGA
TGACTTGCTTCTACTCTCAAATTTTGTCATGTCATCAGAATCATTCAGGACATCAGAATCTTTCTCACCA
ATCTGCCTACCAAGATACAACGCTCAGGCCTTTTTGCATGCCTATGTCCACTTCTTTGATGATGATACAT
ATGTAATATTGCTTACCACACGTTCAGATGCGTTCCATCATCTCAAAGATTGCAGGGTACGCCTTGAGGC
TGTTCTTCTCAAGTCAAATATTCTAAGTGTGGTTCAAAGATCAATCGCGGAAGGTGGAATGCGTGTTGAA
GATGTACCAATAGACCGCAGGCGTCGATCATCTACTACTAATCAAGAACAAGACTCACCTGGTCCCGACA
TATCTGTGGGAACCGGAGGTCCCTTTGGACTTTGGCATTTCATGTACCGTAGTATATACTTAGATCAATA
CATTTCCTCGGAATTCTCACCCCCAGTAACTAGTCACAGACAACAGAAAAGTCTATATCGAGCATACCAG
AAACTTTATGCTTCAATGCATGTAAAAGGATTGGGACCCCACAAGACTCAATATAGAAGAGATGAAAACT
ACACTCTTCTATGTTGGGTCACACCAGATTTTGAACTCTATGCAGCATTTGATCCACTTGCAGACAAGGC
GATGGCGATAAAGATATGCAATCAGGTGTGCCAAAGGGTAAAAGATGTGGAGAATGAAGTGTTCTTGCAA
GGAGCTAGTCCTTTCTCTTGGTGATAATATTTTACTATTCACTCTTTAATATATATGTATTTTTTTTTAA
TCTTTCTACTGGTTTGACCCCCTATATTGTGCTAGTACCACCCACCTTAATAAGGCAATAATGTAATTGT
ACCCAGAAACCCTTGAGAGAAAGCTATTTCATTGCCTTTATTGTTATTAATTAGCTTGAATAGTCAAAAT
TGAGATGATGTAGACAAAAATTGAAACTATTTGAAAAGTGAGCAATAATATTAAGGTTTTGATGGAAGGA

A.4.3 Mitosis protein YLS8

>gi|30682323|ref|NM_120912.2| *Arabidopsis thaliana* YLS8; catalytic (YLS8)

mRNA, complete cds

```
GCAAGAGAGAAAAAAGGTTGAATCGAAACAGATCGGAAAATCGTCGAGAGAGAGAGAGAGAGAGAGAATG
TCGTATCTTCTTCCACATCTGCACTCCGGTTGGGCTGTTGATCAGTCGATTCTGGCCGAGGAAGAGCGTC
TCGTCGTCATTCGTTTCGGCCATGACTGGGATGAGACCTGTATGCAGATGGATGAGGTGCTTGCGTCTGT
TGCTGAGACGATTAAGAACTTTGCAGTCATTTATCTGGTGGACATCACTGAGGTTCCAGACTTCAACACC
ATGTACGAGCTGTACGATCCTTCTACGGTCATGTTCTTCTTCAGGAACAAGCACATCATGATCGATCTTG
GAACTGGTAACAACAACAAGATCAACTGGGCTCTCAAGGACAAGCAGGAGTTCATTGATATCATTGAGAC
TGTCTACCGTGGTGCAAGGAAGGGTCGTGGGTTGGTGATTGCTCCAAAAGATTACTCCACCAAATACCGT
TACTAATCGAGCTTCCCAACACTATCTAGTTTGTTAAAACCATTGAGTCTAGTGATTCTGGTCAGCTGAA
ATATCCCGTGAACTGGTTTCATTTCATATATGCTTTGATGATGATTGTGATTCTGGTTTTTGCTTACTGT
TTCGGTTGTTCTCCATTTATGTATGTAACTACTTGCTTCGAACATGATTCAGTGAAATGAAATTTGGAAG
CCGTTGGGTTTATGT
```

A.4.4 F-box family protein

>gi|186523165|ref|NM_121575.4| *Arabidopsis thaliana* F-box family protein

(AT5G15710) mRNA, complete cds

```
ATCTCTCTCTTCTTCGTGTTACTAAAAAGGACGAAGCTTGTTGCATAATATGTTGAGGTAAATTACTAAT
TACTGATCCAAAGTTCGAATCTTTGCTCCAACTCCAGGCTAGCTGATTGCGTAGCTTCCGATTGATTTCT
ACCTGAGTTTTGAGTTCCTTTGTGGCCACTTCGTTGTTCTTCTGCTGGGTTTTTTGCTCGAGGATCTGAT
ACTTCTGTTTGGTCGATGATCGAGTGATCTTCGTTGGGTTTTGGGGATCTAAGTCGTCTATATAGCTAAT
GGTTTGGATTTGAGTTTGAATGGAGCGTTTAGGATTTTGGGGATTGCTAATGGGTAGTGTGGAAAAGTCA
TTGGATTCTGGAAATTCGTTGGCTTGCTCTGCATCTGCTAAGAATGGAGACGAAGAGAGTAGTACTTCAT
CGAAGCAAGTTTCACCATTGAAGGGTTCTGGGTCGAGAAATACTAGTCCTTTAGGTCGAGTTGGGTCGAG
AAACACGAGTCCTTCTAGGCAGAAAGTGGTGAAGACGAAGCCTCGTGGTCTAGAGGAAGAAACAGTTGCT
TCATTTGGTAAACAAGTTGTTGCTGATGTGCAGATGGAAGATGGTATATGGGCAATGCTTCCAGAGGATT
TGCTCAATGAGATTTTAGCTAGGGTTCCACCGTTTATGATATTTCGAATCCGGTCTGTTTGTAAAAAATG
GAACTTGATTCTTCAGGATAATAGTTTTCTCAAGTTTCACTCAAATGTGTCATCTCATGGGCCTTGTCTT
CTCACTTTCTGGAAGAACTCGCCGCAGATTCCGCAATGCTCAGTTTTTAGTTTGCCATTGAAGACATGGT
ACAAAATTCCATTCACGTTTTTGCCTCCATGGGCTTTTTGGTTGGTTGGTTCTTCAGGTGGTCTCGTTTG
TTTTTCGGGTCTTGATGGTCTAACTTTCAGAACTTTAGTATGCAATCCTCTGATGCAGAGTTGGAGGACT
CTACCGAGTATGCACTATAACCAACAAAGGCAATTGATTATGGTCGTGGATCGCTCAGACAAATCGTTCA
AAGTCATAGCCACAAGTGATATATACGGGGATAAGTCACTTCCTACTGAAGTTTATGATTCCAAAACTGA
CAAATGGTCCTTACATCAGATAATGCCTGCGGTGAACTTATGCTCCTCGAAAATGGCTTATTGTGATTCC
CGGTTATATCTAGAAACTCTTTCGCCTCTTGGTTTGATGATGTATCGGCTTGATTCAGGGCAATGGGAAC
ACATTCCAGCTAAATTCCCGAGATCTTTGTTGGATGGTTACTTAGTTGCTGGAACTCAGAAGAGATTGTT
TCTCGTGGGAAGGATTGGCCTCTACAGTACTCTCCAAAGCATGAGAATATGGGAGCTTGATCACACAAAG
GTCTCTTGGGTAGAGATAAGTAGAATGCCACCAAAGTACTTCCGAGCACTTCTGAGACTTTCGGCTGAGA
GGTTCGAGTGTTTTGGACAAGATAATTTGATCTGCTTTACGTCTTGGAATCAAGGAAAAGGTCTTCTATA
CAATGTGGATAAGAAAATTTGGTCTTGGATTTCCGGTTGTGCTCTTCAGTCATGCAACAGCCAAGTGTGC
TTTTATGAGCCAAGATTTGATGCATCTGTCCTCTGAACAATAAGTTATCGTCTGTCTCACATCATTCTTG
AAAACTTACAAGTTCGCCAGCAAAACATGTCAGAAATATGAAATCAAAGAGGGTTTGATGTGTACCTTCA
GTGTTAATGAAGACCTGGTCAGCAATGATATGCTTCACCAATGGTTAACAATATCGAGGAGAAAAACTGT
AAGATAAACTTGTTTCTAGCTTTCTGTAAATTAGCATTCACTCGATATGAAAACTTTCTCAATA
```

A.4.5 Annexin 1

>gi|4959105|gb|AF083913.1| *Arabidopsis* thaliana annexin (AnnAt1) mRNA,

complete cds

CCACGCGTCCGAAACACTAAAAGTAGAAGAAAAATGGCGACTCTTAAGGTTTCTGATTCTGTTCCTGCTC
CTTCTGATGATGCTGAGCAATTGAGAACCGCTTTTGAAGGATGGGGTACGAACGAGGACTTGATCATATC
AATCTTGGCTCACAGAAGTGCTGAACAGAGGAAAGTCATCAGGCAAGCATACCACGAAACCTACGGCGAA
GACCTTCTCAAGACTCTTGACAAGGAGCTCTCTAACGATTTCGAGAGAGCTATCTTGTTGTGGACTCTTG
AACCCGGTGAGCGTGATGCTTTATTGGCTAATGAAGCTACAAAAAGATGGACTTCAAGCAACCAAGTTCT
TATGGAAGTTGCTTGCACAAGGACATCAACGCAGCTGCTTCACGCTAGGCAAGCTTACCATGCTCGCTAC
AAGAAGTCTCTTGAAGAGGACGTTGCTCACCACACTACCGGTGACTTCAGAAAGCTTTTGGTTTCTCTTG
TTACCTCATACAGGTACGAAGGAGATGAAGTGAACATGACATTGGCTAAGCAAGAAGCTAAGCTGGTCCA
TGAGAAAATCAAGGACAAGCACTACAATGATGAGGATGTTATTAGAATCTTGTCCACAAGAAGCAAAGCT
CAGATCAATGCTACTTTTAACCGTTACCAAGATGATCATGGCGAGGAAATTCTCAAGAGTCTTGAGGAAG
GAGATGATGATGACAAGTTCCTTGCACTTTTGAGGTCAACCATTCAGTGCTTGACAAGACCAGAGCTTTA
CTTTGTCGATGTTCTTCGTTCAGCAATCAACAAAACTGGAACTGATGAAGGAGCACTCACTAGAATTGTG
ACCACAAGAGCTGAGATTGACTTGAAGGTCATTGGAGAGGAGTACCAGCGCAGGAACAGCATTCCTTTGG
AGAAAGCTATTACCAAAGACACTCGTGGAGATTACGAGAAGATGCTCGTCGCACTTCTCGGTGAAGATGA
TGCTTAATCAATCAATCCTCCACAGAGAAACATAAGCTGCTCTACAGCTTCTGTTATCTCTTATCTCCCT
CTCTCTCTCTTTGATGAGTTTCAAATCGTTTGATTTTGTTTCTACAAAAACCTTGTTTGTTTCTGTTGTG
TGTTTTGAGTTCCTAAATAATGCAAAAGAGAGAGACAGAGAGAACCAGTGTGGTCTCTTAAGTTATATAT
ATATGAAGAGCATTGGCCTAAAAAAAAAAAAAAAAAAAAA

A.5 Primers design for reference and target genes

The results for primer pairs used in this thesis were generated by Primer3 (Rozen & Skaletsky, 2000) and Primer-BLAST.

A.5.1 Adenosine phosphoribosyl transferase 1

Primer3 output

Primer	Start	Length	T_m	GC%	any	3'	Sequence (5' > 3')
Left	627	20	59.25	45.00	4.00	1.00	ttggatcgagtgttgatgct
Right	786	20	59.79	45.00	4.00	1.00	cggggattttaagtggaaca

Sequence size: 879

Included region size: 879

Product size: 160, Pair any self-complementary: 4.00, Pair 3' self-complementary: 2.00

Primer-BLAST report

Primer	Sequence (5' > 3')	Length	Start	Stop	T_m	GC%
Forward	TTGGATCGAGTGTTGATGCT	20	627	646	51.42	45.00
Reverse	CGGGGATTTTAAGTGGAACA	20	786	767	49.85	45.00

Product length: 160

Summary of primer pairs:

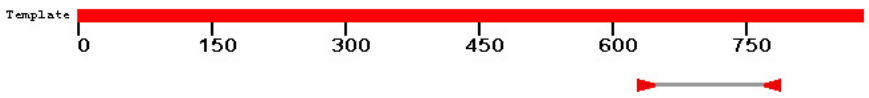

A.5.2 SAND family protein

Primer3 output

Primer	Start	Length	T_m	GC%	any	3’	Sequence (5’ > 3’)
Left	1063	20	60.04	55.00	6.00	0.00	gcgttaaggcaagctacagg
Right	1173	20	60.03	50.00	8.00	2.00	tttctgtgcaccagcaagac

Sequence size: 2170

Included region size: 2170

Product size: 111, Pair any self-complementary: 4.00, Pair 3’ self-complementary: 1.00

Primer-BLAST report

Primer	Sequence (5’ > 3’)	Length	Start	Stop	T_m	GC%
Forward	GCGTTAAGGCAAGCTACAGG	20	1063	1082	53.60	55.00
Reverse	TTTCTGTGCACCAGCAAGAC	20	1173	1154	53.22	50.00

Product length: 111

Summary of primer pairs:

A.5.3 Mitosis protein YLS8

Primer3 output

Primer	Start	Length	T_m	GC%	any	3'	Sequence (5' > 3')
Left	564	20	60.35	45.00	4.00	1.00	tcccgtgaactggtttcatt
Right	706	20	59.94	40.00	6.00	2.00	caacggcttccaaatttcat

Sequence size: 715

Included region size: 715

Product size: 143, Pair any self-complementary: 4.00, Pair 3' self-complementary: 1.00

Primer-BLAST report

Primer	Sequence (5' > 3')	Length	Start	Stop	T_m	GC%
Forward	TCCCGTGAACTGGTTTCATT	20	564	583	51.49	45.00
Reverse	CAACGGCTTCCAAATTTCAT	20	706	687	49.42	40.00

Product length: 143

Summary of primer pairs:

A.5.4 F-box family protein

Primer3 output

Primer	Start	Length	T_m	GC%	any	3’	Sequence (5’ > 3’)
Left	1446	20	60.14	55.00	5.00	2.00	gcacttctgagactttcggc
Right	1602	20	59.99	50.00	4.00	1.00	ggctgttgcatgactgaaga

Sequence size: 1884

Included region size: 1884

Product size: 157, Pair any self-complementary: 4.00, Pair 3’ self-complementary: 1.00

Primer-BLAST report

Primer	Sequence (5’ > 3’)	Length	Start	Stop	T_m	GC%
Forward	GCACTTCTGAGACTTTCGGC	20	1446	1465	53.56	55.00
Reverse	GGCTGTTGCATGACTGAAGA	20	1602	1583	52.71	50.00

Product length: 157

Summary of primer pairs:

A.5.5 Annexin 1

Primer3 output

Primer	Start	Length	T_m	GC%	any	3'	Sequence (5' > 3')
Left	893	20	59.67	50.00	4.00	1.00	ggaacagcattcctttggag
Right	1020	22	59.52	45.45	4.00	1.00	gcagcttatgtttctctgtgga

Sequence size: 1230

Included region size: 1230

Product size: 128, Pair any self-complementary: 4.00, Pair 3' self-complementary: 1.00

Primer-BLAST report

Primer	Sequence (5' > 3')	Length	Start	Stop	T_m	GC%
Forward	GGAACAGCATTCCTTTGGAG	20	893	912	50.94	50.00
Reverse	GCAGCTTATGTTTCTCTGTGGA	22	1020	999	52.82	45.45

Product length: 128

Summary of primer pairs:

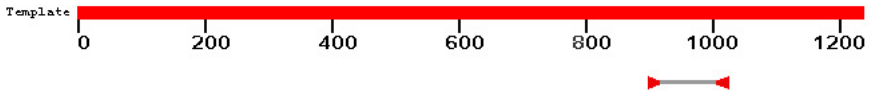

A.6 Computer programs and typesetting

This thesis was typeset with a document processor, LyX, which combines the graphical interface of Words and flexibility of LaTeX. A template was downloaded from the University of Durham (http://maths.dur.ac.uk/Thesis/) and modified using TeXnicCenter version 1.0 according to the thesis format required by the University of Canterbury. The LaTeX distribution used was MiKTeX version 2.7.

All bibliographies were managed by EndNote X2. Then, it was converted into BibTeX format to be intergrated into LyX environment by JabRef version 2.5. The graphs in this thesis were plotted using Microsoft Office Excel 2003 and saved into JPG format using Adobe Photoshop CS2. The latter software was also used for creating, compiling, and labeling figures. Computer programs used during this thesis are shown in Table A.10.

Program	Function	Website
LyX	Document processor	http://www.lyx.org/
LaTeX	Typesetting	http://www.latex-project.org/
MiKTeX	LaTeX distribution	http://www.miktex.org/
TeXnicCenter	Integrated documentation environment for LaTeX	http://www.texniccenter.org/
Endnote	Reference manager	http://www.endnote.com/
JabRef	Reference manager for BibTEX	http://jabref.sourceforge.net/
Excel	Spreadsheet and graphing	http://office.microsoft.com/en-us/excel/default.aspx
STATISTICA	Statistical analysis	http://statsoft.com/
Minitab	Statistical analysis	http://www.minitab.com/
SPSS	Statistical analysis	http://www.spss.com/
REST	Gene expression analysis	http://www.gene-quantification.org/rest-2008.html
BestKeeper	Stability of housekeeping gene	http://www.gene-quantification.org/bestkeeper.html
NormFinder	Stability of housekeeping gene	http://www.mdl.dk/publicationsnormfinder.htm
geNorm	Stability of housekeeping gene	http://medgen.ugent.be/~jvdesomp/genorm/
Primer3	Primer design	http://frodo.wi.mit.edu/
Primer-BLAST	Primer design	http://www.ncbi.nlm.nih.gov/tools/primer-blast/
Image-Pro Plus	Image processing and analysis	http://www.mediacy.com/index.aspx?page=IPP
Photoshop	Image editor	http://www.adobe.com/products/photoshop/photoshop/

Table A.10: Computer programs used during this thesis.